

Please cite the Published Version

Wilson-Nieuwenhuis, Joels (2018) The Interactions Between Bacteria, Platelets Bags and Platelets. Doctoral thesis (PhD), Manchester Metropolitan University.

Downloaded from: <https://e-space.mmu.ac.uk/625111/>

Usage rights:  Creative Commons: Attribution-Noncommercial-No Derivative Works 4.0

Enquiries:

If you have questions about this document, contact openresearch@mmu.ac.uk. Please include the URL of the record in e-space. If you believe that your, or a third party's rights have been compromised through this document please see our Take Down policy (available from <https://www.mmu.ac.uk/library/using-the-library/policies-and-guidelines>)

The Interactions Between Bacteria, Platelets Bags and Platelets

Joels Sebastian Thomas Wilson-Nieuwenhuis

A thesis submitted in partial fulfilment of the requirements of Manchester
Metropolitan University for the degree of Doctor of Philosophy

**Department of Life Sciences,
Manchester Metropolitan University.**

2018

Declaration

I declare that this work has not already been accepted for any degree and is not being currently submitted in candidature for any other than the degree of Doctor of Philosophy at Manchester Metropolitan University.

Contents

Declaration	2
List of Figures.....	10
List of Tables	14
Abstract	15
Publications Arising from this work.....	16
Acknowledgements	17
1.0 Introduction.....	18
1.1 Platelets	20
1.1.1 Significance of Platelets.....	20
1.1.2 Transfusion Risks	21
1.1.3 Origins of Bacterial Contamination in Platelet Units.....	22
1.1.4 Measures for Detecting Bacterial Contamination.....	24
1.2 Surface Characterisation.....	27
1.2.1 Surface Roughness	27
1.2.2 Raman Spectroscopy	28
1.2.4 Attenuated Total Reflection Fourier Transform Infrared Spectroscopy (ATR-FTIR)	29
1.2.5 Surface Physicochemistry.....	29
1.2.6 Energy Dispersive X-ray (EDX)	30
1.3 Low Temperature Atmospheric Pressure Plasma (LTAPP)	31

1.4	Conditioning Films	33
1.5	Bacteria.....	34
1.5.1	<i>Serratia marcescens</i>	34
1.5.2	<i>Staphylococcus epidermidis</i>	35
1.5.3	Bacterial Biofilms	36
1.6	Microbiology Assays	38
1.6.1	Microbial Adhesion to Hydrocarbons (MATH)	38
1.6.2	Biofilm Determination by Crystal Violet.....	38
1.7	Bacterial Interactions with Platelets	39
1.7.1	Methods Used in Understanding Bacterial Interaction with Platelets	41
1.8	Aims and Objectives	43
1.8.1	Aim.....	43
1.8.2	Objectives	43
2.0	Materials and Methods	44
2.1	Materials.....	44
2.1.1	Microorganisms.....	44
2.1.2	Reagents	44
2.1.3	Western Blot Antibodies	46
2.1.4	Buffers:	47
2.2	Surface Modification	48

2.2.1 Flattening.....	48
2.2.2 Low Temperature Atmospheric Pressure Plasma (LTAPP) Treatment.....	48
2.3 Surface Characterisation	49
2.3.1 Coupon Preparation	49
2.3.2 Scanning Electron Microscopy (SEM).....	49
2.3.3 Surface Roughness and Optical Surface Profiles.....	49
2.3.4 Energy Dispersive X-ray (EDX)	49
2.3.5 Attenuated Total Reflection- Fourier Transform Infrared Spectroscopy (ATR-FTIR).....	50
2.3.6 Raman Spectroscopy	50
2.3.7 Physicochemistry of Surfaces	50
2.3.8 Tensile Strength Determination	52
2.3.9 Degeneration of Surface Energy Following LTAPP Treatment.....	52
2.3.10 Batch Testing	52
2.4 Biofilm Formation.....	53
2.4.1 Sterilisation of Coupons	53
2.4.2 Bacterial Growth Conditions	53
2.4.3 Scanning Electron Microscopy	54
2.4.4 Microbial Adhesion to Hydrocarbons (MATH) Assay.....	54
2.4.5 Biofilm Formation.....	55
2.4.6 Crystal Violet Assay.....	56

2.5 Conditioning Films	57
2.5.1 Conditioning Film Preparation	57
2.5.2 Conditioning Film MATH Assay	57
2.6 Effect on Platelet Activity and Function	59
2.6.1 Ethical Approval and Participant Consent	59
2.6.2 Platelet Rich Plasma Extraction	59
2.6.3 Platelet and Bacterial Incubation	59
2.6.4 Aggregometry	60
2.6.5 Flow Cytometry	60
2.6.6 Cytometric Bead Array (CBA)	61
2.6.7 Western Blot Assay	64
2.7 Data Handling and Statistical Analysis	69
3.0 Surface Characterisation and Low Temperature Atmospheric Pressure Plasma Treatment	70
3.1 Introduction	70
3.2 Results	72
3.2.1 Scanning Electron Microscopy	72
3.2.2 Optical Surface Profiling	72
3.2.3 Tensile Strength Measurements	74
3.2.4 Energy Dispersive X-ray	75
3.2.5 Attenuated Total Reflection- Fourier Transform Infrared Spectroscopy	76

3.2.6 Raman Spectroscopy	78
3.2.7 Physicochemistry	79
3.2.8 Effect of LTAPP on Surface Physicochemistry	81
3.3 Discussion	86
3.3.1 Characterisation of Unmodified and Flattened p-PVC Surfaces	86
3.3.2 Effect of LTAPP on Surface Physicochemistry	91
3.4 Conclusion	91
4.0 Bacterial Attachment and Biofilms.....	92
4.1 Introduction.....	92
4.2 Results	94
4.2.1 Scanning Electron Microscopy	94
4.2.2 Microbial Adhesion to Hydrocarbons (MATH) Assays	96
4.2.3 Biofilms at 22 °C.....	99
4.2.4 Biofilms at 37 °C.....	101
4.3 Discussion	103
4.4 Conclusion	105
5.0 Conditioning Films	106
5.1 Introduction.....	106
5.2 Results	108
5.2.1 Scanning Electron Microscopy (SEM).....	108

5.2.2 Optical Surface Profiling	115
5.2.3 Energy Dispersive X-ray (EDX)	118
5.2.4 Attenuated Total Reflection-Fourier Transform Infrared Spectroscopy (ATR-FTIR)	120
5.2.5 Raman Spectroscopy	130
5.2.6 Physicochemistry	136
5.2.7 Microbial Adhesion to Hydrocarbons (MATH) Assay	142
5.3 Discussion	144
5.3.1 Scanning Electron Microscopy	144
5.3.2 Optical Surface Profiling	145
5.3.3 Energy Dispersive X-ray	146
5.3.4 Attenuated Total Reflection-Fourier Transform Infrared Spectroscopy.....	146
5.3.5 Raman Spectroscopy	147
5.3.6 Physicochemistry	147
5.3.7 Microbial Adhesion to Hydrocarbons (MATH) Assays	149
5.4 Conclusion	150
6.0 Bacterial and Biofilm Interactions with Platelets	151
6.1 Introduction	151
6.2 Results	155
6.2.1 Haemostatic Efficacy via Platelet Aggregation	155
6.2.2 Platelet Receptor Activation via Flow Cytometry	159

6.2.3 Western Blots	166
6.2.4 Immunological Activity via Cytometric Bead Array	175
6.3 Discussion	177
6.4 Conclusion	181
7.0 Discussion and Conclusion	182
8.0 References	186

List of Figures

Figure 3.1 SEM images of the un-inoculated p-PVC platelet bags a) rough (inside facing), b) smooth (inside facing) and c) flattened surfaces d) surface roughness (S_a value) of overall rough surface features, pits and ridges of the rough surface features, smooth and flat surfaces Most significant differences annotated with a *. (n = 3).	73
Figure 3.2 Energy Dispersive X-ray of the three surfaces demonstrating little change in their elemental makeup. (n = 3).	75
Figure 3.3 ATR-FTIR spectra (average of n=3) of transfusion bag surfaces; (a) unmodified smooth side, (b) unmodified rough side and (c) flattened surfaces. The carboxylate carbonyl antisymmetric stretching vibrations (at 1577 and 1544 cm^{-1}) are highlighted with arrows. (n = 3).	77
Figure 3.4 Raman spectroscopy of the three surfaces demonstrating no significant changes in any of the peaks. (n = 3).	78
Figure 3.5 Physicochemistry results of the rough, smooth and flattened surfaces a) Gibbs free energy (ΔG), b) surface energy (γ_s), c) Lifschitz van der Waals forces ($\gamma_s LW$), d) acid base components ($\gamma_s AB$), e) acid component ($\gamma_s +$) and f) base component ($\gamma_s -$). Note that a, b and c are on the same scale and d, e and f are on a different scale. (n = 5).	80
Figure 3.6 Surface energy results of untreated and plasma treated surfaces. Graphs represent a. Gibbs free energy (ΔG) b. total surface energy (γ_s) c. Lifschitz van der Waals forces ($\gamma_s LW$) d. acid base energies ($\gamma_s AB$) e. acid energy ($\gamma_s +$) and f. base energy ($\gamma_s -$). (n = 5).	83
Figure 3.7 Surface energy results of plasma treatment degeneration over time. Graphs represent a. Gibbs free energy (ΔG) b. total surface energy (γ_s) c. Lifschitz van der Waals forces ($\gamma_s LW$) d. acid base energies ($\gamma_s AB$) e. acid energy ($\gamma_s +$) and f. base energy ($\gamma_s -$). (n = 5).	84
Figure 3.8 Surface energy results of different batches. Graphs represent a. Gibbs free energy (ΔG) b. total surface energy (γ_s) c. Lifschitz van der Waals forces ($\gamma_s LW$) d. acid base energies ($\gamma_s AB$) e. acid energy ($\gamma_s +$) and f. base energy ($\gamma_s -$). B1.1, B1.2 and B1.3 represent the three bags from batch one and B2.1, B2.2 and B2.3 represent the three bags from the second batch. (n = 5).	85
Figure 3.9 Schematic representation of possible adsorbed structure of calcium stearate on the unmodified p-PVC surfaces. The straight lines represent the $\text{C}_{17}\text{H}_{35}$ chains, the open circles represent the carboxylate group (COO^-) and the closed (black) circles represent the calcium (Ca^{2+}) ions (adapted from) (Lu and Miller, 2002).	90
Figure 4.1 SEM images of the inoculated p-PVC platelet bags a/b) rough (inside facing), c/d) smooth (inside facing) and e/f) flattened surfaces. Black arrows indicate bacterial cells.	95

Figure 4.2 MATH assays of a) <i>Ser. marcescens</i> and b) <i>S. epidermidis</i> demonstrating affinity to the apolar n-alkanes decane and hexadecane and to the solvents chloroform (acidic) and ethyl acetate (basic). (n = 3).	98
Figure 4.3 Five and seven-day biofilm growth of a) <i>Ser. marcescens</i> and b) <i>S. epidermidis</i> on the unmodified (rough and smooth) and flattened p-PVC surfaces at 22 °C. The control surfaces followed the same procedure but were inoculated with sterile distilled water. Most significant differences annotated with a *. (n = 6)	100
Figure 4.4 Five and seven-day biofilm growth of a) <i>Ser. marcescens</i> and b) <i>S. epidermidis</i> on the unmodified (rough and smooth) and flattened p-PVC surfaces at 37 °C. The control surfaces followed the same procedure but were inoculated with sterile distilled water. Most significant differences annotated with a *. (n = 6)	102
Figure 5.1.1 SEM of a/b) rough, c/d) smooth and e/f) flat images after 1h (a, c, e) or 24 h (b, d, f) incubation with a <i>S. epidermidis</i> conditioning film. Blue arrows represent bacterial cells and black arrows represent biomasses.	109
Figure 5.1.2 SEM of a/b) rough, c/d) smooth and e/f) flat images after 1h (a, c, e) or 24 h (b, d, f) incubation with a <i>Ser. marcescens</i> conditioning film. Blue arrows represent bacterial cells.	110
Figure 5.1.3 SEM of a/b) rough, c/d) smooth and e/f) flat images after 1h (a, c, e) or 24 h (b, d, f) incubation with a human plasma conditioning film. Blue arrows represent bacterial cells.	111
Figure 5.1.4 SEM of a/b) rough, c/d) smooth and e/f) flat images after 1h (a, c, e) or 24 h (b, d, f) incubation with a human plasma with <i>S. epidermidis</i> conditioning film. Blue arrows represent bacterial cells.	113
Figure 5.1.5 SEM of a/b) rough, c/d) smooth and e/f) flat images after 1h (a, c, e) or 24 h (b, d, f) incubation with a human plasma with <i>Ser. marcescens</i> conditioning film. Blue arrows represent bacterial cells.	114
Figure 5.2 Average roughness of the conditionings on the a) rough, b) smooth and c) flat surfaces. Most significant differences annotated with a *. (n = 3)	117
Figure 5.3 Determination of elements present according to atomic weight as determined by EDX on the a) rough, b) smooth and c) flat surfaces. Surfaces had CFs applied for 1 h or 24 h with <i>S. epidermidis</i> (Se), <i>Ser. Marcescens</i> (Sm), human plasma or bacteria and human plasma. (n = 3)	119
Figure 5.4.1 ATR-FTIR of <i>S. epidermidis</i> conditioning films, a) 1h and b) 24 h, after subtraction of non-conditioned control surfaces. (n = 3)	121
Figure 5.4.2 ATR-FTIR of <i>Ser. marcescens</i> conditioning films, a) 1h and b) 24 h, after subtraction of non-conditioned control surfaces. (n = 3)	123

Figure 5.4.3 ATR-FTIR of human plasma conditioning films, a) 1h and b) 24 h, after subtraction of non-conditioned control surfaces. (n = 3)	125
<hr/>	
Figure 5.4.4 ATR-FTIR of <i>S. epidermidis</i> and human plasma conditioning films, a) 1h and b) 24 h, after subtraction of non-conditioned control surfaces. (n = 3)	127
<hr/>	
Figure 5.4.5 ATR-FTIR of <i>Ser. marcescens</i> and human plasma conditioning films, a) 1h and b) 24 h, after subtraction of non-conditioned control surfaces. Note that scale differs to other FTIR graphs due to absorbance intensity. (n = 3)	129
<hr/>	
Figure 5.5.1 Raman spectroscopy of surfaces after conditioning with <i>S. epidermidis</i> for a) 1 h or b) 24 h. (n = 3)	131
<hr/>	
Figure 5.5.2 Raman spectroscopy of surfaces after conditioning with <i>Ser. marcescens</i> for a) 1 h or b) 24 h. (n = 3)	132
<hr/>	
Figure 5.5.3 Raman spectroscopy of surfaces after conditioning with human blood plasma for a) 1 h or b) 24 h. (n = 3)	133
<hr/>	
Figure 5.5.4 Raman spectroscopy of surfaces after conditioning with human blood plasma and <i>S. epidermidis</i> for a) 1 h or b) 24 h. (n = 3)	134
<hr/>	
Figure 5.5.5 Raman spectroscopy of surfaces after conditioning with human blood plasma and <i>Ser. marcescens</i> for a) 1 h or b) 24 h. (n = 3)	135
<hr/>	
Figure 5.7 MATH assay of a) <i>S. epidermidis</i> and b) <i>Ser. marcescens</i> with and without the presence of a human plasma conditioning film. Most significant differences annotated with a *. (n = 3)	143
<hr/>	
Figure 6.1 1 Main platelet signalling pathways involved with VASP, PLC β and AKT proteins. Thrombin stimulates the PAR receptor which causes Gq α to mainly activate phospholipase β (PLC β) (and minor activation of Src family kinases (FFK) Lyn in the ADP pathway) which hydrolyses PIP ₂ membrane into IP ₃ triggering an increase in cytosolic Ca ²⁺ levels. ADP stimulates the P2Y ₁₂ receptor and activates Gi which inhibits adenylate cyclase (AC) causing a reduction in cyclic AMP (cAMP) formation leading to the dephosphorylation of VASP. Gi also interacts with SFK (Lyn) which causes Phosphatidylinositol 3-kinase (PI3K) to phosphorylates AKT and also causes PI3K to interact with Protein Kinase C (PKC) to dephosphorylate VASP (Sangkuhl <i>et al.</i> , 2011; Li <i>et al.</i> , 2015).	154
<hr/>	
Figure 6.1.1 Platelet aggregation as assessed by Light Transmission Aggregometry (LTA), in response to ADP (10 μ M), following incubation for a) 1 h or b) 2 h with planktonic bacteria. Data is presented as mean \pm SE after normalisation to the control (incubated in the absence of bacteria but stimulated with ADP). (n = 3)	156
<hr/>	
Figure 6.1.2 Platelet aggregation as assessed LTA, in response to Thrombin (10 U), following incubation for 2 h with planktonic bacteria. Data is presented as mean \pm SE after normalisation to the control (incubated in the absence of bacteria but stimulated with ADP). (n = 3)	157

Figure 6.1.3 Platelet aggregation as assessed by LTA, in response to ADP (10 μ M), following incubation for 2 h with a) 5-day biofilms and b) 7-day biofilms grown on the 3 different surfaces. Data is presented as mean \pm SE after normalisation to the control (incubated in the absence of bacteria but stimulated with ADP). Most significant differences annotated with a *. (n = 3)

158

Figure 6.2.1 CD62P expression as assessed by flow cytometry in response to using ADP (10 μ M), following incubation for a) 1 h or b) 2 h with planktonic bacteria. Data is presented as mean \pm SEM after normalisation to the control (incubated in the absence of bacteria but stimulated with ADP). (n = 3)

160

Figure 6.2.2 CD62P expression as assessed by flow cytometry, in response to Thrombin (10 U), following incubation for 2 h with planktonic bacteria. Data is presented as mean \pm SE after normalisation to the control (incubated in the absence of bacteria but stimulated with ADP). (n = 3)

161

Figure 6.2.3 CD62P expression as assessed by flow cytometry, in response to ADP (10 μ M), following incubation for 2 h with a) 5-day biofilms and b) 7-day biofilms grown on the 3 different surfaces. Data is presented as mean \pm SE after normalisation to the control (incubated in the absence of bacteria but stimulated with ADP). (n = 3)

162

Figure 6.2.4 PAC1 expression as assessed by flow cytometry in response to using ADP (10 μ M), following incubation for a) 1 h or b) 2 h with planktonic bacteria. Data is presented as mean \pm SEM after normalisation to the control (incubated in the absence of bacteria but stimulated with ADP). (n = 3)

163

Figure 6.2.5 PAC1 expression as assessed by flow cytometry, in response to Thrombin (10 U), following incubation for 2 h with planktonic bacteria. Data is presented as mean \pm SE after normalisation to the control (incubated in the absence of bacteria but stimulated with ADP). (n = 3)

164

Figure 6.2.6 PAC1 expression as assessed by flow cytometry, in response to ADP (10 μ M), following incubation for 2 h with a) 5-day biofilms and b) 7-day biofilms grown on the 3 different surfaces. Data is presented as mean \pm SE after normalisation to the control (incubated in the absence of bacteria but stimulated with ADP). (n = 3)

165

Figure 6.2.3.1 Western blot fold difference in phosphorylated VASP quantification for a) *S. epidermidis* and b) *Ser. marcescens* with a protein band representation below each graph with bands in-line with their counterpart in the graphs. Most significant differences annotated with a *. (n = 2)

168

Figure 6.2.3.2 Western blot fold difference in phosphorylated VASP quantification for 5 day biofilms with a) no ADP stimulation and b) with ADP stimulation with a protein band representation below each graph with bands in-line with their counterpart in the graphs. Most significant differences annotated with a *. (n = 2)

169

Figure 6.2.3.3 Western blot fold difference in phosphorylated VASP quantification for 7 day biofilms with a) no ADP stimulation and b) with ADP stimulation with a protein band representation below each graph with bands in-line with their counterpart in the graphs. Most significant differences annotated with a *. (n = 2)	170
<hr/>	
Figure 6.2.4.1 Western blot fold difference in phospho-PLC β 3 quantification for a) <i>S. epidermidis</i> and b) <i>Ser. marcescens</i> with a protein band representation below each graph with bands in-line with their counterpart in the graphs. Most significant differences annotated with a *. (n = 2)	172
<hr/>	
Figure 6.2.4.2 Western blot fold difference in phospho-PLC β 3 quantification for 5 day biofilms with a) no ADP stimulation and b) with ADP stimulation with a protein band representation below each graph with bands in-line with their counterpart in the graphs. (n = 2)	173
<hr/>	
Figure 6.2.4.3 Western blot fold difference in phospho-PLC β 3 quantification for 7 day biofilms with a) no ADP stimulation and b) with ADP stimulation with a protein band representation below each graph with bands in-line with their counterpart in the graphs. (n = 2)	174
<hr/>	
Figure 6.4.1 RANTES release by platelets after incubation with planktonic bacteria, 5 day biofilms or 7 day biofilms for 4 h a) without stimulation and b) with ADP stimulation. Most significant differences annotated with a *. (n = 2)	176

List of Tables

Table 1.1 Physicochemical parameters and their meaning.	30
<hr/>	
Table 3.1 Tensile strength and elongation measurements for the unmodified and flattened surfaces with standard errors. (n = 3)	74
<hr/>	
Table 5.7.1 Physicochemistry of the rough surface after applying 1 h or 24 h conditioning films of the bacteria alone, human plasma alone or a combination of bacteria and human plasma. Se denotes the bacteria <i>Staphylococcus epidermidis</i> and Sm denotes <i>Serratia marcescens</i> . (n = 5)	137
<hr/>	
Table 5.7.2 Physicochemistry of the smooth surface after applying 1 h or 24 h conditioning films of the bacteria alone, human plasma alone or a combination of bacteria and human plasma. Se denotes the bacteria <i>Staphylococcus epidermidis</i> and Sm denotes <i>Serratia marcescens</i> . (n = 5)	139
<hr/>	
Table 5.7.3 Physicochemistry of the flat surface after applying 1 h or 24 h conditioning films of the bacteria alone, human plasma alone or a combination of bacteria and human plasma. Se denotes the bacteria <i>Staphylococcus epidermidis</i> and Sm denotes <i>Serratia marcescens</i> . (n = 5)	141

Abstract

Bacterial contamination of blood products is a major risk in transfusion medicine, with bacterial attachment and biofilm formation a potential source for false negative results of bacterial platelet contamination. Understanding platelet bag (PB) surface properties could improve understanding of how bacteria adhere to these surfaces. PB surfaces were analysed using scanning electron microscopy, optical surface profiling, Fourier transform infrared spectroscopy, RAMAN spectroscopy, goniometry, energy dispersive X-ray and a tensiometer. Initial findings demonstrated that the PBs had two distinct surfaces, a rough diamond patterned surface and a smoother surface. Two surface altering methods were used; PBs surfaces were flattened to remove surface features, which can increase bacterial attachment, and treated with low temperature atmospheric pressure plasma, with flattening demonstrating surface feature changes and plasma treatment being unsuitable. *Staphylococcus epidermidis* and *Serratia marcescens* biofilms grown on the surfaces demonstrated reduced biomass formation on the flattened surface after 5 days.

Conditioning films on the surfaces of the bacteria, human plasma and human plasma combined with one of the bacteria demonstrated that the human plasma alone altered the surface properties the most, especially the roughness, surface chemistry and surface physicochemistry. When human plasma was combined with bacteria, changes were also determined but differed to when human plasma was tested alone.

Finally, testing the effects of bacteria on platelets demonstrated that planktonic bacteria had little effect on platelet activation and viability, whilst biofilms halved platelet aggregation but did not affect activation. Western blots demonstrated that protein expression could be affected, particularly by biofilms. Further, release of RANTES by the platelets was doubled when incubated with bacterial biofilms.

The results demonstrated the significance surface properties had on bacterial attachment and biofilm formation as well as how conditioning films altered the surface properties and how biofilms were able to affect platelets.

Publications Arising from this work

Part of the following work has previously been published in the following peer-reviewed articles or abstracts, as such, some of the following may bear resemblances to the published work:

- Wilson-Nieuwenhuis, J.S.T., Dempsey-Hibbert, N., Liauw, C.M. and Whitehead, K.A. (2017) 'Surface modification of platelet concentrate bags to reduce biofilm formation and transfusion sepsis.' *Colloids and Surfaces B: Biointerfaces*. 160: 126-135.
- Wilson-Nieuwenhuis, J.S.T., Whitehead, K.A. and Dempsey-Hibbert, N.C. (2018) 'Bacterial Contamination of Platelet Transfusion Units Affects Platelets Haemostatic Function and Immunological Activity.' *EMJ Haematol*. 6(1): XX-XX.

Acknowledgements

I would like to thank my Director of Studies Dr Nina Dempsey-Hibbert for the opportunity to do this project and for her guidance and advice for an area that was new to me, enabling me to learn a new area of research in haematology. I would also like to thank my supervisor Dr Kathryn Whitehead for her massive amount of support and guidance throughout this project, enabling me to further my knowledge of surface microbiology research, and my supervisor Dr Chris Liauw who was vital in helping me analysis parts of my data. Without my whole team of supervisors and their expertise I would never have been able to complete this project.

I would also like to thank all the various technical staff who have helped me throughout this project from different teams including microbiology, cellular research and the analytical science teams, with special thanks to Dr Paul Benson who repeatedly provided support throughout the project.

I would like to thank everyone else in the microbiology research lab over the past 3 years for helping me occasionally relax from the project with conversation, joking, food and drinks.

Finally, I would like to thank the Sir Halley Stewart Trust for part funding this project in conjunction with Manchester Metropolitan University.

1.0 Introduction

Bacterial contamination of blood products poses one of the biggest risks of transfusion medicine (Blajchman *et al.*, 2005). This contamination is most commonly associated with transfusion of platelet concentrates (PC) due to their storage conditions within the blood bank, providing ideal conditions for bacterial growth and proliferation. It is reported that approximately 1 in 2000-5000 PCs are contaminated (Greco *et al.*, 2007; Greco-Stewart *et al.*, 2012; Martini *et al.*, 2012). However, use of bacterial detection systems within the national blood banks such as the Bact/Alert microbial detection system minimise the likelihood of transfusing a contaminated unit. Whilst the reported incidence of culture confirmed sepsis in platelet contamination is around 1 in 100,000, a higher incidence rate of 1 in 25,000 has been estimated, with higher rates likely due to under reporting of transfusion-related sepsis (Blajchman *et al.*, 2005; Greco *et al.*, 2007). However, a more recent study has demonstrated that a retrospective review during a study indicated that 1 in 10,720 patients demonstrated clinical symptoms of a transfusion reaction due to high bacterial loads in the transfused unit (Hong *et al.*, 2016). Although systems like the Bact/Alert system significantly reduces the risk of transfusion infections, they still may produce false negative results due to low initial bacterial concentration or due to the formation of bacterial biofilms within the PC during storage. One study demonstrated that 2.6 % of the negative results, when subsequently cultured onto agar, demonstrated bacterial growth (Kocoglu *et al.*, 2005).

Most studies into PC contaminations fall into two categories: (1) data from artificial contamination of PCs, or (2) data from the study of transfusion-related infection cases or infected PCs detected before transfusion. Most data obtained from artificial

contamination is aimed at determining the levels of bacteria required to cause sepsis, how bacteria grow within PC units or influence PCs and the best method to determine contamination. Data obtained from studies involving real-world patient data typically examines different surveillance systems and rates of unit and patient contamination, the amounts of which vary within the literature. Reviews by Hillyer *et al.* (2003) and Blajchman *et al.* (2005), summarising evidence from nine independent studies, concluded that approximately 1 in 3000 units were contaminated and approximately 1 in 25,000 transfusions lead to some form of sepsis. However, the studies reviewed were performed prior to the widespread implementation of additional detection methods such as the BacT/Alert detection system (Corash, 2011). Corash (2011) summarised that four studies using both aerobic and anaerobic cultures had a contamination rate ranging from 1 in 994 to 1 in 1567, two to three times that stated by Blajchman *et al.* (2005). This is notable, as in an American Red Cross (ARC) study, where only positive aerobic cultures were confirmed, it was estimated that 1 in 6041 PC units was contaminated. This meant that studies that used both aerobic and anaerobic bottles detected 4 – 6 times as many contaminated units as the ARC study which only used aerobic bottles. It must be noted though, that all these studies were performed upon initial release units when the bacterial load would be low, rather than on units that had been stored for a period of time. This meant that any bacterial contamination may not yet have proliferated to levels detectable upon initial release as a study by Murphy *et al.* (2008) showed that 1 in 460 expired PCs had contamination, demonstrating significantly greater microbial loads after the extended storage time.

The significance of the number of contaminated units is highlighted when considering that 306,970 PCs were issued in the UK in 2016 alone. In this same year, there were 108 cases

of suspected bacterial transfusion-transmitted infections (TTI) attributed to both PCs and whole blood units. Furthermore, of all the confirmed cases of bacterial TTI throughout the recorded Serious Hazards Of Transfusions (SHOT) history, 37 of the 44 cases were from PC units, with these only accounting for the reported and fully confirmed cases. Thus these results did not include cases which may have not been fully reported or were never confirmed (SHOT, 2017). As these results only account for fully confirmed cases, the actual number of bacteria TTI has the possibility to be much greater and also demonstrates that the incidence of transfusing a contaminated platelet unit is far greater than transfusing a contaminated whole blood unit.

1.1 Platelets

1.1.1 Significance of Platelets

Platelet transfusions are prescribed therapeutically to control active bleeding or prophylactically to reduce the risk of bleeding (Blajchman *et al.*, 2008). Therapeutic platelet transfusions are typically only given to patients with significant clinical bleeding, especially in the presence of thrombocytopenia or functional defects of platelets (Blajchman *et al.*, 2008; Liunbruno *et al.*, 2009). Such patients may be undergoing peripheral blood stem cell transplants, surgery, massive red cell transfusions, or have congenital or acquired platelet function defects (Liunbruno *et al.*, 2009). Further, research into novel therapeutic applications of platelets have led to a platelet gel mimicking the clotting cascade that can be used to control unsuturable bleeding sites or leakage of blood during surgery (Mohanty, 2009).

However, approximately 85% of platelet transfusions are prophylactic transfusions given to reduce a patients' risk of bleeding (Brecher *et al.*, 2005; Blajchman *et al.*, 2008). One of the biggest uses for prophylactic transfusions is to reduce the risk of bleeding during

complex surgical procedures, especially cardiovascular surgeries (Mohanty, 2009). However, they are also extensively used for patients undergoing chemotherapy or bone marrow transplants, typically due to patients becoming thrombocytopenic during these procedures, increasing their risk of bleeding. These patients typically receive multiple transfusions of PC during the period of their other treatment.

1.1.2 Transfusion Risks

There are a variety of risks associated with receiving a platelet transfusion. Whilst blood group antigens are expressed more weakly on platelets than on red blood cells, it has been observed that repeat transfusions with an ABO-mismatched PC can lead to haemolytic transfusion reactions which can be fatal (Sadani *et al.*, 2006). Furthermore, ABO-mismatched PCs may cause refractoriness to the transfusion where the platelet count is not raised post transfusion, but this can also be caused by a PC that has not been properly or fully leukodepleted (Heal *et al.*, 1993). It has also been shown that patients receiving ABO-matched PCs require half the transfusions as those who had ABO-mismatched PCs (Heal *et al.*, 1993). As such, it is commonly agreed that all PCs are leukodepleted and only ABO-matched PCs used when possible (Blumberg *et al.*, 2010).

One of the biggest risks to a patient's health is from the transfusion of a contaminated unit which can lead to a septic infection. The significance of this risk is greater when it is considered that platelet transfusions are often given to oncology, haematology, paediatric and bone marrow transplant patients, all of which have weakened immune systems and are more at risk of infection (Brecher *et al.*, 2005). Not only can a septic infection be fatal to a patient, but even in a case where no infection occurs, it is hypothesised that the transfused PC may not function properly due to being stored whilst contaminated with bacteria or bacterial biofilms. This may be due to bacteria and their biofilms producing

secondary metabolites and/or toxins, which may interfere with platelet function; this exposes a patient to a risk of transfusion with no therapeutic outcome (Kini *et al.*, 2011). This risk of transfusing a PC with no functional platelets is also present from PCs stored for longer periods of time, as storage can cause several complex changes within a PC leading to non-functional platelets and/or partial activation of platelets and/or inflammatory factors, all of which can have undesired side-effects on the patient (Spiess, 2010).

1.1.3 Origins of Bacterial Contamination in Platelet Units

The significant number of transfusion-related sepsis cases and the associated costs of treating such cases has led to various strategies being developed to reduce the number of contaminated units whilst improving detection methods. A study of sepsis infections after general surgery found that the costs were 2.28 times greater than patients without, with an additional average cost of \$ 63,824 per patient to treat the sepsis (Vaughan-Sarrazin *et al.*, 2011). Despite an attempt to control bacterial contamination of PC units by using aseptic technique and sterile working as standard practice, there are still three main sources that result in such contamination: 1) the venepuncture site during phlebotomy, 2) transient donor bacteraemia and 3) contamination during processing within the blood bank (Blajchman *et al.*, 2005; Schrezenmeier *et al.*, 2007).

1.1.3.1 Contamination from the Venepuncture Site during Phlebotomy

As the major source of contamination appears to be from the donor's skin flora at the venepuncture site, there has been a large amount of research and investment into procedures aimed at reducing the numbers of viable bacteria at the venepuncture site and training donor centre staff in the importance of such techniques. Studies have shown that although iodine is the most effective substance for sterilisation, it is considered donor-unfriendly due to the potential for irritation and donor allergy, and thus isopropyl alcohol

(IPA) is the most commonly used agent and next best-choice (De Korte *et al.*, 2006). However, even careful disinfection of the venepuncture site may not result in complete disinfection since bacterial cells such as *Staphylococcus aureus* and *Propionibacterium acnes* are located within the sebaceous glands (Kunishima *et al.*, 2001).

Introduction of a diversion pouch, which collects the first 10 mL - 50 mL of blood containing the skin tag from the puncture wound during the blood collection procedure has been reported to have resulted in a reduction in the number of contaminated units, with a 40% -90% reduction rate quoted in individual studies (Liumbruno *et al.*, 2009). When tested *in vitro*, Wagner *et al.* (2000) demonstrated that diversion of the first 21 mL - 42 mL of saline or whole blood caused approximately a one log drop in colony load of *Staphylococcus aureus* when deliberately inoculated onto the collection surface. Further, whilst the effects of a diversion pouch are only effective against organisms originating from the skin, it has reportedly caused an 85 % reduction of skin flora contaminated units (De Korte *et al.*, 2006; Lee *et al.*, 2012).

1.1.3.2 Transient donor bacteraemia

Whilst transient donor bacteraemia contamination, that is contamination of a PC by organisms in a donor's bloodstream, is uncommon and would usually be accompanied by clinical symptoms identified by donor centre staff at the time of donor selection, it can still occur. Further, it is presumed that Gram-negative organism contamination typically originates from this source and these organisms can lead to more serious incidences if transfused (Brecher *et al.*, 2005). This indicates that whilst the incidence rate for this source of contamination is significantly lower than from the venepuncture site, it may be missed during donor screening due to asymptomatic patients; further, if transfused this can cause more serious adverse reactions.

1.1.3.3 Contamination during processing within the blood bank

Cases of contamination during processing are extremely rare but are suggested to be higher in pooled-donor units than single-donor units, as evidenced by higher rates of septic transfusion reactions reported following transfusion with pooled random-donor PCs (Ness *et al.*, 2001). The cases of contamination during processing, or storage, are typically thought to be due to breaking a sterile closed collection system such as pooling platelet units or inefficient cleaning processes in processing and storage areas (Liumbruno *et al.*, 2009). A case was reported whereby contamination by *Serratia marcescens* was due to clean but not sterile outer plastic packaging of the platelet bags which proliferated in the presence of moisture and nutrients (the plasticizer) in storage, resulting in the bacteria finally gaining entry into the bag (Szewzyk *et al.*, 1993).

1.1.4 Measures for Detecting Bacterial Contamination

After blood collection, the units are screened to ensure that preventative measures have eliminated contamination. The most widely spread screening system is the BacT/Alert automated microbial detection system. The BacT/Alert system operates by detecting CO₂ production caused by microbial proliferation. BacT/Alert sample bottles contain media and a CO₂ sensor bonded to the bottom of the bottle which changes the colour of the media when CO₂ is produced. This colour difference is detected by a change in red light reflected by the sensor (Thorpe *et al.*, 1990). Different sample bottles enable the detection of anaerobic and aerobic species. However, this makes the system reliant upon bacterial proliferation, as well as upon bacteria being present within the aliquot of test sample removed from the PC (Bjarnsholt, 2013). Both are affected if bacteria present within the unit forms a biofilm, since biofilms alter bacterial growth in relation to environment factors with the bacteria forming an almost 'multicellular' lifestyle within a community of bacteria

leading to changes in gene expression, surface molecule expression, nutrient usage, virulence factors and enables bacteria to survive in unfavourable conditions (Kostakioti *et al.*, 2013). This can subsequently alter CO₂ production, and reduce the numbers of planktonic bacteria within the PC. Thus, if bacteria are retained on the surface of the platelet bag in the form of a biofilm they may not be collected into the aliquot. This can lead to false negative results by the system. The final limitation on this system is that bacterial species may remain viable within the PC, but may not proliferate under platelet storage conditions or the bacteria proliferate so slowly that not enough CO₂ is formed to be detectable (Benjamin and Wagner, 2007). Whilst contamination can also be detected by using quantitative real-time PCR or flow cytometry, both systems require significantly higher cell numbers to operate and cannot continually check a PC for contamination like the BacT/Alert system, with PCR having a detection limit of 5 – 50 CFU / mL and Flow cytometry as greater than 10³ CFU / mL (Brecher *et al.*, 2000; GuoHui *et al.*, 2013; Störmer and Vollmer, 2014).

Current guidelines dictate that a unit is screened 24 hours after obtaining the PC, and is continuously screened until unit expiry (Corash, 2011). A unit typically has a shelf life of 5 or 7 days after screening when stored at 22 ± 2 °C with constant gentle agitation. For closed processing systems, where the sterility of a product is not compromised, most units are only stored for 5 days, with 7 days' storage allowed if bacterial contamination assays or pathogen inactivation procedures are performed prior to transfusion. However, any unit that involves an open system process, which involves exposing the unit to the environment to wash or pool units for example, should be used as soon as possible and within 6 hours of storage (UK Blood Transfusion and Tissue Transplantation Services, 2013). In the UK, all platelet units are screened using the BacT/Alert system exclusively for monitoring, as this

allows the PC unit to be constantly monitored for contamination, even after the unit has been released to the hospital for transfusion. This enhances the detection of slow growing bacteria or low initial bacterial levels, and if the aliquot becomes positive for contamination, the unit can be recalled. If the unit has already been transfused when contamination is detected, the species can be fully identified and the patient treated accordingly.

1.2 Surface Characterisation

1.2.1 Surface Roughness

It has been well established that the surface topography has an influence on bacterial adhesion, and of the topographical features, the surface roughness is thought to have a major influence (Whitehead *et al.*, 2005). A surface is made up of various peaks and valleys which vary in height, width and spacing, all of which forms the surface texture and influences the surface roughness. Whilst a surface may appear to be completely flat or smooth to the naked eye, when examined under something like an optical surface profiler, it is typically found that a surface is not a smooth or flat in terms of microbial dimensions. A variety of surface parameters can be assessed when an instrument like an optical surface profiler is used which can take measurements from line profiles across a surface or the surface as a whole (in the imaged area). However, the average roughness is typically used to give an idea as to the deviations in surface texture and guidelines on surfaces for use in hygienic conditions, medical and food settings, are set to ensure that surfaces are suitable for use in such environments (Heubner, 2009). This is because the surface substrata features can influence bacterial functions when in contact with bacterial cells including adhesion and biofilm growth (Whitehead *et al.*, 2005; Wu *et al.*, 2018). In this study, the mean average surface roughness (S_a value) which gives the average height deviation across an area of the surface was used. However, the S_a values do not reflect the shape of the surface features, which can also affect microbial retention. Surface topographical features were typically spilt into three types based on their size (Verran *et al.*, 2010):

1. Macrotopographical features, $S_a \geq 1 \mu\text{m}$.
2. Microtopographical features, $S_a \geq 500 \text{ nm} - 1 \mu\text{m}$.
3. Nanotopographical features, $S_a < 500 \text{ nm}$.

1.2.1.1 Scanning Electron Microscopy (SEM)

The use of SEM allows for the visualisation of a wide variety of surface morphologies, including the surface topographies as well as bacteria or organic matter that has been adsorbed onto a surface. The microscope sends a beam of electrons at a surface through a series of objectives and condenser lenses, which causes secondary electrons and backscattering primary electrons to be generated and emitted from the scanned surface, carried out under vacuum to ensure no particles deflect the electrons. It is the detection and analysis of these emitted electrons which allow for the production of an image. This allows for images of high detail to be produced at significant magnifications (15,000 x magnification) not available via less advanced microscopy methods (McMullan, 2006).

1.2.1.2 Optical Surface Profiling (White Light)

Optical surface profiling is the use of optics to reconstruct the topographic profile of a surface, such as by using white light interferometry. Surface profile measurements by white light interferometry typically employ a technique using a mirror to cause interference between the light reflected from the surface of a sample and a reference light signal (Baryshev *et al.*, 2013). These changes are recorded using a camera and software can reconstruct an image based on the reflected light. The reconstructed image can then be used to determine the overall average roughness, maximum peak height or valley depths as well as produce line profiles and topographic images that detail the shape of the features across the surface.

1.2.2 Raman Spectroscopy

Raman spectroscopy can be used to observe vibrational, rotational and other low-frequency modes to give a chemical fingerprint which can be used to identify molecules. It is a scattering technique that is based on the Raman Effect, measuring inelastic scattering,

where the frequencies between a small fraction of scattered radiation differs from that of monochromatic radiation (Laserna, 2006; Bumbrah and Sharma, 2016). It is the interaction of the monochromatic laser interacting with the molecules of a sample that allow it to be used to determine changes in the molecular structure of surfaces (Bumbrah and Sharma, 2016).

1.2.4 Attenuated Total Reflection Fourier Transform Infrared Spectroscopy (ATR-FTIR)

FTIR spectroscopy relies upon absorbance of light which corresponds with specific molecular vibrations to develop a spectrum of a sample, providing both organic and inorganic molecular-scale information (Kazarian and Chan, 2006; Parikh and Chorover, 2006). The use of an ATR attachment allows samples to be placed in direct contact with a crystal and requires little to no preparation of a sample to use, as the penetration depth of IR light using ATR is not dependant on sample thickness (Kazarian and Chan, 2006).

1.2.5 Surface Physicochemistry

Surface physiochemistry is a wide ranging term used to refer to a variety of chemical bonding forces (**Table 1.1**), including surface energy (wettability), van der Waals forces and Lewis acid-base interactions (surface electric charge) when describing microbial surface interactions. These forces can play a significant role in initial microbial attachment as they can influence adhesion before cells even come into direct contact with a surface (Busscher and van der Mei, 2012). These forces are a mix of long range forces, such as van der Waals forces, and shorter forces, such as Lewis acid-base forces, which together can control the distance between the cells and the surface interface (Korenevsky and Beveridge, 2007). As such, the relationship between surface physicochemistry and cell adhesion has been the focus of many *in vitro* studies (Noro *et al.*, 2013).

Table 1.1 Physicochemical parameters and their meaning.

ΔG_{iwi}	-	Gibbs free energy (Hydrophobicity)
γ_s	-	Total free surface energy
γ_s^{LW}	-	Lifschitz van der Waals forces energy (Electrostatic attraction)
γ_s^{AB}	-	Acid-Base energy (Polar charge)
γ_s^+	-	Acid energy (Electron accepting)
γ_s^-	-	Basic energy (Electron donating)

1.2.6 Energy Dispersive X-ray (EDX)

Energy Dispersive X-ray (EDX) is a technique that is used for the analysis of elemental or chemical characterisation of a sample, relying on the interaction between an X-ray radiation source and a sample. Under vacuum, a high energy beam of X-rays is used to excite characteristic X-ray emissions from a sample, which is used to determine the elemental components in a sample due to the unique atomic structure of each element (Goldstein *et al.*, 2003). This allows a user to determine the specific elements present in a sample as well as estimate their abundance.

1.3 Low Temperature Atmospheric Pressure Plasma (LTAPP)

Initially bacteria are weakly attached to a surface via Lifshitz Van der Waals forces, after which a stronger adhesion is formed by bacterial cell adhesion structures (Busscher and van der Mei, 2012). Lifshitz Van der Waals forces are properties of both the bacteria and the surfaces, and understanding them can lead to understanding how the bacteria interact with a surface. By causing changes in these forces, as well as other surface properties, it may be hypothesized that it is possible to alter how bacteria interact with a surface and potentially reduce bacterial attachment. As such, whilst it may be possible to develop more sensitive detection systems, modifying the platelet bag surfaces in a way so that bacterial cells are either unable or take longer to attach to the platelet bag surface could play a role in reducing false negatives in already established systems.

Changes in these forces can be done via both physical changes to the surface (such as flattening) or via chemical treatment of the surface (such as with energy induced plasma). One physical approach to reducing initial surface attachment of the bacteria, potentially leading to a reduction in biofilm formation, is by modifying the surface topography (Whitehead *et al.*, 2005). However, whilst several studies have been carried out to determine the effects of surface topography on bacterial retention, findings have been conflicting, especially when different topographies may be present on a surface. These topographies, macro ($> 10 \mu\text{m}$), micro ($< 10 \mu\text{m} - 0.5 \mu\text{m}$) and nano ($< 0.5 \mu\text{m}$), can all have different effects on the initial conditioning film and bacterial attachment to a surface.

LTAPP based treatments have gained popularity for altering bio-interfaces; that is surfaces that encounter biological environments (Siow *et al.*, 2006). The development of LTAPP has increased in interest due to its ability to operate without requiring a vacuum, which limited traditional plasma implementation (Tendero *et al.*, 2006). Plasmas have a wide range of

applications: surface coatings, waste destruction, gas treatments and chemical synthesis, with more potential applications possible (Tendero *et al.*, 2006). LTAPP can be generated using a variety of gasses to achieve different effects, and by using different gasses, the surface energy of the treated surface can potentially be altered to be more suitable for the surface's application (Tendero *et al.*, 2006; Bárdos and Baránková, 2010; Yaghoubi and Taghavinia, 2011; Bozaci *et al.*, 2013).

1.4 Conditioning Films

Any clean sterile surface that becomes exposed to an environment containing organic material will begin to form a conditioning film (CF) (Loeb and Neihof, 2009). It has been demonstrated that whilst surface properties massively influence bacterial adhesion, bacterial cells often do not attach to the surface directly but instead attach to an interface of the surface which has been exposed to its surrounding environment and 'conditioned' (Donlan, 2002). This conditioning film on a surface is typically made up of a huge variety of molecules adsorbed onto the substrate and thus can influence the properties of a surface and hence the effect the surface/CF has on bacterial attachment and adhesion (Donlan, 2002). Further, bacterial cells can also form a conditioning film when exposed to various proteins and other molecules that are capable of binding to receptors present on the cell surface, further influencing initial bacterial adhesion (Lorite *et al.*, 2011). These conditioning films when present on substrate surfaces and/or cell surfaces have the capability to both reduce and increase bacterial adhesion, depending on the composition of the CF, the properties of the surface and the properties of the bacterial cell and how their individual properties influence their biochemical interactions (Donlan, 2002; Lorite *et al.*, 2011).

1.5 Bacteria

1.5.1 *Serratia marcescens*

Ser. marcescens is a motile, rod-shaped, Gram-negative environmental organism which has only been considered an opportunistic pathogen over the last 30 years (Kim *et al.*, 2015). *Serratia spp.* are known to secrete numerous substances, including extracellular DNase, gelatinase, lipase, proteases, prodigiosin (a red pigment), chitinases and a chitin binding protein, however, in *Ser. marcescens* they do not appear to act as virulence factors (Aucken and Pitt, 1998; Hover *et al.*, 2016). However, *Ser. marcescens* does produce pore forming toxins, hemolysin ShIA via activation by ShIB, which can lead to cell toxicity and cell lysis (Hertle, 2005).

Due to its abundance in the environment it has been implicated in some hospital acquired infections in immunocompromised patients due to its opportunistic nature (Silva, 2010). The infections caused by *Ser. marcescens* include urinary tract, respiratory, biliary tract, peritonitis, wound and intravenous catheter related infections (Kim *et al.*, 2015). One study stated that *Serratia spp.* accounted for 6.5 % of all Gram negative intensive care unit (ICU) infections and 3.5 % of all non-ICU Gram negative infections, whilst a report by the European Centre for Disease Prevent and Control stated it as the tenth most common cause of bloodstream infection with a 2 % incidence rate (ECDC, 2013; Sader *et al.*, 2014). It is likely its abundance in the environment that has caused it to be identified as a platelet concentrate contaminant. Due to most patients typically receiving platelet transfusions being immunocompromised patients, as well as *Ser. marcescens* becoming more resistant to many antibiotics used to treat infections, accidental transfusion due to undetected contamination is a serious concern (Kim *et al.*, 2015).

1.5.2 *Staphylococcus epidermidis*

Whilst *Staphylococcus aureus* is typically the most common pathological *Staphylococcus* species, in the case of platelet contamination it is *Staphylococcus epidermidis* that is most prevalent (Taha *et al.*, 2018). It demonstrates similar traits to *S. aureus*, being Gram-positive, non-motile and non-spore forming, however, it does not produce coagulase and it is this trait that is often determined from the contaminants, with the species simply stated as a 'coagulase-negative staphylococci' (CNS). However, if identified in more detail, most CNS species tend to be *S. epidermidis* (Kleinschmidt *et al.*, 2015). It is highly implicated in platelet contamination as it is abundant as a commensal skin flora, more so than *S. aureus*, but has lower virulence and is an opportunistic pathogen (Widerström *et al.*, 2012; Becker *et al.*, 2014). Whilst *S. epidermidis* infections rarely become life-threatening, once they are established they can be harder to treat than *S. aureus* infections and most *S. epidermidis* infections are acquired in hospitals (Otto, 2009; Widerström *et al.*, 2012).

Infections caused by *S. epidermidis* are highly implicated in infections from indwelling medical devices, such as catheters, as well as potentially playing a role in shunt, prosthetic joint, vascular and surgical site infections (McCann *et al.*, 2008; Rogers *et al.*, 2009). Further, *S. epidermidis* accounted for at least 22 % of bloodstream infections in intensive care patients in the US (National Nosocomial Infections Surveillance System, 2004). These infections are also becoming harder to treat as many strains of *S. epidermidis* are becoming multidrug resistant, with significance placed on the increase in methicillin resistant *S. epidermidis* strains (Otto, 2009; Decousser *et al.*, 2015).

1.5.3 Bacterial Biofilms

Bacteria typically exist in one of two forms: planktonic, which are single cells freely existing within a suspension, or sessile, which are bacteria attached to a surface and which may form part of a biofilm. A biofilm is a highly complex community formed by bacteria encased within an extracellular polymeric substance (EPS) in which the bacteria increase their virulence, increase their gene exchange and a decrease in growth which may result in a reduction in CO₂ production and hence detection (Donlan, 2002; Busscher and van der Mei, 2012; Desrousseaux *et al.*, 2013). The EPS can provide many benefits to the bacteria in a biofilm including adhesion, protection and structure, and is usually comprised of mostly water and polysaccharides with some DNA, proteins, lipids and lectins (Bjarnsholt, 2013; Limoli *et al.*, 2015).

The process of biofilm development is complex and multifactorial, with the attachment of bacteria influenced by the surface properties, such as wettability, structure and roughness (Lorite *et al.*, 2011). In most models of biofilm formation, there are certain steps that are characteristic of the development of a biofilm, starting with bacterial cells initially weakly adhering to a substrate via non-specific interactions and are relatively easy to remove (Donlan, 2002). However, they quickly become irreversibly attached using specific surface interactions including pili (or fimbriae), flagella or adhesive proteins, with the physical structure being significant as one study demonstrated the bacteria's inability to land on surfaces and / or attach to surfaces (O'Toole and Kolter, 1998; Lorite *et al.*, 2011). Upon becoming bound to a substrate other bacterial cells start adhering to already bound cells and proliferation occurs until maturation of the biofilm, whilst encased within an EPS matrix (Donlan, 2002; Lorite *et al.*, 2011).. Finally, upon a biofilm growing large enough a

detachment of cells occurs, and the detached cells can colonise new substrates (Petrova and Sauer, 2016).

Biofilms grant a large number of benefits to the bacterial community, with significant increase in the resistance of bacteria to numerous antimicrobials as well as to host defences potentially being the biggest benefit (Ito *et al.*, 2009; Lorite *et al.*, 2011; Dias *et al.*, 2018). Biofilms can reduce antimicrobial diffusion, bacterial cells tend to have an altered metabolism due to changes in oxygen and nutrient availability and bacterial cells can exchange resistance genes whilst contained in the biofilm (Anderson and O'Toole, 2008; Dias *et al.*, 2018). The combination of altered gene expression and changes in metabolism can make the detection of bacteria more difficult for some analytical systems especially those that are reliant upon bacterial proliferation. Therefore, if the bacteria have adhered to the surface of the platelet bag and formed biofilms, then the bacteria may not be planktonic within the unit and with a reduced metabolism and reduced CO₂ production, their detection becomes more difficult, potentially leading to false negatives (Benjamin and Wagner, 2007). Further, a study by Ali *et al.* (2014) demonstrated that biofilm-positive *S. epidermidis* strains typically grew slower in platelet concentrates and were therefore more likely to be missed with automatic systems.

1.6 Microbiology Assays

1.6.1 Microbial Adhesion to Hydrocarbons (MATH)

Like surfaces, microbial adhesion is influenced by forces involving electrostatic interactions, van der Waals forces and Lewis acid-base interactions. To calculate acid-base properties and cell hydrophobicity, the 'Microbial Adhesion to Hydrocarbons' (MATH) assay is used. It was developed by Rosenberg *et al.* (1980) and uses pairs of monopolar and apolar solvents to determine the bacterial surface physicochemistry. Two sets of solvents are used; chloroform with hexadecane and ethyl acetate with decane. Hexadecane and decane are both apolar n-alkanes, whilst chloroform is a strong electron accepting acidic solvent and ethyl acetate is a strong electron donating basic solvent. The assay was devised to determine the affinity of the test organism to the four solvents by determining their percent adhesion using spectroscopy.

1.6.2 Biofilm Determination by Crystal Violet

As biofilms grow on surfaces it becomes possible to quantify the biomass present on the surface by performing a crystal violet staining assay. A biofilm is grown and rinsed to remove non-adhered cells and biomass before the crystal violet stain is applied to stain all the biomass of a grown biofilm on a surface, which can then be elucidated out of the stained cells by using glacial acetic acid. The elucidate is then measured using a spectrophotometer to give a semi-quantitative measurement of the total biomass formed and can be used to compare against other biofilms stained in a similar manner (Merritt *et al.*, 2005; O'Toole, 2011).

1.7 Bacterial Interactions with Platelets

Whilst increasing knowledge on the role that platelets play in the immune system is becoming evident, there is still only a basic understanding of the ways in which bacteria interact with the platelets (Arman *et al.*, 2014). Bacterial interaction with platelets is thought to cause serious complications leading to diseases including infective endocarditis, disseminated intravascular coagulation, immune thrombocytopenia purpura and even increased risk of myocardial infarction or stroke (Fitzgerald *et al.*, 2006). Three main mechanisms exist for how bacteria and platelets interact, but are mediated by a range of strain-specific surface proteins and secretions (Arman *et al.*, 2014). These include;

- 1) Direct bonding of a bacterial cell to platelet receptors
- 2) Indirect bonding of a bacterial cell to a plasma protein which bonds to a platelet receptor or the bonding of metabolites
- 3) The effect of toxins excreted by bacterial cells to platelets (Hamzeh-Cognasse *et al.*, 2015).

Whilst these mechanisms are a result of the interactions between the bacteria and the platelets or plasma proteins, typically a co-signal or a secondary factor, is required to cause aggregation rather than just adherence. This secondary factor may be one of the other mechanisms that are used for adherence, or potentially a new secretion resulting from the binding of a bacterial cell to a platelet (Fitzgerald *et al.*, 2006; Kerrigan and Cox, 2010). This contributes to the complexity of bacterial-platelet interactions and is one of the reasons why it is still only partially understood.

Receptors that are typically involved in platelet-bacteria interactions include the glycoproteins (GP) GPIIb-IIIa, GPIb α , Fc γ RIIa, complement receptors and Toll-like receptors (Cox *et al.*, 2011). Of these, the GPIIb-IIIa receptor, an integrin complex receptor for

fibrinogen and von Willebrand factor that aids platelet activation, appears to be the most common receptor and is most often bound with bacteria indirectly via fibrinogen or fibronectin, with a couple of bacterial species directly binding to these receptors such as *S. aureus* or *Streptococcus gordonii*. Aggregation has been observed via this indirect binding to other fibrinogen-coated surfaces, however, less aggregation has been observed when bacteria directly interacting with the receptor (Hamzeh-Cognasse *et al.*, 2015). It is speculated that this may potentially be due to a weaker affinity to the receptor via the direct adherence, instead of via the use of an intermediary molecule (such as fibronectin) (Hamzeh-Cognasse *et al.*, 2015). Of the other receptors, GPIb α typically binds either directly or via the use of von Willebrand factor (vWF), Fc γ RIIIa typically uses immunoglobulin G (IgG), Toll-like receptors typically bind directly and the complement receptors bind indirectly using C1 (Cox *et al.*, 2011). Whilst a few main platelet receptors are used, along with other host factors, the bacterial factors are much more varied and greater than the scope of this work (Fitzgerald *et al.*, 2006; Cox *et al.*, 2011).

The presence and binding of some organisms may lead to the inhibition of aggregation instead of activation. Some organisms may find it to their advantage to prevent aggregation of the platelets and have evolved methods of preventing aggregation, such as the use of enterotoxin B by *S. aureus* (Fitzgerald *et al.*, 2006). Further, other molecules and secretions have been found to show inhibition where platelet agonists have been involved. Beachey *et al.* (1977) demonstrated that lipoteichoic acid secreted by Gram-positive organisms inhibited collagen activation of platelets and partial inhibition of aggregation was observed where monoclonal antibodies directed against von Willebrand Factor were present (Pawar *et al.*, 2004). Whilst inhibition of aggregation does not pose an issue whilst during storage, if inhibition of aggregation is still present upon transfusion of a unit, then

not only would the transfused unit not have a therapeutic use but may instead be further damaging to a patient. If platelets in a patient are unable to or have a reduced aggregation, the patient may experience haemorrhaging or delayed wound healing (Fitzgerald *et al.*, 2006).

1.7.1 Methods Used in Understanding Bacterial Interaction with Platelets

1.7.1.1 Aggregometry

The clumping together of platelets upon activation is described as aggregation and is part of the sequence of events that leads to the formation of clots. The aggregation of platelets can be measured to determine the viability of the platelets. Platelet aggregation is measured using an aggregometer, with different types of measurements possible, including light transmission (optical) or impedance aggregometry. Since the focus of this work was platelet transfusion units rather than whole blood units, optical aggregation was used as this uses platelet rich plasma (PRP). This measures the ability of agonists to induce platelet activation and aggregometry *in vitro*. The test involves the use of a platelet poor plasma (PPP) as a blank whilst a PRP sample with a stirrer is baselined before an agonist is added. As the platelets aggregate, the light passed through the sample is impeded and a measurement of the aggregation is possible, thus determining how strongly the platelets have aggregated (Koltai *et al.*, 2017).

1.7.1.2 Flow Cytometry

A flow cytometer uses lasers at various wavelengths to perform cell counting, cell sorting and biomarker detection as cells pass through an electronic detection apparatus. It can be used, in conjunction with fluorochrome antibodies, to determine changes in cell surface receptors. For example, when platelets have been activated with agonists or combined with other compounds, and a quantitative value can be determined. Further, as multiple

lasers can be used in conjunction with one another, multiple parameters can be tested simultaneously (Givan, 2011).

1.7.1.3 Cytometric Bead Array

Cytometric bead array (CBA) is a flow cytometry procedure that allows for the simultaneous quantification of multiple proteins by using the diverse range of fluorescence detection possible with flow cytometry. Whilst the method of detection is similar to a traditional enzyme-linked immunosorbent assay (ELISA), the test can detect up to 30 unique proteins per test sample and has a detection ability as low as 0.274 pg / mL, whilst using a sample of similar volume to that used in an ELISA. This is possible by using a wide range of beads that each have a unique fluorescent signal, allowing for the detection of multiple beads with specific antibodies whilst maintaining fluorescent intensity accuracy. Further, whilst many sets are commercially available for many proteins, sets also exist which enable any antibody to be attached to the beads which thus, in theory, will enable the detection of any protein using the CBA (Castillo and MacCallum, 2012).

1.7.1.4 Western Blot

Western blots are a widely used technique for the detection of specific proteins from cell extracts. Cells are treated or left untreated and lysed to collect the protein before run through an acrylamide gel and then transferred onto a blotting membrane. After transfer, specific protein antibodies are used to bind to those proteins present on the blot, with a secondary antibody used for visualisation. This allows for a semi-quantitative estimation of protein dependant on the size and intensity of the protein band (Mahmood and Yang, 2012).

1.8 Aims and Objectives

1.8.1 Aim

The aim of the study was to characterise and alter the platelet bag surfaces so as to maintain platelet viability, activation and function, whilst reducing the amount of bacterial retention and biofilm formation on the platelet bag surface.

1.8.2 Objectives

- Characterise the surface properties of the inside of the unmodified plasticized poly(vinyl chloride) (p-PVC) platelet bag surfaces (smooth and rough) including; chemistry (ATR-FTIR and Raman), roughness (optical surface profiler and scanning electron microscopy) and physicochemical characteristics (surface energies via contact angles).
- Modify and characterise the platelet bag surface after flattening via hot press.
- Modify and determine the viability of using low temperature atmospheric pressure plasma to modify the surface energy of the platelet bags.
- Determine the effect of the surface modification on platelet viability and function.
- Characterise biofilm growth on all surfaces via crystal violet staining when grown in standard laboratory broth.
- Treat all surfaces with conditioning films (broth and human plasma) and characterise difference in surface characteristics post treatment.
- Determine the effects on platelets by planktonic bacteria and biofilms via aggregation, flow cytometry, western blot and cytometric bead array.

2.0 Materials and Methods

2.1 Materials

pPVC transfusion bags obtained from Terumo BCT (USA) were used for this work. The inside had two faces designated a rough side and a smooth side. When the surfaces had been flattened using the press, they were designated the 'flat' surfaces.

2.1.1 Microorganisms

Serratia marcescens (NCTC 9741)

Staphylococcus epidermidis (DSM 28319)

2.1.2 Reagents

Acetone (Fisher, UK)

Adenosine diphosphate (ADP) (Sigma, UK)

Ammonium Persulfate > 98% (Sigma, UK)

BD™ Cytometric Bead Array (CBA) (558265) (BD Biosciences, USA)

Bovine Serum Albumin (Sigma, UK)

Bromophenol Blue (Sigma, UK)

CBA Flex Kits; RANTES (558324), IL-6 (558276), IL-1 β (558279) and TNF (558273) (BD Biosciences, USA)

Chloroform (Sigma, UK)

Crystal Violet (BDH, UK)

Decane (Sigma, UK)

Diiodomethane (Alfa Aesar, UK)

Disodium Phosphate (Fisher Scientific, UK)

Ethylenediamine tetraacetic acid (EDTA) (BDH, UK)

Ethanol (IMS) (Fisher Chemicals, UK)

Ethanol (Absolute) (Fisher, UK)

Ethyl Acetate (Sigma, UK)

Ethylene Glycol (Sigma-Aldrich, UK)

Fluorochrome Conjugated Antibodies; PE Mouse Anti-Human CD62P (555524) and FITC Mouse Anti-human PAC-1 (340507) (BD Biosciences, USA):

Glacial Acetic Acid (Fisher Scientific, UK)

Gluteraldehyde

Glycerol (Fisher, UK)

Glycine (Fisher, UK)

HEPES (BDH, UK)

Hexadecane (Sigma, UK)

HPLC grade water (BDH, UK)

Human Blood Components; Human Platelets and Human Plasma

Hydrochloric Acid (Fisher, UK)

Magnesium Chloride (Sigma-Aldrich, UK)

Magnesium Sulfate Heptahydrate (Fisher, UK)

Methanol (Fisher, UK)

Monopotassium Phosphate (Sigma, UK)

Nonidet p-40 (NP40) (85124) (Thermo Scientific, USA)

Paraformaldehyde (Fisher, UK)

Phosphatase Inhibitor Cocktail (Sigma, UK)

Pierce™ Bicinchoninic Acid (BCA) Protein Assay Kit (23227) (Thermo Scientific, USA)

Platelet Storage Bags (Terumo BCT, UK)

Ponceau S (BDH, UK)

Potassium Phosphate Dibasic Trihydrate (Fisher Scientific, UK)

Precision Plus Protein™ Dual Colour Standards (Bio-Rad Laboratories, UK)

Protease Inhibitor Cocktail (Sigma, UK)

Restore™ Western Blot Stripping Buffer (Thermo Scientific, USA)

Sodium Bicarbonate (BDH, UK)

Sodium Chloride (Fisher, UK)

Sodium Dodecyl Sulfate (SDS) (Sigma, UK)

SuperSignal™ West Pico Chemiluminescent Substrate (Thermo Scientific, USA)

TEMED (Fluka, Switzerland)

TGX Stain-Free™ FastCast™ Acrylamide Starter Kit (161-0182) (Bio-Rad Laboratories, UK)

Thrombin (Chronolog, USA)

Trans-Blot Turbo™ RTA Transfer Kit, Nitrocellulose (170-4270) (Bio-Rad Laboratories, UK)

Tris Base (Fisher, UK)

Tryptone Soy Agar (Oxoid, UK)

Tryptone Soy Broth (Oxoid, UK)

Tween-20 (Fisher, UK)

2.1.3 Western Blot Antibodies

Phospho-PLCβ3 (Ser537) Polyclonal Antibody (Thermo Fisher Scientific, USA)

B-Actin Antibody (Cell Signalling Technology, USA)

Phospho-Akt (Ser473) Antibody (Cell Signalling Technology, USA)

Akt Antibody (Cell Signalling Technology, USA)

Phospho-VASP (Ser239) Antibody (Cell Signalling Technology, USA)

VASP (9A2) Rabbit monoclonal Antibody (Cell Signalling Technology, USA)

Anti-rabbit IgG HRP-linked Antibody (Cell Signalling Technology, USA)

2.1.4 Buffers:

Modified RIPA Buffer without Inhibitors

NaCl 0.88 g / 100 mL plus 5 mL of 1 M Tris base, 10 mL of 10 % (v/v) NP-40, 10 mL Glycerol, 1 mL of 0.5 M EDTA (pH 8.0) and ultrapure water up to 100 mL.

PUM buffer

K₂HPO₄·3H₂O 22.2; KH₂PO₄ 7.26; Urea 1.8; MgSO₄·7H₂O 0.2 g / L.

SDS Loading Buffer

10 x stock: SDS 5; Bromophenol Blue 0.1 g / L plus 25 mL Glycerol, 10 mL of 1 M Tris base (pH 6.8) and 14 mL ultrapure water.

SDS Running Buffer

10 x stock: Glycine 144.2; Tris base 30.3; SDS 10 g / L

TBS-Tween

1 mL Tween-20 and 1 L of TBS.

Tris Buffered Saline (TBS)

10 x stock: NaCl 87.6; Tris base 24.22 g / L (pH 7.5 with HCl).

Tyrodes Buffer

NaCl 7.83; HEPES 4.7662; NaHCO₃ 1.008; Glucose 0.9008; KCl 0.216; Na₂HPO₄ 0.048 g / L plus 1 M MgCl₂ 1 mL / L.

2.2 Surface Modification

2.2.1 Flattening

Strips of plasticized poly (vinyl chloride) (p-PVC) platelet storage bags were cut from whole platelet bags obtained from Terumo BCT (USA), 150 mm x 25 mm, and were placed between two sheets of Kapton. A template made of polyethylene terephthalate (PET) was used to ensure the p-PVC was not flattened beyond the depth of the PET for consistency, with a thickness of 0.24 mm. This was placed in between stainless steel sheets (300 x 100 x 1.5 mm), which was subsequently placed between two plates of steel (300 x 200 x 45 mm) which had been pre-heated to 150 °C in the hot press (Bradley & Turton LTD, UK). The p-PVC / PET / Kapton and stainless steel sheets were placed into the hot press and 10 tonnes of pressure was applied at 150 °C for 10 min. The plates were transferred to a cold press and cooled with 10 tonnes of pressure for 10 min.

2.2.2 Low Temperature Atmospheric Pressure Plasma (LTAPP) Treatment

LTAPP treatment was performed via an internally built dielectric barrier discharge rig consisting of two dielectric alumina plates measuring 240 mm by 50 mm, with sputtered copper electrodes. The plasma was generated using a custom-built power supply consisting of a function generator (AIM-TTi TG1000 Function Generator single channel 10 Mhz DDS, UK), audio amplifier (ProSound 2 Channel 1600W Power Amplifier, USA), and transformer (Custom design by Amethyst Designs Ltd, UK) delivering a voltage (10 kV) and alternating current of 10 kHz. Nitrogen gas was flowed through the dielectric barrier discharge at a flow-rate of five slm.

2.3 Surface Characterisation

2.3.1 Coupon Preparation

Coupons of 11 mm in diameter were punched from p-PVC platelet bags using an 11 mm disc punch (Agar Scientific, UK) or punched from the previously flatted p-PVC bags.

2.3.2 Scanning Electron Microscopy (SEM)

p-PVC coupons were attached to 12 mm SEM stubs (Agar Scientific, UK) with 12 mm carbon tabs (Agar Scientific, UK) prior to being sputter coated with a gold and palladium coating (Model: SC7640, Polaron, Au/Pd target, deposition time: 1.5 min). Samples were stored in a dessicator containing silicon beads until imaged.

2.3.3 Surface Roughness and Optical Surface Profiles

Surface roughness (S_a) values were calculated from surface profiles measured using a ZeGage 3D Optical Surface Profiler (Zygo; USA) for all p-PVC coupons. Measurements were taken using 50 x magnification with a scanning distance of 50 μm from the centre position ($n = 3$).

2.3.4 Energy Dispersive X-ray (EDX)

Surfaces were prepared treated the same as SEM samples but were not sputter coated. Samples were then imaged using the SEM at 20 KV with a 15 mm working distance before EDX was run on the samples using the EDX attachment on the SEM ($n = 3$).

2.3.5 Attenuated Total Reflection- Fourier Transform Infrared Spectroscopy (ATR-FTIR)

ATR-FTIR was used to measure the molecular structures and chemical bonds of the untreated and modified p-PVC (Nicolet 380 FTIR with a Smart iTR attachment, Thermo Scientific, UK). Background spectra was captured prior to each measurement and spectra were acquired at room temperature using Omnic 5.2 (Thermo Scientific, UK) software with each run made up of 16 scans and a resolution of 4 cm⁻¹. Analysis of each sample was performed in triplicate and average spectra used (n = 3).

2.3.6 Raman Spectroscopy

Raman spectra was measured at room temperature using a DXR 532nm laser on a DXR Raman microscope (Thermo Scientific, UK). The laser was focused on the sample surface using 50 x magnification with a long working distance optical objective, and a laser power of 10 mW, with sample exposure time of 3 s. The Raman was performed in triplicate on each surface, with each run containing 20 scans, and a mean spectra taken (n = 3).

2.3.7 Physicochemistry of Surfaces

Contact angles (θ) using HPLC grade water, ethylene glycol or diiodomethane were measured with a MobileDrop goniometer (Krüss GMBH, Germany). Both left and right side angles were determined, with five measurements of each chemical on each sample taken (n = 10). Fresh coupons were used for each solvent to ensure there was no cross contamination of solvents on the surfaces. The method of van Oss *et al.* (1988) was used for calculating the surface energy (γ_s^{SE}) of the films from these measurements, according to the following equation:

$$(1 + \gamma_l) \cos\theta = 2 \left(\sqrt{\gamma_s^{LW} \gamma_l^{LW}} + \sqrt{\gamma_s^A \gamma_l^B} + \sqrt{\gamma_s^B \gamma_l^A} \right) \quad [1]$$

Where the subscripts *l* and *s* denote the surface energy of the solid and liquid respectively. The superscript *LW* denotes the Lifshitz-van der Waals components of the surface energy, and the superscripts *A* and *B* denote the Lewis acid and Lewis base parameters of the surface energy. The acid and base terms can be combined into the Lewis acid base (superscript *AB*) component of the surface energy:

$$\gamma_i^{AB} = 2 \sqrt{\gamma_i^A \gamma_i^B} \quad [2]$$

Subsequently the overall surface energy was calculated as the sum of the Lifshitz-van der Waals and Lewis acid base components:

$$\gamma_i = \gamma_i^{LW} + \gamma_i^{AB} \quad [3]$$

The components of the surface energy were then used to assess the hydrophobicity, or Gibbs free energy of attraction between the surface and water (surface energies are denoted by subscript *w*), and were calculated using the following (Van Oss and Giese, 1995):

$$\Delta G_{sw} = -2 \left(\left(\sqrt{\gamma_s^{LW}} - \sqrt{\gamma_w^{LW}} \right)^2 + 2 \left(\sqrt{\gamma_s^a \gamma_s^b} + \sqrt{\gamma_w^a \gamma_w^b} - \sqrt{\gamma_s^a \gamma_w^b} - \sqrt{\gamma_w^a \gamma_s^b} \right) \right) \quad [4]$$

2.3.8 Tensile Strength Determination

Tensile strength of the PVC was determined using a Tinius Olsen (UK) H10KS tensiometer running Qmat 5.53 (Tinius Olsen, UK). Samples were run with a 4 mm width and a 200 mm / min speed (n = 5). Unmodified surface Mpa was calculated considering the effect of the diamond cross sectional area, as the thickness for the surface was not consistent due to the patterning on one side of the surface (n = 3).

2.3.9 Degeneration of Surface Energy Following LTAPP Treatment

Pieces of smooth p-PVC surfaces were plasma treated and control strips were left untreated. The untreated coupons as well as three plasma treated coupons had contact angle measurements taken immediately for 0 h measurements. The coupons were left in the dark at room temperature and contact angle measurements of the plasma treatment was taken after 24 h, 48 h, 72 h, 96 h, 120 h and 168 h, with three coupons used at each time point (n = 3).

2.3.10 Batch Testing

The smooth side of three platelet bags from two separate batches were cut into strips and contact angle measurements were taken (n = 12).

2.4 Biofilm Formation

2.4.1 Sterilisation of Coupons

Coupons were placed into a 30 mL sterile plastic universal containing 70 % (v/v) ethanol and vortexed for one min. The coupons were then soaked for 15 min in ethanol. The ethanol was removed and the coupons were aseptically transferred to a sterile Petri dish containing sterile distilled water (dH₂O) to remove the ethanol before being aseptically transferred to another sterile Petri dish containing sterile dH₂O. The washing sequence was performed in triplicate to ensure all the excess ethanol was removed before the coupons were air dried in a class II microbiological cabinet for 1 h.

2.4.2 Bacterial Growth Conditions

Strains of *Serratia marcescens* (NCTC 9741) and *Staphylococcus epidermidis* (DSM 28319) were obtained from frozen pure culture stock, plated onto tryptone soya agar (TSA) and incubated at 37 °C overnight. New plates were streaked from freezer stock every four weeks to ensure the continuity of the bacteria was maintained for all experiments, with streaked plates stored at 4 °C. A single colony was removed from the TSA plate and inoculated into a volume (10 mL) of sterile tryptone soya broth (TSB) which was incubated overnight at 37 °C with shaking (150 rpm). The bacterial culture was centrifuged at 2210 g for 10 min, the supernatant removed and the cells washed with 10 mL of sterile dH₂O before repeating. The cells were re-suspended in sterile dH₂O and diluted to an OD of 1.0 ± 0.05 at 540 nm using a spectrophotometer (Jenway 6305, UK). A serial dilution with spread plates was performed in duplicate with three separate bacterial broth cultures to obtain 1.25 x 10⁹ colony forming units per mL (CFU mL⁻¹) for *Ser. marcescens* and 1.44 x 10⁸ CFU mL⁻¹ for *S. epidermidis* at an OD of 1.0 ± 0.05 at 540 nm.

2.4.3 Scanning Electron Microscopy

An overnight culture was prepared and the washed bacterial inoculum was diluted to an optical density (OD) of 1.0 ± 0.05 at 540 nm. Ten microliters of bacterial inoculum was pipetted onto a coupon and dried in a class II cabinet for 1 h before being processed by placing into 4 % glutaraldehyde (made up in phosphate buffered saline) overnight. The coupons were removed from the glutaraldehyde using tweezers and rinsed with sterile dH₂O to remove the remaining solvent. The coupons were dried in a fume hood for 1 h before an ethanol gradient of 10 %, 30 %, 50 %, 70 %, 90 % and 100 % made up from absolute ethanol diluted with sterile dH₂O was performed. Each coupon was left in each ethanol concentration for 10 min moving from the lowest ethanol concentration to the greatest. Once removed from the 100 % ethanol solution, the coupons were placed into a desiccator and when dry were attached to SEM stubs with carbon tabs prior to being sputter coated with a gold and palladium coating (Model: SC7640, Polaron, Au/Pd target, deposition time: 1.5 min) before being stored in a desiccator until imaged.

2.4.4 Microbial Adhesion to Hydrocarbons (MATH) Assay

Cultures were grown at 37 °C overnight in TSB. Bacterial cells were harvested via centrifugation at 2210 *g* for 10 min, washed 3 times using PUM buffer pH 7.1 and re-suspended to an OD 1.0 at 400 nm in PUM buffer. A 1.5 mL volume of washed cells suspended in PUM buffer was added to a round bottomed test tube, 15 mm in diameter. A 250 µL volume of one of the test liquids (Chloroform, Hexadecane, Ethyl Acetate or Decane) was added to the suspension. Suspensions were incubated at 37 °C for 10 min to equilibrate. The test suspension was vortexed for 2 min before re-incubation for 30 min at 37 °C to allow separation of the lower aqueous phase. The lower aqueous phase was

removed from the test tube and the OD determined at 400 nm. This was used with a calculation developed by Rosenberg *et al.* (1980) to determine cell surface hydrophobicity;

$$Adhesion = \left(\frac{1 - A}{A\emptyset} \right) \times 100 \quad [5]$$

Where $A\emptyset$ was the optical density of the microbial suspension when measured at 400 nm before adding test chemical and A was the optical density measured at 400 nm of the extracted lower aqueous phase after mixing with the hydrocarbon ($n = 3$).

2.4.5 Biofilm Formation

A 1.8 mL volume of sterile TSB was added to each well of a sterile 12-well plate (Nunc Non-Treated Multidishes, Thermo Fisher Scientific, UK) along with a sterilised p-PVC coupon, 11 mm in diameter, test side of the surface face up. The reverse end of a sterile swab was used to push the coupon to the bottom of the well. The 12 well plates were left at room temperature overnight to check for any contaminant growth and to check that all coupons were fully sterilised. An overnight culture was prepared and diluted to obtain 1.0×10^8 CFU mL^{-1} . Two hundred microliters of the bacterial suspension was added to the appropriate wells to give a working concentration of 1.0×10^7 CFU mL^{-1} . The 12 well plates were parafilmmed to prevent the media from evaporating from the plates. The plates were incubated at either 22 °C or 37 °C for either 5 or 7 days with gentle shaking (68 rpm). Following incubation, all the media in each well was removed by pipetting, leaving just the coupon behind and the wells containing the coupons were washed by adding 2 mL of sterile dH_2O to each well; carefully against the side of the well so as not to disturb the biofilm formed on each coupon. The liquid was gently swirled around the wells manually

for 5 s before pipetting out the liquid to remove any unbound planktonic cells. The 12 well plates and coupons were air dried in a class II cabinet for 1 h.

2.4.6 Crystal Violet Assay

One millilitre of 0.03 % w/v crystal violet solution was added to each well following drying, ensuring full coupon coverage, and left for 30 min. The stain was pipetted out of each well and 2 mL of sterile dH₂O was added and manually gently swirled around for 10 s to remove the excess stain. This was repeated once and the coupons were removed after the second time and transferred to a fresh 12 well plate. To each well in the new plate, 2 mL of 33 % (v/v) glacial acetic acid solution was added and left for 15 min with manual agitation every 5 min to elute the bound crystal violet from the biofilm. The absorbance of the eluted stain in the glacial acetic acid was measured at 590 nm to determine the optical density, thus quantifying biofilm growth. The absorbance value obtained was doubled to convert it to absorbance per mL. When the absorbance was too high to be read, the remaining 1 mL in the well was diluted down with another 1 mL of 33 % (v/v) glacial acetic acid solution and measured, with values obtained multiplied by four to account for the dilution. (n = 6).

2.5 Conditioning Films

2.5.1 Conditioning Film Preparation

Conditioning films of human plasma were made alone and in the presence of bacteria, as well as bacteria in water as a control. For inoculated conditioning films, an overnight culture was centrifuged at 2210 *g* and washed once with sterile dH₂O before re-centrifugation and suspension in sterile dH₂O. The suspension was diluted to a CFU / mL of 1×10^8 before diluting into either sterile dH₂O or human plasma to obtain a working concentration of 1×10^7 CFU / mL. Once prepared, sterile test p-PVC coupons were added to a 12 well plate with the test side facing up and 1 mL of the suspension was added to each well, ensuring the coupon remained at the bottom of the well and covered. The 12 well plate was left for either 1 h or 24 h at 22 °C with gentle agitation (68 *rpm*) on an orbital shaker. After incubation, the contents of each well were removed with pipetting and the coupons washed by adding 2 mL of sterile dH₂O to each well and using sterile forceps to transfer the coupon to a new 12 well plate which was placed in a class II cabinet for 1 h to dry the coupons. Once dry, the coupons were then examined using FTIR, RAMAN, EDX and WLP. A separate batch was prepared for SEM and processed per SEM preparation instructions. Fresh samples were also prepared for the Goniometer as the coupons were disposed of after applying the solvents.

2.5.2 Conditioning Film MATH Assay

The MATH assay was performed as described in *2.4.4 Microbial Adhesion to Hydrocarbons (MATH) Assay* with the addition of a conditioning film. After washing and prior to testing, 7.5 mL of standardised bacterial suspension (OD 1.0 at 540 nm) was added to 3.25 mL of human plasma or TSB and vortexed for one min. This was centrifuged at 2210 *g* for ten min

and rinsed once with PUM buffer before re-centrifugation. The pellet was re-suspended in PUM buffer and an OD of 1.0 at 400 nm was obtained before the MATH assay was performed. A MATH assay without the conditioning film was performed as a control and the assay was performed in triplicate.

2.6 Effect on Platelet Activity and Function

2.6.1 Ethical Approval and Participant Consent

The Manchester Metropolitan University ethics board granted approval for the study. Healthy volunteers were recruited for blood collection and gave written informed consent before donating a blood sample. The study was performed conforming to the Declaration of Helsinki.

Participants who had taken anti-platelet medication, anti-inflammatory medications, herbal medicines that may interfere with platelet function (Ginkgo Biolba, St John's Wort) or Selective Serotonin Reuptake Inhibitors in the past fortnight were excluded from the study. The study involved a total of 41 participants (n = 24 male, n= 17 female). Samples from some participants (chosen at random) were used for analysis of multiple markers of platelet activation and function.

2.6.2 Platelet Rich Plasma Extraction

A total of 20 mL of whole blood was collected from healthy voluntary donors into 4 mL vacutainers containing 3.2 % sodium citrate. The vacutainers were centrifuged at 180 g to compact the blood cells into the lower section of the tube, leaving the platelet rich plasma (PRP) as the supernatant. The PRP from all the centrifuged tubes was extracted without disturbing the compacted red blood cells into sterile 50 mL falcon tubes.

2.6.3 Platelet and Bacterial Incubation

For planktonic bacteria, the PRP was diluted with bacteria suspended in Tyrodes buffer back to physiological levels using either *Ser. marcescens* or *S. epidermidis* at working concentrations of both 2×10^7 or 2×10^6 . The bacteria were prepared as in 2.4.2 *Bacterial*

Growth Conditions but were rinsed with and suspended in Tyrodes buffer. For biofilm work, the PRP was diluted with Tyrodes buffer prior to being added to biofilms. The biofilms were also prepared as in *2.4.5 Biofilm formation* but were rinsed with Tyrodes buffer instead of sterile dH₂O. These were then incubated at 22 °C for either 1 h, 2 h or 4 h with gentle agitation (68 rpm) prior to experimental work.

2.6.4 Aggregometry

Samples for aggregation were prepared by adding 450 µL of test PRP to two aggregation cuvettes with a mini stirrer. A platelet poor plasma (PPP) sample was prepared by centrifuging 600 µL of PRP at 5000 g for 5 min and transferring 500 µL of the supernatant to a clean aggregation cuvette. The PPP sample was placed into the PPP slot of a aggregometer (Chrono-log 700, Chrono-log, USA) pre-warmed to 37 °C. Test samples were stored in the spare slots in the aggregometer to warm to 37 °C before running. Each sample was run by being placed into the PRP slot with a stirrer speed of 1200 rpm and the baseline was obtained. The trace was run and after 30 s, 50 µL of the agonist (50 µM ADP or 10 U Thrombin) was added and the recording of the aggregation began. Each trace was run until it reached the 4 min mark and was stopped, and the max aggregation was recorded, (n = 6).

2.6.5 Flow Cytometry

Flow cytometer tubes were prepared by initially adding 90 µL of the PRP preparation to two tubes per test sample, plus 3 additional tubes of the control sample. To all tubes, 10 µL of the chosen agonist (50 µM ADP or 10 U Thrombin) was added. For the 3 additional tubes, 1 tube was not stained with any fluorochrome antibody, 1 tube was stained with

only the FITC conjugated anti-human CD62P antibody and 1 tube was only stained with the PE conjugated PAC1. To all the other tubes, 10 μL of each fluorochrome antibody being used was added. All the tubes were incubated for 10 min in the dark before 100 μL 4% paraformaldehyde was added to fix the cells. Each tube was then made up to 500 μL with Dulbecco's phosphate buffered saline (DPBS), wrapped with foil to keep light off the samples and stored in the fridge until analysis. All samples were analysed using a BD Accuri C6 Flow Cytometer (BD Biosciences, USA), ($n = 3$).

2.6.6 Cytometric Bead Array (CBA)

2.6.6.1 CBA Sample Preparation

Samples of planktonic or biofilm bacteria were incubated with PRP for 4 h or 24 h. Each sample had 450 μL of biofilm-treated PRP or bacteria-treated PRP as described in 2.6.3 *Platelet and Bacterial Incubation* transferred to two Eppendorf tubes to which either 50 μL of Tyrodes buffer or 50 μL of 50 μM ADP was added. The Eppendorf tubes were mixed via inversion and left for 5 min before centrifugation at 3000 g for 10 min. The supernatants were harvested from each Eppendorf tube and transferred into clean Eppendorf tubes, which were stored at $-80\text{ }^{\circ}\text{C}$ until the samples were analysed.

2.6.6.2 Human Soluble Protein Flex Set Standards

Cytometric bead array (CBA) standards were prepared according to manufacturer's instructions. One vial of lyophilized standard for each BD CBA Human Soluble Protein flex tested (RANTES) was opened and pooled in a 15 mL falcon tube as the 'Top Standard'. The standards were reconstituted using 4 mL of Assay Diluent and equilibrated for at least 15 min without vortexing. The standard was diluted by pipetting 500 μL of the top standard

into an additional 500 μL for the 1:2 dilution and mixed by pipetting. Dilutions were carried on to obtain 1:4, 1:8, 1:16, 1:32, 1:64, 1:128 and 1:256 concentrations and a blank containing just assay diluent was prepared.

2.6.6.3 Capture beads and PE Detection Reagent Preparation

The number of tests in the experiment were determined as the number of test samples plus 10 for the standards and 2 added on to account for pipetting error. The capture bead (CB) stock vials were vortexed for 15 s to ensure thorough resuspension of the beads. Undiluted capture beads were provided so that 1 μL was used for 1 test. The volume required of each capture bead stock was scaled according to the number of tests run and the volume of capture bead diluent required was calculated as follows:

$$\text{CB diluent } (\mu\text{L}) = (\text{Test Number} \times 50 \mu\text{L}) - (\text{Cytokine Number} \times \text{Test Number}) \quad [6]$$

The capture beads were added to a tube containing the appropriate volume of CB diluent labelled as calculated using the above equation to prepare the 'Mixed Capture Beads'. The same procedure was followed to prepare the 'Mixed PE Detection Reagent', using the PE detection reagent provided in each kit and the detection reagent diluent. The mixed PE detection reagent was stored at 4 °C and protected from light until ready to use. The capture beads in each kit have a unique fluorescence and are coated in a specific antibody for the analyte the kit was made for. The PE detection reagent contains detector antibodies with a conjugated reporter molecule that binds to the analyte.

2.6.6.4 Performing the Human Soluble Protein Flex Set Assay

Clean Eppendorf tubes were prepared by adding 50 μL of either a standard or a test sample. The mixed capture beads were vortexed for 5 s and 50 μL was added to each tube and gently mixed via inversion. The tubes were incubated at room temperature for 1 h. After incubation, 50 μL of the mixed PE detection reagents were added to each tube, gently mixed via inversion and incubated at room temperature for 2 h in the dark. Whilst incubating, the flow cytometer was set up for the CBA samples. After incubation, 1 mL of wash buffer was added to each tube, mixed via inversion and the tubes were centrifuged at 200 g for 5 min. The supernatant was carefully aspirated and 300 μL of wash buffer was added to each tube. Tubes were vortexed for 1 s to resuspend the beads. The standards were analysed, starting at the lowest concentration, and then the samples were analysed. The data was then exported to FCAP Array software (Version 3.0).

2.6.6.5 Flow Cytometer Setup for CBA

Two flow cytometer tubes were prepared containing the CBA set up beads for the flow cytometer, one tube containing the F1 + A1 beads with another containing the F1 + F9 beads. To both tubes, 350 μL of wash buffer was added along with 25 μL of each of the beads required for the tube. The tubes were vortexed for 1 s. The CBA template was opened and the 2 *blue*, 2 *red* instrument configuration was selected and the filter for the FL3 laser was changed to the 780/60 filter. The setup beads were run with a 2000 event limit in the R1 gate with a medium flow rate. Data was acquired for the F1 + A1 tube, ensuring bead population was within the R1 gate and the thresholds excluded the debris but not the beads. Once acquisition was complete, colour compensation was performed to correct FL4 by subtracting a percentage of FL3, starting low to avoid overcompensation.

The beads were compensated so that the A1 bead population moved from the upper-right quadrant to the upper-left quadrant. Once the compensation was optimised, the compensation was applied to all the samples. The F1 + F9 beads were run and the colour was compensated by correcting FL3 by subtracting a percentage of FL4. Compensation was performed until the median FL3 value for the lower-right quadrant matched the median FL3 value for the lower-left quadrant (Compensation should typically be < 5 %). Once compensated, it was applied to all the results and the file was saved as a template for future acquisition of CBA flex kits.

2.6.7 Western Blot Assay

2.6.7.1 Western Blot Sample Preparation

Samples for Western blot were prepared after incubation using a modified radioimmunoprecipitation assay (RIPA) buffer. Prior to use, both protease and phosphatase inhibitor cocktails were added to the RIPA buffer, with a 1:1000 dilution of each added. To Eppendorf tubes, 450 μ L of test PRP was added. To each sample, 50 μ L of either Tyrodes buffer, 50 μ M ADP or 10 U Thrombin was added and the Eppendorf tubes were inverted to mix before being centrifuged at 1500 g for 5 min to pellet the cells. The supernatant was removed and the samples were kept on ice whilst processing. To each sample, 200 μ L of modified RIPA buffer was added before the sample was vortexed at high speed for 10 s and pipetted vigorously to mix. The samples were left on ice for 30 min, with vortexing of each sample every 5 min for 30 min. Subsequently, the samples were vortexed for 3 min to ensure full breakdown of the platelet membranes. Samples were centrifuged at 13500 g (Prism chilled centrifuge, Labnet, USA) for 20 min in a pre-chilled 4 $^{\circ}$ C centrifuge

and the supernatants were transferred to clean chilled Eppendorf tubes. Samples were run using the bicinchoninic acid (BCA) protein assay and frozen at -20 °C until analysed.

2.6.7.2 Protein Assay

Bicinchoninic acid (BCA) protein assays were performed on each sample to ensure correct protein concentration of the samples. Standards were made up according to the manufacturer's instructions, with standards containing increasing levels of bovine serum albumin; 0 µg / mL, 25 µg / mL, 125 µg / mL, 250 µg / mL, 500 µg / mL, 750 µg / mL, 1000 µg / mL, 1500 µg / mL and 2000 µg / mL. To a 96 well plate, 25 µL of each standard and of each test sample was added in duplicate. To each of these wells, 200 µL of the working reagent (made up of 50 parts BCA reagent A with 1 part BCA reagent B) was added and the wells were mixed by pipetting back and forth. The plate was incubated at 37 °C for 30 min before being cooled back to room temperature. The plate was read using a plate reader with a measured absorbance of 562 nm. The average absorbance of the blank standard, 0 µg / mL BSA, was subtracted from all the other measurements. A standard curve was plotted using the blank corrected measurements of the standards vs. its concentration in µg / mL. The standard curve was used to determine the protein concentration of each unknown samples.

2.6.7.3 Gel Electrophoresis

Bio-Rad handcast glass plates (Bio-Rad Laboratories, UK) were stabilised using a mini-PROTEAN Tetra cell casting stand (Bio-Rad Laboratories, UK) during casting. Resolver solution was prepared by adding equal portions (3 mL of each per gel) of the TGX Stain-Free FastCast acrylamide kit's resolver A and Resolver B with 30 µL of 10 % ammonium

persulfate (APS) and 3 μ L of TEMED and pulse vortexed for 5 s to mix. The mixture was carefully added to the cassette using an appropriate pipette, ensuring that no bubbles formed and that the solution did not mix with air, filling the cassette to 0.5 cm – 1 cm below the bottom of the comb teeth. To this, a stacker solution was carefully added by pipetting down the middle of the cassette and filling to the top of the short plates, ensuring the mixture did not mix with the resolver solution. The stacker solution was prepared using equal portions (1 mL of each per gel) of the TGX Stain-Free FastCast acrylamide kit's stacker A and stacker B with 10 μ L of 10 % APS and 2 μ L of TEMED and pulse vortexed for 5 s to mix. The comb was aligned and inserted into the cassette carefully to prevent air being trapped under the comb teeth, and the gel was left to polymerize for 30 min - 45 min before electrophoresis. Gels were either used immediately or wrapped in a paper towel wetted with deionized water and then stored in an airtight container for up to 4 weeks at 4 °C. Gel cassettes were installed into a mini-PROTEAN tetra electrode assembly or companion running module (Bio-Rad Laboratories, UK), placed into a buffer tank and running buffer was added into the assembly or companion module to check for leaks. If any leakage was determined, the gel cassettes were adjusted to ensure no leaks, and the outer chamber was filled to the '2 gels' or the '4 gels' mark. Samples were diluted to obtain 20 μ g of protein in 15 μ L of RIPA buffer, to which 5 μ L of loading buffer was added (a 3:1 ratio). Samples were mixed and put on ice for 10 min before incubating at 100 °C for another 10 min in a heat block. The samples were centrifuged at high speed, 16,000 *g*, for 1 min to collate the sample at the bottom of the Eppendorf tube. The comb was gently removed from the gel and the first well was loaded with 20 μ L of Precision Plus Protein™ Dual Colour Standards and the samples were loaded into the remaining wells. The chamber was connected to the power supply and run at 400 MA with 100 Volts for 10 min. Once it

was confirmed that the proteins were moving through the gel, the voltage was increased to 125V for approximately 45 min until the bands of dye reached around 1 cm from the bottom of the gel.

2.6.7.4 Nitrocellulose Transfer

Transfer buffer was used to wet two filter papers and a nitrocellulose membrane for 2.5 min before assembling the transfer stack in the Trans-Blot Semi-Dry SD Transfer Cell system (Bio-Rad Laboratories, UK). One of the filter papers was placed at the bottom, the membrane was placed onto this filter paper, then the gel was carefully removed from the glass plates and added with the other filter paper placed on top. During each addition, the roller provided was used to remove any air bubbles from the stack. The lid was locked in place on the Trans-Blot cassette and the cassette was placed into the machine. The transfer was run at 400 MA with 10 V for 40 min. The transfer was checked by submerging the membrane into Ponceau S staining solution (0.2% (w/v) Ponceau S in 5% (v/v) acetic acid) for up to 1 h.

2.6.7.5 Protein detection

After transfer, the membrane was placed into Tris Buffer Saline with 0.1% Tween 20 (TBST) for 5 min with agitation to wash. The membrane was placed into a 5% BSA blocking solution at room temperature for 1 h with agitation. After blocking, the diluted primary antibody (Table 2.6.7.1) was added and incubated overnight at 4 °C. The primary antibody was removed and the diluted secondary antibody (15 µL Anti-Rabbit IgG (Whole molecule)-Peroxidase (A615W) antibody produced in goat (Sigma, MFCD00162788) in 15 mL of 2 % BSA) was added and incubated at room temperature for 1 h with agitation. The membrane

was removed from the secondary antibody and washed with TBST 3 times as earlier. SuperSignal™ West Pico Chemiluminescent Substrate was prepared by combining 1 mL SuperSignal™ West Pico Stable-Peroxide Solution to 1 mL of SuperSignal™ West Pico Luminol/Enhancer Solution in a universal tube and protected from light. The membrane was incubated with the chemiluminescent substrate for 5 min at room temperature before being exposed in the Chemi Doc Touch Imaging System (Bio-Rad Laboratories, UK) to visualise and detect the protein bands.

2.6.7.6 Membrane Stripping and Re-probing

After visualisation, the membrane was incubated in Restore™ Western Blot Stripping Buffer for 15 min on a shaker to strip previously bound antibodies so that the control antibodies could be tested. After incubation, the membrane was washed 3 times in TBST as earlier and placed into blocking solution for 1 h at room temperature on an orbital shaker (68 rpm). The membrane was incubated the corresponding primary antibody B (Table 2.6.7.1) antibody overnight at 4 °C. The membrane was washed and incubated with the secondary antibody, incubated with the chemiluminescent and visualised as described in 2.6.7.5 *Protein detection*.

2.6.7.7 Protein Densitometry Measurements and Normalisation

Images obtained for the western blots were opened in Image Lab 6.0.1 (Bio-Rad Laboratories, UK) and lanes were manually arranged over the lanes present in the blot images. Bands on the Images were manually placed over the bands in the ladder lane to determine protein size of bands present on the blot. Lanes were checked with the lane profile tool to ensure that removal of excess background (Disk Size of 70 mm) was

standardised and the background did not contain any peaks. Band volume (Intensity) for each band was determined and recorded. Once band for both protein of interest and housekeeping antibody were determined. The housekeeping antibody was standardised by dividing each intensity by the intensity of the band with the highest intensity. The protein of interest was standardised by dividing each band by its standardised housekeeping intensity. The fold difference was determined by dividing the standardised protein of interest intensity by the standardised protein of interest control value.

2.7 Data Handling and Statistical Analysis

All results were presented as mean \pm standard error (SE). Mean values were compared using analysis of variance (ANOVA) to determine significant differences between mean values at the 95% confidence level ($p < 0.05$).

3.0 Surface Characterisation and Low Temperature Atmospheric Pressure Plasma Treatment

3.1 Introduction

It has been well established that surface properties play a significant role in microbial attachment and biofilm formation. A variety of features can influence the attachment of microorganisms to a surface, including surface topography / roughness, chemistry and physicochemistry. The surface roughness, caused by the topographical features present on a surface, can play a major role depending on the size of the topography and also the shape of the surface features. Surface features similar in size to the microorganism have been suggested to have the most significant effect on microbial retention (Whitehead and Verran, 2006).

Surface chemistry plays a role in microbial attachment by providing functional groups that increase bacterial adhesion (Parreira *et al.*, 2011). In the study by Parreira *et al.* (2011), it was demonstrated that *Helicobacter pylori* preferentially adhered to self-assembled monolayers (SAMs) that exposed a CH₃ functional group whilst SAMs with an ethylene glycol (EG4) functional group reduced *H. pylori* adhesion. Further, the EG4-SAMs samples also both reduced the viability and influenced the morphology of adhered cells, whilst the CH₃-SAMs were mostly still viable and had standard morphologies. A previous study had demonstrated similar results using *Pseudomonas aeruginosa* and *S. epidermidis*. In this study the *S. epidermidis* preferentially adhered to the CH₃ group whilst the *P. aeruginosa* preferentially adhered to the ethylene glycol group, demonstrating that different bacteria interact with functional groups differently (Cheng *et al.*, 2007).

The surface chemistry links into surface physicochemistry, which contributes to the effectiveness of microbial attachment in the initial reversible attachment stage (Tuson and Weibel, 2013). This is due to microorganisms typically initially adhering weakly to surfaces via Lifschitz van der Waals forces, whilst other forces including hydrophobicity and acid-base energies can also influence bacterial attachment and adhesion (Loza-Correa *et al.*, 2017). Since it is difficult to change the chemistries of the surfaces of the transfusion bags, due to the regulations concerning such modifications, the aim of this chapter was to modify the surface properties of the pPVC bags both by using a hot press to flatten the surfaces, and /or followed by use of a gas plasma, to alter the surface physicochemical properties by changing the electrochemical properties of the surface (Chapter 3), in order to reduce bacterial retention and biofilm formation (Chapter 4)

3.2 Results

3.2.1 Scanning Electron Microscopy

Upon initial analysis of the bags, it was determined that they were made of two sheets of p-PVC melded together. The analysis of the PC bags was carried out on the inside faces of the bags against which the platelet concentrates (PCs) would come into contact. SEM images demonstrated that one inside face of the p-PVC had a diamond patterned surface, which showed roughened features (rough surface) (**Fig. 3.1a**). The rough surface showed pits along the edges of the diamond imprints of varying sizes. In comparison to this, the other inward facing side of the p-PVC polymer demonstrated a smoother, more featureless surface (smooth surface) (**Fig. 3.1b**). Due to the unexpected surface features, flattening of the surfaces was performed to remove any surface features and determine whether this was enough to reduce biofilm growth. Post flattening of the p-PVC, the surface was demonstrated to be smoother still and without any discernible surface features (flat surface) (**Fig. 3.1c**).

3.2.2 Optical Surface Profiling

Following quantification of the surface roughness, optical surface profiling demonstrated that the rough surface inside of the platelet bag had the greatest levels of differing surface topography (**Fig. 3.1d**). The mean surface roughness (S_a) of the rough surface varied between the diamond bottom, ridges and the sides of the diamonds which were demonstrated as having pits. A statistically significant reduction in the S_a values were observed from the rough surface (3549.8 nm) to the smooth surface (1021.2 nm) and a further significant reduction was observed on the flattened surface (108.1 nm).

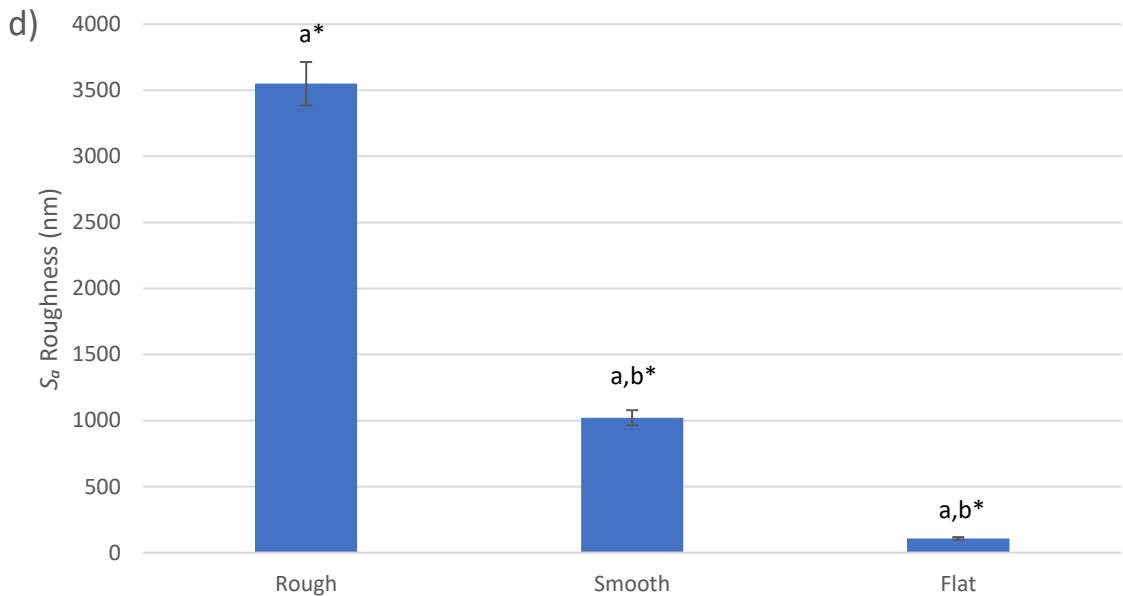
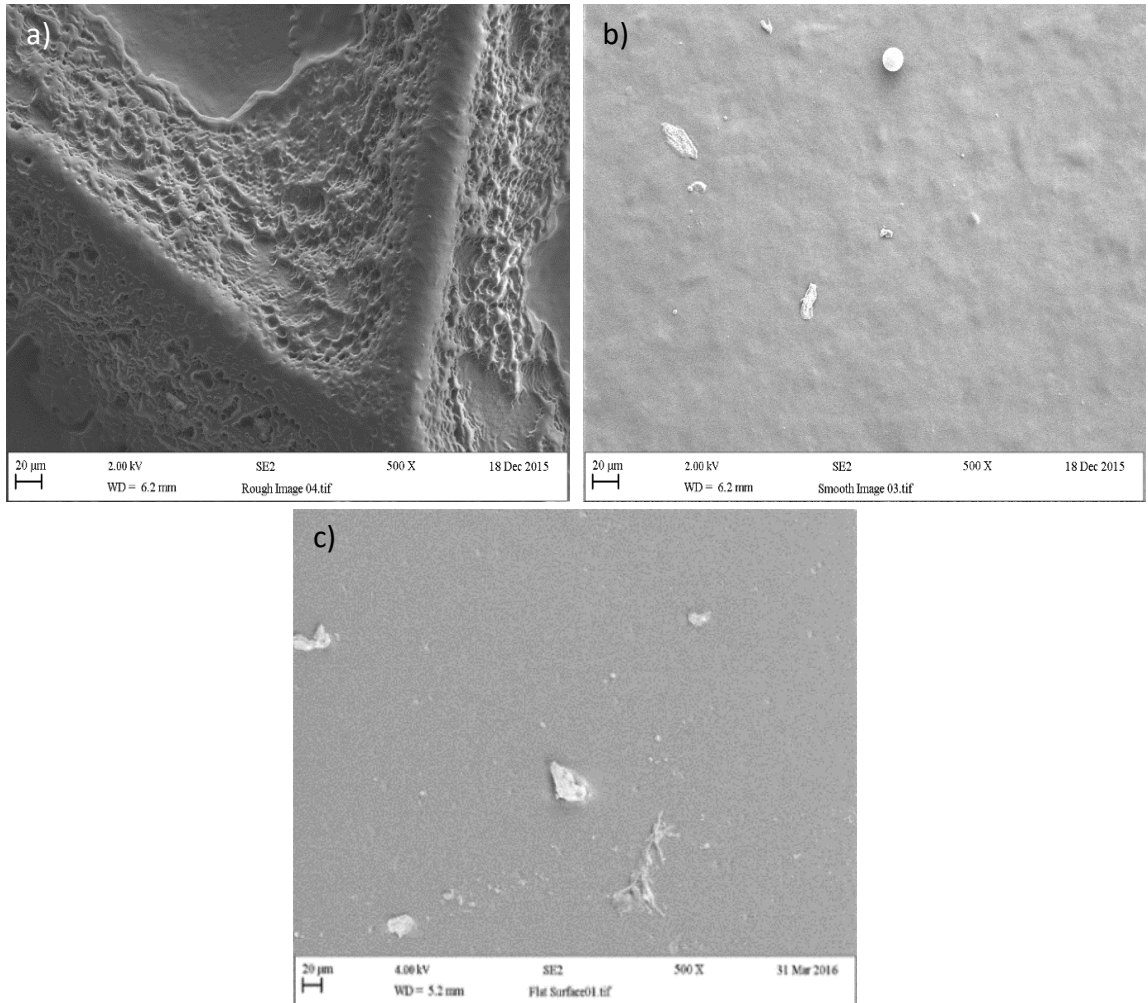


Figure 3.1 SEM images of the un-inoculated p-PVC platelet bags a) rough (inside facing), b) smooth (inside facing) and c) flattened surfaces d) surface roughness (S_a value) of overall rough surface features, pits and ridges of the rough surface features, smooth and flat surfaces Most significant differences annotated with a *. (n = 3).

3.2.3 Tensile Strength Measurements

Tensile strength measurements of both surfaces determined that there was no statistically significant difference between the average tensile strength of the unmodified surface (18.332 Mpa) and the flattened surface (15.145 Mpa), despite the higher average obtained for the unmodified surface. Further, there was also no significant difference between the elongation percentage for the unmodified surface (329.760 %) and the flattened surface (358.720 %) (**Table. 3.1**).

Table 3.1 Tensile strength and elongation measurements for the unmodified and flattened surfaces with standard errors (n = 3).

	Tensile Strength (Mpa)		Elongation (%)	
Unmodified PVC	18.332	± 0.301	329.76	± 19.373
Flattened PVC	15.145	± 1.531	358.72	± 25.019

3.2.4 Energy Dispersive X-ray

EDX determined that all three surfaces had no significant differences in the atomic weight of their elemental makeup, typically between 78 % - 80 % Carbon, 12 % – 14 % Chlorine and 7 % - 8 % Oxygen (**Fig. 3.2**).

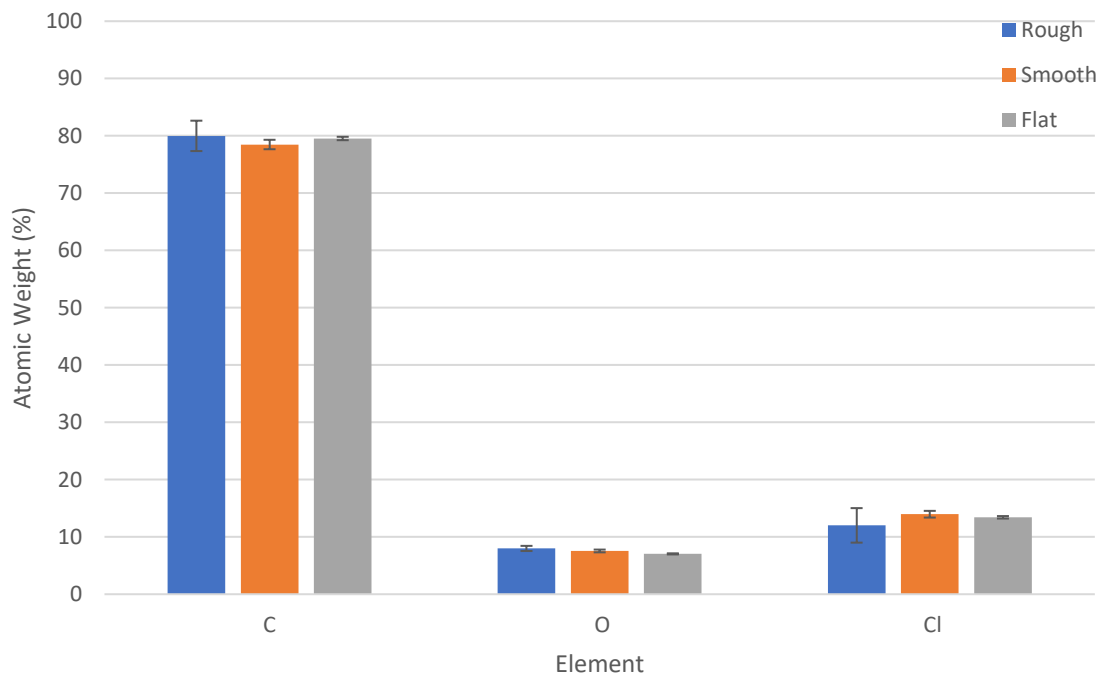


Figure 3.2 Energy Dispersive X-ray of the three surfaces demonstrating no significant difference in their elemental makeup (n = 3).

3.2.5 Attenuated Total Reflection- Fourier Transform Infrared Spectroscopy

The ATR-FTIR spectra of the surfaces were dominated by the major absorptions expected in p-PVC (**Fig. 3.3**). The most dominant were C-H stretching (centred at ca 2900 cm^{-1}), ester carbonyl stretching from the plasticiser (1740 cm^{-1}) and C-O bending of the plasticiser ester (1170 cm^{-1}). The C-Cl stretching vibration from the PVC itself at ca. 690 cm^{-1} was also present. Two very small absorptions appeared between the phthalate ester carbonyl stretch and the C-H bending vibration of the PVC / plasticiser at 1458 cm^{-1} (see **Fig. 3.3** inset). The smooth unmodified surface (**Fig. 3.3a**) showed two small absorption peaks at 1576 cm^{-1} and 1541 cm^{-1} , however, on the rough unmodified surface (**Fig. 3.3b**) only one peak at 1539 cm^{-1} was evident. Interestingly both peaks were absent on the flattened surface (**Fig. 3.3c**). The peak positions matched the antisymmetric $\nu_{\text{as}}\text{COO}^-$ stretching vibration of carboxylate groups in unidentate (1577-1575 cm^{-1}) and bidentate (1544-1540 cm^{-1}) coordination with calcium (Gönen *et al.*, 2010). The carboxylate carbonyl absorptions for the zinc stearate were simpler, just a single peak at ca 1540 cm^{-1} (National Institute of Standards and Technology (NIST) Web Book).

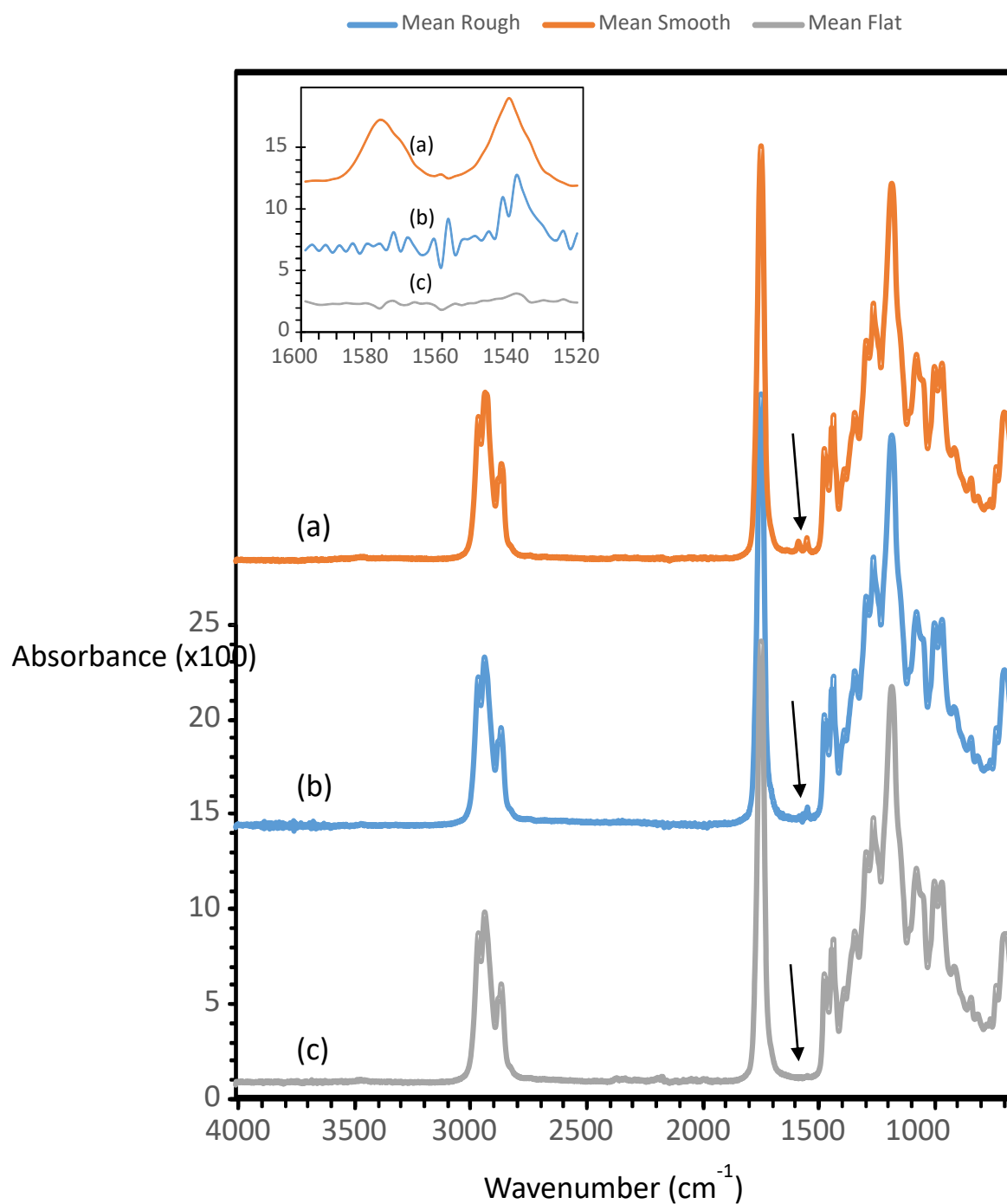


Figure 3.3 ATR-FTIR spectra (average of $n=3$) of transfusion bag surfaces; (a) unmodified smooth side, (b) unmodified rough side and (c) flattened surfaces. The carboxylate carbonyl antisymmetric stretching vibrations (at 1577 and 1544 cm^{-1}) are highlighted with arrows. ($n = 3$)

3.2.6 Raman Spectroscopy

Raman spectroscopy (**Fig. 3.4**) demonstrated no discernible differences in the peaks observed. The PVC was identifiable by the two peaks at 635 cm^{-1} and 695 cm^{-1} representing the C-Cl stretching vibration bonds and the high intensity determined at 2916 cm^{-1} was assigned to the stretching vibrations of the C-H bonds present in the PVC (Solodovnichenko *et al.*, 2016). The peak around 1440 cm^{-1} also represents the C-H stretching, whilst the CH bending of the CHCl group was observed at 1326 cm^{-1} (Kerr *et al.*, 2013). The small peak around 1750 cm^{-1} was one of the characteristic peaks of phthalate esters, such as the DEHP present in the p-PVC bags (Nørbygaard and Berg, 2002).

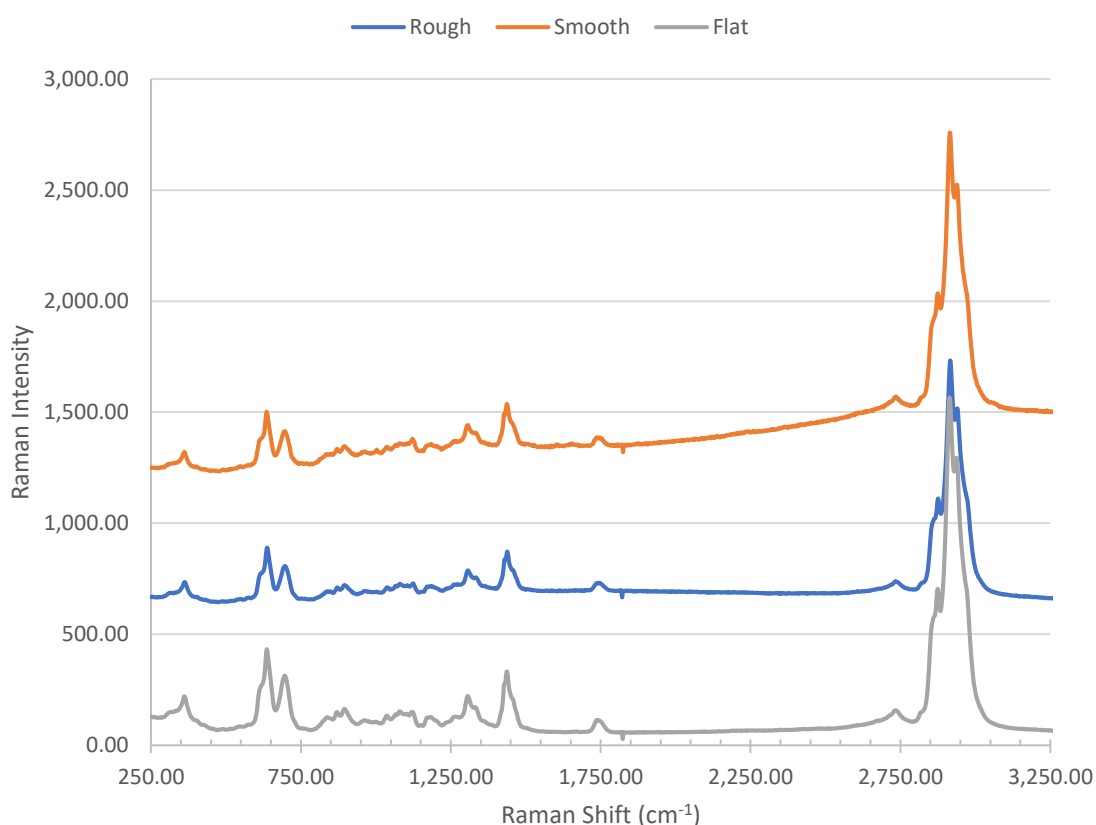


Figure 3.4 Raman spectroscopy of the three surfaces demonstrating no significant changes in the peaks. (n = 3)

3.2.7 Physicochemistry

Physicochemistry measurements between the smooth and rough surfaces demonstrated that there were no significant differences in the results (**Fig. 3.5**). An increase in the Gibbs Free (ΔG) (**Fig. 3.5a**) energy (to -40.2 mj/m^2) demonstrated that flattening of the surfaces resulted in the surface becoming less hydrophobic. However, the flat modified surface maintained similar Lifschitz van der Waals force (γ_{sLW}) (**Fig. 3.5c**) values (45.2 mj/m^2) as the unmodified (smooth (48.9 mj/m^2) and rough (45.6 mj/m^2)) surfaces. The higher base energy (γ_{s-}) (**Fig. 3.5e**) on all the surfaces (rough (7.3 mj/m^2), smooth (7.5 mj/m^2) and flat (9.7 mj/m^2)) demonstrated that the surfaces were electron donating rather than electron accepting. Flattening the p-PVC resulted in an increase in both the acid (γ_{s+}) (**Fig. 3.5e**) (from $0.4\text{-}0.5 \text{ mj/m}^2$ to 1.8 mj/m^2) and base (γ_{s-}) (**Fig. 3.5f**) (from $7.3\text{-}7.5 \text{ mj/m}^2$ to 9.7 mj/m^2) energies demonstrating the surfaces' ability to donate and accept electrons had both increased.

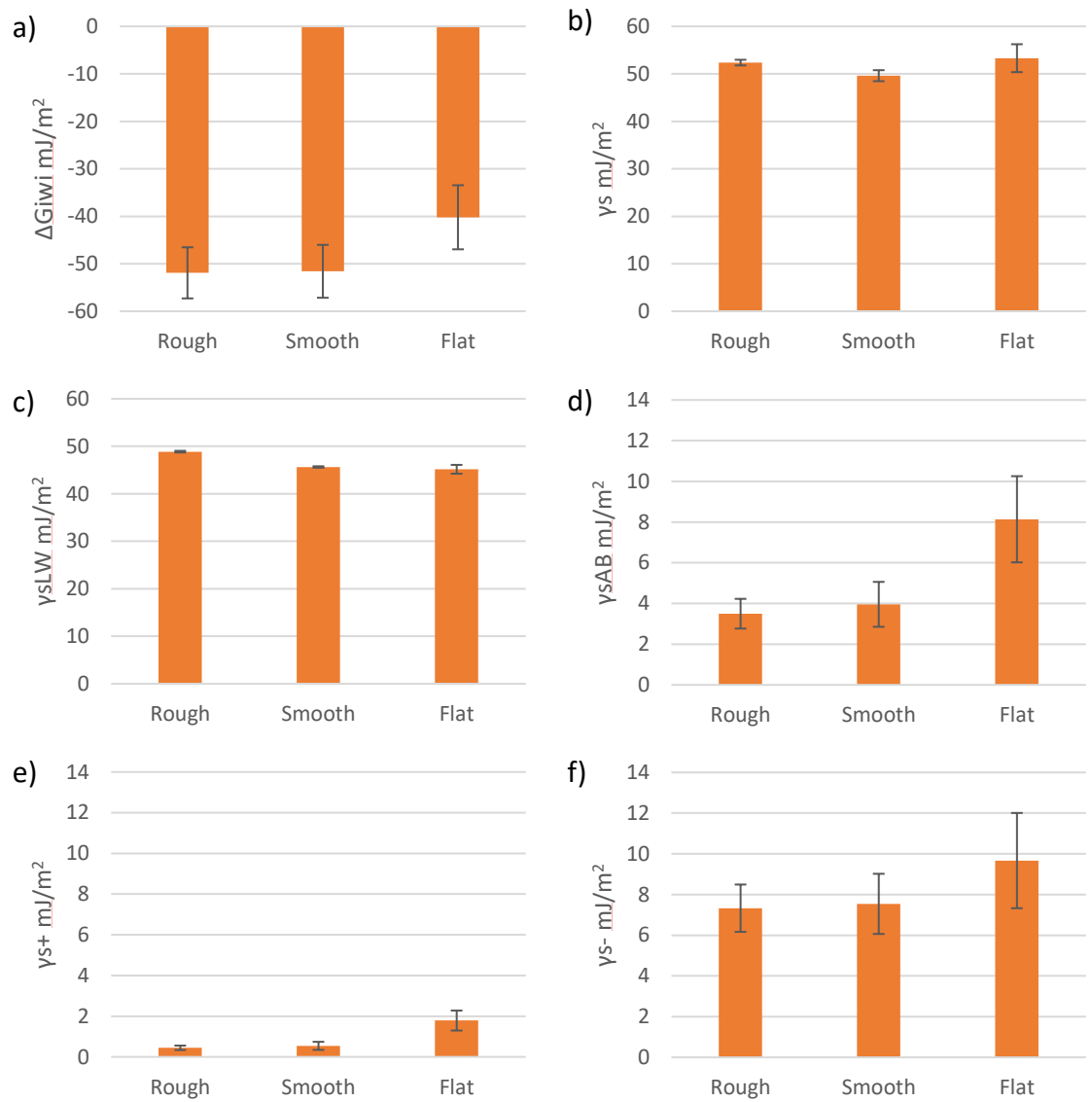


Figure 3.5 Physicochemistry results of the rough, smooth and flattened surfaces a) Gibbs free energy (ΔG), b) surface energy (γ_s), c) Lifschitz van der Waals forces (γ_{sLW}), d) acid base components (γ_{sAB}), e) acid component (γ_{s+}) and f) base component (γ_{s-}). Note that a, b and c are on the same scale and d, e and f are on a different scale. (n = 5)

3.2.8 Effect of LTAPP on Surface Physicochemistry

The rough, smooth and flattened surfaces were treated with LTAPP, via dielectric barrier discharge to determine whether this treatment could alter the surface physicochemistry of the polymer (**Fig. 3.6**). Analysis of the physicochemistry revealed that the overall surface energy of all the surfaces decreased after either 1 or 10 second treatments. Further, a reduction in the acid and base energies was observed, indicating a reduction in the surfaces ability to donate or accept electrons post treatment.

The stability of a surface in terms of its surface energy following LTAPP treatment was investigated to ensure that any alterations to the surface properties of the p-PVC were stable over time. The surface energy results following LTAPP treatment of the p-PVC demonstrated an inconsistent degeneration over time, where certain surface energies fluctuated up and down (**Fig. 3.7**). For example, the Gibbs Free energy increased from -31.88 mJ/m² to -23.16 mJ/m² after 24 h but then decreased to -29.67 mJ/m² after 48 h then increased again after 120 h to -12.01 mJ/m² before decreasing again to -18.53 mJ/m² after 168h.

It was important to determine whether the physicochemistry of the platelet bags was consistent between different bags within the same batch, and between different batches (**Fig. 3.8**). Only the Lifschitz van der Waals forces ($\gamma_s LW$) appeared to be consistent throughout, within the same batch or between batches. The Gibbs free energy (ΔG) has the highest variance of around 25 % difference between the lowest and highest values, whilst the acid base energies ($\gamma_s AB$) had the smallest variation value.

Whilst ATR-FTIR, Raman and surface roughness were measured for the LTAPP treated surfaces, their results did not differ from those of the untreated surfaces. Due to them being the same as the unmodified surfaces the data has not been presented.

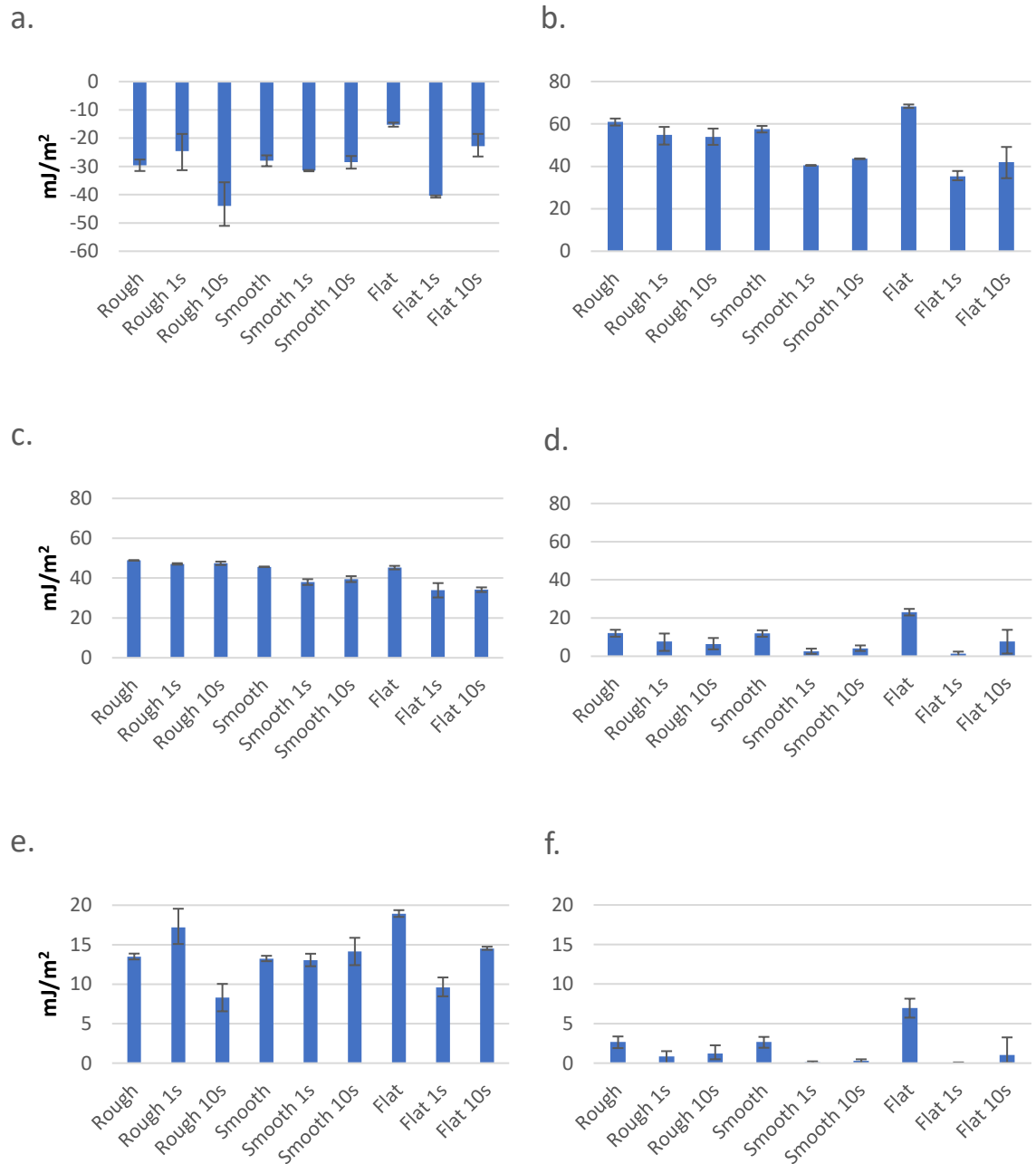


Figure 3.6 Surface energy results of untreated and plasma treated surfaces. Graphs represent a. Gibbs free energy (ΔG) b. total surface energy (γ_s) c. Lifschitz van der Waals forces ($\gamma_s LW$) d. acid base energies ($\gamma_s AB$) e. acid energy (γ_s+) and f. base energy (γ_s-). (n = 5)

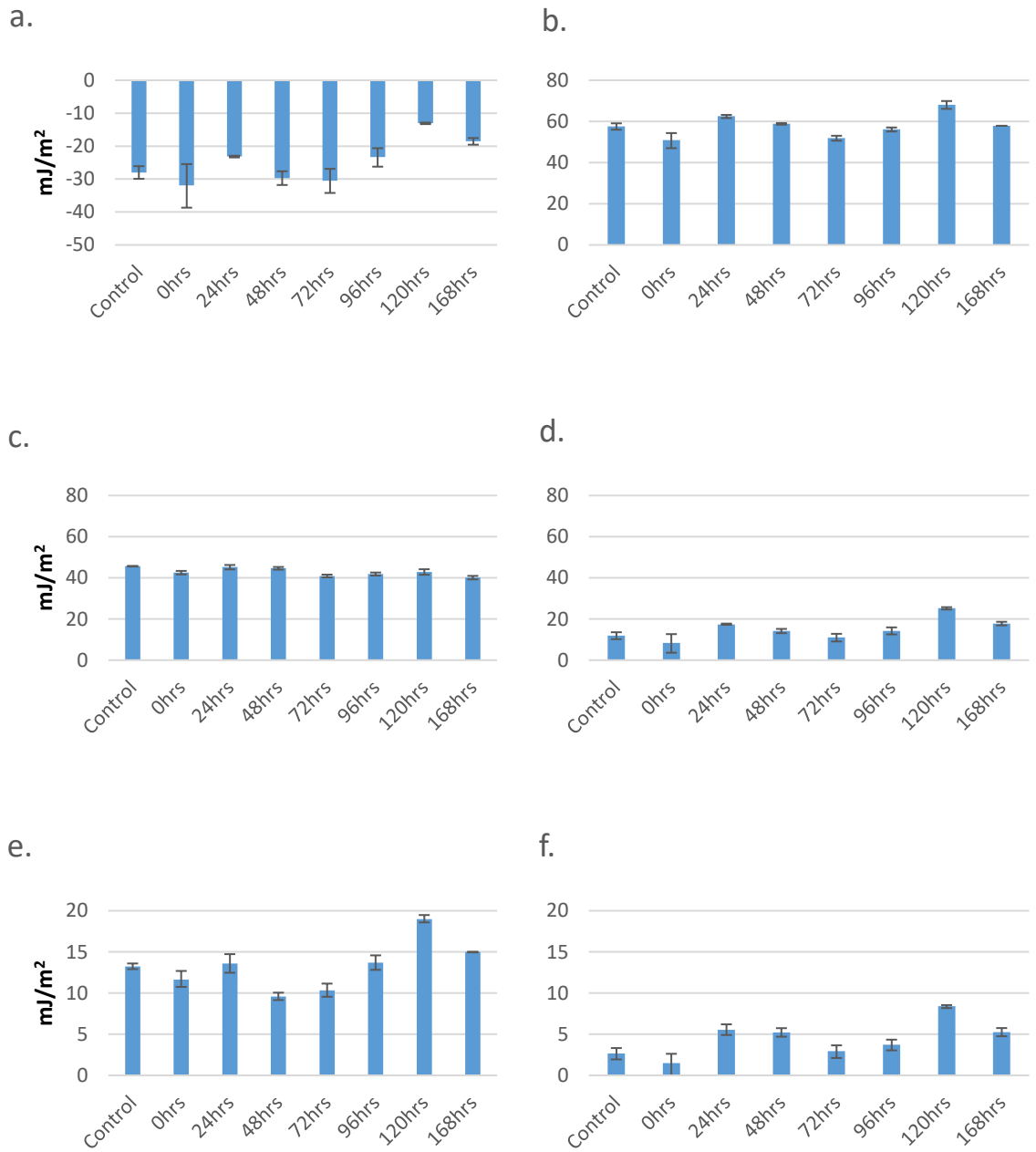


Figure 3.7 Surface energy results of plasma treatment degeneration over time. Graphs represent a. Gibbs free energy (ΔG) b. total surface energy (γ_s) c. Lifschitz van der Waals forces (γ_{sLW}) d. acid base energies (γ_{sAB}) e. acid energy (γ_{s+}) and f. base energy (γ_{s-}). (n = 5)

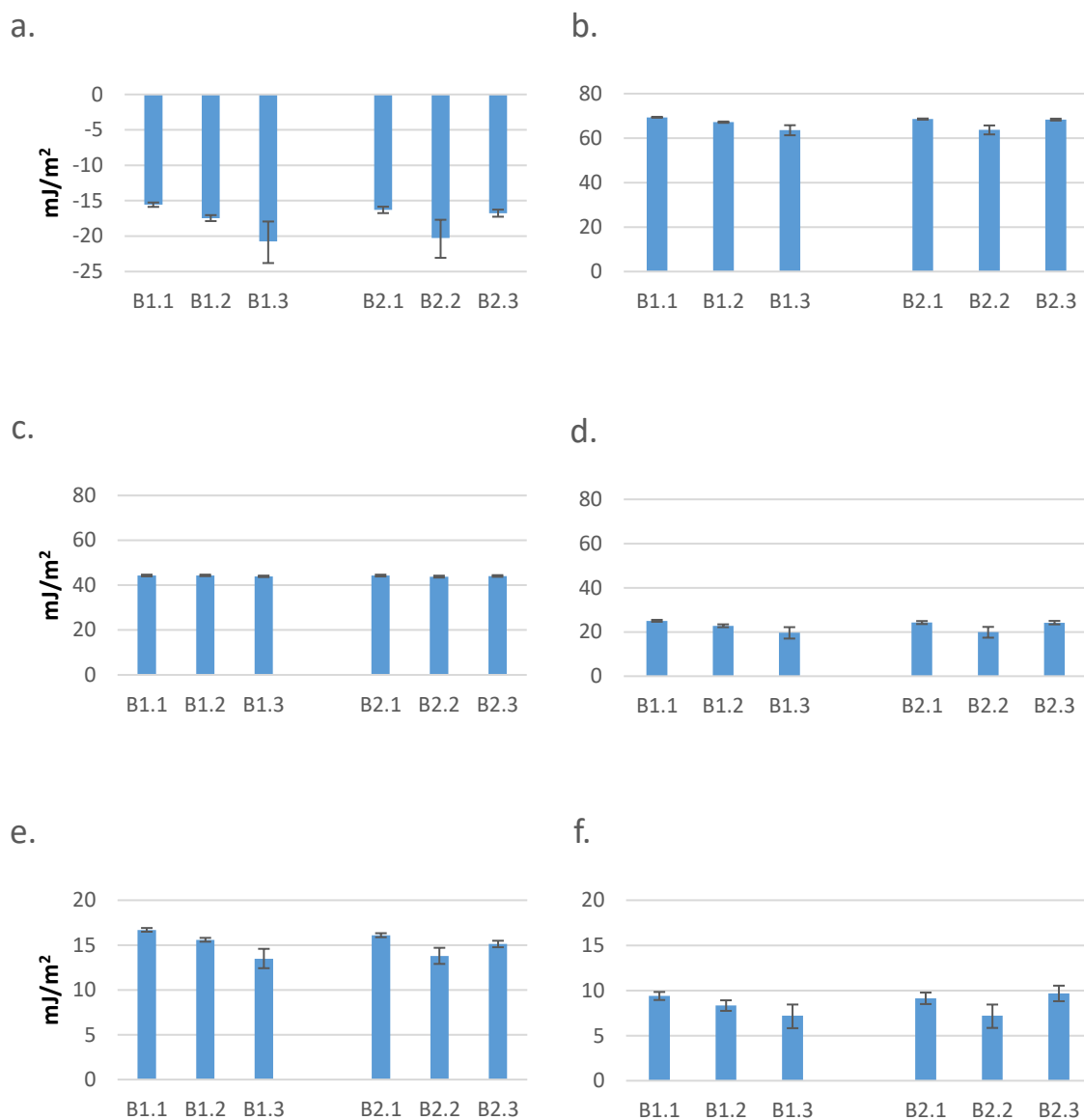


Figure 3.8 Surface energy results of different batches. Graphs represent a. Gibbs free energy (ΔG) b. total surface energy (γ_s) c. Lifschitz van der Waals forces (γ_{sLW}) d. acid base energies (γ_{sAB}) e. acid energy (γ_{s+}) and f. base energy (γ_{s-}). B1.1, B1.2 and B1.3 represent the three bags from batch one and B2.1, B2.2 and B2.3 represent the three bags from the second batch. (n = 5)

3.3 Discussion

3.3.1 Characterisation of Unmodified and Flattened p-PVC Surfaces

The surface properties of PC bags were characterised to determine the effect of a physical alteration, that was lowering the surface topography by flattening the surfaces using a hot press. Observations of the topography of the surfaces via SEM and optical surface profiling demonstrated that the diamond cross-print pattern observed on the rough surface demonstrated a highly roughened surface, whilst the flattening of the surface significantly reduced the overall surface roughness. This was significant as the preference for defined surface features by bacteria has been previously demonstrated, with increases in roughness linked to an increase in bacterial retention due to greater surface contact area between the surface and a bacterium (Whitehead *et al.*, 2005; Whitehead and Verran, 2006). The surface roughness did not appear to affect the surface energies, as the surface energy properties of both the rough and smooth surfaces were similar. However, the flattened surface which demonstrated no surface features did present differences in surface energies, indicating that the flattening procedure changed the surface energy. The changes observed in the surface energy of the flattened surface led to the surface having a reduction in hydrophobicity as well as increasing its overall ability to accept and donate electrons, whilst maintaining a preference for accepting electrons. These changes could reduce or increase bacterial adherence to the flattened surface, depending on the surface energy components of the bacteria themselves.

No significant changes were determined in the tensile strength between the unmodified and the modified surfaces, indicating that the ability of the modified surface to withstand handling had not been compromised despite physical modifications to the surfaces of the bags.

No significant changes were detected in the chemical composition of the three surfaces when analysed via EDX. This indicated that whilst some changes were detected in other surface analysis techniques, the chemical elements that made up the three surfaces were retained in similar proportions. Further, the slight changes that were visible were on the rough surface, which was likely caused due to the uneven surface potentially altering the emission of characteristic X-rays from its surface, but when the error bar was taken into account then no difference was determined.

The analysis of the surface chemistry via Raman and ATR-FTIR demonstrated that most of the spectra for all the surfaces were significantly similar, with only small differences determined in the ATR-FTIR spectra. Whilst the C-CL stretching vibration of PVC would be a strong band in non-plasticised PVC, the high level of plasticiser in the samples caused absorptions from the latter to dominate the spectrum. Aromatic C-H stretching and deformation absorptions (3060 cm^{-1} - 3100 cm^{-1} and 1600 cm^{-1} - 1580 cm^{-1} , respectively) were absent from the spectrum confirming that a phthalate plasticiser had not been used in this particular platelet bag formulation. Absence of phthalates was further supported by the specific wavenumber of the ester carbonyl stretching absorption; phthalate carbonyl groups absorb at ca. 1730 cm^{-1} , whereas adipate and sebecate carbonyl groups absorb at ca 1740 cm^{-1} (Wypych, 2017).

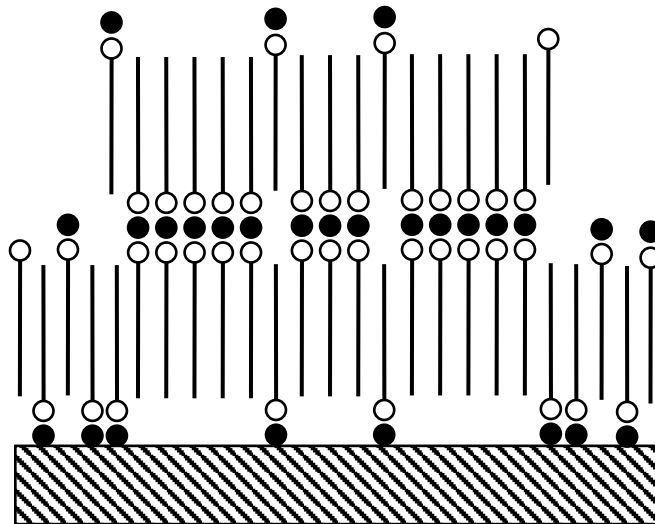
The two carboxylate carbonyl peaks (1576 cm^{-1} and 1541 cm^{-1}), indicated the presence of calcium / zinc stearates on the surface and / or within ca. $1.8\text{ }\mu\text{m}$ of the surface, and were present for the smooth, and to a degree the rough surfaces. However, after the flattening process the two carboxylate carbonyl absorptions were no longer present, suggesting that during the flattening process the calcium stearate either diffused more deeply (i.e., deeper than ca $1.8\text{ }\mu\text{m}$) into the p-PVC or was preferentially adsorbed on to the polyester

separating sheets, either way, calcium / zinc stearate could no longer be resolved by ATR-FTIR. An identical observation has been made by Bodecchi *et al.* (2005) in ATR-FTIR studies on plasticised PVC that had been sterilised by γ -irradiation, where it was argued that the stearate diffused further into the p-PVC. Combinations of calcium and zinc stearates have been reported to form complexes during the stabilisation of PVC, with the combined carboxylate carbonyl stretching vibrations of the complex resulting in an absorption at 1600 cm^{-1} , but no such absorption was evident (Benavides *et al.*, 1995). This indicated that the stearates had been removed or diffused deeper into the substrate, rather than becoming complexed / combined because of elevated temperatures experienced by the p-PVC during the flattening operation. The spectrum of the rough surface was noisier than the smooth and flat surface due to the rough surface having an impaired contact with the internal reflection element of the ATR accessory.

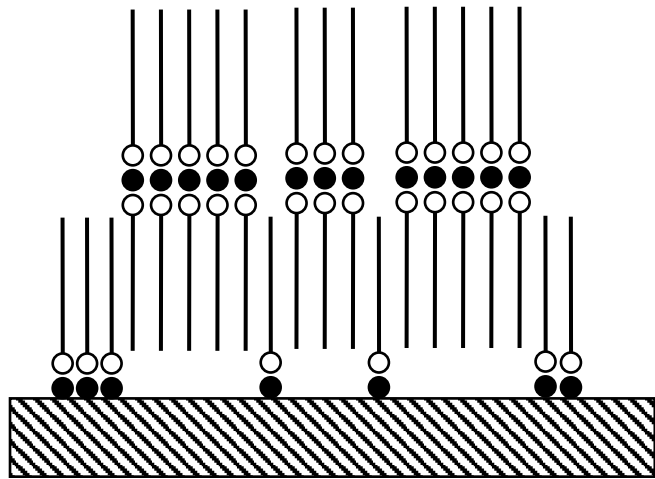
The contact angle measurements demonstrated that the unmodified surfaces had lower surface energies than the flattened surface, and this observation indicated that a fraction of the stearates had bloomed to the surface of the unmodified substrates; the increase in surface energy of the flattened substrate is corroborated by the absence of stearates on this sample. As the p-PVC had a relatively polar surface it may be that the bloomed calcium / zinc stearates were adsorbed with the carboxylate groups facing the surface, leaving the stearyl ($\text{C}_{17}\text{H}_{35}$) tails pointing away from the surface. The latter may account for the unidentate form of calcium stearate, absorbing at ca. 1576 cm^{-1} . If the local surface concentration of calcium stearate was high enough, the stearyl tails of the bidentate form (absorbing at ca. 1541 cm^{-1}) in the form of a bi-layer with Ca^{2+} ions in between, could incorporate the unidentate forms in wax-like self-assembled surface structures (Lu and Miller, 2002). Such structures could have contributed to the reduced surface energy of the

unmodified surfaces. The marginally higher values of γ^- , γ^+ and γ_s^{AB} obtained for the smooth unmodified surface, relative to the rough unmodified surface, may have been due to incorporation of some unidentate carboxylate, with the carboxylate group pointing away from the p-PVC, within the self-assembled structures. The rough unmodified surface showed only one carboxylate absorption at 1539 cm^{-1} , indicating the presence of bidentate calcium stearate, possibly with a small amount of zinc stearate. However, a uniform monolayer of stearate composed of stearyl chains, pointing away from the substrate in a self-assembled array, will have a very low surface energy of $22\text{-}24\text{ mJ/m}^2$. However, the latter here was clearly not the case and the implication is that the surface coverage with calcium / zinc stearate was not uniform (Shafrin and Zisman, 1960). It may be that the stearates exist as micron-scale patches on the surface of the p-PVC.

Unlike FTIR, Raman spectroscopy demonstrated no noticeable differences in the spectrum obtained for all three surfaces. This may be due to how Raman works in comparison to FTIR, such as Raman spectroscopy measuring relative frequencies whilst FTIR measures absolute frequencies. Further, FTIR is sensitive to hetero-nuclear functional group vibrations and polar bonds, especially OH stretching, which may have enabled FTIR to detect the changes in the stearyl chains whilst Raman spectroscopy did not.



(a)



(b)

Figure 3.9 Schematic representation of possible adsorbed structure of calcium stearate on the unmodified p-PVC surfaces. The straight lines represent the $C_{17}H_{35}$ chains, the open circles represent the carboxylate group (COO^-) and the closed (black) circles represent the calcium (Ca^{2+}) ions (adapted from) (Lu and Miller, 2002).

3.3.2 Effect of LTAPP on Surface Physicochemistry

The fluctuating surface energies observed when testing plasma degeneration over time demonstrated that this method could not be used in its current form to modify the p-PVC platelet bags. Since there was variability across a single bag, it was difficult to differentiate the effect the plasma had on the surfaces. However, whilst the surface energy readings of the unmodified platelet bag fluctuated, they appeared to be between a selected range of values. Thus, using plasma treatment on this surface with such variables could lead to unexpected and unreliable data. However, it may be possible to use on a more controlled surface.

3.4 Conclusion

The results demonstrated that hot pressing the p-PVC surface significantly reduced the surface topography that was observed using SEM and optical surface profiling, whilst maintaining surface tensile strength. Further, the surface chemistry remained mostly unchanged, with only a change in two small peaks determined by FTIR and no changes via Raman spectroscopy. Physicochemical measurements determined more changes in the flattened surface, with increases in both the Gibbs free energy and the acid-base energies observed. Finally, atmospheric plasma treatment of the surfaces was determined to be unsuitable due to the inconsistency and fluctuation observed in the treated surfaces over time.

4.0 Bacterial Attachment and Biofilms

4.1 Introduction

Bacterial adhesion and biofilm formation is a very complex and multifactorial process, with differences in the bacteria, the surface and the environment all contributing to biofilm development (Desrousseaux *et al.*, 2013). Initial weak adhesion to a surface originates mostly from Lifshitz Van der Waals forces, but is also influenced by surface and bacterial hydrophobicity and their electrostatic properties (Busscher and van der Mei, 2012). Once weakly adhered, a stronger adherence is established via the use of cell adhesin structures, such as pili, flagellum or adhesive substances (Persat *et al.*, 2015). These cell adhesin structures may make it significantly more difficult to remove the bacteria and they start to produce an extracellular polymeric substance, or 'slime', which encases the bacterial community (Donlan, 2002; Busscher and van der Mei, 2012). This extracellular substance is usually primarily composed of polysaccharides, but can also contain DNA, lectins, lipids and proteins (Bjarnsholt, 2013). Upon biofilm maturation, the bacterial population can communicate via quorum sensing (QS), which allows the biofilm to regulate gene expression and overall behaviour, leading to increased resistance to antimicrobials and altered proliferation (Miller and Bassler, 2001). This ability to communicate within a biofilm is not limited to just a single species but allows communication across multiple species contained within a given biofilm (Miller and Bassler, 2001).

Of the two species used throughout this work, both demonstrated different cell adhesion methods other than physical cell structures such as pili. The adhesions used for attachment to a surface also differs depending on the surface type, as one study found that *Ser. marcescens* attachment to an abiotic surface was regulated by the QS based *N*-acyl

homoserine lactone whilst the biotic surface was not. However, the study also discovered that two genes, *bsmA* and *bsmB*, were involved in both biotic and abiotic surface adhesion. The study also discovered that QS regulated two other cell surface adhesins, exopolysaccharide and outer membrane protein OmpX (Labbate *et al.*, 2007). *S. epidermidis* has multiple cell adhesion mechanics, especially a few that enable it to adhere to plastics such as autolysin AtlE, as an *S. epidermidis* mutant with a defect of an *atlE::Tn917* transposon lost its ability to adhere to plastic surfaces (Heilmann *et al.*, 1997). However, it may be that the effect of AtlRE on attachment is secondary as activation of AtlE induced significant changes in cell surface hydrophobicity (Otto, 2014). Further, *S. epidermidis* biofilms contain polysaccharide intercellular adhesion (PIA), which is mediated by *icaADBC*, that increases the adherence of *S. epidermidis* to polymers (de Allori *et al.*, 2006; Frank *et al.*, 2007).

This chapter aimed to demonstrate how changes in the surface properties can alter how bacteria interact with the surface and form biofilms.

4.2 Results

4.2.1 Scanning Electron Microscopy

SEM of the surfaces with bacteria demonstrated that the density of *Ser. marcescens* and *S. epidermidis* was similar on all surfaces (**Fig. 4.1**). The bacteria were observed to be clumped in and around the pits of the rough surface with fewer cells spread around the other surface features (**Fig. 4.1a/b**). The number of cells present on the smooth surface appeared significantly reduced, and most cells formed small clusters (**Fig. 4.1c/d**). On the flat surface, both species demonstrated very low coverage with only a few cells visible (**Fig. 4.1e/f**).

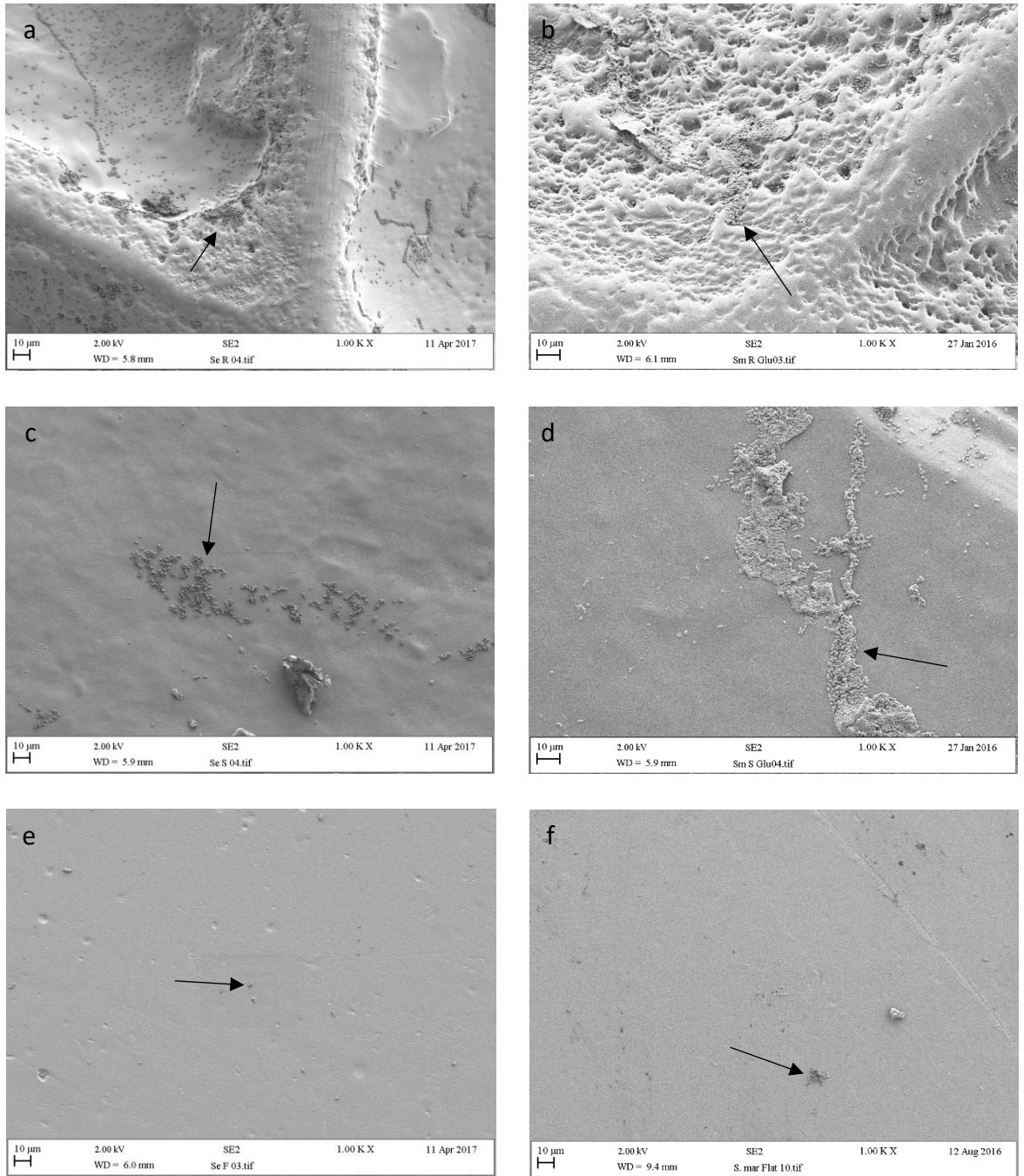


Figure 4.1 SEM images of the inoculated p-PVC platelet bags a/b) rough (inside facing), c/d) smooth (inside facing) and e/f) flattened surfaces. Images a,c and e contain *S. epidermidis* and images b, d and f contain *Ser. marcescens*. Black arrows indicate bacterial cells.

4.2.2 Microbial Adhesion to Hydrocarbons (MATH) Assays

The MATH assay for *Ser. marcescens* (**Fig. 4.2a**) demonstrated a low affinity for the apolar n-alkanes decane (6.33 %) and hexadecane (5.24 %), whilst having a moderate affinity for the acidic (Lewis-acid) solvent chloroform (43.97 %) and the basic (Lewis-base) solvent ethyl acetate (50.12 %). Pairs were chosen as having one polar and one non-polar liquid, both with similar Lifschitz van der Waals forces (Bellon-Fontaine *et al.*, 1996). The extremely low affinity (< 10 %) towards both non-polar hydrocarbons decane and hexadecane determined that *Ser. marcescens* was highly hydrophilic, which was supported by the bacteria having a greater affinity to the polar solvents chloroform and ethyl acetate (Min *et al.*, 2006; Skovager *et al.*, 2012; Szlavik *et al.*, 2012). The stronger affinity for both of the polar solvents (chloroform and ethyl acetate) when compared with their non-polar counterpart (hexadecane with chloroform and decane with ethyl acetate) further indicated that *Ser. marcescens* was both a moderate electron donor and a moderate electron acceptor (Skovager *et al.*, 2012). However, when compared in their pairs (chloroform and hexadecane against ethyl acetate and decane), the value for ethyl acetate and decane was higher, which demonstrated that the bacteria were better electron donors than acceptors (Skovager *et al.*, 2012). This was further supported by the higher affinity to chloroform than to hexadecane (Bellon-Fontaine *et al.*, 1996).

In contrast, *S. epidermidis*' MATH assay results (**Fig. 4.2b**) were significantly different to that of *Ser. marcescens*, demonstrating a high affinity to the apolar n-alkanes decane (98.21 %) and hexadecane (97.76 %) whilst also having a high affinity to the acidic solvent chloroform (98.44 %). The high affinity (> 55.00 %) to both non-polar hydrocarbons decane and hexadecane determined that *S. epidermidis* was highly hydrophobic. This was supported by the higher combined affinity to the non-polar hydrocarbons (decane and

hexadecane) when compared against the polar hydrocarbons (chloroform and ethyl acetate). The significantly higher affinity of *S. epidermidis* to the acidic solvent chloroform compared to the basic solvent ethyl acetate (30.67 %) indicated that the bacteria were strong electron donors. *S. epidermidis* as an electron donor was further supported by a higher combined value of chloroform and hexadecane compared to ethyl acetate and decane. *S. epidermidis* also had a moderate affinity to the basic solvent ethyl acetate indicating that whilst it was a strong electron donor it also had moderate electron accepting properties. This determined that *S. epidermidis* was highly hydrophobic and was a strong electron donor, with lesser electron accepting properties.

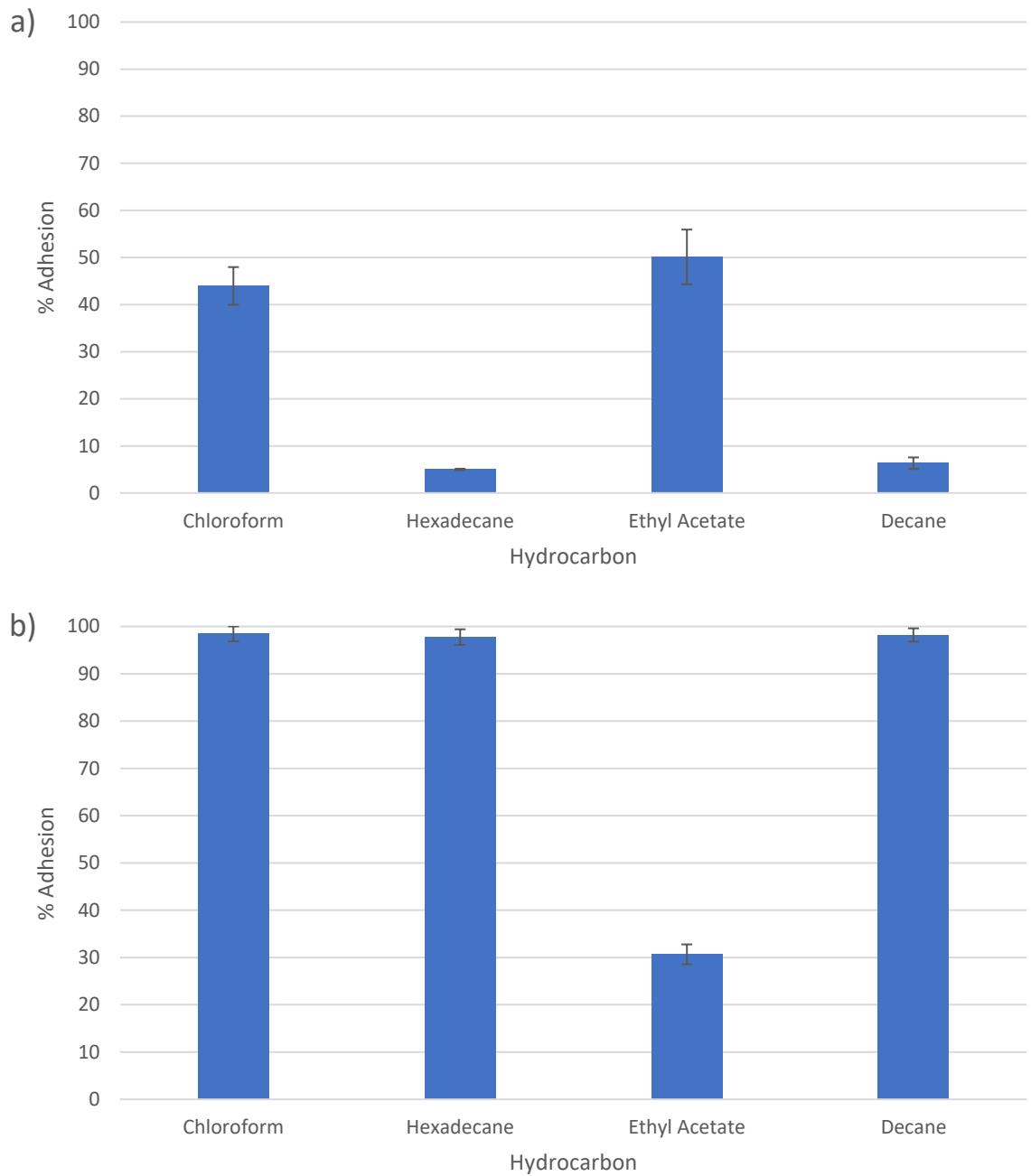


Figure 4.2 MATH assays of a) *Ser. marcescens* and b) *S. epidermidis* demonstrating affinity to the apolar n-alkanes decane and hexadecane and to the solvents chloroform (acidic) and ethyl acetate (basic). (n = 3)

4.2.3 Biofilms at 22 °C

Biofilm growth of both *Ser. marcescens* and *S. epidermidis* following incubation in platelet storage conditions (22 °C) on the p-PVC for 5 or 7 days was assessed using a crystal violet assay (**Fig. 4.3**). Following 5 days' incubation, *Ser. marcescens* demonstrated a significant decrease in the amount of biofilm formed on the flattened (1.75) surface when compared to the rough (3.26) or smooth (2.94) surfaces (**Fig. 4.3a**). Whilst a decrease in the amount of growth on the flattened (2.60) surface compared to with that on the rough (3.66) surface was observed at day 7, it was less apparent than after 5 days, and no significant decrease was observed between the smooth and flat surfaces after 7 days (**Fig. 4.3a**). Similarly, *S. epidermidis* demonstrated a reduced growth on the flat (1.06) surface compared to the rough (1.96) and smooth (1.42) surfaces after 5 days of incubation, despite demonstrating significantly less growth overall (**Fig. 4.3b**). However, after 7 days' incubation there was no significant difference between the rough (2.13), smooth (1.94) or flat (2.04) surfaces (**Fig. 4.3b**).

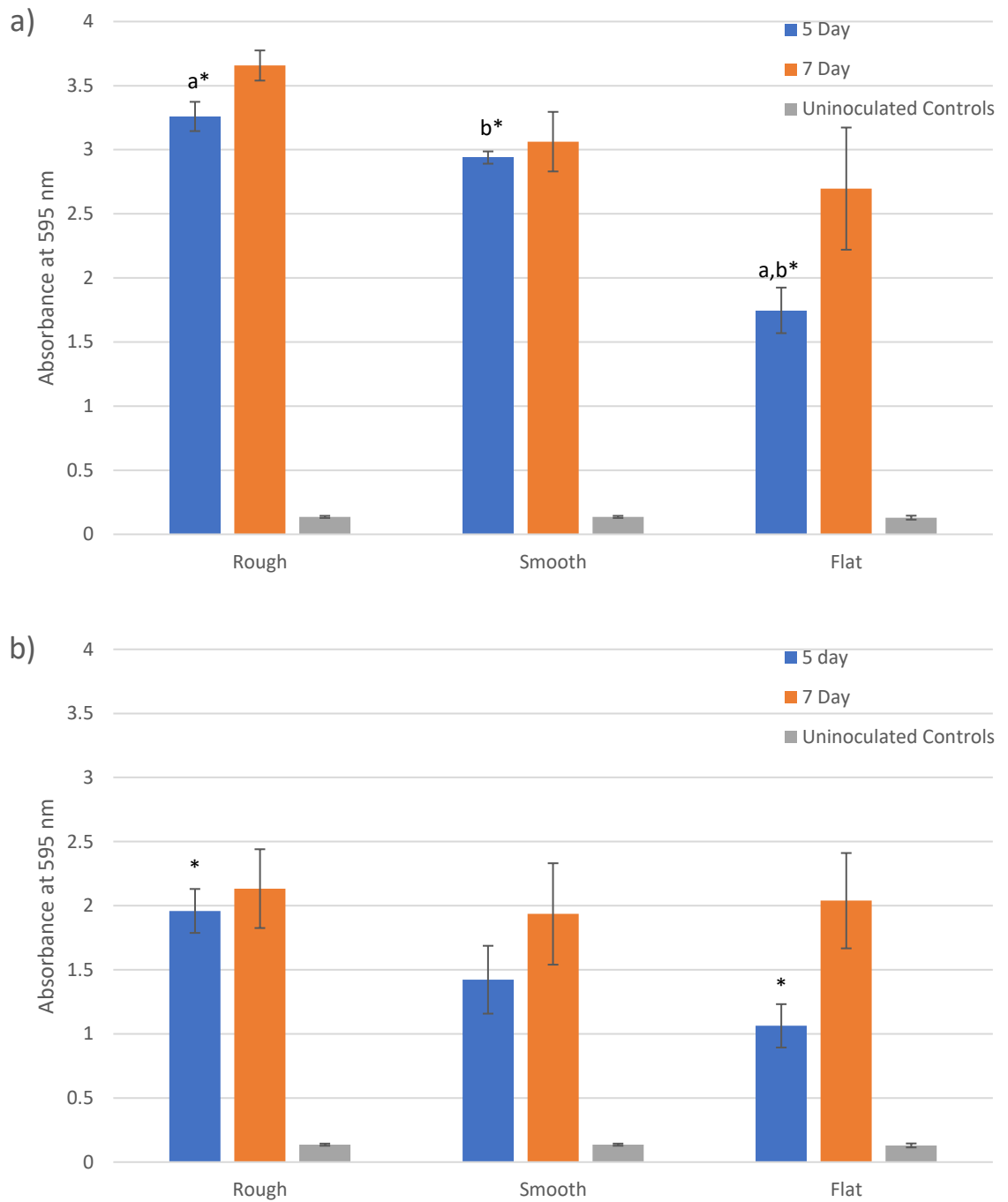


Figure 4.3 Five and seven-day biofilm growth of a) *Ser. marcescens* and b) *S. epidermidis* on the unmodified (rough and smooth) and flattened p-PVC surfaces at 22 °C. The control surfaces followed the same procedure but were inoculated with sterile distilled water. Most significant differences annotated with a *. (n = 6)

4.2.4 Biofilms at 37 °C

Biofilm growth of both *Ser. marcescens* and *S. epidermidis* following incubation at 37 °C on the p-PVC for 5 or 7 days was assessed using a crystal violet assay as previously described (**Fig. 4.4**). Following 5 days' incubation, *Ser. marcescens* demonstrated a significant decrease in the amount of biofilm formed on the flattened (0.49) surface when compared to the rough (1.24) or smooth (1.10) surfaces (**Fig. 4.4a**). A reduction in the amount of growth on the flattened (0.86) surface compared to both the rough (1.70) and smooth (1.41) surfaces was also observed at day 7 (**Fig. 4.4a**). However, whilst *S. epidermidis* appeared to demonstrate a reduced growth on the flat (2.40) or smooth (2.38) surface compared to the rough (2.87) surfaces after 5 days of incubation, it was not a significant difference (**Fig. 4.4b**). Further, after 7 days' incubation the difference was reduced between the rough (3.06), smooth (2.79) or flat (2.55) surfaces (**Fig. 4.4b**).

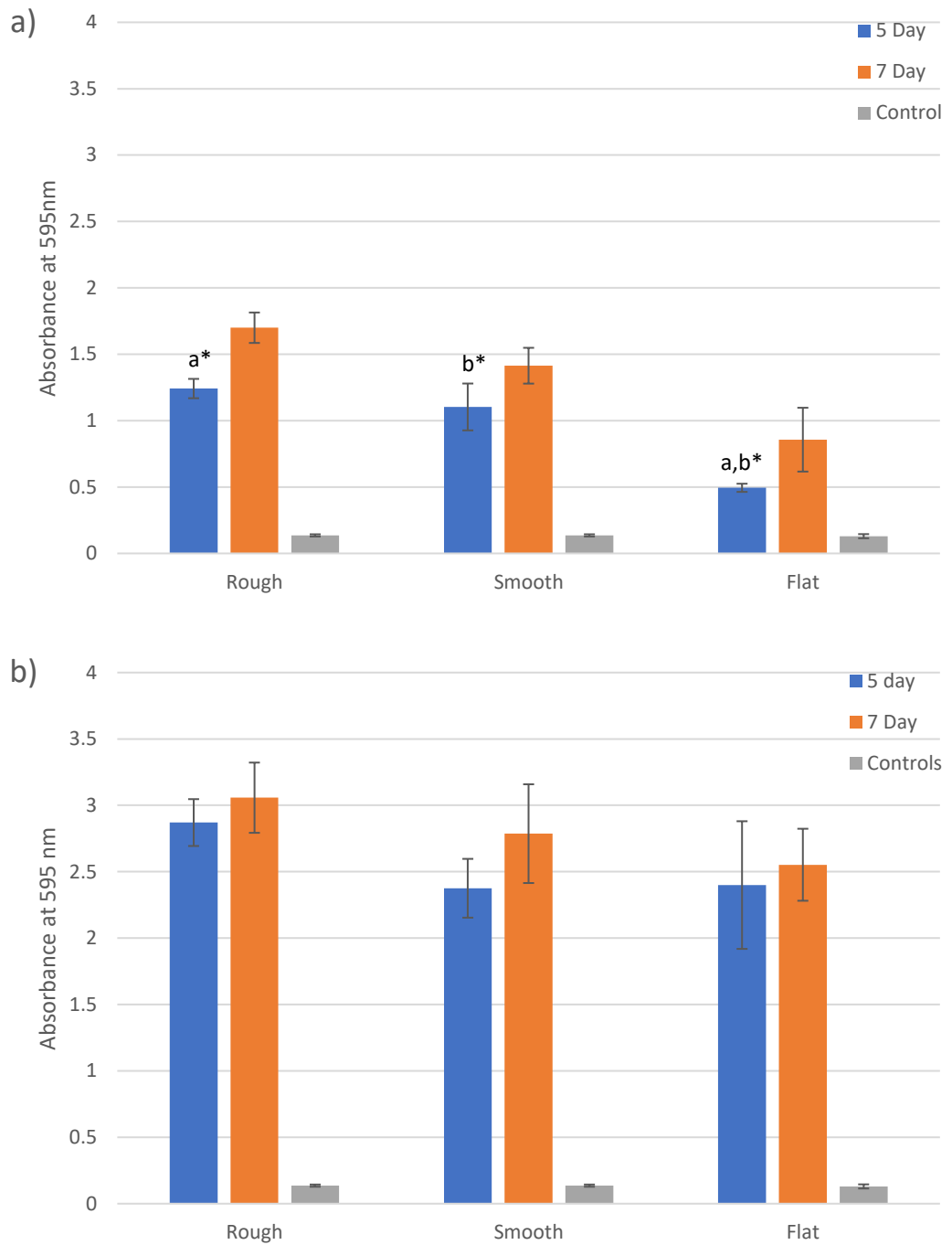


Figure 4.4 Five and seven-day biofilm growth of a) *Ser. marcescens* and b) *S. epidermidis* on the unmodified (rough and smooth) and flattened p-PVC surfaces at 37 °C. The control surfaces followed the same procedure but were inoculated with sterile distilled water. Most significant differences annotated with a *. (n = 6)

4.3 Discussion

The biofilms were grown for 5 or 7 days to simulate the real time spans that platelets are stored between. When observing biofilm growth at 22 °C of both bacterial species on the smooth and flattened surfaces and comparing this with growth observed on the rough surface, it was demonstrated that there was significantly more growth on the rough surface. The only exception to this was after 7 day's incubation with *S. epidermidis* where no significant differences were determined. Since the chemistry and physicochemistry of the rough and smooth surfaces were the same, this could only be due to a topographical effect with respect to the smooth surface. The similar growth on all the surfaces after 7 day's incubation with *S. epidermidis* may have been caused by a build-up of conditioning film and cells after the 5 days which meant that any surface topography, chemistry or physicochemistry effects on biofilm growth were negated. When the biofilms were grown at 37 °C, fewer differences were observed between the three surfaces. Whilst *Ser. marcescens* still demonstrated a difference in biofilm growth observed on the flat surface, *S. epidermidis* demonstrated no significant differences between any of the surfaces. This may be due to the higher temperature increasing growth and reducing any limitation the surfaces may have had on the growth ability of the organism.

The effect of flattening the surface resulted in the most pronounced biofilm reduction with *Ser. marcescens* after 5 days at 22°C. It is suggested that for *Ser. marcescens*, which demonstrated moderate electron donor and accepting properties, as well as highly hydrophilic properties, the reduction in hydrophobicity of the flattened surface reduced initial adherence of the bacteria to the surface (Bellon-Fontaine *et al.*, 1996; Min *et al.*, 2006; Skovager *et al.*, 2012; Szlavik *et al.*, 2012). However, the reduced biofilm growth could also be due to the lack of features present on the flattened surface which reduced

surface area contact between the bacteria and the surface. A combination of both factors was most likely to be the cause of the lowered retention of *Ser. marcescens* to the flattened surface. However, it is difficult to determine which surface parameter had the most influence.

With respect to *S. epidermidis*, this organism was found to be highly hydrophobic and have strong electron donor properties. Therefore, it would not be unreasonable to assume that on the flattened surface which has reduced hydrophobicity and electron accepting properties, there would be an increase in total biofilm mass due to a potential initial increase (Dunlap *et al.*, 2005; Min *et al.*, 2006; Skovager *et al.*, 2012; Szlavik *et al.*, 2012). However, our results demonstrated initial decreased biofilm growth on the flattened surface when compared to the rough after 5 days, which may be attributed to the lack of surface features. Further, it is uncertain as to how long the surface features would be able to contribute to biofilm growth and formation due to build-up of growth, as well as how viable the bacterial cells present in the biofilms would be.

Although data exists to support the theory that bacteria, which are generally negatively charged, will preferentially adhere to negatively charged surfaces, there are conflicting results in this area due to assays being carried out in a number of different ways and under different environmental conditions (Min *et al.*, 2006; Zeraik and Nitschke, 2010; Whitehead *et al.*, 2015). However, it is clear from the present study that a reduction in surface topography of the smooth and flattened surface resulted in a reduction in biofilm formation for both bacterial species after 5 days incubation, and after 7 days' for *Ser. marcescens*.

Over time, it appeared that the reduction of biofilm formation between the unmodified surfaces and the flattened surface was lessened as the reduction in growth was much

greater at the 5-day point than what was observed after 7 days. This may be due to a build-up of adhered cells to the surfaces, which would gradually mask the underlying surface properties and allow adherence of further cells.

There is conflicting evidence regarding how significant the surface properties such as the roughness and physicochemistry are in determining bacterial retention, and hence biofilm formation. It has previously been determined that under the conditions of flow on p-PVC surfaces, bacterial adhesion was influenced by the surface roughness (Katsikogianni and Missirlis, 2004; Katsikogianni *et al.*, 2006). However, it has also been demonstrated that p-PVC surface colonisation by *Pseudomonas aeruginosa* and *S. epidermidis* was independent of surface roughness and wettability (Eginton *et al.*, 1995). Furthermore, previous work completed by our group has demonstrated that whilst hydrophobic bacteria tend to adhere more to a hydrophilic surface and vice versa, some bacterial species can adhere better to a surface that has the same wettability (Whitehead *et al.*, 2015).

4.4 Conclusion

Whilst reduction in biofilm growth was observed for *Ser. marcescens* at both temperatures, reduction was only observed for *S. epidermidis* at 22 °C after 5 days. Further, both organisms demonstrated different amount of growth depending on the temperature, with *Ser. marcescens* demonstrated greater growth at 22 °C and *S. epidermidis* demonstrating greater growth at 37 °C. It also appeared that neither surface chemistry or physicochemistry had a significant influence on the biofilm growths in this instance, with the topography, specifically the surface roughness, having the greatest influence on biofilm biomass.

5.0 Conditioning Films

5.1 Introduction

It has been well established that once a surface becomes exposed to the environment it immediately starts to adsorb a conditioning film and thus becomes fouled (Loeb and Neihof, 2009). This conditioning film acts as a layer between the surface and the environment, altering how the surface interface interacts with external materials (Garrett *et al.*, 2008). A significant area of research surrounding conditioning films is how they can influence and alter interactions between a surface and bacteria, with significant importance placed on their effects on bacteria. It is understood that a conditioning film on a surface can mask the underlying features of the surface and alter the ability of bacteria to be retained, with the adsorbed molecules potentially stimulating or decreasing bacterial attachment (Greco-Stewart *et al.*, 2013). However, it is also understood that the nature of the CF can vary significantly depending upon the conditions of the environment in which the substrate is within (Lorite *et al.*, 2011). For example, environment CFs can be formed on surfaces exposed to seawater as described by Loeb and Neihof (2009), but can also be formed by bodily fluids (such as blood, tears, saliva and urine) on biomaterials (Lorite *et al.*, 2011).

Due to a conditioning film's ability to alter the forces that enable the initial weak attachment of bacteria, such as Lifschitz van der Waals forces, before becoming adhered using adhesion structures it is important to understand how CFs affect attachment (Busscher and van der Mei, 2012). One study by Cardile *et al.* (2014) demonstrated that the addition of human plasma to media increased *S. aureus* biofilm formation, with differences in biofilm phenotypes and cell morphology also determined. However,

another study by She *et al.* (2016) demonstrated that human serum components had antibiofilm effects on *S. epidermidis* biofilms, but not on established biofilms. Further, a study by Linnes *et al.* (2012) demonstrated that surfaces conditioned with adsorbed fibronectin reduced the adhesion of *S. epidermidis* to a surface dependent upon the amount of adsorbed fibronectin. However, *S. epidermidis* can produce a binding protein that enables it to bind to a different human plasma component, fibrinogen, that has been conditioned onto a surface (Hartford *et al.*, 2001). These studies demonstrated the complexity of surfaces that have been conditioned and how they can significantly alter the interactions between bacteria and a substrate. Therefore, this chapter was aimed at demonstrating the importance of conditioning films their effects on surface properties.

5.2 Results

5.2.1 Scanning Electron Microscopy (SEM)

SEM images of *S. epidermidis* (**Fig. 5.1.1**) demonstrated that almost no bacteria were adhered to any of the surfaces following 1 h or 24 h incubation. However, debris was present which may have come from lysed bacteria. On the rough surfaces after 24 h, there appeared to be a significant amount of material on the surface within the pits present compared to the 1 h rough surface or the control surface, which looked as though there may be bacteria retained within the surface features (**Fig. 5.1.1b**). Both the rough surface after 1 h and the smooth surface after 24 h (**Fig. 5.1.1a/d**) demonstrated what appeared to be a clump of bacteria on the surface, with the masses of bacteria bound together. However, whilst clumps also appeared on the 1 h flat surface the clumps appeared to be more likely to be dust without anything resembling bacteria.

When *Ser. marcescens* was imaged under SEM (**Fig. 5.1.2**) only the rough surface after 1 h (**Fig. 5.1.2a**) appeared to have any bacteria present. However, they appeared to be distorted in shape, perhaps indicating that the cell shape had become damaged. Further, little debris was found on the surfaces, with only the smooth and flat surfaces after 24 h (**Fig. 5.1.2d/f**) demonstrating a large amount of debris that may have come from lysed bacteria.

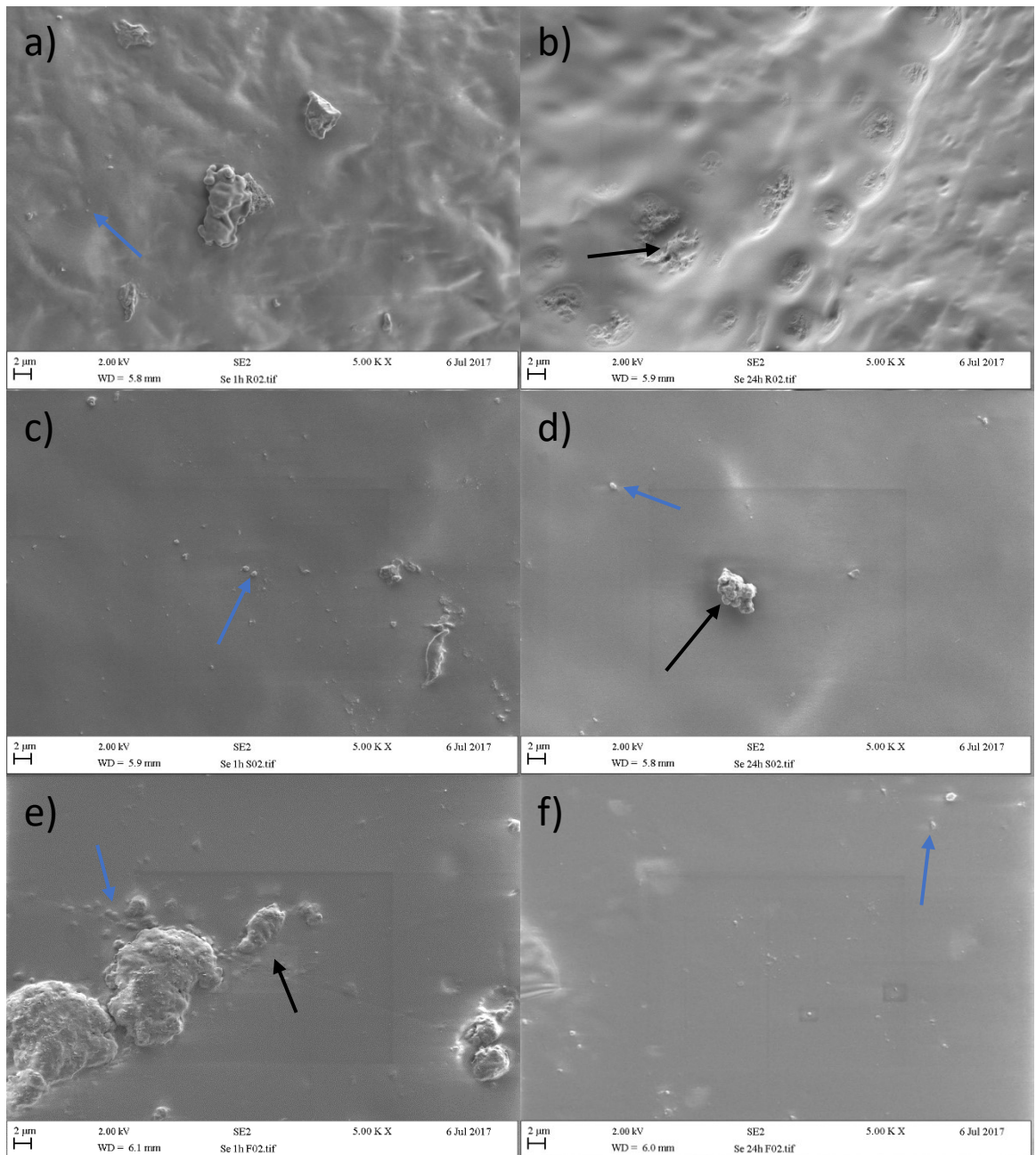


Figure 5.1.1 SEM of a/b) rough, c/d) smooth and e/f) flat images after 1h (a, c, e) or 24 h (b, d, f) incubation with a *S. epidermidis* conditioning film. Blue arrows represent bacterial cells and black arrows represent biomasses.

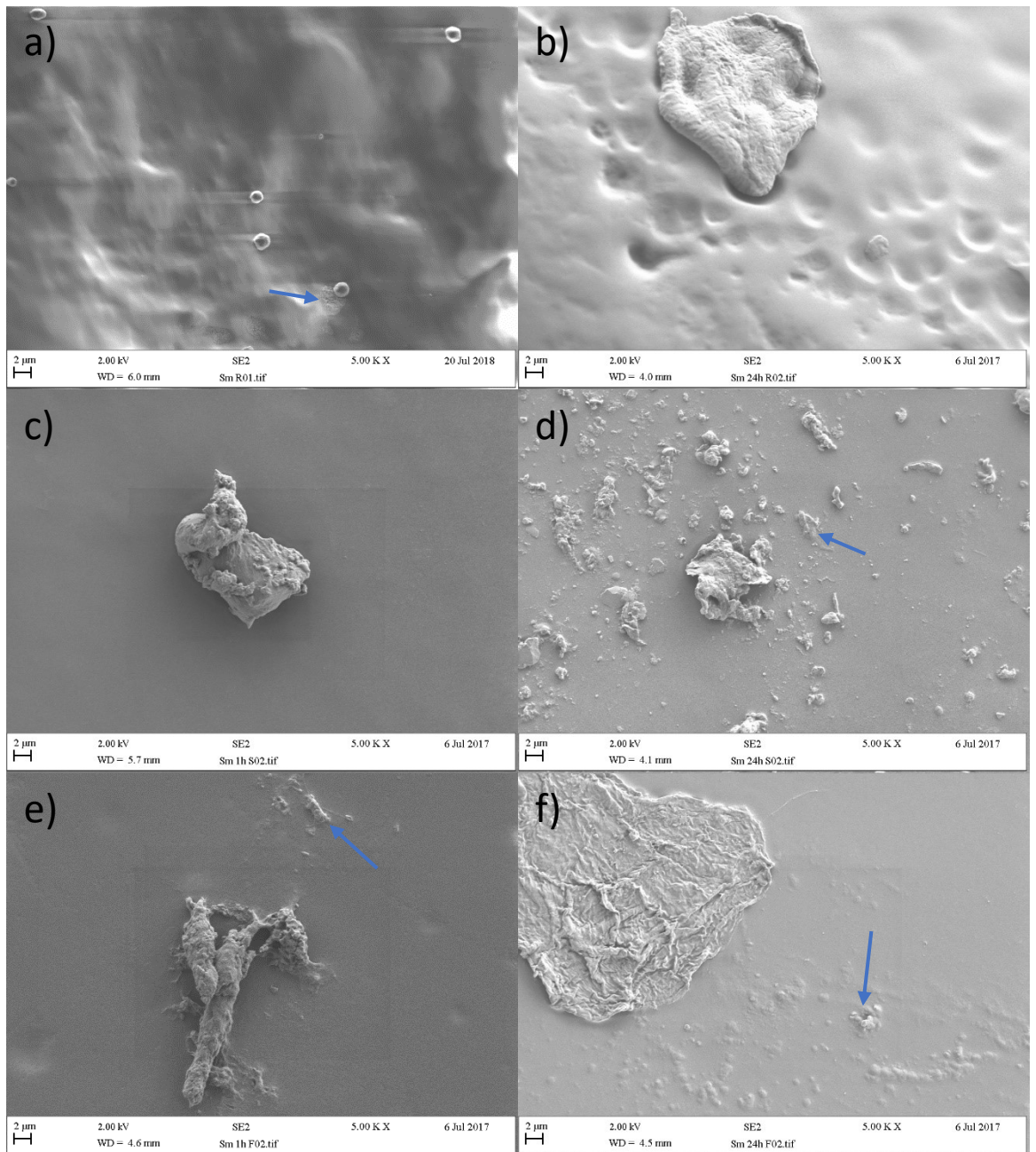


Figure 5.1.2 SEM of a/b) rough, c/d) smooth and e/f) flat images after 1h (a, c, e) or 24 h (b, d, f) incubation with a *Ser. marcescens* conditioning film. Blue arrows represent bacterial cells.

When the surfaces were fouled with a human plasma CF (**Fig 5.1.3**), as expected no bacteria were observed on the surfaces. However, all the surfaces had observable debris which was likely from adsorbing molecules, such as fibrinogen, fibrin or albumin, from the human plasma. Further, the rough surface after 24 h (**Fig. 5.1.3b**) demonstrated the most significant amount of debris/molecules adsorbed onto its surface, likely due to retention of the organic material in the surface features.

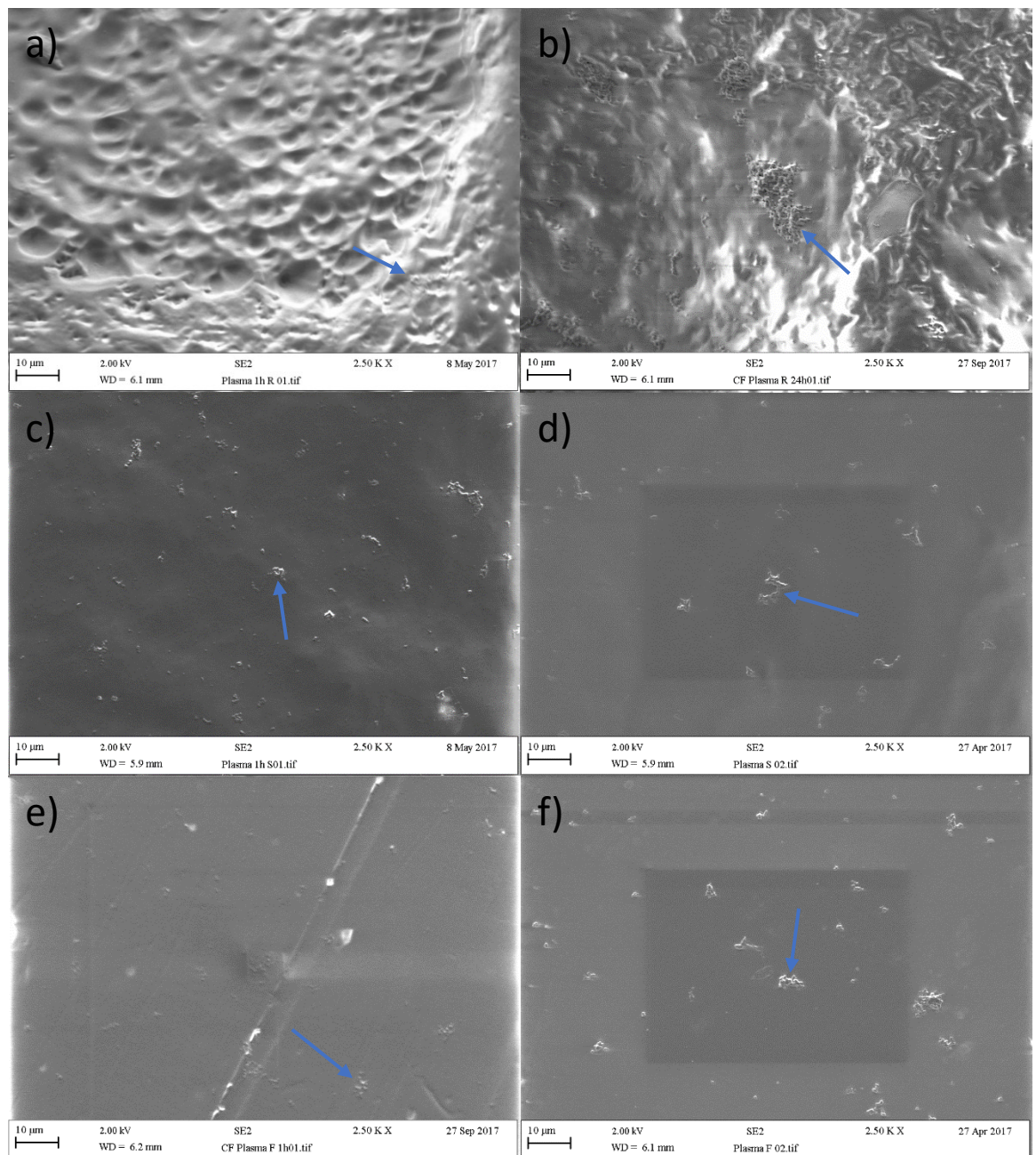


Figure 5.1.3 SEM of a/b) rough, c/d) smooth and e/f) flat images after 1h (a, c, e) or 24 h (b, d, f) incubation with a human plasma conditioning film. Blue arrows represent bacterial cells.

The combination of human plasma and *S. epidermidis* (**Fig. 5.1.4**) had both bacteria and particles from the human plasma observable on all the surfaces, with only the rough surface after 1 h (**Fig. 5.1.4a**) having no observable cells. Both the smooth and flat surfaces with a 1 h incubation (**Fig. 5.1.4c/e**) only had a low number of particles and only a few bacteria observable. However, after 24 h all the surfaces demonstrated a significant increase in bacteria and particles present on the surfaces. After 24 h the rough surface (**Fig. 5.1.4a**) demonstrated small clumps of bacteria that were concentrated around pits present on the surface with a spread of particles across the whole surface. The smooth surface after 24 h (**Fig. 5.1.4d**) demonstrated small clumps of bacteria on the surface with some particles present. Finally, the flat surface after 24 h (**Fig. 5.1.4f**) demonstrated a significant increase in the number of bacteria present, which again formed clumps, and a significant increase in particles spread over the surface.

When human plasma and *Ser. marcescens* were combined (**Fig. 5.1.5**) a substantial difference between the 1 h and 24 h CFs was observed. After 1 h, some particles and a few cells were observable on the surfaces, but the number of cells was significantly increased after 24 h. All three surfaces demonstrated a layer of cells spread over them with a 24 h incubation, with a coverage of greater than 50 %, with both the rough and smooth surfaces (**Fig. 5.1.5 b/d**) appearing to have the most cells present. However, how much human plasma was adsorbed on the surfaces was not visible due this layer of cells.

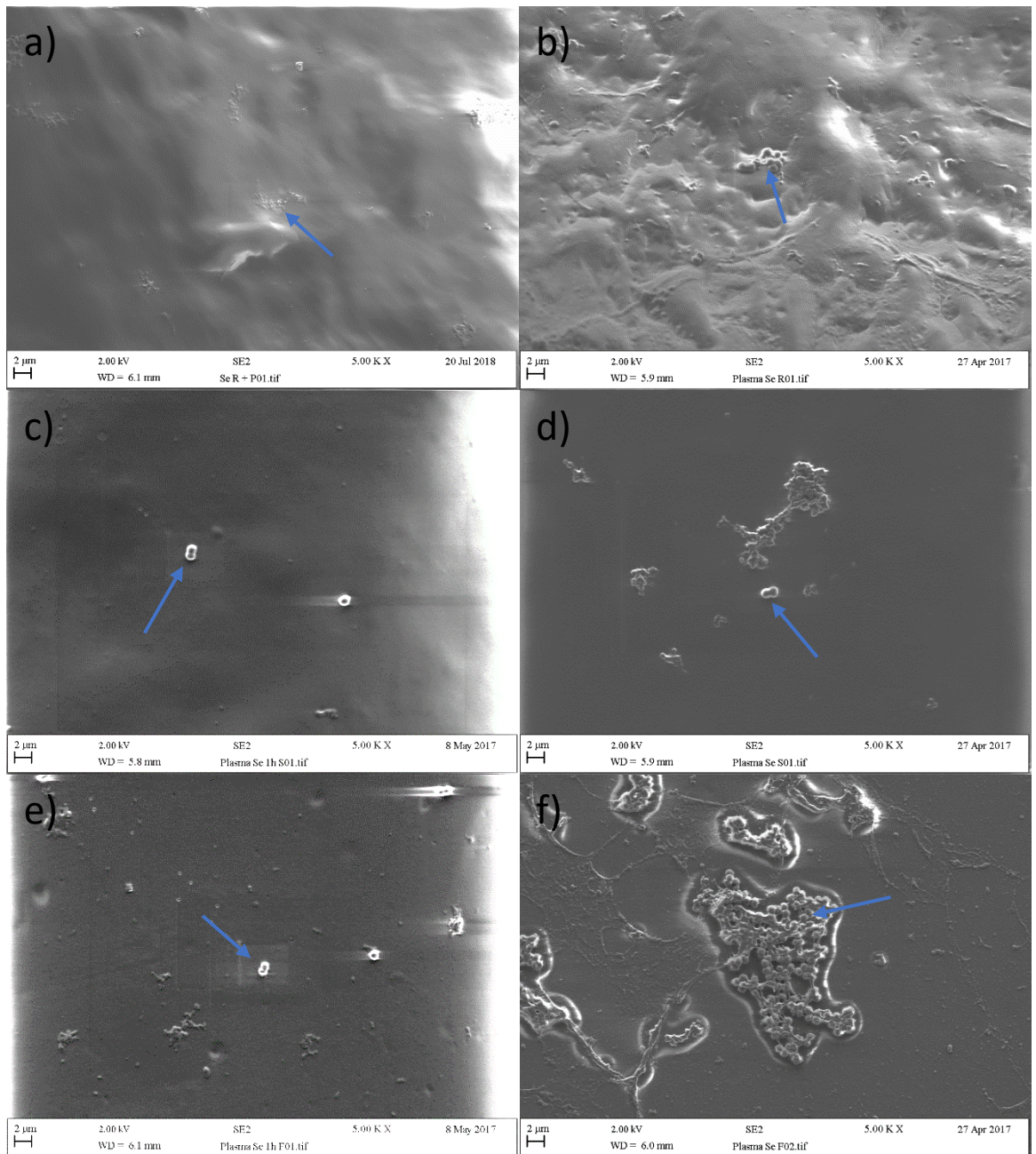


Figure 5.1.4 SEM of a/b) rough, c/d) smooth and e/f) flat images after 1h (a, c, e) or 24 h (b, d, f) incubation with a human plasma with *S. epidermidis* conditioning film. Blue arrows represent bacterial cells.

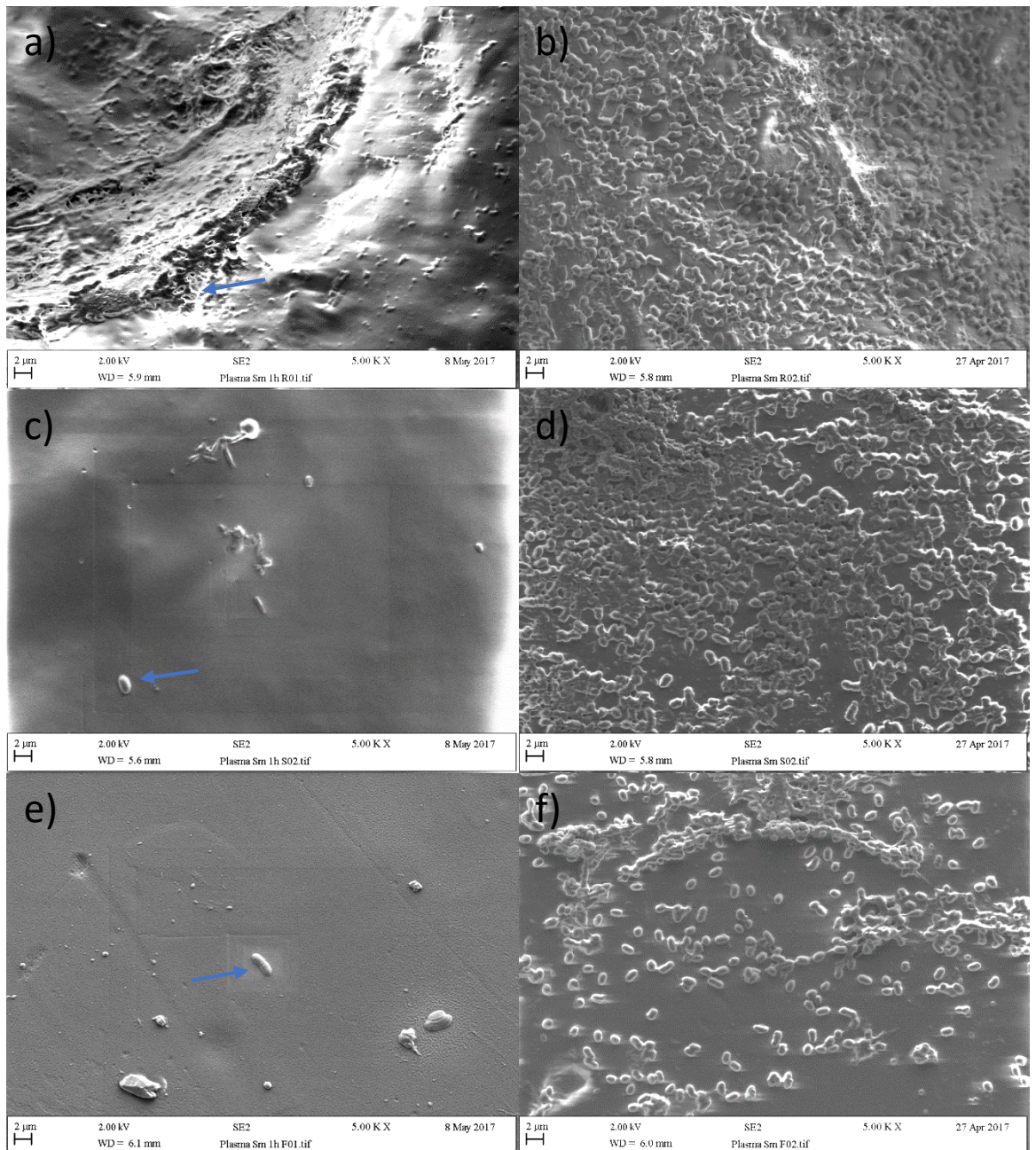


Figure 5.1.5 SEM of a/b) rough, c/d) smooth and e/f) flat images after 1h (a, c, e) or 24 h (b, d, f) incubation with a human plasma with *Ser. marcescens* conditioning film. Blue arrows represent bacterial cells (24h has no arrows as the surfaces are covered in cells).

5.2.2 Optical Surface Profiling

Optical surface profiling of the surfaces was performed to determine average surface roughness of each surface after CF treatments. The average roughness (S_a Value) of the rough surface demonstrated a reduction in the roughness following surface treatment for all the conditioning films after 1 h or 24 h except for the *Ser. marcescens* 24 h conditioning film. The CF that demonstrated the greatest reduction on the rough surface compared to the rough control value (3.55 μm) was the 24 h human plasma CF (2.05 μm) closely followed by the 24 h *Ser. marcescens* in human plasma CF (2.10 μm). Further, all the CF involving human plasma on the rough surface demonstrated greater reductions in the average roughness than those without.

Unlike the rough surface, the smooth surface demonstrated both reductions and increases in the average roughness of the surface after CF treatment compared to the smooth control (1.02 μm). The 24 h human plasma CF (0.7 μm) demonstrated the greatest reduction in roughness on the smooth surface, with both the 24 h *S. epidermidis* in dH₂O (0.79 μm) and the 24 h *Ser. marcescens* in human plasma (0.86 μm) demonstrating reductions also. However, whilst the 24 h *Ser. marcescens* in human plasma demonstrated reductions it also demonstrated the greatest increase at 1h (1.35 μm).

Finally, for the flat surface, due to the surface roughness already being significantly low (0.11 μm) when compared to the other two surfaces, most of the CFs demonstrated an increase in the average roughness or no significant change. The three that demonstrated a reduction in roughness on the flat surface were the 1 h *S. epidermidis* in dH₂O (0.07 μm), 1 h *Ser. marcescens* in dH₂O (0.08 μm) and the 1 h *S. epidermidis* in human plasma (0.1 μm). Further, in contrast to the rough surface, the 24 h *Ser. marcescens* in human plasma

on the flat surface demonstrated the greatest increase (0.29 μm) closely followed by the 1 h human plasma CF (0.25 μm).

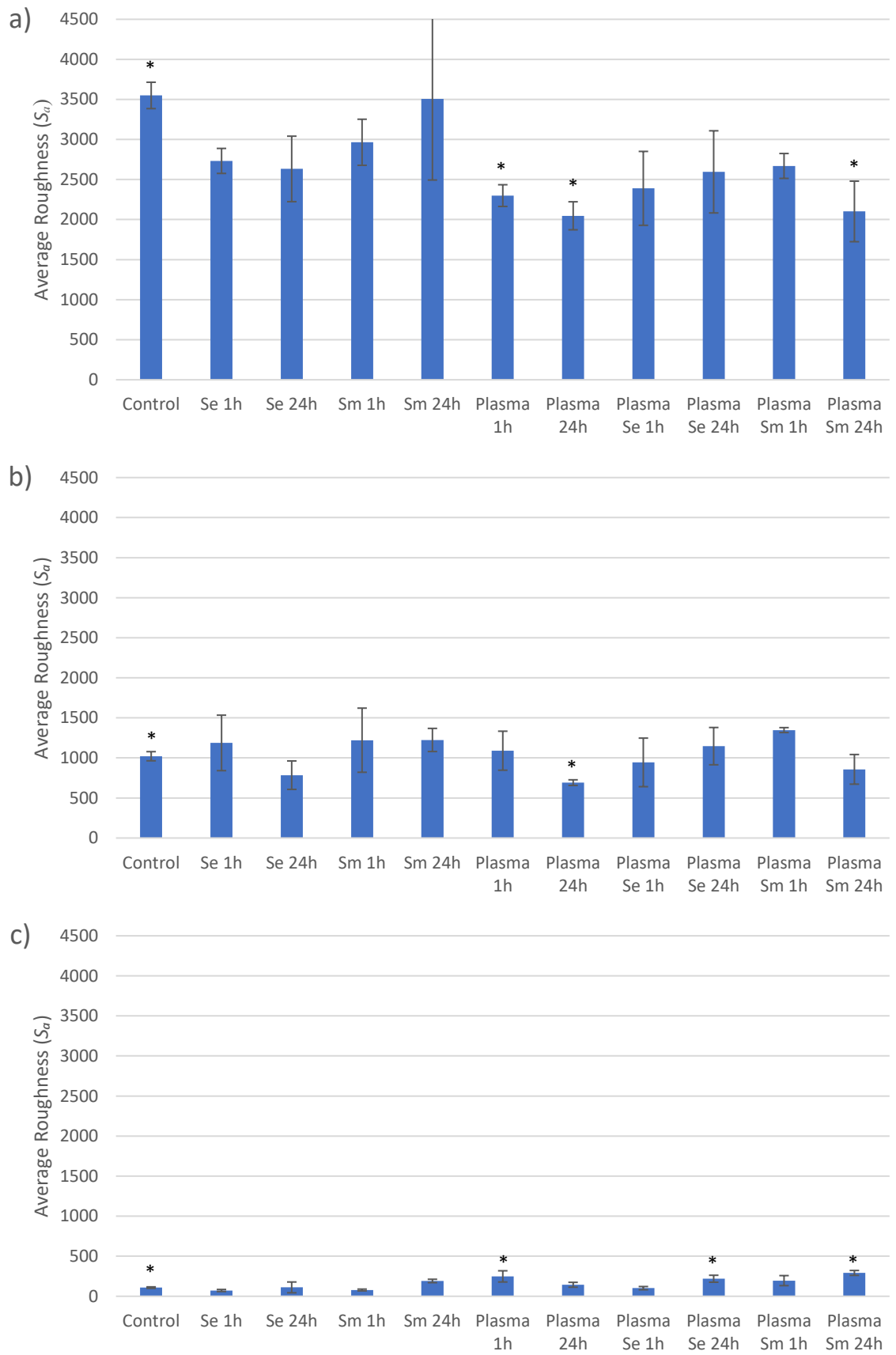


Figure 5.2 Average roughness of the conditionings on the a) rough, b) smooth and c) flat surfaces. Most significant differences annotated with a *. (n = 3)

5.2.3 Energy Dispersive X-ray (EDX)

All three surfaces had very similar atomic weight of their elemental makeup when determined using EDX, typically between 78 - 80 % carbon, 12 – 14 % chlorine and 7 - 8 % oxygen. After treatment with the CFs, all the surfaces had a change in these values, averaging 68 – 75 % Carbon, 12 – 22 % Chlorine and 8 – 12 % Oxygen, with variation between the different CF types.

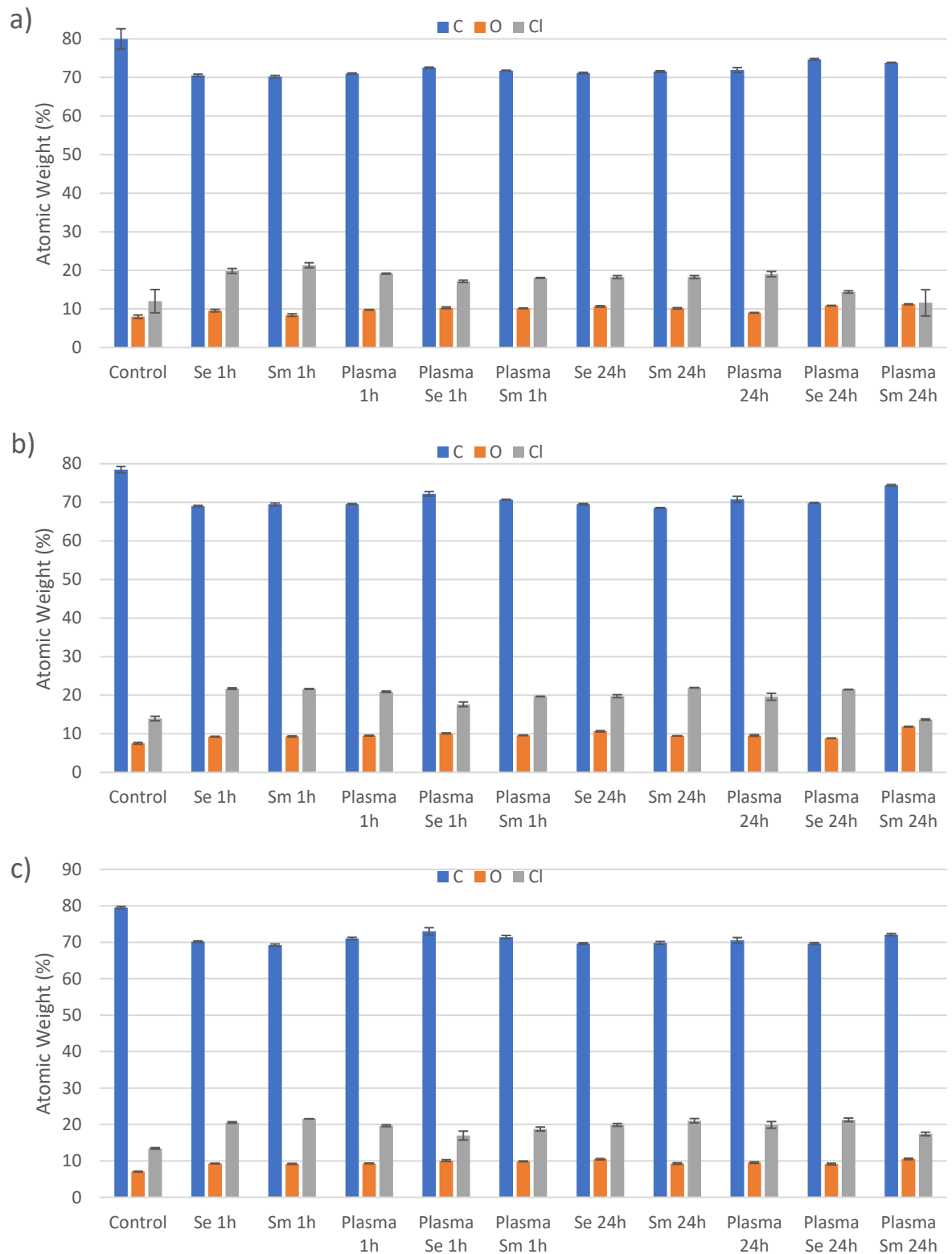


Figure 5.3 Determination of elements present according to atomic weight as determined by EDX on the a) rough, b) smooth and c) flat surfaces. Surfaces had CFs applied for 1 h or 24 h with *S. epidermidis* (Se), *Ser. marcescens* (Sm), human plasma or bacteria and human plasma. (n = 3)

5.2.4 Attenuated Total Reflection-Fourier Transform Infrared Spectroscopy (ATR-FTIR)

The surfaces were analysed using ATR-FTIR after applying a CF to determine changes in the surface chemistry.

5.2.4.1 ATR-FTIR of *S. epidermidis* Conditioning Films

The addition of a *S. epidermidis* CF (Figure 4.4.1) demonstrated no significant differences between the 1 h and 24 h timepoint but did cause some changes to the spectra. Changes were observed in the C-H stretching region (centred at ca 2900 cm^{-1}), with the smooth surface demonstrating a reduced absorption whilst the rough and flat surfaces demonstrated no significant changes. Changes were also observed from the ester carbonyl stretching caused by the surface plasticiser (ca 1740 cm^{-1}), where the opposite trend was observed with both the rough and smooth surfaces demonstrating increased absorbance and the flat surface demonstrating a reduced absorbance. The C-O bending of the plasticiser ester (1170 cm^{-1}) demonstrated no changes in the rough surface, an increase for the smooth surface and a reduction for the flat surface. As for the C-CL stretching vibration of the PVC itself (ca 690 cm^{-1}), the rough surface demonstrated no changes but both the smooth and flat surfaces demonstrated an increased absorbance. The two peaks that represent the antisymmetric $\nu_{\text{as}}\text{COO}^-$ stretching vibration of carboxylate groups in unidentate (1577-1575 cm^{-1}) and bidentate (1544-1540 cm^{-1}) coordination with calcium (Gönen *et al.*, 2010) or carboxylate carbonyl zinc stearate absorption (ca 1540 cm^{-1}) (National Institute of Standards and Technology (NIST) Web Book) both demonstrated changes. A reduced absorption on the smooth surface where they were both present, a reduction on the rough surface at 1540 cm^{-1} (which was the only one present) and an increased absorbance on the flat surface at 1540 cm^{-1} , which originally demonstrated neither peak.

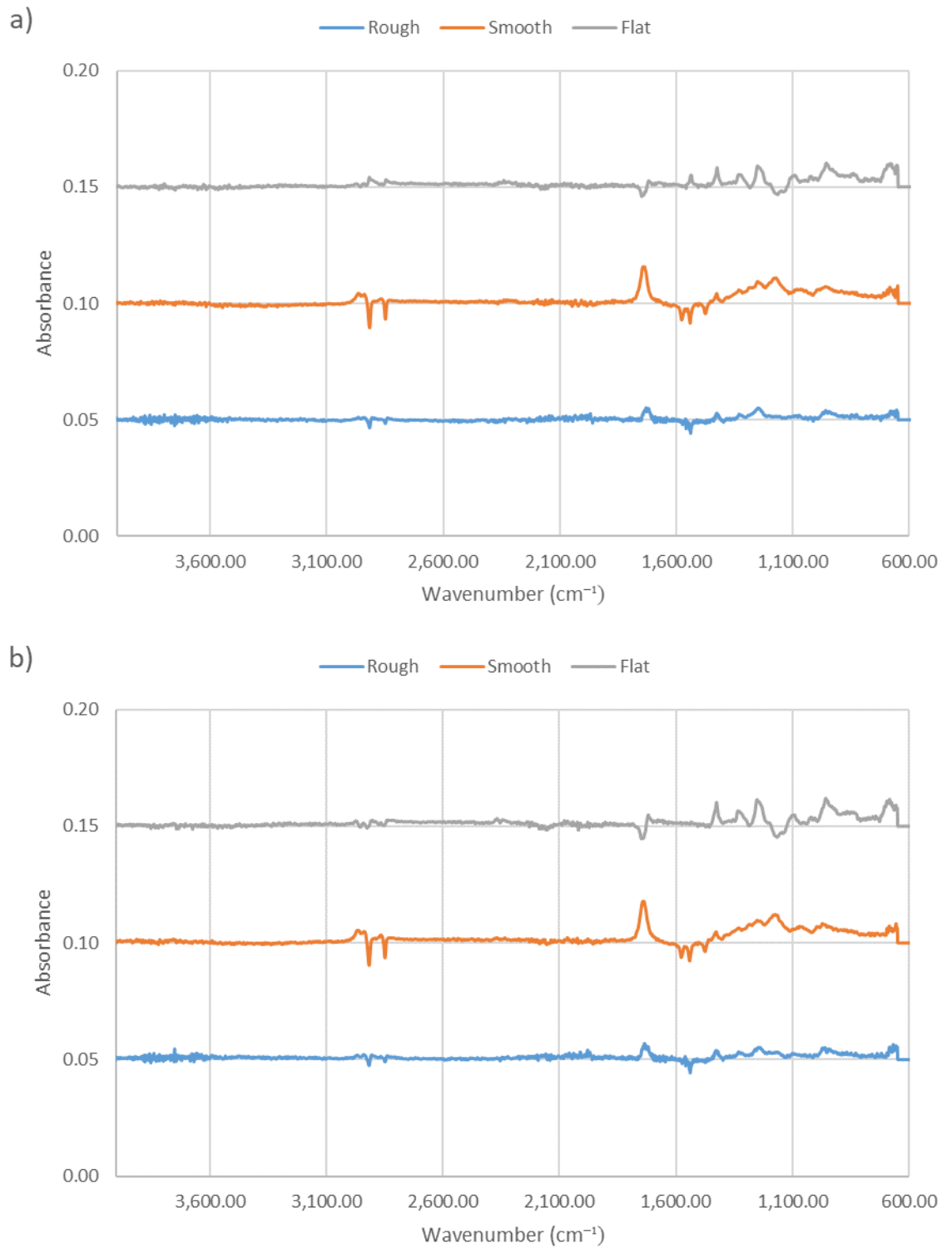


Figure 5.4.1 ATR-FTIR of *S. epidermidis* conditioning films, a) 1h and b) 24 h, after subtraction of non-conditioned control surfaces. (n = 3)

5.2.4.2 ATR-FTIR of *Ser. marcescens* Conditioning Films

When a *Ser. marcescens* CF was applied (Figure 5.4.2) the 1 h spectra demonstrated similar differences to those observed with an *S. epidermidis* CF with minor differences such as not demonstrating an increased absorbance at 1540 cm^{-1} for the calcium / zinc stearate. After 24 h the CF demonstrated significant changes in the spectra. The overall absorbance was decreased across the whole spectra for all three surfaces. A reduction in the C-H stretching region (centred at ca 2900 cm^{-1}) was observed with both the rough and smooth, whilst the flat surface demonstrated no significant changes. Both the rough and flat surfaces demonstrated reduced absorbance in the ester carbonyl stretching caused by the surface plasticiser (ca 1740 cm^{-1}), whilst the smooth surface demonstrated an increase. Whilst the plasticiser ester C-O bending (1170 cm^{-1}) was reduced in all three surfaces it was most apparent in the rough and flat surfaces. Finally, both the smooth and flat surfaces demonstrated a greater reduction in the absorbance for the C-CL stretching vibration of the PVC itself (ca 690 cm^{-1}) than the rough surface, which may have been due to the patterning on the rough surface.

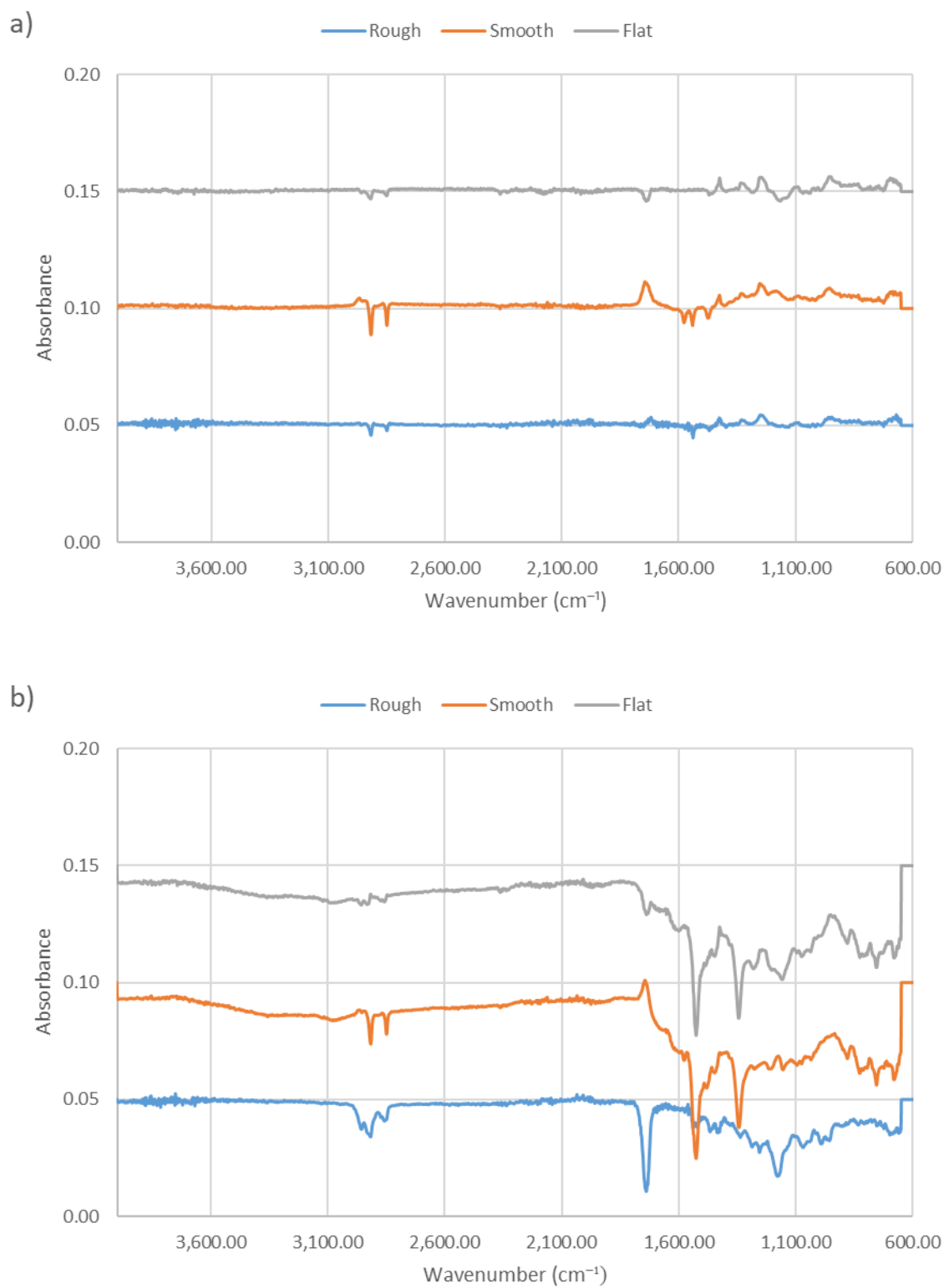


Figure 5.4.2 ATR-FTIR of *Ser. marcescens* conditioning films, a) 1h and b) 24 h, after subtraction of non-conditioned control surfaces. (n = 3)

5.2.4.3 ATR-FTIR of Human Plasma Conditioning Films

When a human plasma CF was applied (Figure 5.4.3) no significant differences were observed between the 1 h and 24 h spectra. A peak at ca 3266 cm^{-1} was observed only on the rough surface, representing the O-H stretching present in water. The rough surface also demonstrated a peak at ca 1635 cm^{-1} , demonstrating an increased absorbance of the H-O-H scissor-bending bond in water (Mojet *et al.*, 2010). All three surfaces demonstrated reductions in the absorbance of the C-H stretching region (ca 2900 cm^{-1}), but only the smooth surface demonstrated a significant reduction. Both the rough and flat surfaces demonstrated a significant reduction in absorbance at the ester carbonyl stretching region of the plasticiser (1740 cm^{-1}) whilst the smooth surface demonstrated a slight increase. A reduced absorption on the smooth surface of two peaks that represent the antisymmetric $\nu_{\text{as}}\text{COO}^-$ stretching vibration of carboxylate groups in unidentate (1577-1575 cm^{-1}) and bidentate (1544-1540 cm^{-1}) coordination with calcium (Gönen *et al.*, 2010) or carboxylate carbonyl zinc stearate absorption (ca 1540 cm^{-1}) was observed. However, a significant increase on the rough surface at 1540 cm^{-1} and no changes in the flat surface were also observed. The plasticiser ester C-O bending (1170 cm^{-1}) demonstrated reduced absorption on the rough and flat surfaces but no significant changes on the smooth surface. Finally, all the surfaces demonstrated an increase in the absorbance for the C-Cl stretching vibration of the PVC itself (ca 690 cm^{-1}), indicating that the FTIR was able to detect the PVC vibrations more with a CF.

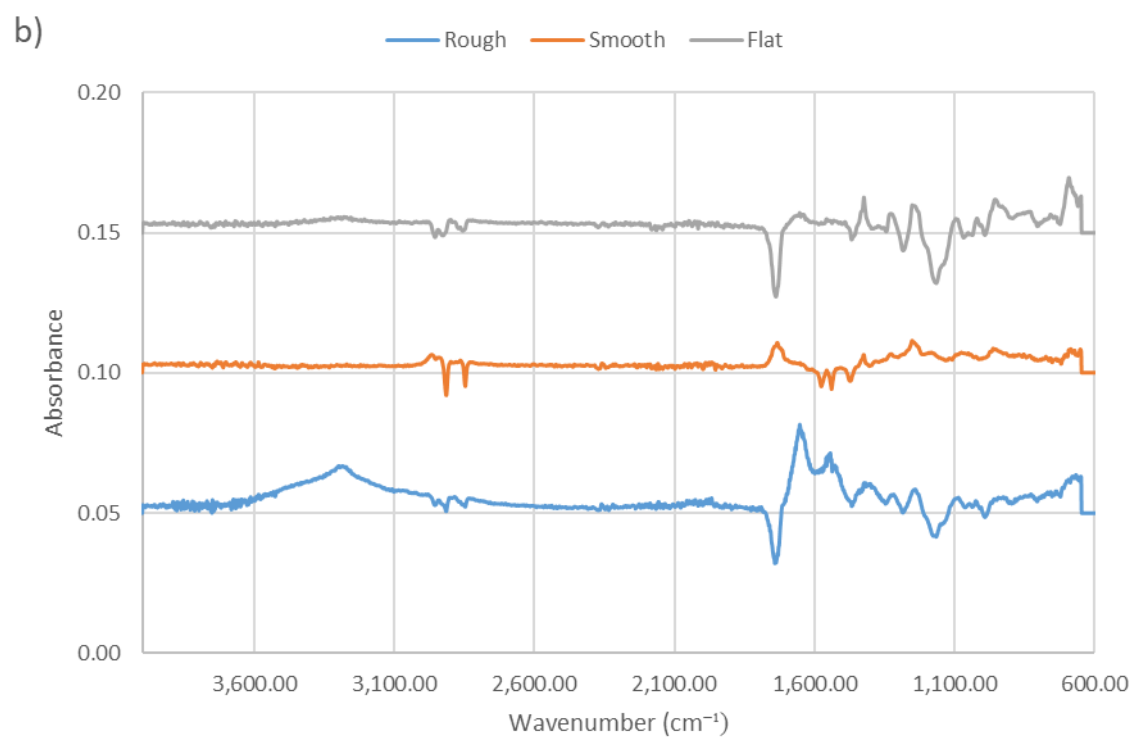
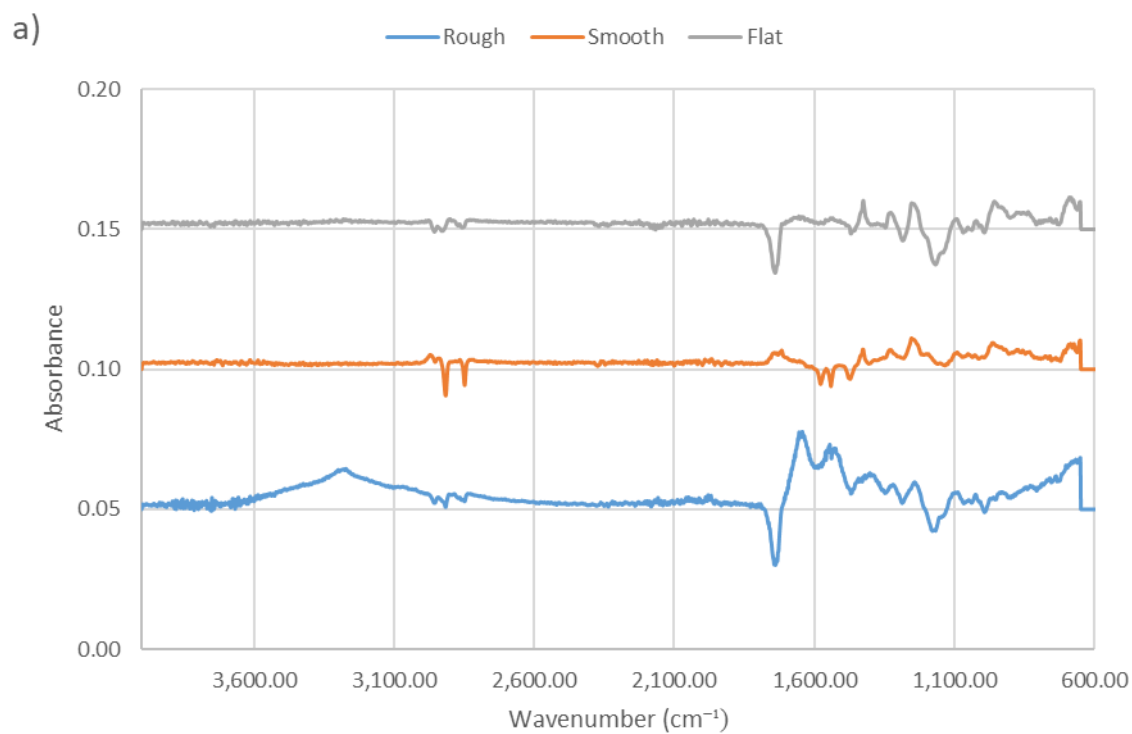


Figure 5.4.3 ATR-FTIR of human plasma conditioning films, a) 1h and b) 24 h, after subtraction of non-conditioned control surfaces. (n = 3)

5.2.4.4 ATR-FTIR of Human Plasma and *S. epidermidis* Conditioning Films

When a human plasma and *S. epidermidis* CF was applied (Figure 5.4.4), the 1h spectra demonstrated the same differences as the human plasma CF alone for the smooth and flat surfaces, and whilst the spectra for the rough surface demonstrated the same peaks the absorbances were different. After 24 h, the smooth and flat surfaces still demonstrated a similar spectrum to that obtained with human plasma alone. However, the rough surface demonstrated further significant reduction in the absorbances obtained with some of the peaks no longer as discernible. This applied to the two peaks associated with water on the surface, the O-H stretching (range of 3000 – 4000 cm^{-1}) and the H-O-H scissor-stretch (1635 cm^{-1}) (Mojet *et al.*, 2010). The main components of the surface that still demonstrated a reduction in absorbance were the ester carbonyl stretching region of the plasticiser (1740 cm^{-1}) and the plasticiser ester C-O bending (1170 cm^{-1}). A further reduction was observed for the antisymmetric $\nu_{\text{as}}\text{COO}^-$ stretching vibration of carboxylate groups in bidendate (1544-1540 cm^{-1}) coordination with calcium (Gönen *et al.*, 2010) or carboxylate carbonyl zinc stearate absorption (ca 1540 cm^{-1}).

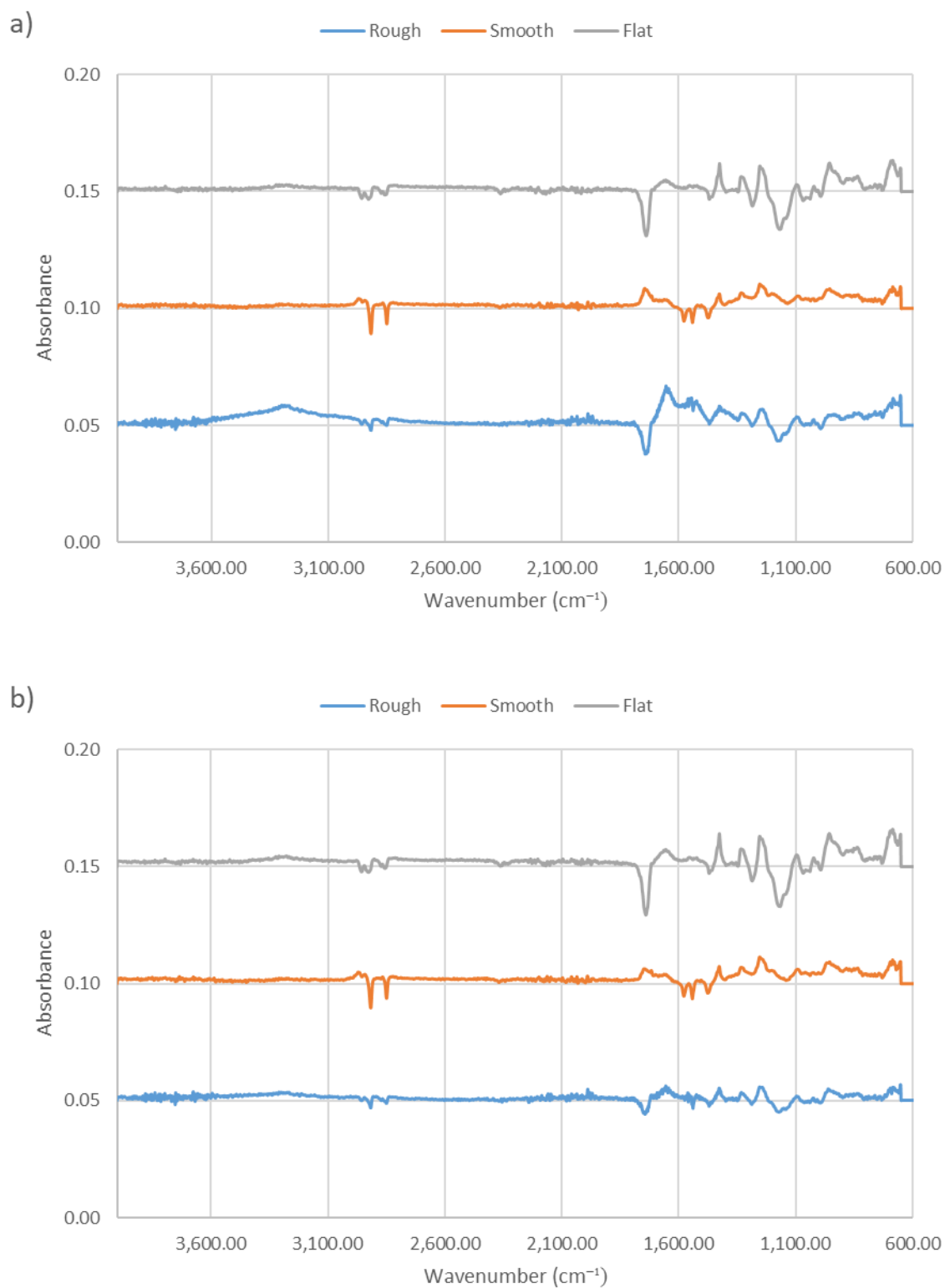


Figure 5.4.4 ATR-FTIR of *S. epidermidis* and human plasma conditioning films, a) 1h and b) 24 h, after subtraction of non-conditioned control surfaces. (n = 3)

5.2.4.5 ATR-FTIR of Human Plasma and *Ser. marcescens* Conditioning Films

The CF formed by the combination of human plasma with *Ser. marcescens* (Figure 5.4.5) demonstrated the same spectrum as just a human plasma CF after 1 h. However, after 24 h the spectrum was significantly different, with all surfaces demonstrated peaks associated with water on the surface, the O-H stretching (range of 3000 – 4000 cm^{-1}) and the H-O-H scissor-stretch (1635 cm^{-1}) (Mojet *et al.*, 2010), with the flat surface demonstrating the greatest increase. Both the rough and flat surfaces demonstrated a reduction in the absorption for the ester carbonyl stretching region of the plasticiser (1740 cm^{-1}) and the plasticiser ester C-O bending (1170 cm^{-1}) whilst the smooth surface demonstrated no change. Finally, all the surfaces demonstrated an increase in the absorbance for the C-CL stretching vibration of the PVC itself (ca 690 cm^{-1}).

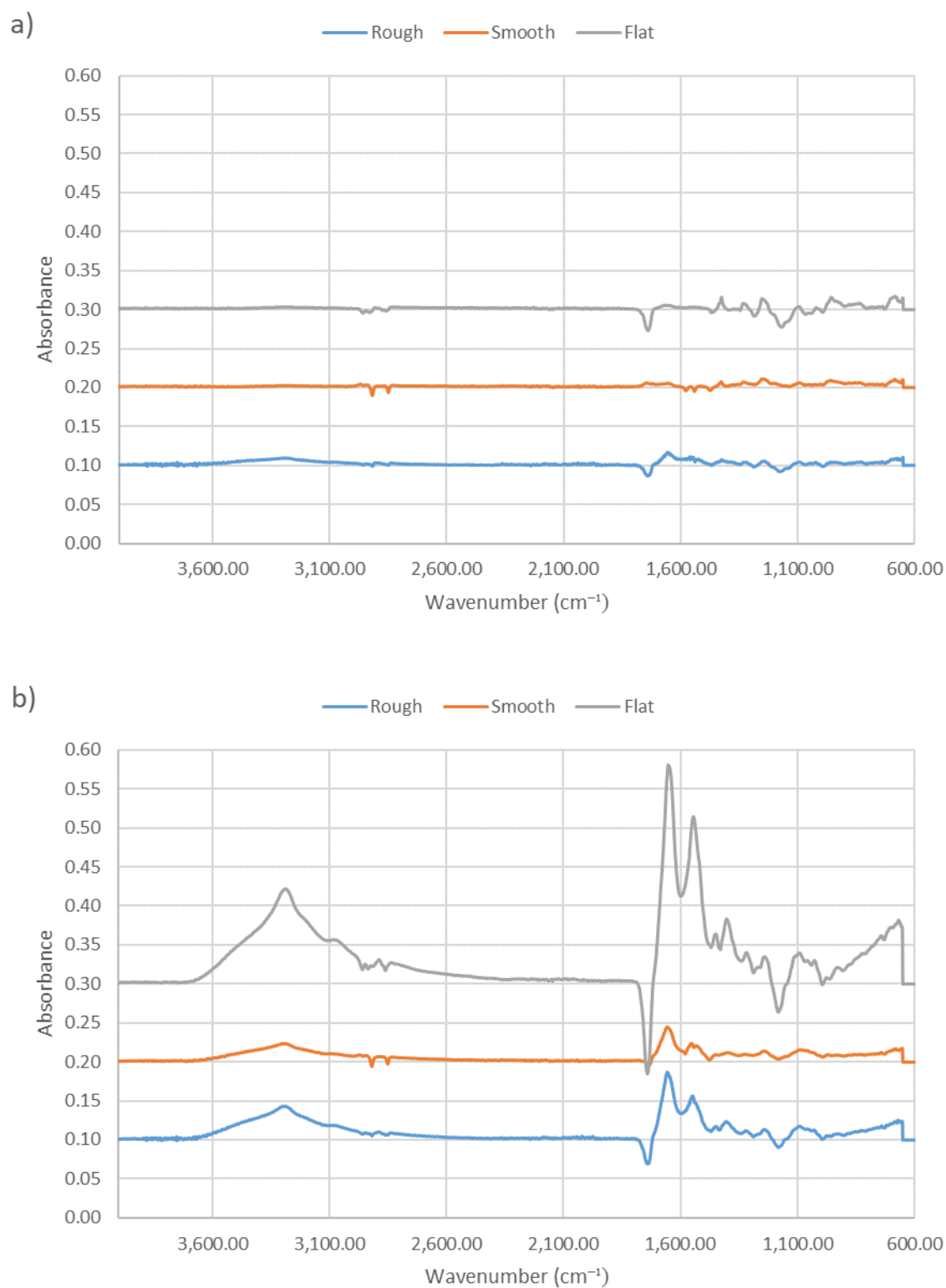


Figure 5.4.5 ATR-FTIR of *Ser. marcescens* and human plasma conditioning films, a) 1h and b) 24 h, after subtraction of non-conditioned control surfaces. Note that scale differs to other FTIR graphs due to absorbance intensity. (n = 3)

5.2.5 Raman Spectroscopy

The surfaces were analysed using Raman spectroscopy after applying a CF to determine changes in the surface chemistry. Only one of the conditioning films demonstrated a change in the spectra obtained when compared to the control surfaces, which was when *Ser. marcescens* combined with human plasma was conditioned onto the flat surface for both 1 h or 24 h (**Fig. 5.5.5a/b**). This CF appeared to mask the two peaks at 635 cm^{-1} and 695 cm^{-1} representing the C-Cl stretching vibration bonds of the PVC, whilst the intensity of the stretching vibrations of the C-H bonds present in the PVC at 2916 cm^{-1} was significantly reduced with a 24 h CF, which further indicated the CF was masking the PVC surface (Solodovnichenko *et al.*, 2016).

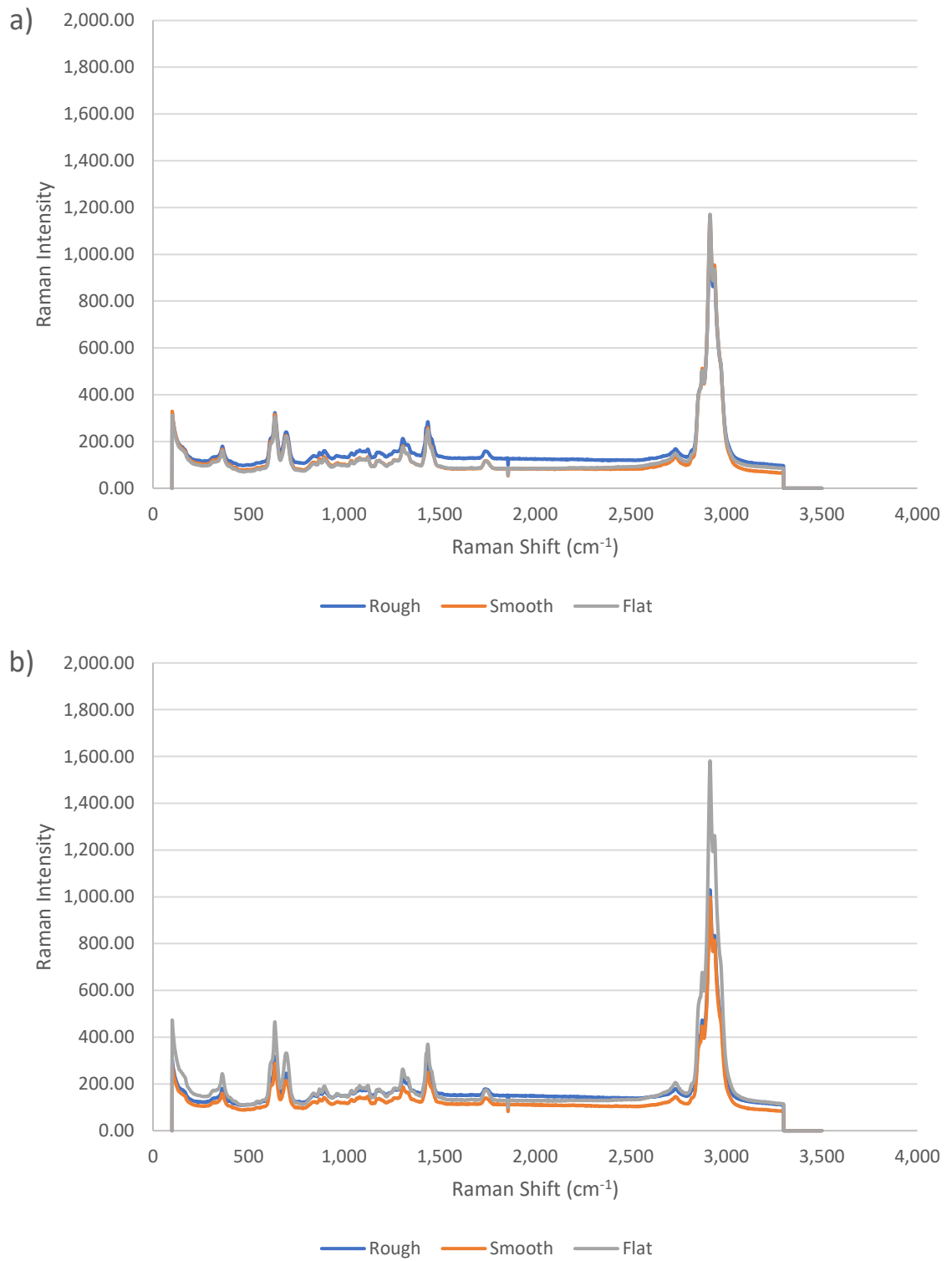


Figure 5.5.1 Raman spectroscopy of surfaces after conditioning with *S. epidermidis* for a) 1 h or b) 24 h. (n = 3)

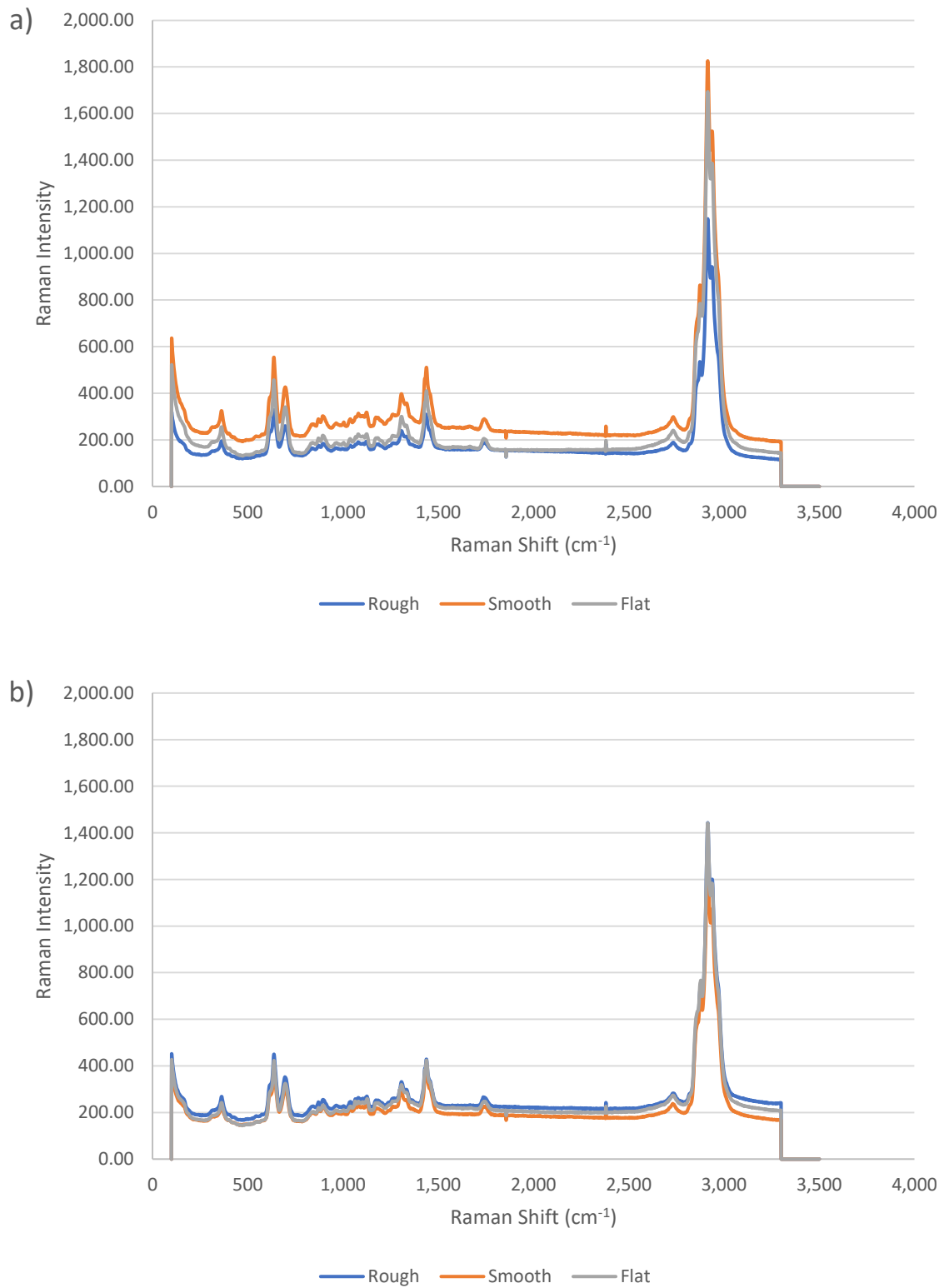


Figure 5.5.2 Raman spectroscopy of surfaces after conditioning with *Ser. marcescens* for a) 1 h or b) 24 h. (n = 3)

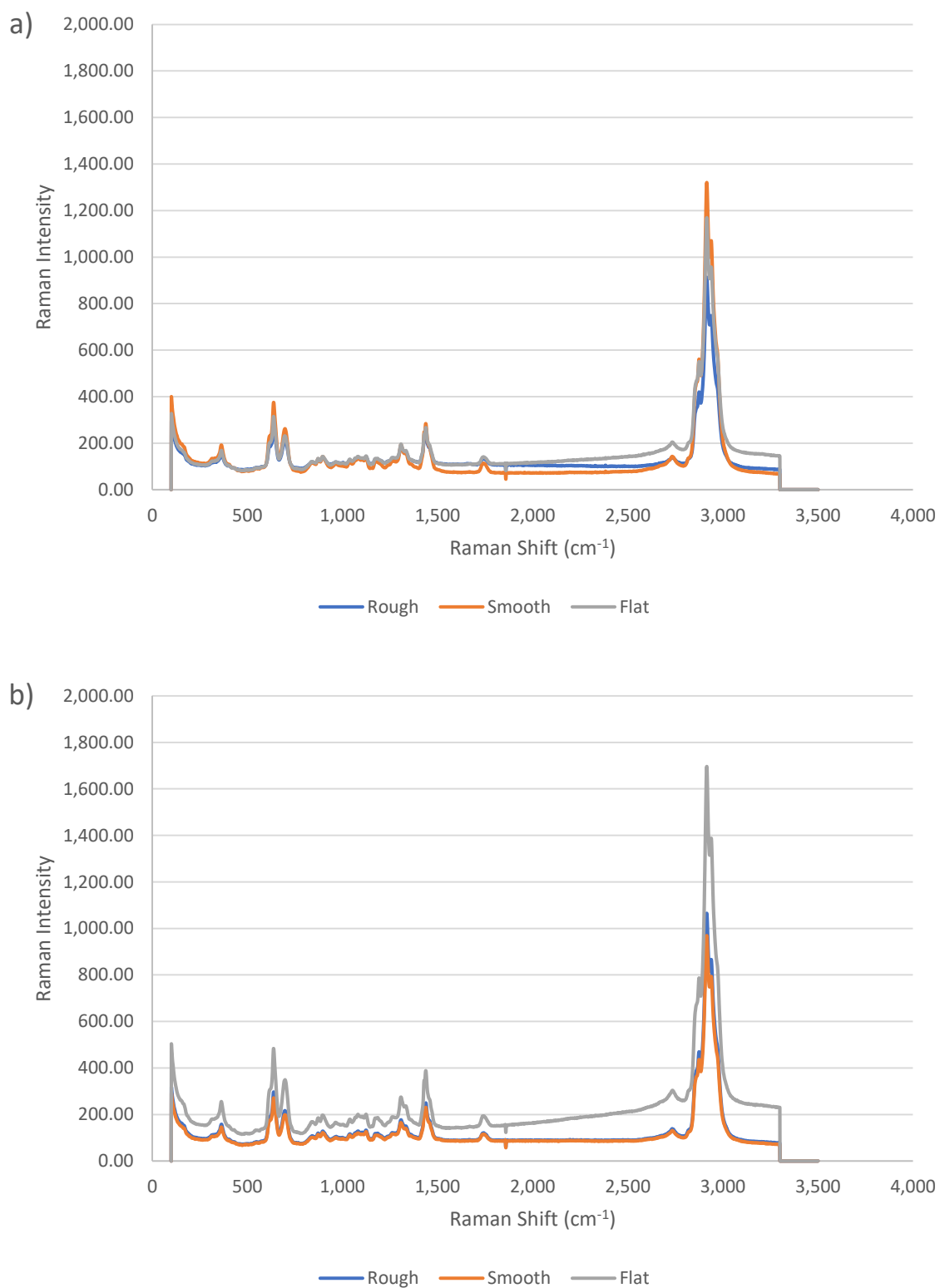


Figure 5.5.3 Raman spectroscopy of surfaces after conditioning with human blood plasma for a) 1 h or b) 24 h. (n = 3)

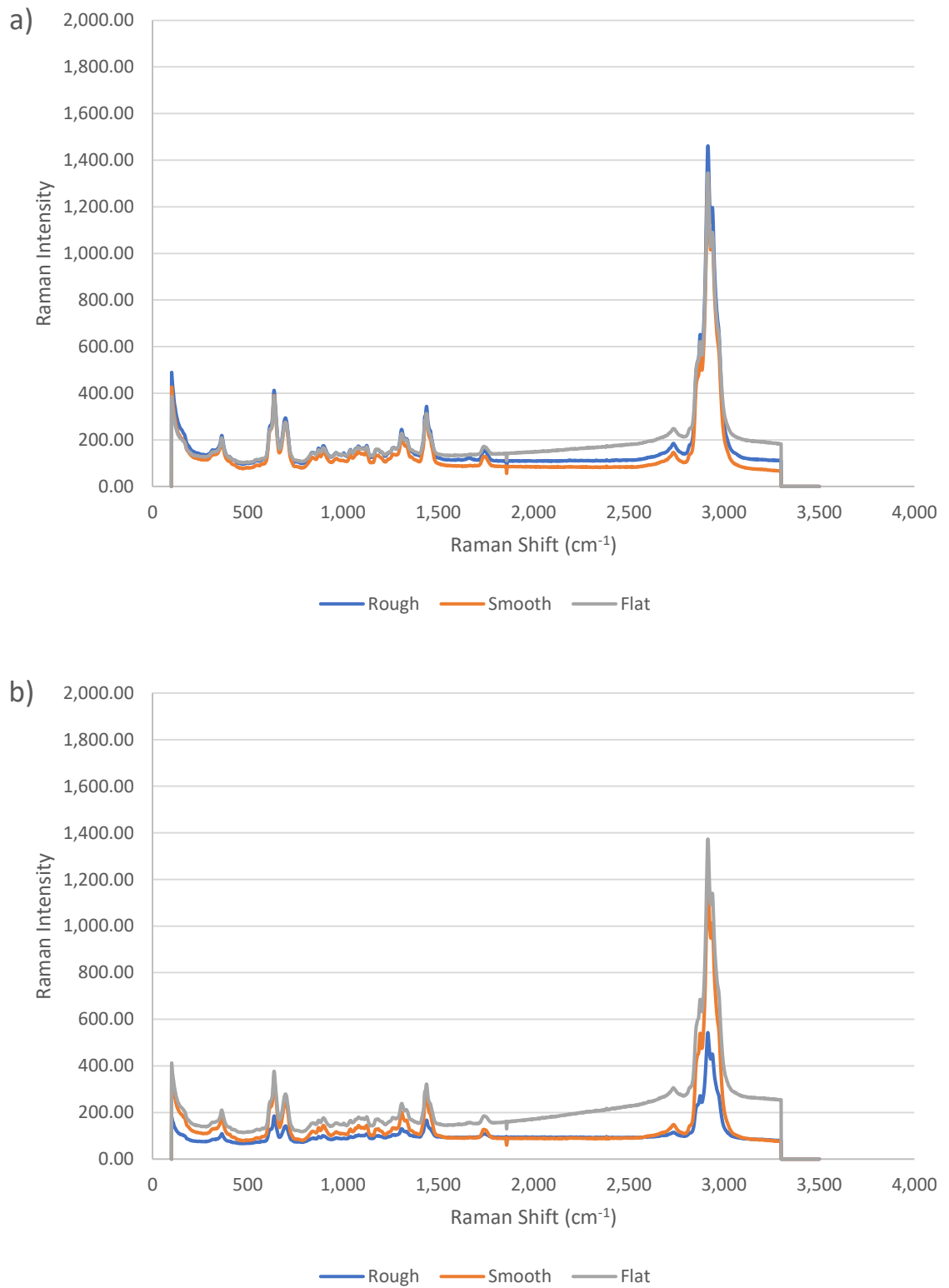


Figure 5.5.4 Raman spectroscopy of surfaces after conditioning with human blood plasma and *S. epidermidis* for a) 1 h or b) 24 h. (n = 3)

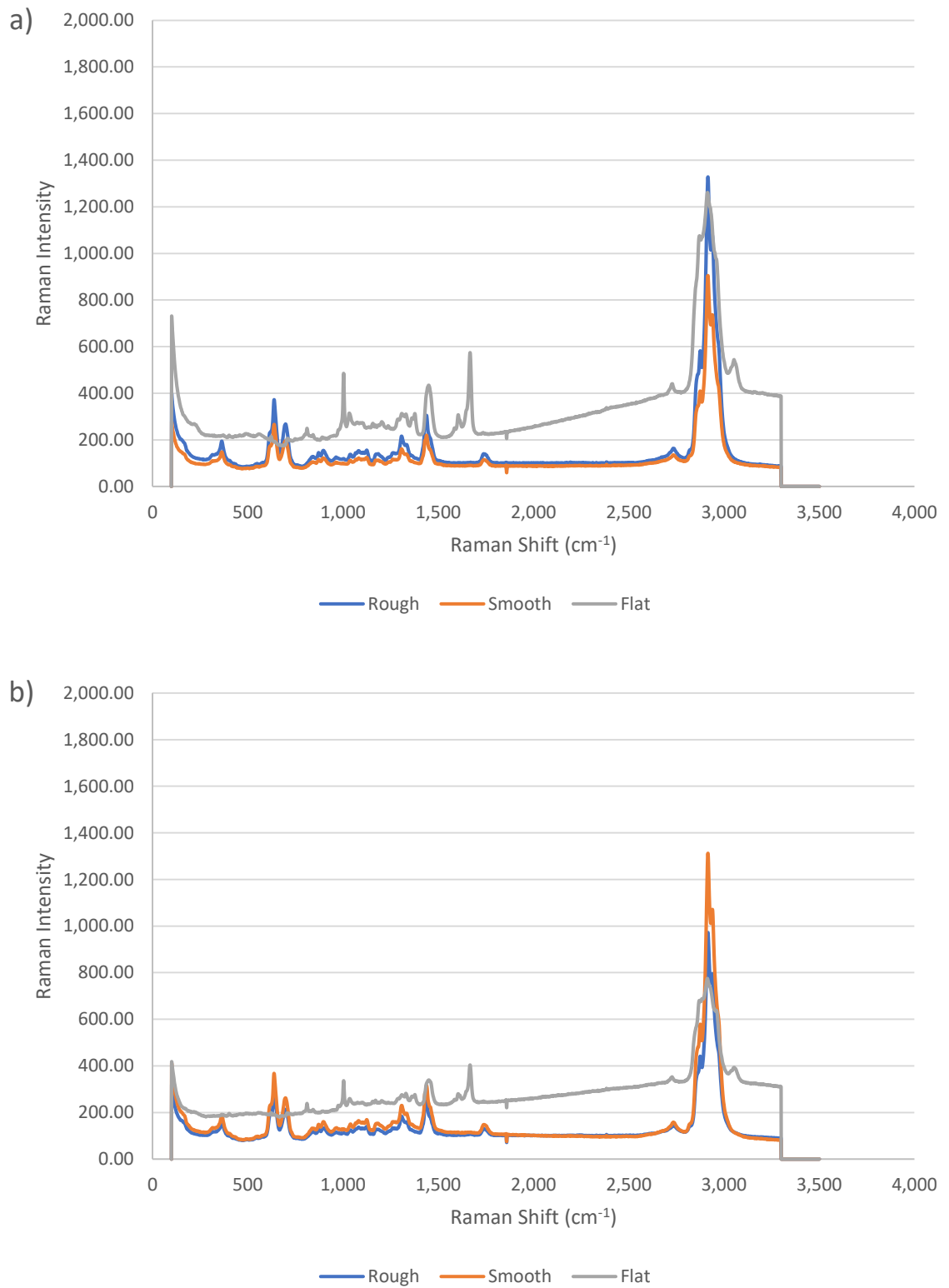


Figure 5.5.5 Raman spectroscopy of surfaces after conditioning with human blood plasma and *Ser. marcescens* for a) 1 h or b) 24 h. (n = 3)

5.2.6 Physicochemistry

Goniometry was carried out using water, ethylene glycol and diiodomethane to determine the physicochemical characteristics of the surfaces after application of a CF.

5.2.6.1 Physicochemistry of the Rough Surface

Physicochemical properties of the rough surface (Table 5.7.1) after the application of a CF to the surface caused no significant changes in any of the physicochemical parameters of a 1 h or 24 h *S. epidermidis* CF. Only a trend of a reduction in Gibbs Free energy (ΔG) after 24 h (-62.3 mJ/m^2) was observed, whilst the application of a *Ser. marcescens* CF demonstrated the opposite trend, with an increase in Gibbs free energy for both 1 h and 24 h (-41.1 mJ/m^2 and -40.5 mJ/m^2 respectively). The *Ser. marcescens* CF also demonstrated another trend, with an increase in base energy (γ_s) for after 1 h or 24 h was also determined, but no significant changes were determined.

The application of a human plasma CF had a greater effect on the surface physicochemistry after 1 h or 24 h, with both the Gibbs Free energy and the base energy demonstrating significant changes. The Gibbs Free energy increased from -53 mJ/m^2 for the control surface to -28.5 mJ/m^2 after 1 h and -6 mJ/m^2 after 24 h whilst the base energy increased from 7.3 mJ/m^2 for the control surface to 16.8 mJ/m^2 after 1 h and 27.2 mJ/m^2 after 24 h. When a CF was applied combining the bacteria with human plasma, the combination of human plasma with *S. epidermidis* caused a significant increase in the Gibbs Free energy, from -53 mJ/m^2 to -31.3 mJ/m^2 after 24 h, whilst a significant increase in the basic energy was observed after 24 h, from 7.3 mJ/m^2 to 14.9 mJ/m^2 . However, when *Ser. marcescens* and human plasma combined demonstrated a significant increase after 1 h, with the Gibbs Free energy increasing to -21.5 mJ/m^2 and the basic energy increasing to 21.5 mJ/m^2 . However, after 24 h no significant changes were apparent.

Table 5.7.1 Physicochemistry of the rough surface after applying 1 h or 24 h conditioning films of the bacteria alone, human plasma alone or a combination of bacteria and human plasma. Se denotes the bacteria *Staphylococcus epidermidis* and Sm denotes *Serratia marcescens*. (n = 5)

	ΔG mJ/m ²	γ_s mJ/m ²	γ_{sLW} mJ/m ²	γ_{sAB} mJ/m ²	γ_{s+} mJ/m ²	γ_{s-} mJ/m ²
Rough	-53.0 ± 6.1	52.4 ± 1.2	48.9 ± 0.1	3.5 ± 1.1	0.4 ± 0.2	7.3 ± 1.5
Rough 1h Se	-56.2 ± 7.2	46.2 ± 0.5	45.6 ± 0.4	0.7 ± 0.2	0.0 ± 0.0	7.4 ± 1.8
Rough 24h Se	-62.3 ± 2.2	45.8 ± 0.7	44.9 ± 0.6	0.9 ± 0.2	0.0 ± 0.0	5.2 ± 0.5
Rough 1h Sm	-41.4 ± 3.8	45.8 ± 1.1	44.8 ± 0.6	1.1 ± 0.5	0.0 ± 0.0	11.4 ± 1.2
Rough 24h Sm	-40.5 ± 6.4	47.3 ± 0.7	45.0 ± 0.7	2.3 ± 0.4	0.1 ± 0.0	11.6 ± 2.3
Rough 1h Plasma	-28.5 ± 7.1	52.7 ± 4.1	46.0 ± 1.1	6.7 ± 3.7	1.0 ± 0.7	16.8 ± 3.5
Rough 24h Plasma	-6.0 ± 6.1	52.0 ± 4.0	43.4 ± 2.3	8.6 ± 3.2	1.0 ± 0.5	27.2 ± 3.4
Rough 1h Plasma + Se	-43.3 ± 9.6	45.7 ± 0.3	44.0 ± 0.6	1.7 ± 0.4	0.2 ± 0.1	11.0 ± 3.5
Rough 24h Plasma + Se	-31.3 ± 2.2	46.1 ± 1.1	44.6 ± 0.9	1.5 ± 0.5	0.1 ± 0.0	14.9 ± 0.8
Rough 1h Plasma + Sm	-21.5 ± 9.2	48.4 ± 1.1	45.4 ± 0.8	3.0 ± 1.4	0.1 ± 0.1	21.5 ± 5.0
Rough 24h Plasma + Sm	-43.1 ± 5.0	45.3 ± 0.8	43.2 ± 0.9	2.1 ± 0.5	0.2 ± 0.1	10.1 ± 1.9

5.2.6.2 Physicochemistry of the Smooth Surface

When the CF's were applied to the smooth surface (Table 5.7.2), the application of a *S. epidermidis* CF demonstrated a trend in Gibbs Free energy reduction after 1 h (-58.5 mJ/m²) and a further reduction after 24 h (-67.1 mJ/m²) but this was not significant. No other bacteria in water CF demonstrated any trends and no significant changes were observed.

The application of a human plasma CF to the smooth surface significantly increased the Gibbs Free energy. After 1 h the Gibbs Free energy increased to -7.5 mJ/m² and after 24 h it increased to 9.5 mJ/m². Further, the acid-base energy increased to 13.9 mJ/m² after 1 h and 11.4 mJ/m² after 24 h, due to the significant increases in the base energy component which increased from 7.5 mJ/m² to 37.9 mJ/m² after 1 h and 50 mJ/m² after 24 h.

When the smooth surface was conditioned with human plasma and either *S. epidermidis* or *Ser. marcescens* both organisms demonstrated a reduction in Gibbs Free energy after 1 h, from -50.1 mJ/m² to -68.2 mJ/m² for *S. epidermidis* and -57.9 mJ/m² for *Ser. marcescens*. However, after 24 h the Gibbs Free energy values were similar to human plasma alone, with 7.6 mJ/m² for human plasma with *S. epidermidis* and 4.8 mJ/m² for human plasma with *Ser. marcescens*. However, both organisms demonstrated significantly different values for the other physicochemical properties after 24 h. The combined human plasma and *Ser. marcescens*' CF demonstrated an increase in acid-base energies at 9.2 mJ/m² due to the significant increase in base energy (34.7 mJ/m²). However, human plasma and *S. epidermidis* combined 24 h CF demonstrated a significantly reduced the total free energy, Lifschitz van der Waals forces and the base energies (1.2 mJ/m², 1.7 mJ/m² and 0.9 mJ/m² respectively) when compared to the controls (49.6 mJ/m², 45.7 mJ/m² and 7.5 mJ/m²).

Table 5.7.2 Physicochemistry of the smooth surface after applying 1 h or 24 h conditioning films of the bacteria alone, human plasma alone or a combination of bacteria and human plasma. Se denotes the bacteria *Staphylococcus epidermidis* and Sm denotes *Serratia marcescens*. (n = 5)

	ΔG mJ/m ²	γ_s mJ/m ²	γ_{sLW} mJ/m ²	γ_{sAB} mJ/m ²	γ_{s+} mJ/m ²	γ_{s-} mJ/m ²
Smooth	-50.1 ± 6.1	49.6 ± 1.2	45.7 ± 0.2	4.0 ± 1.1	0.5 ± 0.2	7.5 ± 1.5
Smooth 1h Se	-58.5 ± 4.3	49.2 ± 1.3	45.8 ± 0.8	3.3 ± 0.6	0.6 ± 0.1	5.0 ± 0.8
Smooth 24h Se	-67.1 ± 5.4	46.9 ± 1.4	44.8 ± 0.8	2.0 ± 0.7	0.3 ± 0.1	3.6 ± 0.8
Smooth 1h Sm	-53.7 ± 2.5	50.1 ± 0.9	46.0 ± 0.3	4.1 ± 0.6	0.7 ± 0.2	5.8 ± 0.5
Smooth 24h Sm	-51.3 ± 6.6	50.7 ± 1.9	46.1 ± 0.9	4.6 ± 1.2	0.8 ± 0.2	7.0 ± 2.0
Smooth 1h Plasma	-7.5 ± 21.3	57.8 ± 7.0	44.0 ± 0.3	13.9 ± 6.7	1.3 ± 0.7	37.9 ± 16.2
Smooth 24h Plasma	9.5 ± 30.7	50.7 ± 3.7	39.3 ± 0.6	11.4 ± 4.0	0.8 ± 0.2	50.0 ± 19.4
Smooth 1h Plasma + Se	-68.2 ± 3.4	45.6 ± 0.5	44.1 ± 0.7	1.5 ± 0.4	0.2 ± 0.1	3.3 ± 0.4
Smooth 24h Plasma + Se	7.6 ± 4.3	1.2 ± 0.5	1.7 ± 0.6	0.9 ± 0.2	0.1 ± 0.0	0.9 ± 0.6
Smooth 1h Plasma + Sm	-57.9 ± 5.2	47.2 ± 1.3	44.5 ± 0.4	2.7 ± 0.9	0.5 ± 0.2	5.4 ± 1.1
Smooth 24h Plasma + Sm	4.8 ± 5.6	51.4 ± 5.4	42.2 ± 1.3	9.2 ± 4.3	0.8 ± 0.5	34.7 ± 5.8

5.2.6.3 Physicochemistry of the Flat Surface

After applying CFs to the flat surface (Table 5.7.3), the *S. epidermidis* CF significantly reduced the Gibbs Free energy from -40.2 mJ/m^2 to -64.6 mJ/m^2 after 1 h and to -75.6 mJ/m^2 after 24 h. When *Ser. marcescens* was conditioned onto the flat surface, a significant reduction was determined in the Gibbs Free energy after 1 h (from -40.2 mJ/m^2 to -59.1 mJ/m^2) but this increased after 24 h (-48.8 mJ/m^2).

A human plasma CF on the flat surface caused an increase in the Gibbs Free energy, with a 1 h incubation increasing it to 22 mJ/m^2 and a 24 h incubation increasing it to -5.5 mJ/m^2 . Whilst small changes in values were observed, the only other significant change was the increase in base energy from 9.7 mJ/m^2 to 22.7 mJ/m^2 after 1h and then 29.3 mJ/m^2 after 24 h.

The combination of human plasma and *S. epidermidis* to create a CF caused the Gibbs Free energy to reduce from -40.2 mJ/m^2 to -60.5 mJ/m^2 after 1 h and -58.6 mJ/m^2 after 24 h. A slight reduction in the total free energy was observed after one hour (46.8 mJ/m^2) but was not significant until 24 h where the total free energy was reduced from 53.3 mJ/m^2 to 38.3 mJ/m^2 . However, when a human plasma and *Ser. marcescens* CF was applied the Gibbs Free energy was initially reduced to -63.2 mJ/m^2 after 1 h but significantly increased to 6.9 mJ/m^2 after 24 h. The total free energy for *Ser. marcescens* followed the same trend as *S. epidermidis*, where an initial slight reduction was observed after 1 h (45.5 mJ/m^2) but then a further reduction to 38.7 mJ/m^2 was observed after 24 h. Finally, the basic energy did not have a significant change after 1 h, but after 24 h was significantly increased from 9.7 mJ/m^2 to 32.2 mJ/m^2 .

Table 5.7.3 Physicochemistry of the flat surface after applying 1 h or 24 h conditioning films of the bacteria alone, human plasma alone or a combination of bacteria and human plasma. Se denotes the bacteria *Staphylococcus epidermidis* and Sm denotes *Serratia marcescens*. (n = 5)

	ΔG mJ/m ²	γ_s mJ/m ²	γ_{sLW} mJ/m ²	γ_{sAB} mJ/m ²	γ_{s+} mJ/m ²	γ_{s-} mJ/m ²
Flat	-40.2 ± 6.1	53.3 ± 1.2	45.2 ± 0.1	8.1 ± 1.1	1.8 ± 0.2	9.7 ± 1.5
Flat 1h Se	-64.6 ± 6.2	43.9 ± 0.6	42.6 ± 0.1	1.4 ± 0.6	0.1 ± 0.1	4.4 ± 1.0
Flat 24h Se	-75.6 ± 3.5	44.5 ± 0.2	44.0 ± 0.4	0.5 ± 0.2	0.0 ± 0.0	2.6 ± 0.5
Flat 1h Sm	-59.1 ± 2.5	46.6 ± 0.7	44.2 ± 0.2	2.3 ± 0.6	0.3 ± 0.1	5.0 ± 0.4
Flat 24h Sm	-48.8 ± 7.2	49.3 ± 1.6	45.7 ± 0.6	3.6 ± 1.2	0.4 ± 0.1	8.7 ± 2.5
Flat 1h Plasma	-22.0 ± 19.4	47.4 ± 3.9	40.6 ± 1.4	6.8 ± 3.2	0.7 ± 0.5	22.7 ± 10.9
Flat 24h Plasma	-5.5 ± 19.2	46.0 ± 5.3	40.4 ± 3.5	5.7 ± 2.5	0.5 ± 0.3	29.3 ± 10.1
Flat 1h Plasma + Se	-60.5 ± 6.1	46.8 ± 1.2	44.5 ± 0.6	2.3 ± .8	0.3 ± 0.1	5.2 ± 1.5
Flat 24h Plasma + Se	-58.6 ± 3.3	38.3 ± 0.2	36.9 ± 0.2	1.3 ± 0.3	0.2 ± 0.1	4.7 ± 1.1
Flat 1h Plasma + Sm	-63.2 ± 3.1	45.5 ± 0.4	44.2 ± 0.4	1.3 ± 0.2	0.1 ± 0.0	4.6 ± 0.8
Flat 24h Plasma + Sm	6.9 ± 7.9	38.7 ± 1.1	36.8 ± 0.9	1.9 ± 0.9	0.0 ± 0.0	32.2 ± 4.0

5.2.7 Microbial Adhesion to Hydrocarbons (MATH) Assay

The effect of a human plasma conditioning film on *Ser. marcescens* (Figure 5.7b) lowered the polar energy of the cells. Both the acid (chloroform) and basic (ethyl acetate) hydrocarbons demonstrated a reduction in the percent adherence after exposing the cells to the conditioning film (from 42.2% to 21.9 % for chloroform and from 48.3 % to 33.9% for ethyl acetate), demonstrating that the ability for the cell to donate and accept electrons had been reduced, but was still within the moderate adhesion range (between 10 % and 55 %). The highly hydrophilic properties of *Ser. marcescens* did not change, with both non-polar hydrocarbons (decane and hexadecane) demonstrating almost no adherence (0.29 % and 0.58 % respectively).

S. epidermidis (Figure 5.7a) demonstrated a reduced adherence to both non-polar (decane and hexadecane) hydrocarbons and the polar hydrocarbon chloroform (reductions from 98.2 %, 95.8 % and 98.4 % to 90.8 %, 89.2 % and 93.8 % for decane, hexadecane and chloroform respectively), but the reductions were a trend and were not significant. As this was still classed as high adhesion (> 55 %), whilst the cells may be slightly less hydrophobic the changes were unlikely to affect the hydrophobicity or the electron donating properties. However, a significant increase in the adherence of *S. epidermidis* to the basic hydrocarbons ethyl acetate (30.67 % without and 59.74 % with the conditioning film) signified that the cells ability to accept electrons had increased significantly, especially as the cells were classed as moderately adhered without the CF (between 10 % and 55 %) but strongly adhered with the CF (> 55 %).

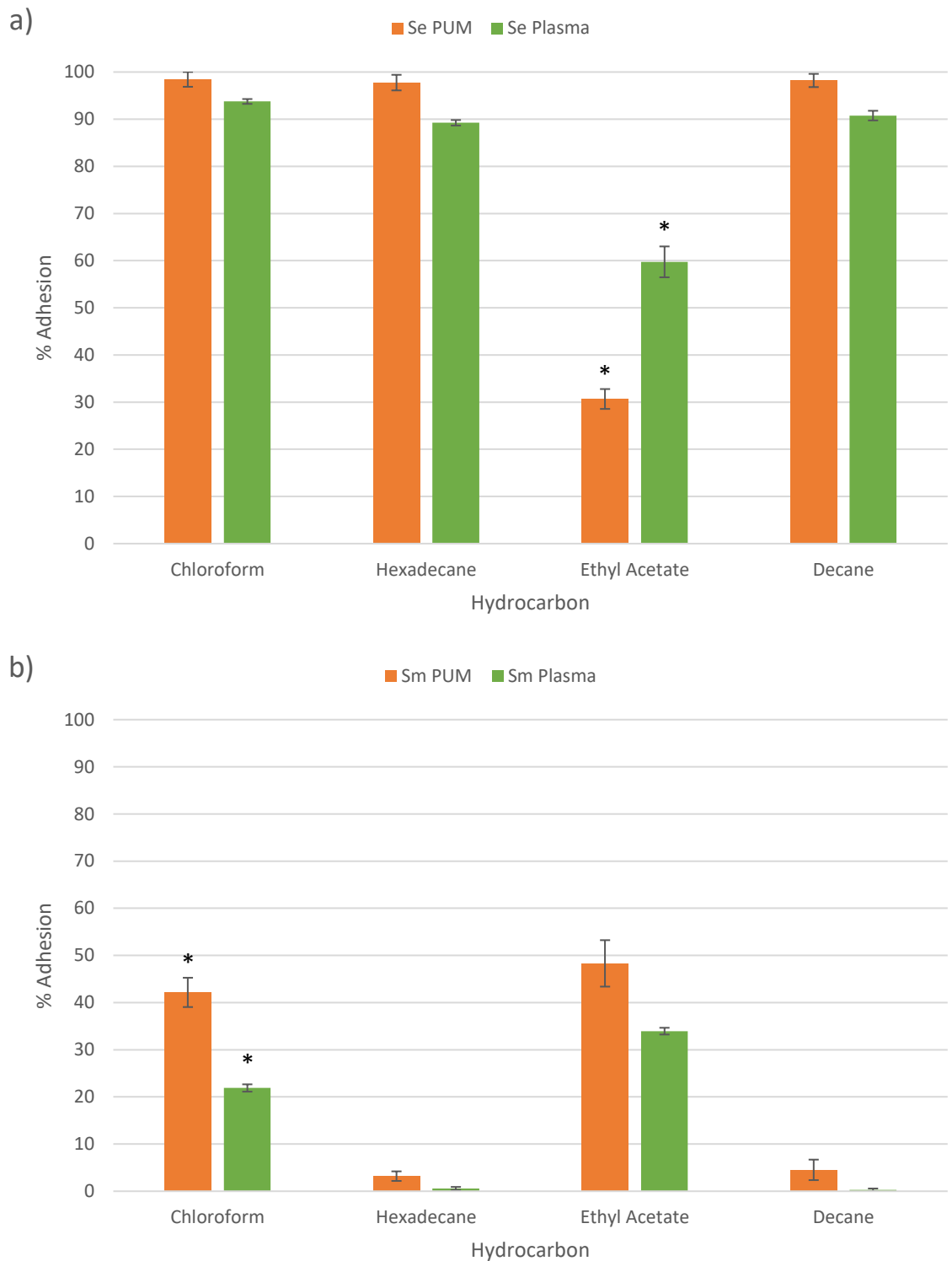


Figure 5.7 MATH assay of a) *S. epidermidis* and b) *Ser. marcescens* with and without the presence of a human plasma conditioning film. Most significant differences annotated with a *. (n = 3)

5.3 Discussion

5.3.1 Scanning Electron Microscopy

When the conditioning films were imaged under SEM the bacteria alone did not appear to have any difference between the 1 h and 24 h timepoints, likely due to a lack of nutrients available for proliferation. However, it was apparent that when *S. epidermidis* was applied to the rough surface, especially after 24 h (Figure 5.1.1b), it preferentially adhered within the pits present. The human plasma conditioning film appeared to have a visible increase on the rough surface from 1 h to 24 h (Figure 5.1.3a/b), which is likely caused by a continuous building up of molecules being adsorbed onto the surface and onto other molecules already adsorbed (Lorite *et al.*, 2011). This was only apparent on the rough surface, as both the smooth and flat did not appear to demonstrate any significant differences between the timepoints, with the effect appearing on the rough surface due to the pits making it harder to wash away the excess CF. The most significant change observable for any of the CFs was the significant increase in cells observable on any of surfaces after a 24 h human plasma and *Ser. marcescens* CF was applied (Figure 5.1.5). This demonstrated that the *Ser. marcescens* proliferated during the 24 h incubation period using nutrients present in the human plasma, as this same effect was not observed when *Ser. marcescens* was incubated without the addition of human plasma. It also demonstrated that *S. epidermidis* either was not capable of using the nutrients as efficiently as *Ser. marcescens* or that something within the human plasma was reducing *S. epidermidis*' proliferation, some studies have demonstrated that bacteria can be sensitive to plasma serum, as whilst it appeared that an increase in cells occurred when human plasma and *S. epidermidis* were combined (Figure 5.1.4) this was significantly less than human plasma and *Ser. marcescens* combined (Ramírez-Arcos *et al.*, 2007).

5.3.2 Optical Surface Profiling

On the roughest surface, the changes observed with the rough surface were the most noticeable and significant. The CF that had the greatest effect on the surface roughness were the human plasma CF's, with both 1 h and 24 h conditioning films significantly reducing the roughness values (5.2a). The reduction in roughness was likely to be caused by molecules in the human plasma adsorbing onto the surface and possibly filling in the pits that were present, which appeared to be the case when imaged under SEM (Figure 5.1.3). Further, it has previously been demonstrated that the addition of a conditioning film has drastically reduced surface roughness of glass (Lorite *et al.*, 2011). On the smooth surface human plasma had no significant difference after 1 h, but after 24 h a reduction in surface roughness was also observed. Whilst the smooth surface did not have the pits that were present on the rough surface, it still had a greater surface roughness than the flattened surface which could have been smoothed out by the adsorption of molecules. Finally, on the flat surface a slight increase in roughness was observed after 1 h but then no difference was observed after 24 h. This could potentially be due to an uneven adsorption of molecules onto the surface after 1 h, causing more irregularity in the surface features, but was smoothed out as more molecules were adsorbed onto the surface.

When conditioned alone *S. epidermidis* 1 h or 24 h and *Ser. marcescens* 24 h demonstrated a reduction in surface roughness, whilst *Ser. marcescens* 1 h demonstrated no change. The greater reduction caused by *S. epidermidis* was possibly due to the shape of the cell, as *S. epidermidis* is a cocci and smaller than *Ser. marcescens*, it was possible that it was more likely to reside within smaller pits on the surface that *Ser. marcescens* is unable to fully reside within without protruding, which is also what may have caused the increase in roughness after 24 h. Unlike the rough surface, when conditioned onto the smooth surface

no significant changes were determined for CFs formed by bacteria alone. Similarly, the flat surface demonstrated no significant changes. For both surfaces, the lack of any significant change was likely due to the surface already being relatively smooth with no large surface features present like the rough surface.

When human plasma and bacteria were conditioned onto the rough surface a reduction in roughness was observed for all the CF's. Whilst the roughness for the human plasma and *S. epidermidis* CF's demonstrated no significant differences between the 1 h and 24 h CF, *Ser. marcescens* demonstrated a further reduction from 1 h to 24 h. The changes may be due to the strain of *S. epidermidis* used demonstrating little growth in the human plasma whilst the strain of *Ser. marcescens* demonstrated plenty of growth. Further, bacteria typically preferentially adhere within gaps or pits on a surface due to protection from unfavourable environmental factors and increase in surface area contact (Mitik-Dineva *et al.*, 2008; Lorenzetti *et al.*, 2015). As such, the growth of *Ser. marcescens* may have caused some pits to be filled in by a combination of bacterial cells, human plasma and products produced by the bacteria, such as extracellular polymeric substances (EPS).

5.3.3 Energy Dispersive X-ray

Whilst some small changes were detected via EDX analysis following the application of the CFs, they were not significant. This demonstrated that whilst other methods of analysis determined changes in the surface properties, the elemental makeup of the surfaces were not significantly altered. Overall the small changes appeared to be a reduction in the detection of carbon and subsequent increases in the oxygen and chlorine detected.

5.3.4 Attenuated Total Reflection-Fourier Transform Infrared Spectroscopy

The analysis of the surface chemistry via ATR-FTIR demonstrated that the addition of a CF altered a number of spectra, however most of the changes were consistent across the

different CFs applied. Most of the surfaces demonstrated increases in the C-CL stretching region, with only human plasma alone demonstrating a reduction in this absorption. As the absorption for the PVC was already reduced, due to the high levels of plasticiser dominating the spectrum, the changes were potentially due to the CFs interacting with the plasticiser which reduced the domination of it across the spectrum. This would be supported by both the ester carbonyl stretching region of the plasticiser and the plasticiser ester C-O bending region demonstrating a reduced absorption across almost all the surfaces. The application of a CF also appeared to mask the presence of the antisymmetric $\nu_{as}COO^-$ stretching vibration of carboxylate groups in unidentate and bidentate calcium or carboxylate zinc stearates for all surfaces where it was detected on the control surface.

5.3.5 Raman Spectroscopy

All of the Raman spectra demonstrated no significant differences compared to the control spectra, except human plasma combined with *Ser. marcescens* spectra demonstrating a difference on the flat surface. The difference is likely to be due to *Ser. marcescens* being able to proliferate significantly within the human plasma whilst *S. epidermidis* appeared to demonstrate a very low rate of proliferation.

5.3.6 Physicochemistry

One of the biggest changes demonstrated due to the surfaces being fouled in the presence of CFs was how the CFs influenced the physicochemical characteristics. The changes not only differed depending on what CF was applied to a surface but also upon the surface the CF was applied to. However, whilst all the properties demonstrated changes, the most significant changes in physicochemistry occurred to the Gibbs Free energy and the basic energy.

The physicochemical force that demonstrated the greatest change was the Gibbs Free energy, which can be used to determine surface hydrophobicity. Whilst most of the surfaces demonstrated a negative Gibbs Free energy value, indicative of a hydrophobic surface, many demonstrated increases in this value, but only when human plasma was used in the CF, and some CFs demonstrated increases great enough to become positive values. This indicated that whilst many of the surfaces remained hydrophobic, the intensity of the hydrophobicity was potentially reduced. Some of the surfaces demonstrating positive Gibbs Free energy values indicated that they had become hydrophilic, even if only weakly. Most of the surfaces that changed to display hydrophilic properties were on the smooth surface and all involved human plasma, with or without bacteria, that had been conditioned on the surface for 24 h with the only other hydrophilic surface being the flat surface with human plasma and *Ser. marcescens* after 24 h.

The changes determined in the basic energy were likely also due to the effects of macromolecules adsorbed from the human plasma, as the significant changes in values obtained all had human plasma conditioned onto them. An increase in basic energy indicated an increase in the negative charge of the energy present within a surface. This change was significant as all of the physicochemical factors can influence the attachment and adhesion of bacteria. Further, bacteria in solution are typically negatively charged and an increase in surface negative charge may create a repulsion effect which could reduce attachment, however, surface charge on bacterial attachment has not been clearly defined (Katsikogianni and Missirlis, 2004).

These changes in the Gibbs Free energy and basic-energy demonstrated how an initial conditioning film can significantly differ from a conditioning film that has been allowed to develop over a longer period, increasing the amount or types of macromolecules adsorbed

and how well they are adsorbed. The longer incubation time increased the amount of adsorbed macromolecules whilst increasing their adherence to the surfaces, which caused a greater effect on the surface physicochemistry. The increase in adsorbed macromolecules over time and the effects of physicochemical changes of a surface has previously been demonstrated by Lorite *et al.* (2011).

5.3.7 Microbial Adhesion to Hydrocarbons (MATH) Assays

When MATH assays were performed using a human plasma CF, most of the levels of adherence to any of the hydrocarbons for either *S. epidermidis* or *Ser. marcescens* was reduced with the exception of *S. epidermidis* to ethyl acetate. The varying reduction indicated that properties of the human plasma were interfering with the adherence of the bacteria to the hydrocarbons. In one study, it was found that platelet bags preconditioned with human plasma demonstrated a significant increase in bacterial adhesion by *S. epidermidis* (Loza-Correa *et al.*, 2017). This signified that bacteria may be influenced by the presence of plasma factors in their adherence capabilities. Further, the only increase observed in the MATH assays of *S. epidermidis* to ethyl acetate may have been facilitated by the use of plasma factors to increase adherence in this instance. This indicated that the plasma factors could increase or decrease different aspects of bacterial adherence, or the plasma factors were binding to bacterial receptors and altering how they interact with their environment. This has previously been demonstrated by Schuster *et al.* (2014) using *Staphylococcus aureus* with bovine serum albumin, γ -globulins and plasma serum and changes in *S. aureus*' adhesion after removal of its IgG binding protein. As such, it is likely that the changes observed in the MATH assays was due to the binding of blood plasma molecules with the bacteria.

5.4 Conclusion

Conditioning films can affect surface properties in a variety of ways dependent upon the original surface properties and the properties of the conditioning film applied. It was apparent that when applied to a rougher surface CFs are capable of reducing surface roughness potentially by greater adsorption within surface features. It was also apparent that the adsorption of a CF was capable of masking certain surface chemistry features, as was determined via FTIR. CFs were also capable of altering the physicochemical properties by increasing the hydrophilic property, especially human plasma due to the large variety of plasma factors present. The human plasma was finally also able to reduce overall adhesion of the bacteria to most of the hydrocarbons, indicating that the plasma factors can play a role in altering physicochemical interactions and affect bacterial adherence. Overall, it was apparent that it was important to take into account that the platelet bags will become conditioned with human plasma factors that could significantly alter the way a contaminant interacting with the platelet bag surfaces.

6.0 Bacterial and Biofilm Interactions with Platelets

6.1 Introduction

It has already been established that bacteria, and their products, are capable of interacting with platelets (Arman *et al.*, 2014). Bacterial interactions with platelets are thought to contribute to diseases including infective endocarditis, disseminated intravascular coagulation, immune thrombocytopenia purpura and myocardial infarction or stroke (Fitzgerald *et al.*, 2006). Further, therapeutic platelets are often transfused into patients with weak immune systems whose own platelets may not be fully functioning. Therefore, platelet viability, activation and function within the transfusion unit are vital, and any changes in these caused by bacteria could be detrimental to a transfusion recipient (Fitzgerald *et al.*, 2006).

Platelet activation and aggregation enable platelets to aggregate and form clots, potentially stopping patients from bleeding out, with more recent studies indicating that platelets play a role in intercellular communication (Edelstein, 2017). At a basic level, platelet activation by an agonist results in calcium signalling, a cascade of phosphorylation events and expression of specific surface proteins which aid in further activation of neighbouring resting platelets and also end-point aggregation (Vinik *et al.*, 2001). Surface activation markers such as CD62P and activated GP IIb/IIIa (measured by PAC1 binding) can be detected by flow cytometry, while end point aggregation can be assessed by light-transmission aggregometry (LTA) (Lu and Malinauskas, 2010). Platelet surface P-selectin (CD62P) translocates to the platelet surface upon platelet activation, but in resting platelets is expressed on α -granules internally (Lu and Malinauskas, 2010; Wasiluk *et al.*, 2013). PAC1 monoclonal antibody only binds to GP IIb/IIIa complexes on the platelet

surface after the GP IIb/IIIa complexes have undergone conformational changes due to platelet activation (Shattil *et al.*, 1985; Lim *et al.*, 2008; Lu and Malinauskas, 2010).

The phosphorylation status of signalling proteins can be examined by western blotting. Some important proteins that are affected by phosphorylation include Vasodilator-stimulated Phosphoprotein (VASP), Akt (protein kinase-B) and Phospholipase C- β (PLC- β) (Sangkuhl *et al.*, 2011; Li *et al.*, 2015). VASP is phosphorylated by both the cAMP- and cGMP-dependent protein kinases in resting platelets, but upon activation by an agonist becomes rapidly dephosphorylated and helps in the control of activated platelets (Benz *et al.*, 2016). In contrast Akt and PLC- β exist in a non-phosphorylated form in resting platelets but rapidly become phosphorylated in response to the correct stimulation. AKT phosphorylation has multiple functions including platelet granule secretion, integrin activation and platelet activation mediation, whilst PLC- β is involved in signalling calcium release within platelets (Lian *et al.*, 2005a; Guidetti *et al.*, 2015). Consensus was that specific agonists induced phosphorylation of a distinct set of signalling proteins, with activation of the Protease-Activated Receptor 1 (PAR-1) or PAR-4 by thrombin causing phosphorylation of PLC- β and IP3 (**Fig 6.1**) (Li *et al.*, 2015). Although this model is still considered accurate in many respects, there is evidence to suggest that the signalling pathways are more 'fluid' and activation of multiple pathways via a single agonist is expected (Lian *et al.*, 2005a; Sangkuhl *et al.*, 2011; Li *et al.*, 2015).

In addition to their major role in haemostasis, platelets play critical roles in immunological responses, releasing a vast array of cytokines and chemokines in order to direct a host-pathogen response (Cognasse *et al.*, 2007; Mussano *et al.*, 2016). These cytokines and chemokines are responsible for the activation, and also the migration of many different leukocyte populations, most notably neutrophils and monocytes (Von Hundelshausen *et*

al., 2001; von Hundelshausen *et al.*, 2005). Cytometric Bead Array (CBA), an adaptation of traditionally flow cytometry can be used to identify these cytokines/chemokines (specifically RANTES) in the platelet releasate as a direct measure of platelet activation. RANTES is a significant releasate as it is involved in platelet activation inhibition and monocyte recruitment, but can also be a marker for infection severity (Von Hundelshausen *et al.*, 2001; Shenkman *et al.*, 2004; von Hundelshausen *et al.*, 2005; Stojewska *et al.*, 2016). The aim of this part of the work was to determine whether the presence of planktonic or biofilm forms of *S. epidermidis* or *Ser. marcescens* affect the activation status, aggregation potential or immunological potential of healthy platelets, by examining changes in activation markers, signalling pathways and cytokine profiles of bacterially contaminated platelet rich plasma.

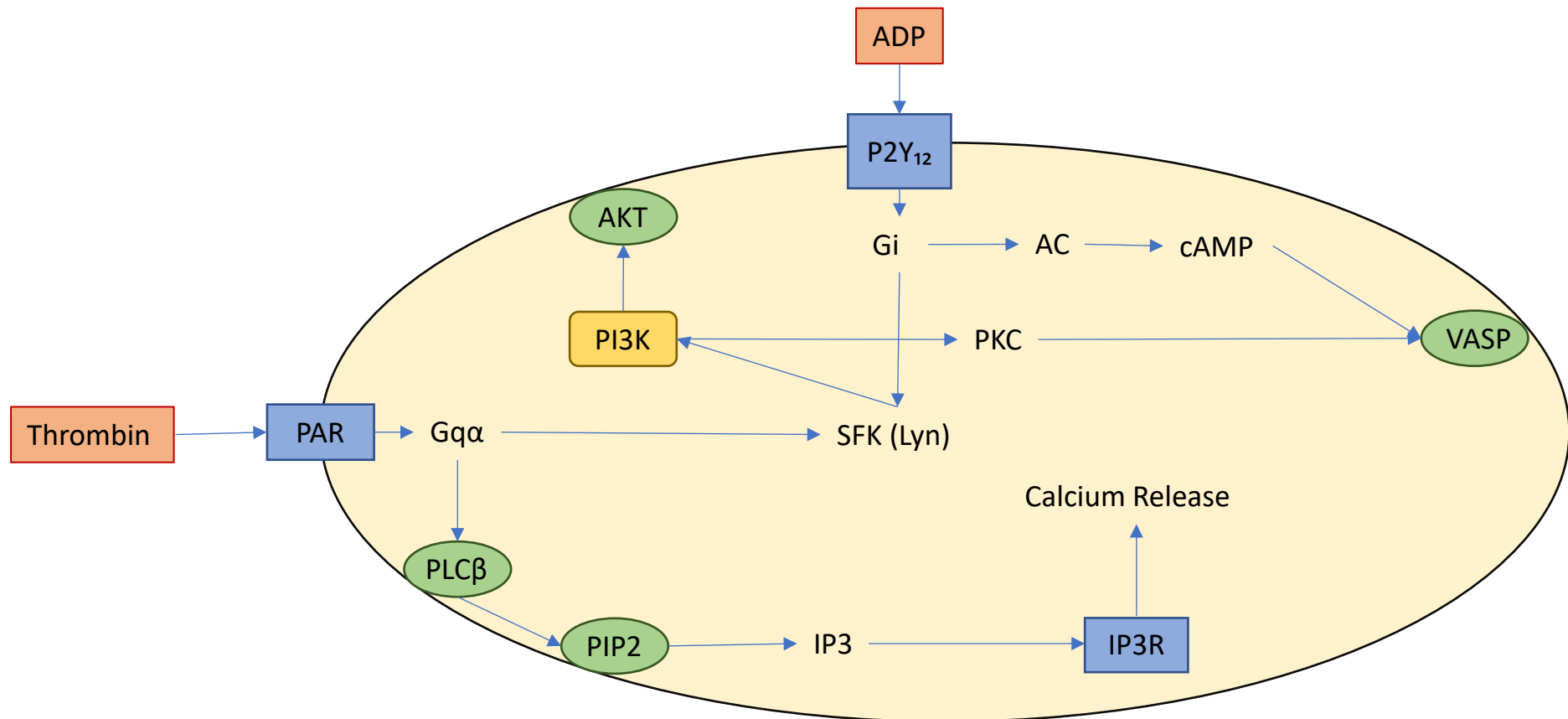


Figure 6.1 Main platelet signalling pathways involved with VASP, PLC β and AKT proteins. Thrombin stimulates the PAR receptor which causes Gq α to mainly activate phospholipase β (PLC β) (and minor activation of Src family kinases (FFK) Lyn in the ADP pathway) which hydrolyses PIP₂ membrane into IP₃ triggering an increase in cytosolic Ca²⁺ levels. ADP stimulates the P2Y₁₂ receptor and activates Gi which inhibits adenylate cyclase (AC) causing a reduction in cyclic AMP (cAMP) formation leading to the dephosphorylation of VASP. Gi also interacts with SFK (Lyn) which causes Phosphatidylinositol 3-kinase (PI3K) to phosphorylates AKT and also causes PI3K to interact with Protein Kinase C (PKC) to dephosphorylate VASP (Sanguhl *et al.*, 2011; Li *et al.*, 2015).

6.2 Results

6.2.1 Haemostatic Efficacy via Platelet Aggregation

Platelets were incubated with either planktonic bacteria or biofilms and tested using light transmission aggregometry with a platelet agonist to determine bacterial effects on platelet aggregation.

When platelets were incubated with planktonic bacteria and activated using ADP (**Fig. 6.1.1**) no significant changes with either a 1 h or 2 h incubation were determined. However, a trend was demonstrated showing a reduction in platelet aggregation when incubated with *S. epidermidis* at 1×10^7 colony forming units / mL (CFU / mL) was observed. When thrombin was used as an agonist (**Fig. 6.1.2**), a trend in the reduction in aggregation (15 - 24 % relative aggregation reduction) was observed with no significant differences between the bacteria or bacterial concentration.

However, significant reductions in platelet aggregation were observed when platelets were incubated with bacterial biofilms (**Fig 6.1.3**). *S. epidermidis* biofilms appeared to have had a greater effect on platelet aggregation than biofilms formed by *Ser. marcescens*, with most significant changes being from *S. epidermidis* biofilms grown on the rough and flat (57.8 % and 44.9 % relative aggregation) surfaces after 5 days. After 7 days growth, the *S. epidermidis* biofilms demonstrated no significant differences between the rough, smooth or flat (53.9 %, 63.6 % and 57.5 % relative aggregation) surfaces.

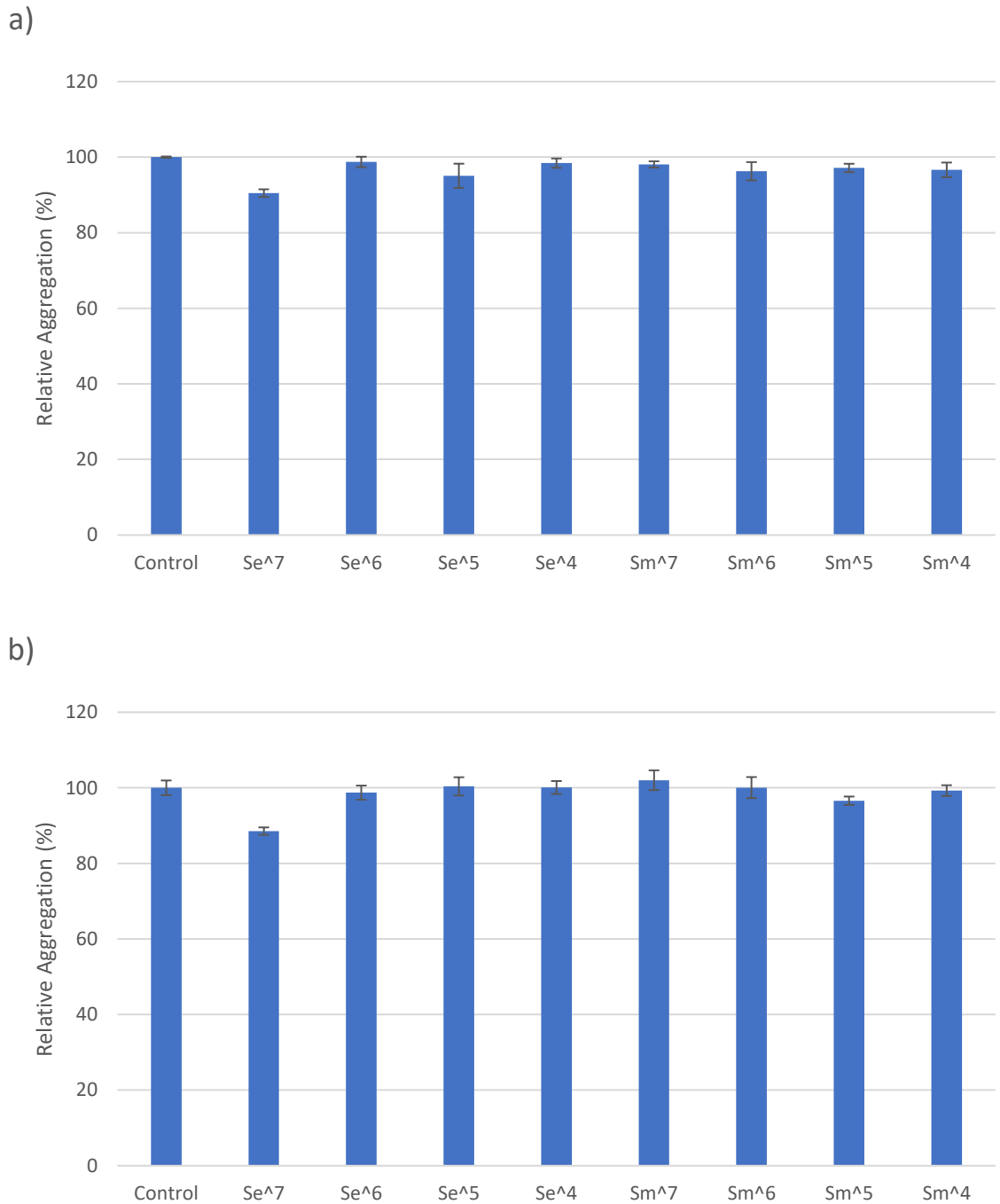


Figure 6.1.1 Platelet aggregation as assessed by Light Transmission Aggregometry (LTA), in response to ADP (10 μ M), following incubation for a) 1 h or b) 2 h with planktonic bacteria. Data presented as mean \pm SE after normalisation to the control (incubated in the absence of bacteria but stimulated with ADP). (n = 3)

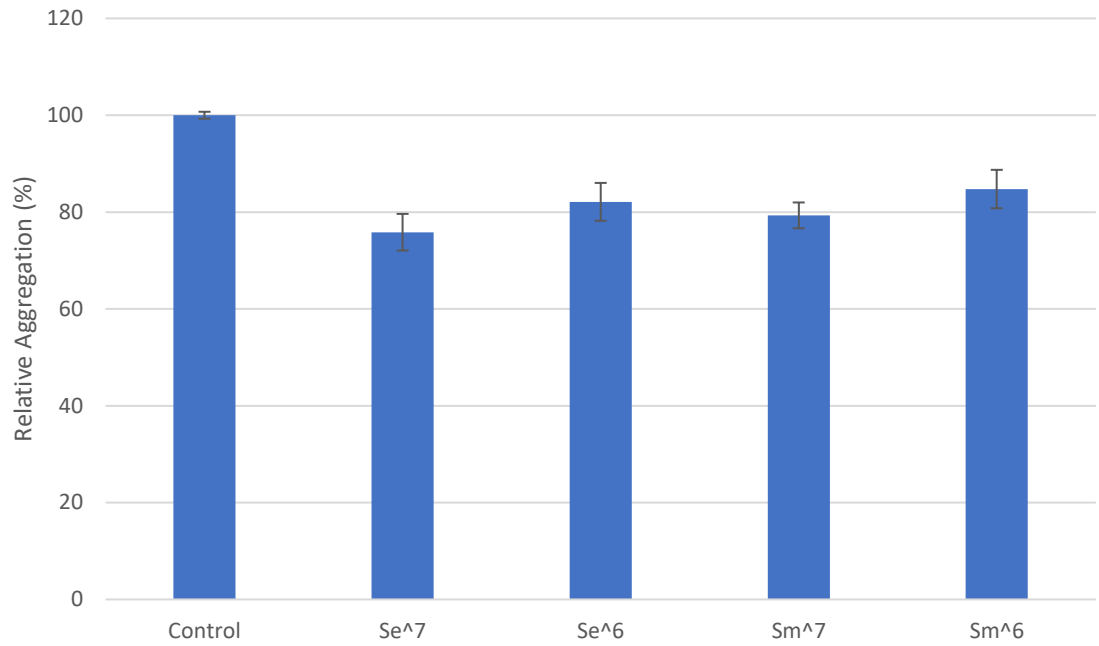


Figure 6.1.2 Platelet aggregation as assessed LTA, in response to Thrombin (10 U), following incubation for 2 h with planktonic bacteria. Data presented as mean \pm SE after normalisation to the control (incubated in the absence of bacteria but stimulated with ADP). (n = 3)

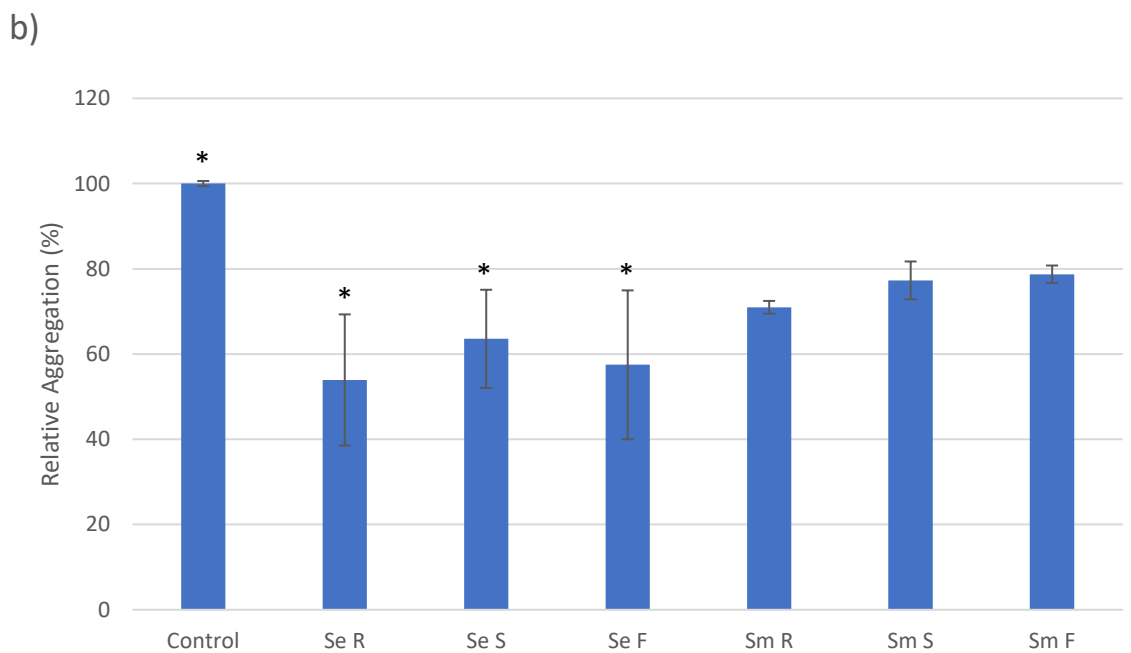
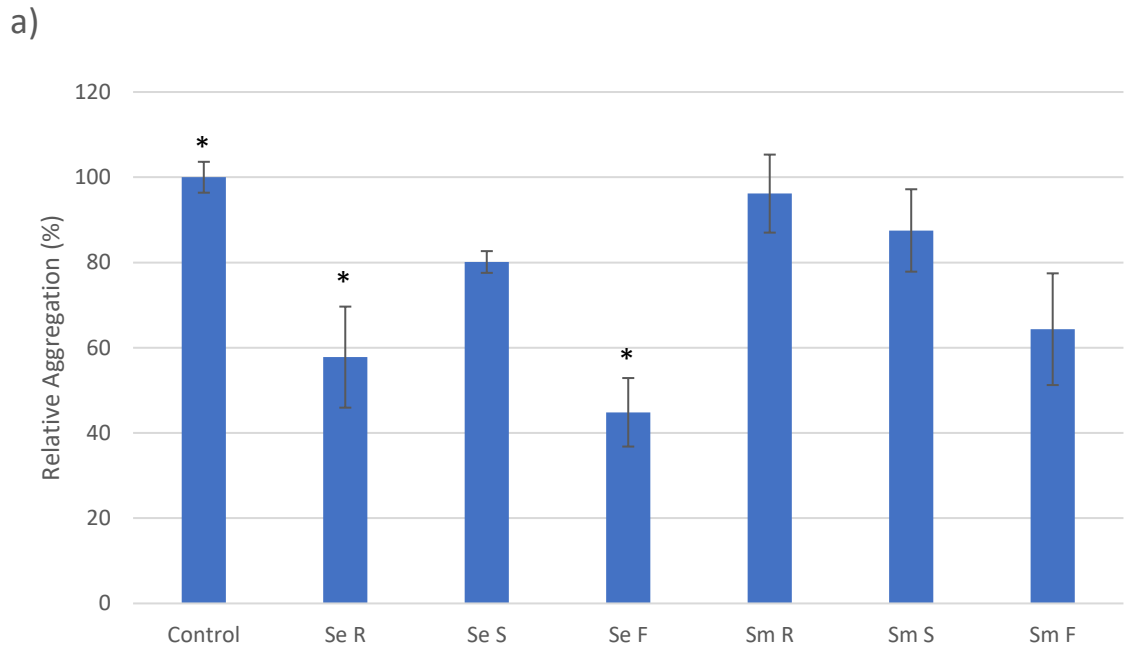


Figure 6.1.3 Platelet aggregation as assessed by LTA, in response to ADP (10 μ M), following incubation for 2 h with a) 5-day biofilms and b) 7-day biofilms grown on the 3 different surfaces. Data presented as mean \pm SE after normalisation to the control (incubated in the absence of bacteria but stimulated with ADP). Most significant differences annotated with a *. (n = 3)

6.2.2 Platelet Receptor Activation via Flow Cytometry

Platelets were incubated with either planktonic bacteria or biofilms, bound with a PE conjugated CD62P antibody (**Fig 6.2.1 - 6.2.3**) or FITC conjugated PAC1 (**Fig. 6.2.4 – 6.2.6**) and analysed via flow cytometry to determine changes in receptor binding.

No significant changes were determined following incubation of the platelets with either planktonic cells or biofilms. Some trends were present, with planktonic bacteria slightly reducing the amount of receptor expression, regardless of whether ADP or Thrombin was used, for both CD62P and PAC1. However, when platelets were incubated with biofilms data was inconsistent, with some increase and some decrease in receptor expression but no significant changes.

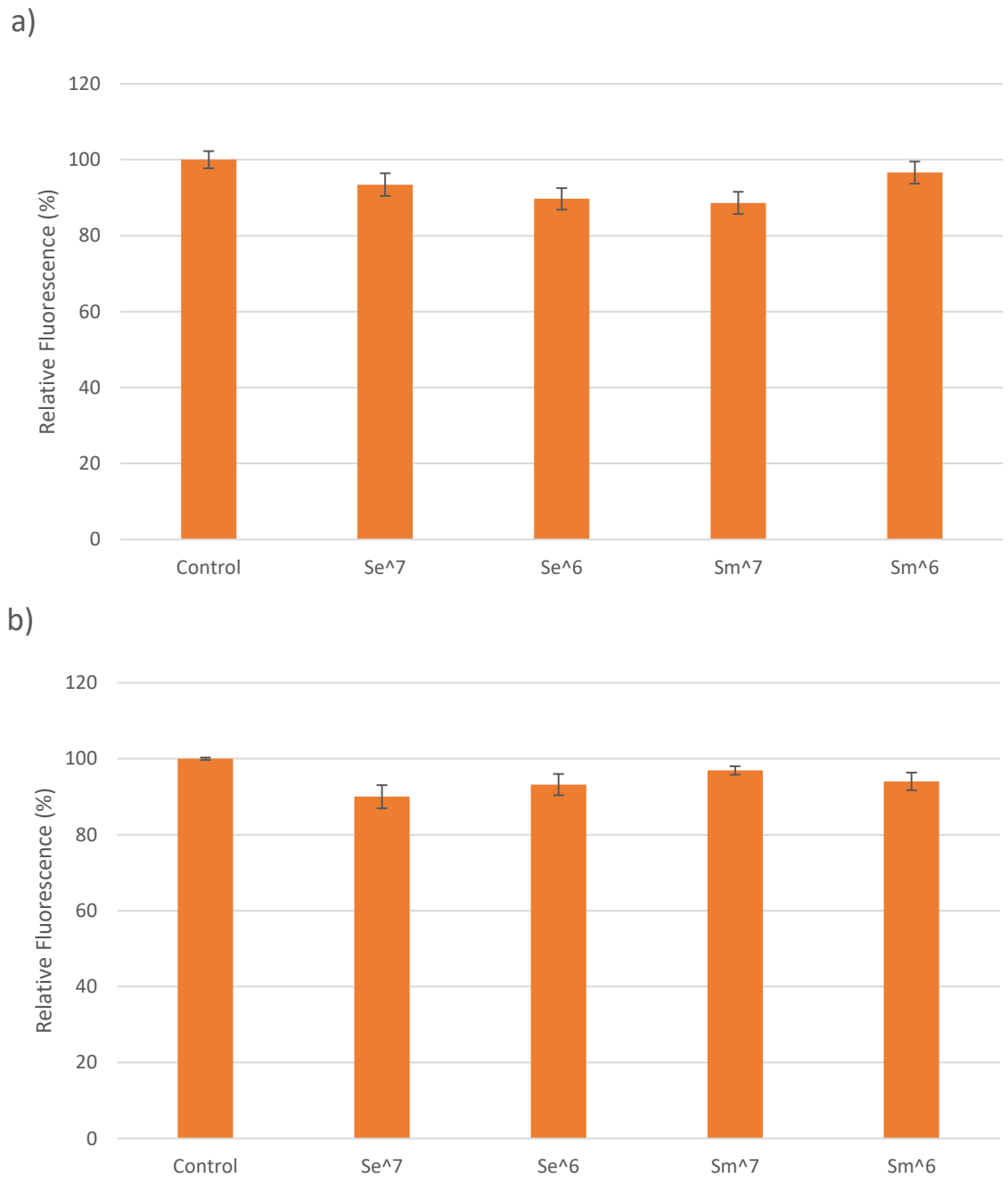


Figure 6.2.1 CD62P expression as assessed by flow cytometry in response to using ADP (10 μ M), following incubation for a) 1 h or b) 2 h with planktonic bacteria. Data presented as mean \pm SEM after normalisation to the control (incubated in the absence of bacteria but stimulated with ADP). (n = 3)

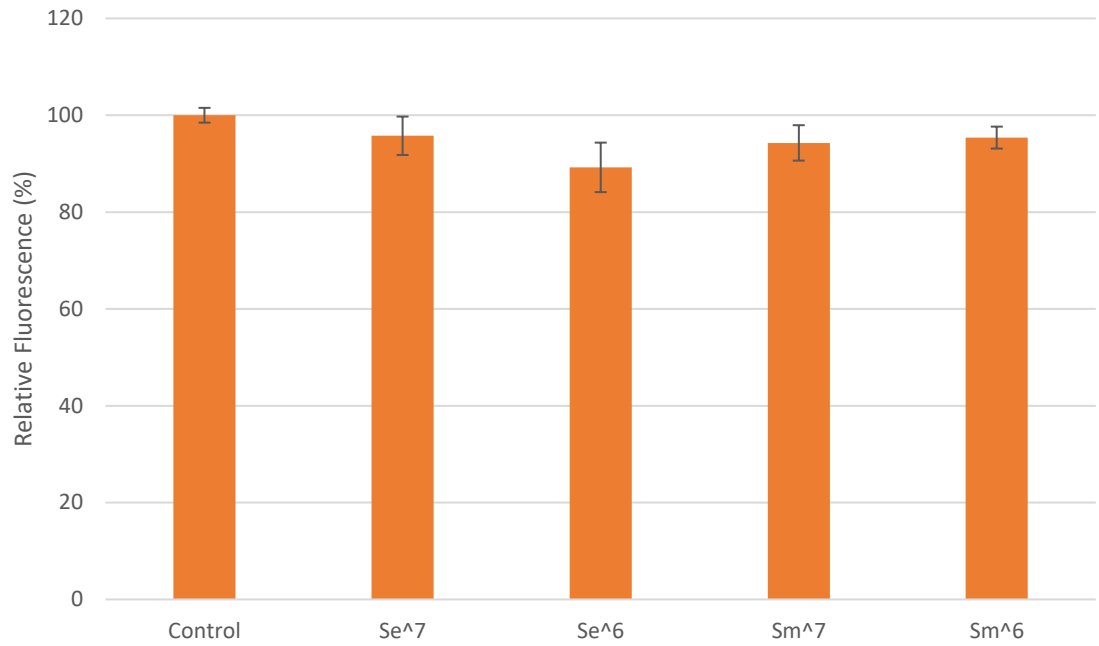


Figure 6.2.2 CD62P expression as assessed by flow cytometry, in response to Thrombin (10 U), following incubation for 2 h with planktonic bacteria. Data presented as mean \pm SE after normalisation to the control (incubated in the absence of bacteria but stimulated with ADP). (n = 3)

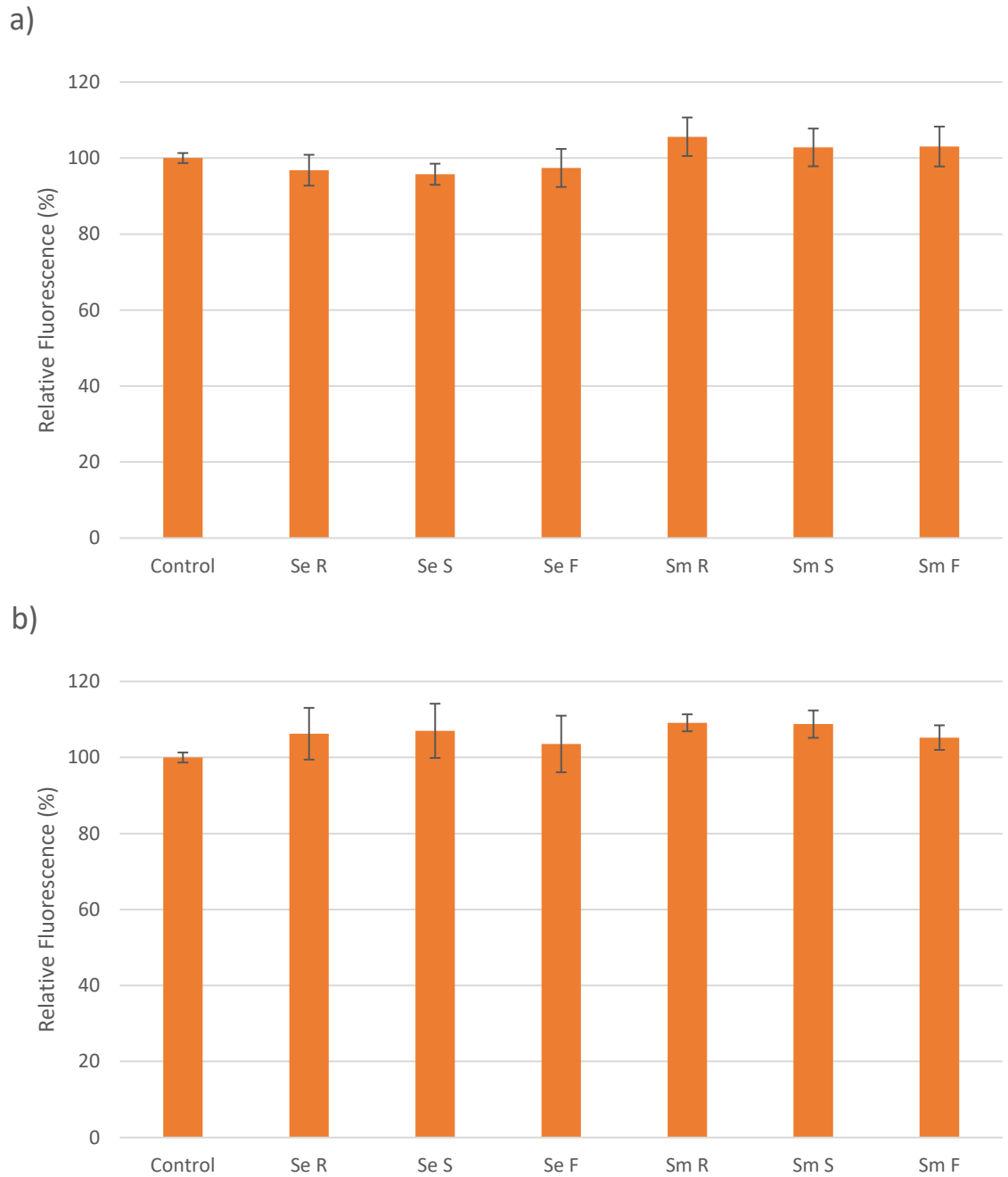


Figure 6.2.3 CD62P expression as assessed by flow cytometry, in response to ADP (10 μ M), following incubation for 2 h with a) 5-day biofilms and b) 7-day biofilms grown on the 3 different surfaces. Data presented as mean \pm SE after normalisation to the control (incubated in the absence of bacteria but stimulated with ADP). (n = 3)

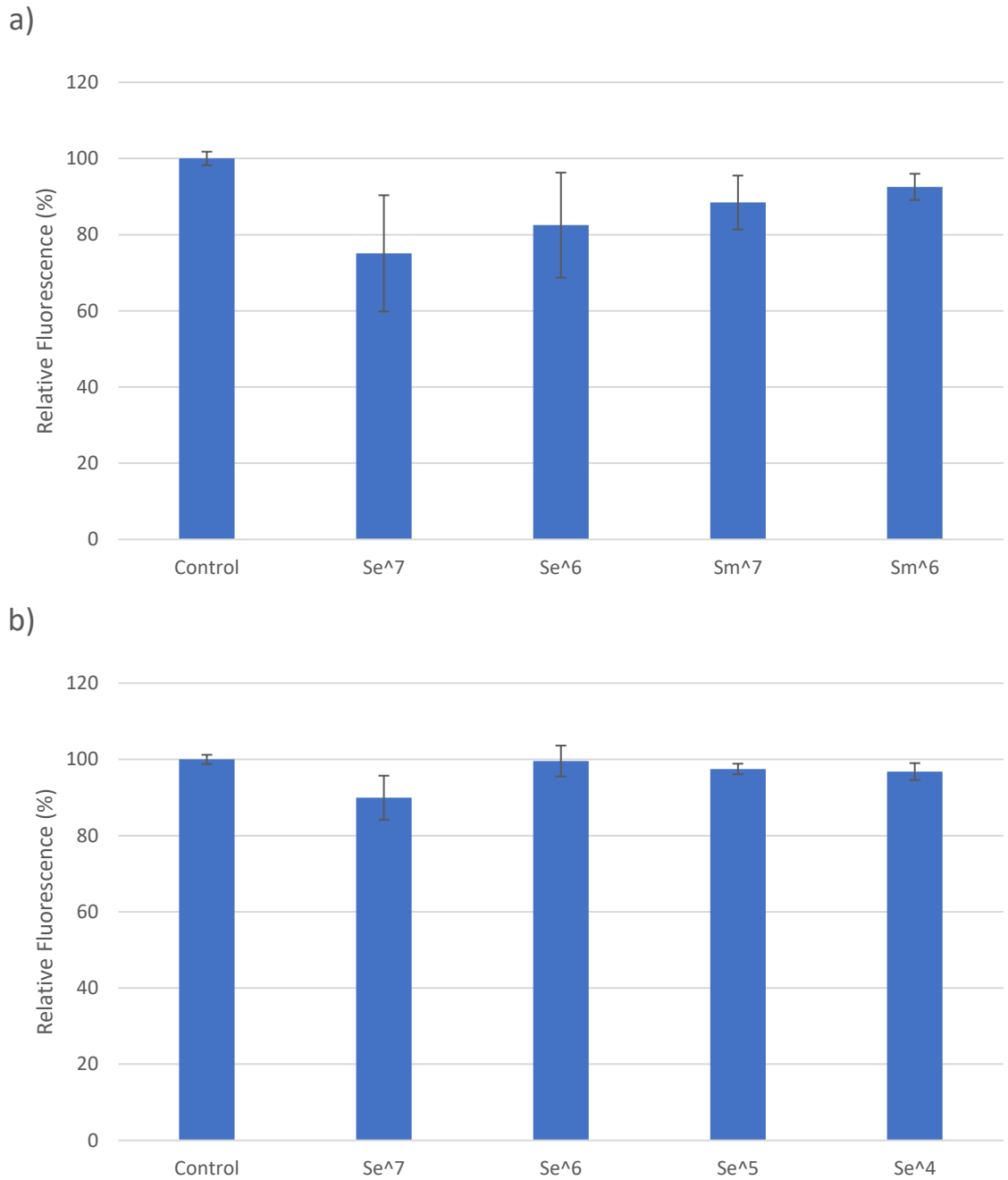


Figure 6.2.4 PAC1 expression as assessed by flow cytometry in response to using ADP (10 μ M), following incubation for a) 1 h or b) 2 h with planktonic bacteria. Data presented as mean \pm SEM after normalisation to the control (incubated in the absence of bacteria but stimulated with ADP). (n = 3)

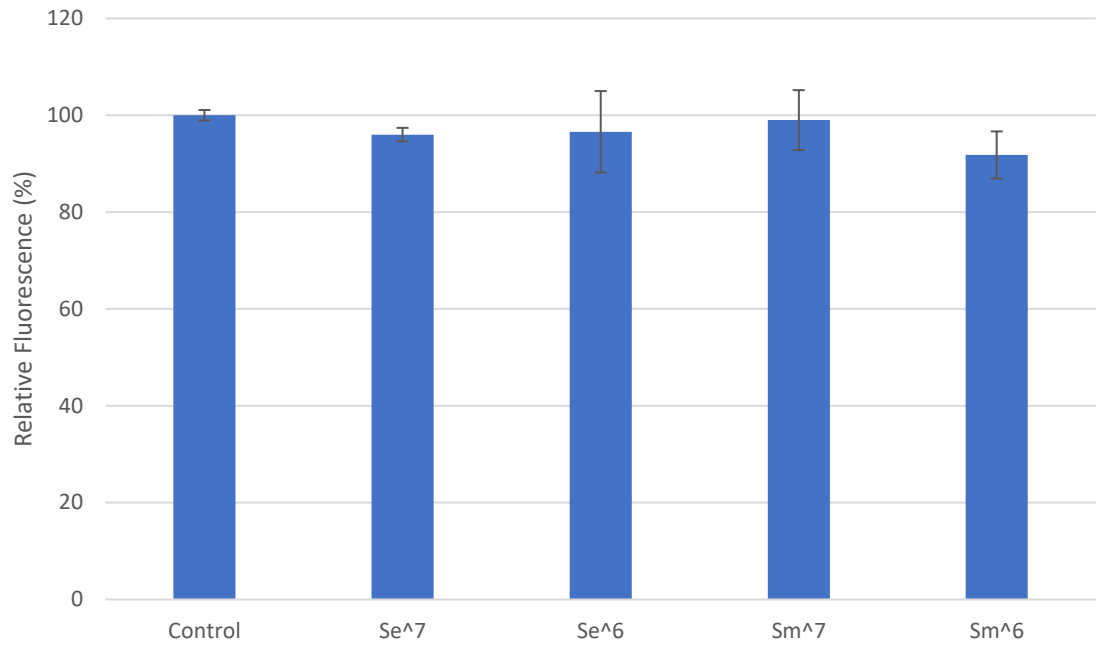


Figure 6.2.5 PAC1 expression as assessed by flow cytometry, in response to Thrombin (10 U), following incubation for 2 h with planktonic bacteria. Data presented as mean \pm SE after normalisation to the control (incubated in the absence of bacteria but stimulated with ADP). (n = 3)

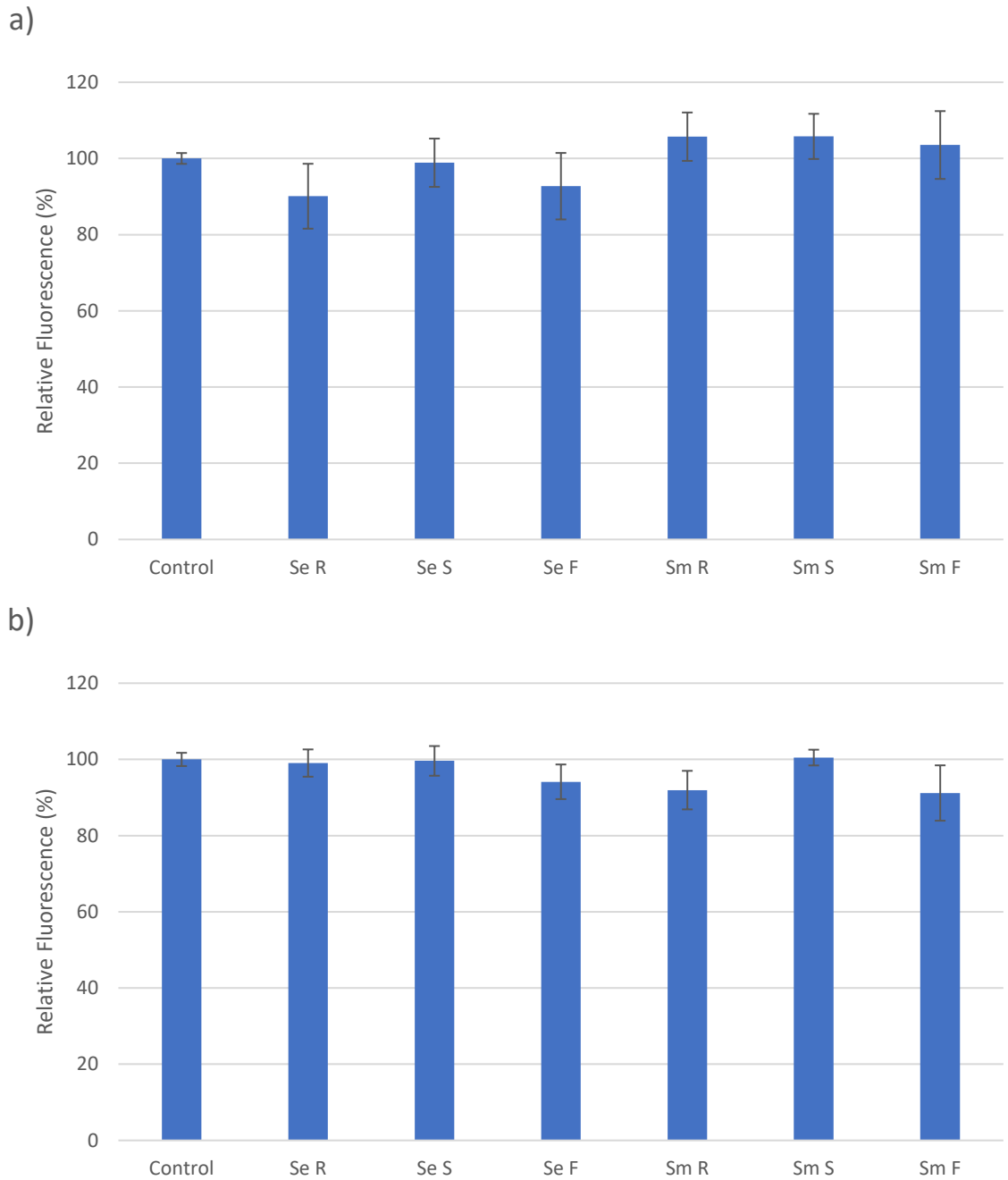


Figure 6.2.6 PAC1 expression as assessed by flow cytometry, in response to ADP (10 μ M), following incubation for 2 h with a) 5-day biofilms and b) 7-day biofilms grown on the 3 different surfaces. Data presented as mean \pm SE after normalisation to the control (incubated in the absence of bacteria but stimulated with ADP). (n = 3)

6.2.3 Western Blots

Proteins were collected from lysed platelets that had been incubated with both planktonic bacteria and biofilms, then processed via western blot to determine changes in protein expression of phosphorylated vasodilator-stimulated phosphoprotein (p.VASP), phospholipase C isoform β (p-PLC β) and phosphorylated AKT (p.AKT). However, Akt had no determinable amount of phosphorylation with the western blots and as such the data has not been presented.

6.2.3.1 Phosphorylated VASP

The expression of p.VASP when platelets were incubated with planktonic bacteria (**Fig. 6.2.3.1**) demonstrated that *Ser. marcescens* had a greater effect on the expression of p.VASP, with both starting concentrations demonstrating a 2-fold increase in p.VASP expression. When the platelets were stimulated with ADP this increased more with a 4-fold increase in p.VASP expression. Further, *S. epidermidis* also demonstrated an increase in p.VASP when the platelets were stimulated with ADP but was significantly lower than *Ser. marcescens* and also had large error bars. However, when the platelets were stimulated with Thrombin, no p.VASP expression was determined for the controls or platelets incubated with bacteria.

When platelets were incubated with biofilms the expression of p.VASP had a greater variation than with planktonic bacteria causing the error bars to be significantly greater. When platelets were incubated with a 5 day biofilm without stimulation (**Fig. 6.2.3.2a**) of *S. epidermidis* on the flat surface the expression of p.VASP was significantly increased by 5.6 fold, demonstrating the greatest increase in p.VASP. *S. epidermidis* also demonstrated an increase on the smooth surface (1.9 fold) and *Ser. marcescens* demonstrated an increase on the flat surface (2.6 fold). However, when platelets incubated with 5 day

biofilms were stimulated with ADP (**Fig. 6.2.3.2b**) only *S. epidermidis* on the smooth surface demonstrated a significant increase (1.9 fold) but was the same as unstimulated. The incubation of platelets with 7 day biofilms without stimulation (**Fig. 6.2.3.3a**) demonstrated a significant increase in p.VASP expression with *S. epidermidis* biofilms grown on the smooth surface (3.1 fold) and *Ser. marcescens* biofilms grown on the smooth (3 fold) and flat surfaces (3.7 fold). When the platelets incubated with 7 day biofilms were stimulated with ADP (**Fig. 6.2.3.3b**) both *S. epidermidis* and *Ser. marcescens* demonstrated significant increases in p.VASP expression for biofilms grown on the flat surface (1.8 fold and 2.5 fold respectively). However, none of the other biofilms demonstrated significant increases.

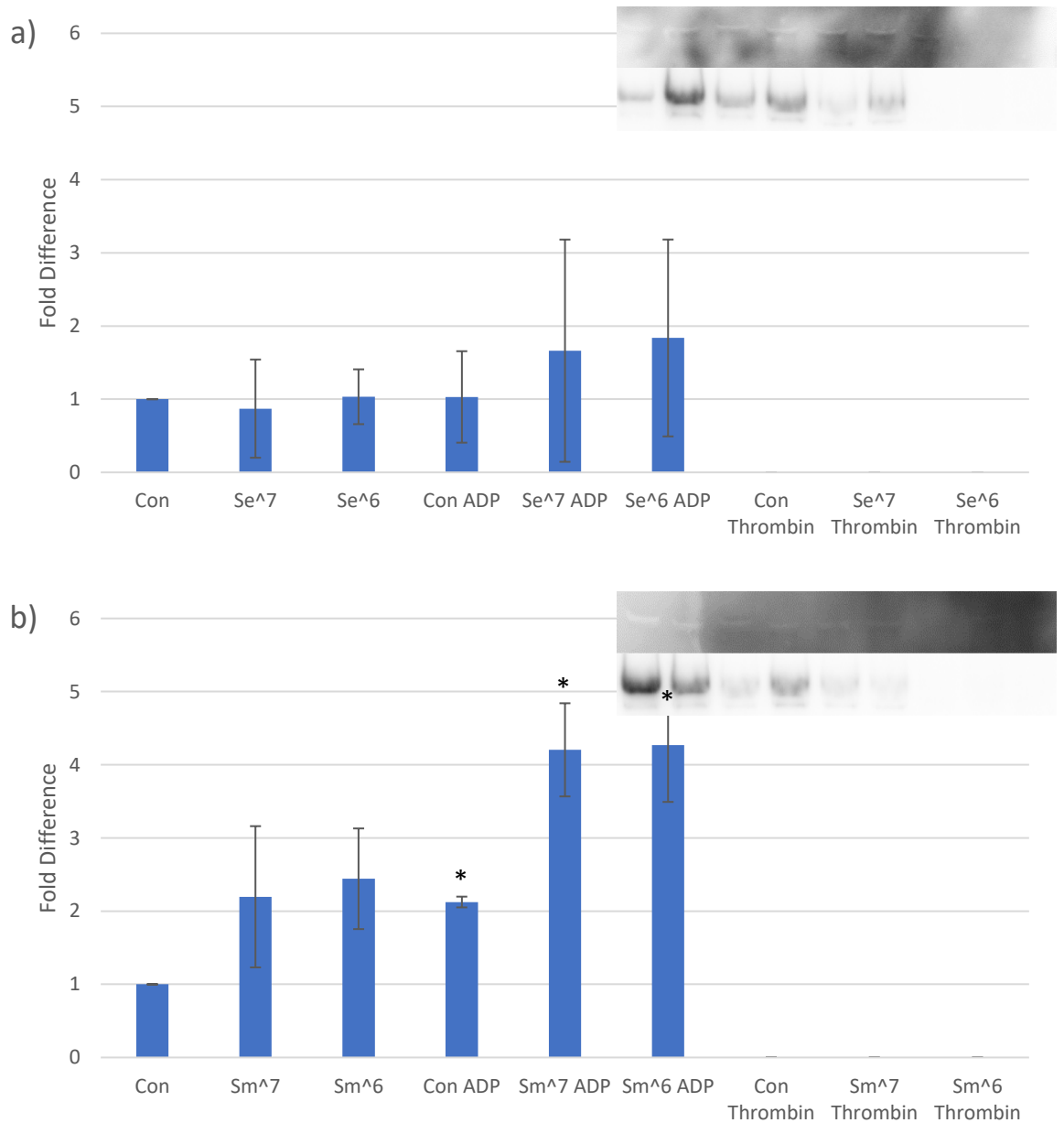


Figure 6.2.3.1 Western blot fold difference in phosphorylated VASP quantification for a) *S. epidermidis* and b) *Ser. marcescens* with a protein band representation below each graph with bands in-line with their counterpart in the graphs. Most significant differences annotated with a *. (n = 2)

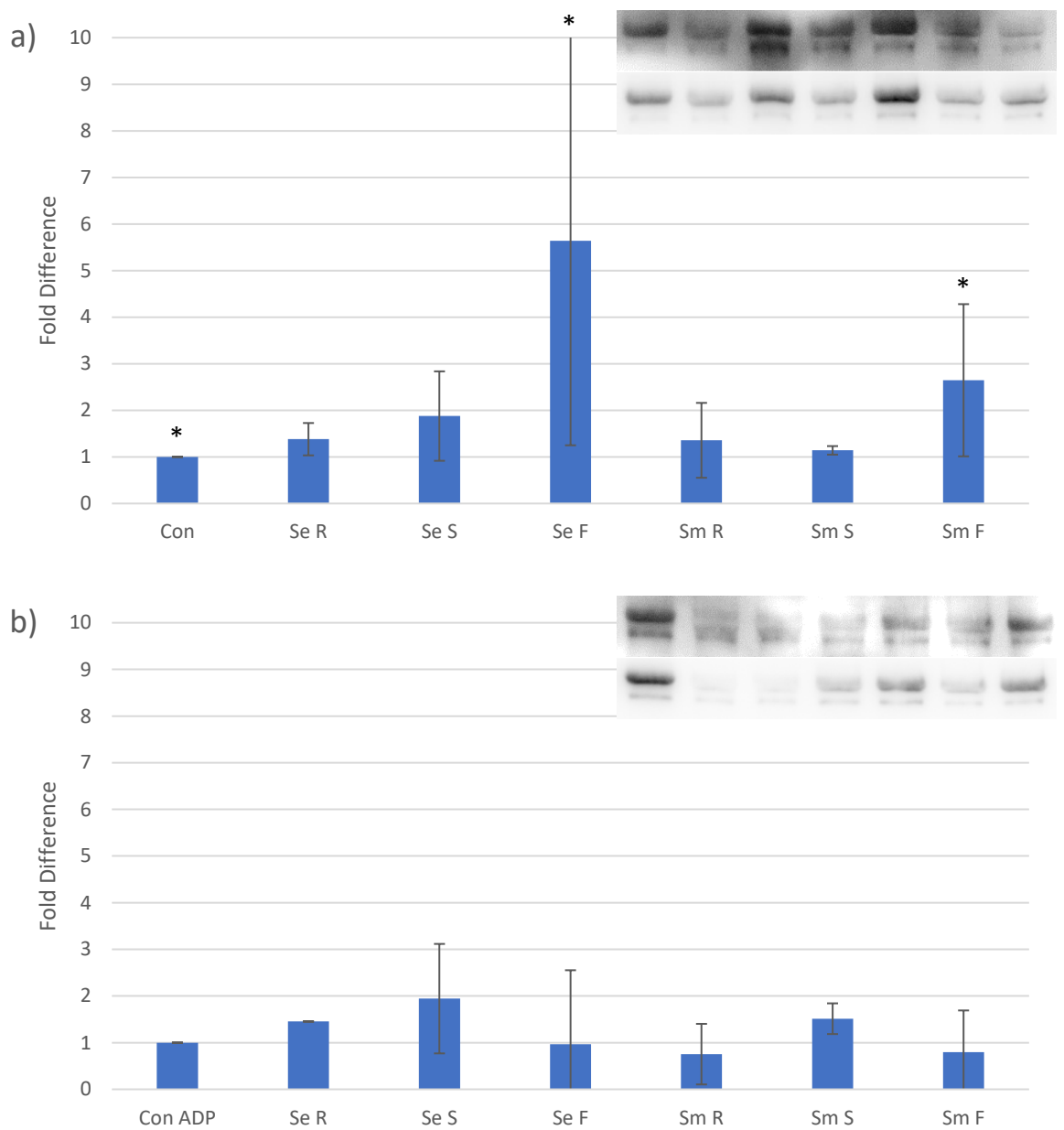


Figure 6.2.3.2 Western blot fold difference in phosphorylated VASP quantification for 5 day biofilms with a) no ADP stimulation and b) with ADP stimulation with a protein band representation below each graph with bands in-line with their counterpart in the graphs. Most significant differences annotated with a *. (n = 2)

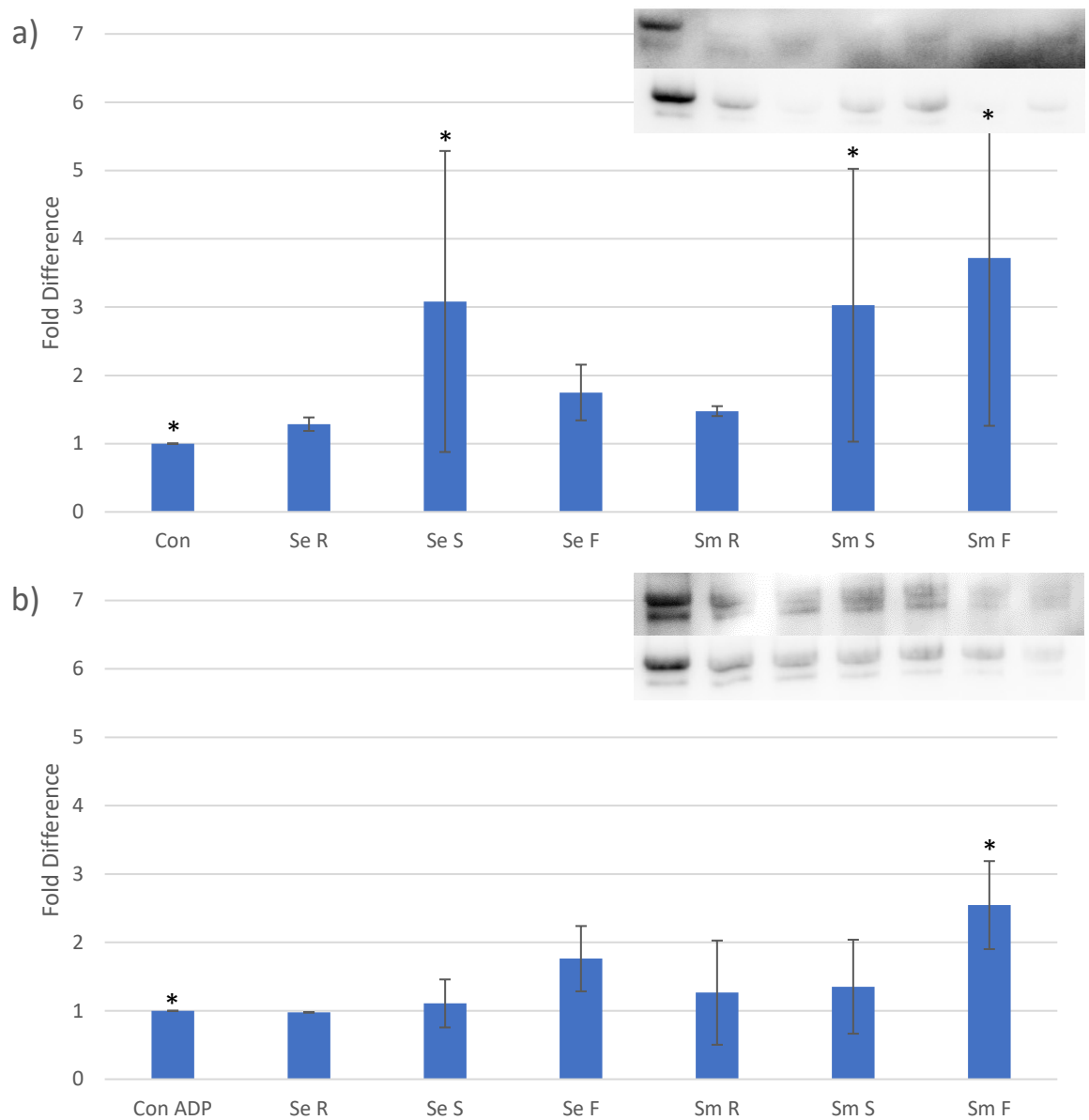


Figure 6.2.3.3 Western blot fold difference in phosphorylated VASP quantification for 7 day biofilms with a) no ADP stimulation and b) with ADP stimulation with a protein band representation below each graph with bands in-line with their counterpart in the graphs. Most significant differences annotated with a *. (n = 2)

6.2.3.2 Phospho-PLC β 3

Phospho-PLC β expression by platelets incubated with planktonic bacteria (**Fig. 6.2.4.1**) demonstrated a trend of increasing expression with a lower starting inoculum when *S. epidermidis* was used, with *S. epidermidis* at 10^6 CFU / mL with no stimulation (from 1 to 1.6 fold increase) and with Thrombin stimulation (from 2.2 to 2.9 fold increase) demonstrating the greatest increases compared to their controls. When *Ser. marcescens* was incubated with the platelets (**Fig. 6.2.4.1b**), increases and decreases in phospho-PLC β were both determined with the lower starting inoculum (10^6 CFU / mL) again demonstrating a greater effect, with a 40% reduction phospho-PLC β expression without stimulation. However, with ADP stimulation had no significant effect and Thrombin stimulation demonstrated a significant increase of 4.4 fold.

However, when platelets were incubated with 5 day biofilms without stimulation (**Fig. 6.2.4.2a**), whilst some variation in the expression of phospho-PLC β was observed, no significant differences were determined. Further, whilst stimulation of the platelets with ADP (**Fig. 6.2.4.2b**) had a trend that all the biofilms demonstrated a reduction in phospho-PLC β expression, no significant differences were determined.

The incubation of platelets with 7 day biofilms demonstrated that when unstimulated (**Fig. 6.2.4.3a**) both *S. epidermidis* and *Ser. marcescens* biofilms on the smooth surface were significantly increased (1.5 fold and 1.8 fold increases respectively) with no other significant increases. Similar to the 5 day biofilms, when the platelets incubated with 7 day biofilms were stimulated with ADP (**Fig. 6.2.4.3b**) a trend demonstrating a reduction in phospho-PLC β expression was determined but no significant differences were observed.

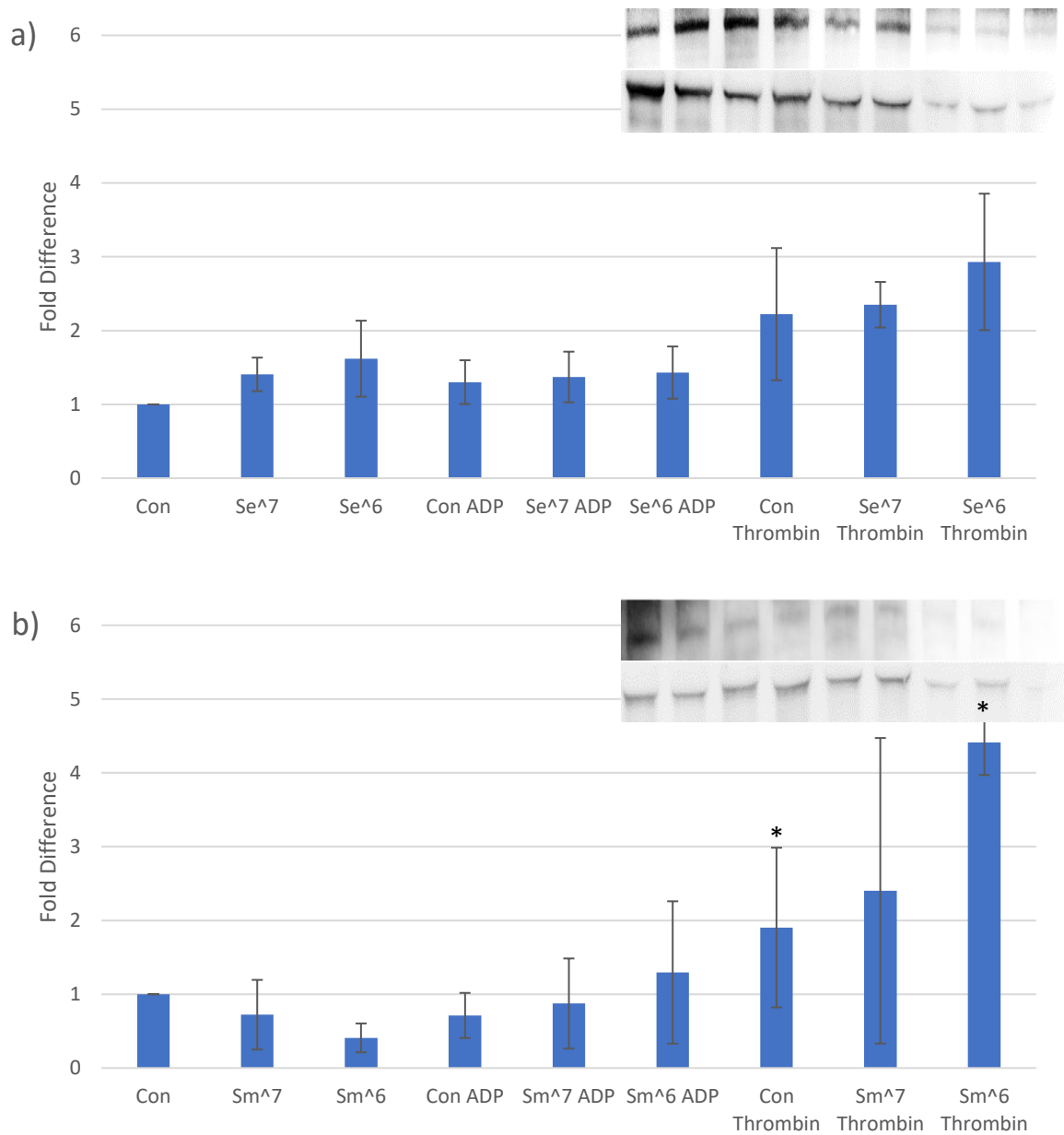


Figure 6.2.4.1 Western blot fold difference in phospho-PLC β 3 quantification for a) *S. epidermidis* and b) *Ser. marcescens* with a protein band representation below each graph with bands in-line with their counterpart in the graphs. Most significant differences annotated with a *. (n = 2)

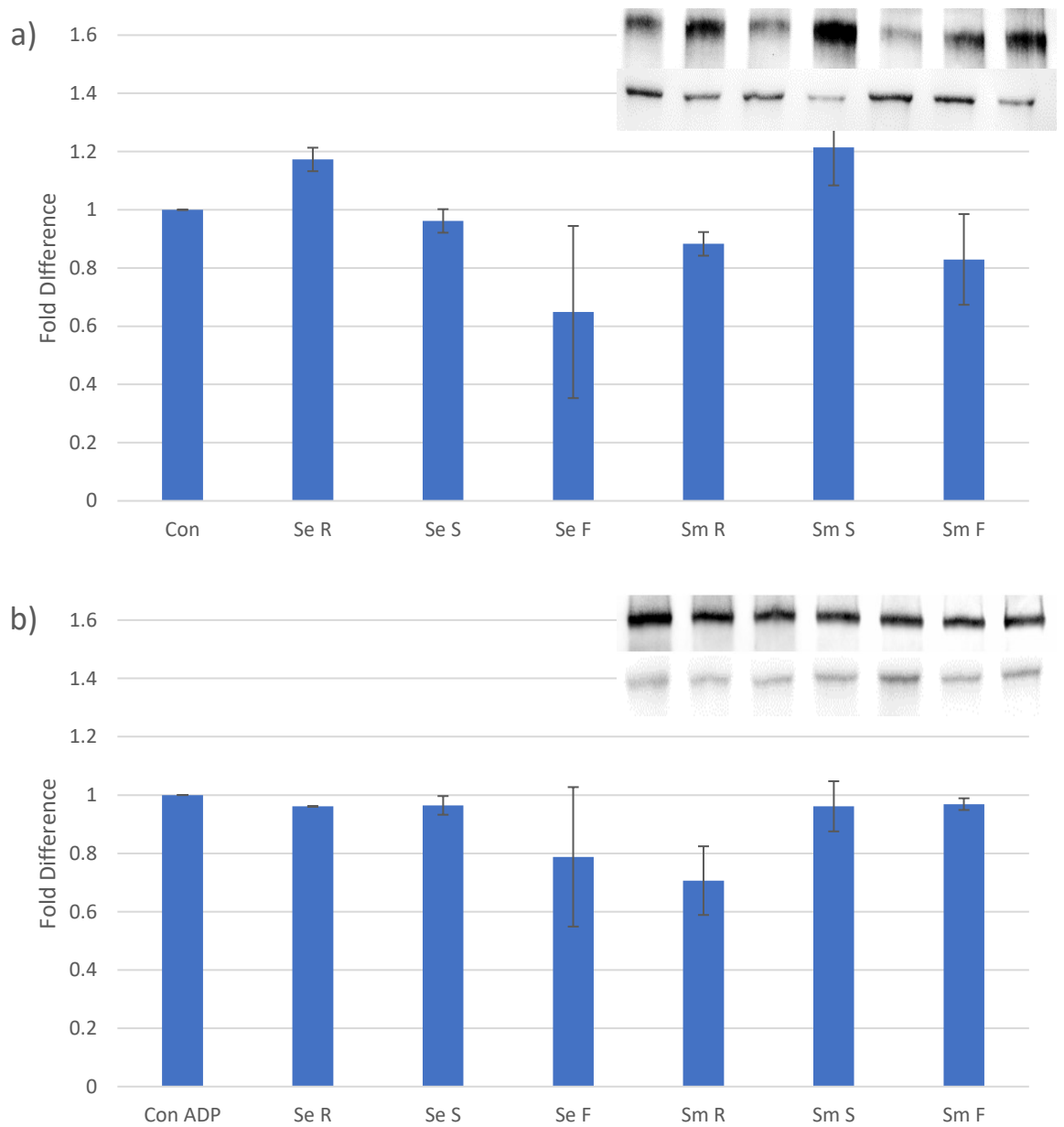


Figure 6.2.4.2 Western blot fold difference in phospho-PLC β 3 quantification for 5 day biofilms with a) no ADP stimulation and b) with ADP stimulation with a protein band representation below each graph with bands in-line with their counterpart in the graphs. (n = 2)

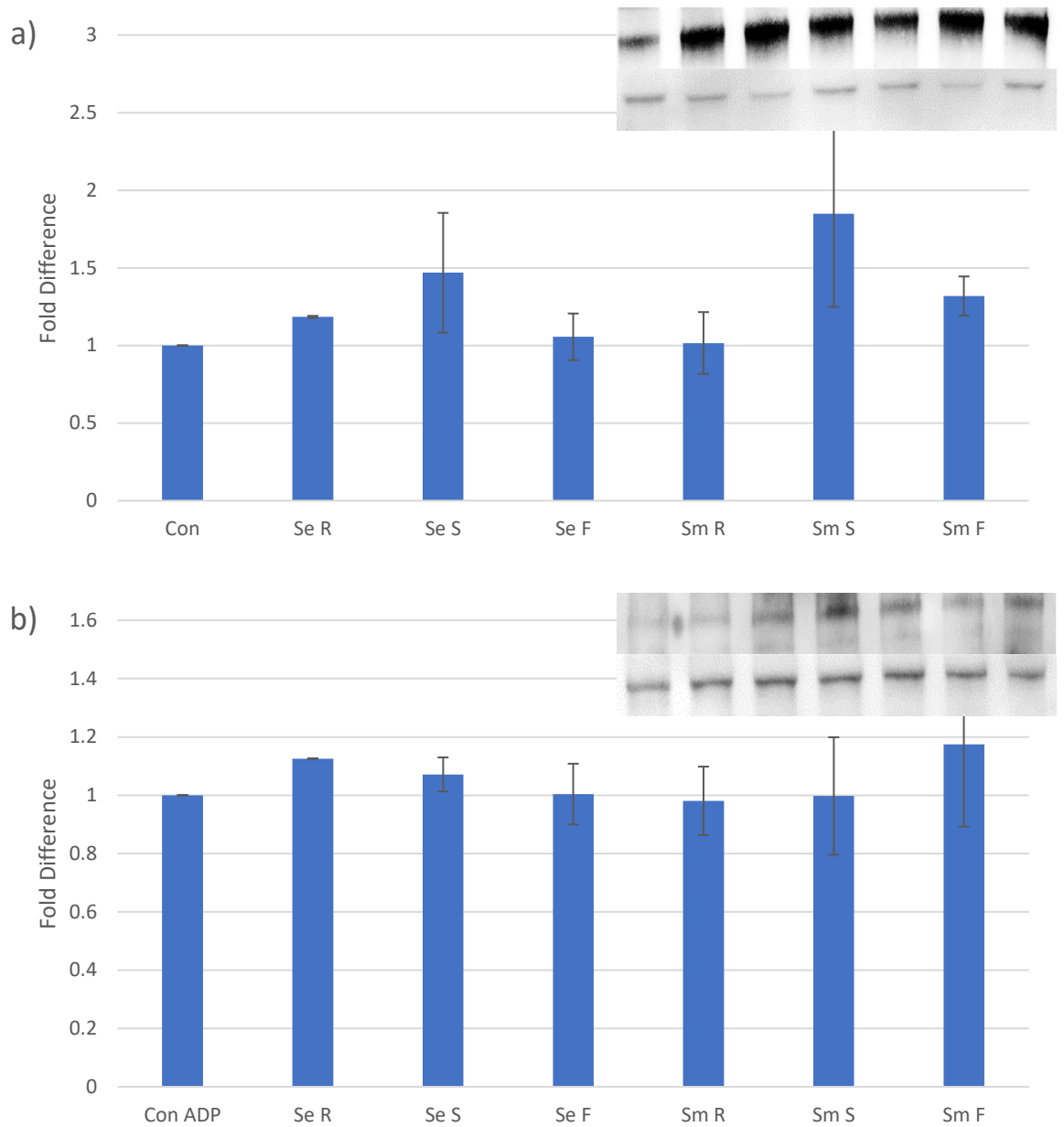


Figure 6.2.4.3 Western blot fold difference in phospho-PLC β 3 quantification for 7 day biofilms with a) no ADP stimulation and b) with ADP stimulation with a protein band representation below each graph with bands in-line with their counterpart in the graphs. (n = 2)

6.2.4 Immunological Activity via Cytometric Bead Array

Platelets were incubated with both planktonic bacteria or bacterial biofilms (5 day or 7 day) for 4 h and supernatants collected both before and after stimulation with ADP. Release of RANTES, IL-6, IL-1 β and TNF were determined, with only RANTES release demonstrating significant concentrations. As concentrations of IL-6, IL-1 β and TNF were too low the data has not been presented.

6.2.4.1 RANTES Release

When platelets were incubated for 4 h with planktonic bacteria (**Fig. 6.4.1a**) RANTES release was reduced for both *S. epidermidis* (4774 pg / mL) and *Ser. marcescens* (4323 pg / mL) compared to the control (6009 pg / mL). However, after stimulation with ADP (**Fig. 6.4.1b**) *S. epidermidis* (3846) demonstrated no significant difference whilst *Ser. marcescens* (5368 pg / mL) demonstrated an increase when compared to the control (4079 pg / mL). When platelets were incubated with a 5 day biofilm (**Fig. 6.4.1a**) both *S. epidermidis* and *Ser. marcescens* demonstrated a trend increase in RANTES release (6662 pg / mL and 6675 pg / mL respectively) compared to the control, but did not significantly change after stimulated with ADP (**Fig. 6.4.1b**). The platelets incubated for 4 h with 7 day biofilms (**Fig. 6.4.1a**) demonstrated a significant increase in RANTES release for both *S. epidermidis* and *Ser. marcescens* biofilms (10945 pg / mL and 10013 pg / mL respectively), and also did not display any significant changes after stimulation with ADP (**Fig. 6.4.1b**).

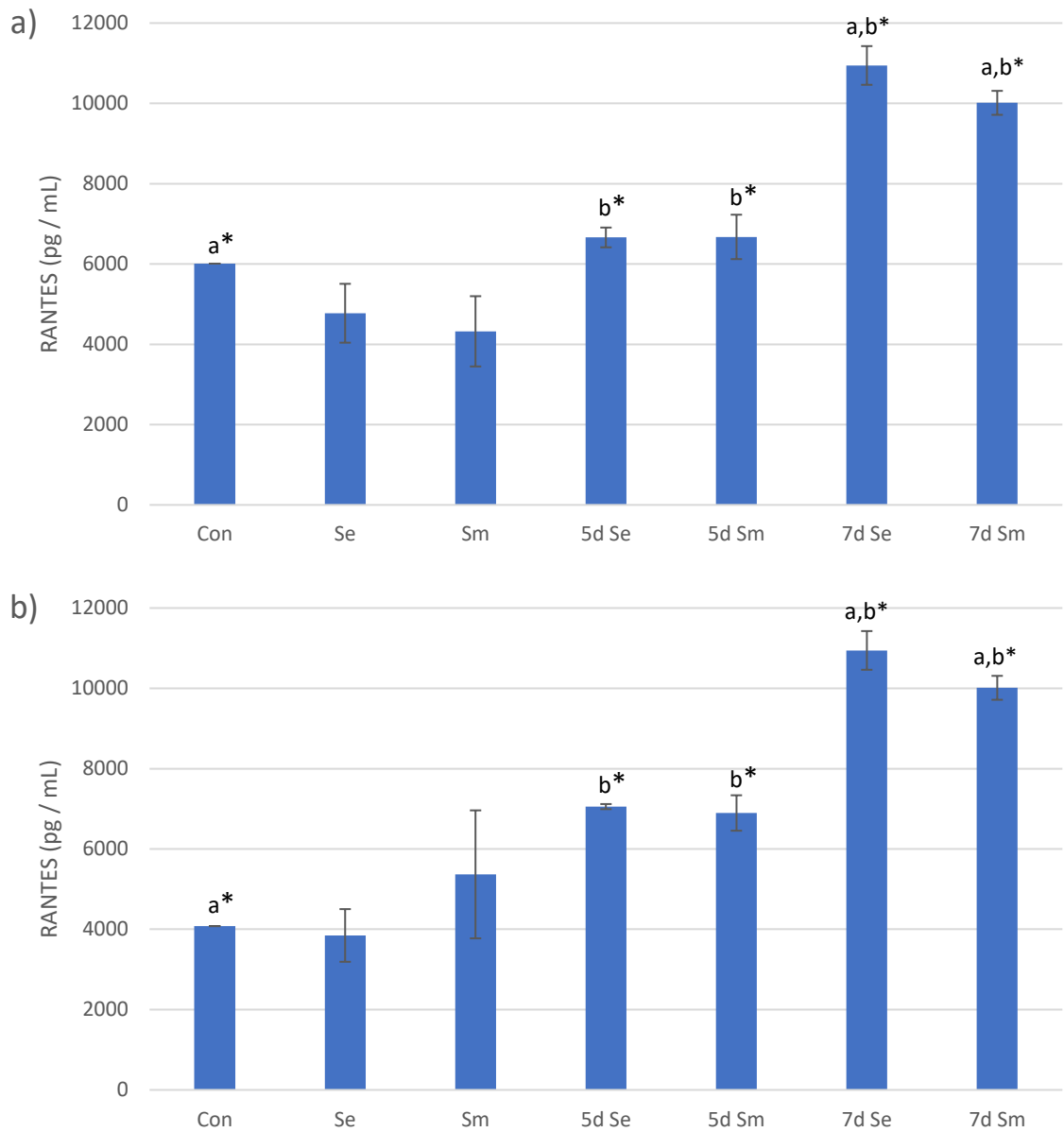


Figure 6.4.1 RANTES release by platelets after incubation with planktonic bacteria, 5 day biofilms or 7 day biofilms for 4 h a) without stimulation and b) with ADP stimulation. Most significant differences annotated with a *. (n = 2)

6.3 Discussion

Light transmission aggregometry is an important tool in understanding platelet function, and in this work, allowed the effects of both planktonic cells and bacterial biofilms on the haemostatic potential of the platelets to be assessed. This allowed the modelling of platelet behaviour in a bacterially contaminated transfusion unit. Platelets that were incubated with biofilms demonstrated a significant reduction in aggregation, and this was likely due to production of a by-product of the biofilms, such as a metabolite or toxin. The presence of the planktonic bacteria had a minimal effect on aggregation as no significant changes with planktonic bacteria were determined. The reduction in aggregation is important as it indicates that a contaminated unit that has biofilm growth may no longer have the therapeutic effect/haemostatic potential that is expected.

The testing of two platelet activation markers, PAC1 and CD62P, demonstrated no significant changes in platelet activation in the presence of either planktonic cells or biofilms. This indicated that the presence of bacteria in planktonic or biofilm form was not inhibiting platelet activation. However, as the biofilm platelets did demonstrate a significant reduction in aggregation it was apparent that whilst the platelets were activating, the biofilm or a product of the biofilm was interfering with the aggregation process. It could be that the biofilms were producing something that was interacting with other platelet receptors that were not tested or the biofilms could be interacting with chemokines released upon platelet activation that enable platelet aggregation.

VASP functions are controlled by the phosphorylation of three phosphorylation sites (Lin *et al.*, 2010). One of these sites include Ser-157, which generally serves as a signal for membrane localisation (Döppler and Storz, 2013). In platelets, VASP plays a major role in negatively regulating secretory and adhesive events with site Ser-157 being the site of

preferential phosphorylation (Wentworth *et al.*, 2006). However, the full role of VASP in platelet aggregation is still unclear (Ito *et al.*, 2018). As such the increase in p.VASP observed when platelets were incubated with planktonic bacteria indicated that the presence of the bacteria was stimulating the phosphorylation of VASP, and subsequently increasing the negative regulation of secretory and adhesive events. The increases in p.VASP were further increased when the platelets were stimulated with ADP, however, ADP activation of the P2Y₁₂ receptor is meant to prevent the phosphorylation of VASP or actively dephosphorylate p.VASP (Mallouk *et al.*, 2018). Due to this, the planktonic bacteria were or potentially interfering with this signalling pathway or that during the incubation time the platelet receptors have started to become unstable or internalised and are no longer as reactive to particular stimuli. Yet Thrombin was able to completely dephosphorylate p.VASP which suggested that the thrombin receptor or signalling pathway were unaffected and that neither bacteria were able to affect the dephosphorylation of p.VASP. However, when 5 day biofilms were incubated with platelets, increases in p.VASP were determined which could indicate an increase in difficulty of platelet activation due to an increase in p.VASP requiring a greater amount of agonist required to achieve dephosphorylation. However, after stimulation with ADP no spikes in p.VASP were determined which demonstrated that some dephosphorylation may have occurred.

PLC β is one of three PLC enzymes expressed and are solely regulated by G protein-coupled receptors (GPCRs), with PLC β 3 being a predominant form in humans (Varga-Szabo *et al.*, 2009). PLC β isoforms can trigger a sequence of events that lead to intracellular release of calcium stores and has been suggested as being a critical part of platelet signalling (Lian *et al.*, 2005b). When platelets were incubated with planktonic bacteria *S. epidermidis*

appeared to have activated PLC β 3 alone when platelets were unstimulated but did not exacerbate not inhibit ADP or Thrombin induced activation of PLC β 3. Whilst increase in PLC β 3 were determined for with both ADP and thrombin stimulated platelets, the greater increases in PLC β 3 demonstrated with Thrombin stimulated platelets is reasonable as Thrombin has a direct effect on PLC β 3 signalling via the Par-1 or Par-4 receptors (Li *et al.*, 2015). Further, this pathway directly causes an upregulation of calcium release within platelets, with platelet activation being heavily reliant upon increases in intracellular calcium, especially within the early stages of platelet activation (Li *et al.*, 2015; Davlouros *et al.*, 2016). This suggests that changes in the levels of phosphorylated PLC β observed when platelets were incubated with bacteria could effect platelet signalling. Unlike *S. epidermidis*, unstimulated platelets incubated with *Ser. marcescens* demonstrated decreases in PLC β 3 activation. Further, when stimulated with Thrombin it appeared that the presence of *Ser. marcescens* exacerbated the activation of PLC β 3, which indicated that *Ser. marcescens* were interacting with the platelets or producing a metabolite / toxin that could interact with the platelets differently to *S. epidermidis*. Further, the upregulation of calcium release within platelets is significant as it is known that platelet activation is heavily reliant upon increases in intracellular calcium, especially within the early stages of platelet activation (Li *et al.*, 2015; Davlouros *et al.*, 2016). However, when the platelets were incubated with biofilms most demonstrated no significant changes in the expression of phosphorylated PLC β with only *S. epidermidis* and *Ser. marcescens* biofilms on the smooth surface even after stimulation. This indicated that potentially due to the bacteria being within a biofilm and enclosed within an extracellular polymeric substance they were not directly interacting with the platelets as the planktonic bacteria were which caused minimal changes in phosphorylated PLC β expression. However, it could likewise be that

the ADP receptors have started to become unstable or internalised and are no longer as reactive to particular stimuli. This is a problem known about working with platelets, and future work could try to counter this effect by adding prostacyclin to the platelets during preparation to minimise potential activation during incubation times.

RANTES is a chemokine stored in α -granules and released upon platelet activation. It is capable of triggering responses from the immune system such as triggering monocyte arrest or increasing the proadhesive and promigratory response of T-lymphocytes (Shenkman *et al.*, 2004). The greater increase in RANTES release after incubation with a 7 day biofilm compared to a 5 day biofilm indicates that a difference between the two biofilms exist. It may be that the increased growth time for a 7 day biofilm has increased the amount of metabolites or toxins produced by the bacteria which may then be interacting with the platelets to cause RANTES release. Further, as increased RANTES release has been demonstrated to be related to infection severity this indicated that the 7 day biofilm potentially could cause a greater infection if transfused (Cavaillon *et al.*, 2003; Ness *et al.*, 2004; Stojewska *et al.*, 2016). RANTES can also inhibit activation of platelets via ADF-1 α potentially as a regulatory role, however, an increase in RANTES could exacerbate platelet aggregation inhibition and reduce the therapeutic use of platelet transfusions (Shenkman *et al.*, 2004). However, the work in this study did not demonstrate any significant changes in platelet activation markers when platelets were incubated in samples that likely contained elevated RANTES and mixed reactions in regard to platelet aggregation, but this cannot be definitively attributed to RANTES. Further, it was also demonstrated that RANTES can reduce the adhesion of platelets to endothelial cells and modulate the innate immune response to sepsis (Ness *et al.*, 2004; Shenkman *et al.*, 2004).

6.4 Conclusion

It was apparent that planktonic bacteria had little effect on platelet aggregation or cell surface receptor display, whilst biofilms had a significant effect on inhibiting platelet aggregation. The effect of planktonic bacteria on cytokine release was also minimal and whilst both 5 and 7 day biofilms significantly increase RANTES release the 7 day biofilm had a greater effect on increasing RANTES release. Planktonic bacteria, especially *Ser. marcescens*, did appear to affect the dephosphorylation of VASP and the presence of biofilms appeared to increase levels of p.VASP prior to platelets activation, demonstrating an increase in difficulty for platelet activation. A similar trend was found in PLC β 3 phosphorylation with planktonic bacteria, whilst the biofilms appeared to have had little effect on PLC β 3 phosphorylation. Overall, it was apparent that the presence of bacteria had a detrimental effect on platelet function, especially when platelets were in the presence of a biofilm.

7.0 Discussion and Conclusion

The initial understanding of the surface properties enabled the progression of this work. The surface analysis demonstrated that the inner lining of the platelet transfusion bag had two unique surfaces present, a rough diamond surface and a smoother surface. This developed into two potential ways of altering the platelet bags to reduce bacterial attachment and subsequent biofilm formation, by physically altering the topographical properties of the platelet bag surfaces via hot press and by attempting to alter the physicochemical properties of the platelet bag surfaces via low temperature atmospheric pressure plasma (LTAPP) treatment.

Analysis of the surfaces following these two treatment methods demonstrated different results. Flattening of the surfaces enabled the removal of major topographical features which enable bacterial attachment, thereby reducing biofilm formation. Only the surface roughness was shown to be significantly different between the different surfaces (rough, smooth and flat), with surface chemistry, physicochemistry and tensile strength only demonstrating minor differences. When the LTAPP treatment was tested, changes in the physicochemistry were determined as predicted, however the results were inconsistent. After testing of multiple platelet bags it was determined that the bags themselves had minor fluctuations present within bags of the same batch and across batches. Further, when treatment was tested over time it was found that changes in the physicochemistry fluctuated over a span of a week demonstrating both increases and decreases. As platelet bags may be stored for months prior to use any treatment with LTAPP may have dissipated prior to use. Due to these various factors the use of LTAPP for this work was discontinued but the flattening of the bags was continued.

After defining the surface properties of the three surfaces, the unmodified rough and smooth surfaces with the modified flattened surfaces, bacterial attachment and biofilm formation was determined. Scanning electron microscopy demonstrated that bacteria preferentially attached within the pits present in the diamond cross print pattern, and it is known that surface features similar in size to bacteria can increase attachment. This could be what caused the rough surface to demonstrate the greatest amount of biofilm and biomass formation. Further, it appeared that the other surface properties had little to no effect on the biofilm formation as the surface energies of the bacteria and the small changes in the physicochemistry of the flat surface should have demonstrated an increase in biofilm formed on the flat surface not the decrease that was observed. However, it may be that the changes in the surface physicochemistry were too small to be able to influence any potential increase biofilm formation.

As any clean surface becomes conditioned upon exposure to the environment, it was important to understand how conditioning films could alter the surface properties. When bacteria by themselves were conditioned onto the surfaces it was apparent that they had the smallest effect on the surface properties. This was likely due to the cells not completely covering a surface, with only a few cells spread out that may influence the surface properties, whilst also because the bacteria would have no readily available nutrient sources when conditioned alone, thereby reducing their activity. The conditioning film that exhibited the greatest effect on the surface properties was the human plasma CF. This was likely due to the variety of molecules present within human plasma which enabled a greater amount of molecules adsorption due to binding to different parts of the surface. When bacteria were combined with human plasma and conditioned onto the surfaces similar changes to those observed when just human plasma was conditioned were

observed. However, due to the presence of bacteria with the human plasma the changes were less pronounced in some instances, such as the physicochemistry, and more pronounced in other instances, such as SEM or FTIR. Overall, when human plasma was involved in the CF the effects on the surface properties can be highly significant.

After understanding how bacteria interact with the surfaces it was also important to understand how bacteria interacted with the platelets themselves. After incubating platelets with either planktonic bacteria or biofilms, it was apparent that planktonic bacteria affected the platelets less than biofilms, but also differently. This was likely due to products produced by biofilms compared to those of unbound planktonic bacteria. Whilst the bacteria appeared to have minimal effect on platelet receptors the biofilms had a significant effect on platelet aggregation, with some demonstrating less than half the aggregation ability than the control. Western blots demonstrated that planktonic bacteria, especially *Ser. marcescens*, affected the dephosphorylation of VASP whilst biofilms appeared to increase levels of p.VASP prior to platelet activation. A similar trend was found in PLC β 3 phosphorylation with planktonic bacteria, whilst the biofilms appeared to have had little effect on PLC β 3 phosphorylation. Further, the cytokine release was upregulated when platelets were in the presence of biofilms but demonstrated both increases and decreases when in the presence of planktonic bacteria.

The work done in this study forms the basis of what could potentially be a significantly larger amount of work, as such some limitations exist. One is that whilst the biofilms were grown in the same conditions for all experiments, the actual number of bacterial cells present, either viable or total, was not quantified and could provide further insight. Also, whilst it is likely that some differences between bacteria may be attributed to their metabolites/toxins produced, these were not identified. As such, work could be carried

out to determine what these substances are, such as via liquid chromatography mass spectroscopy, and also what the effect of the isolated substances had on platelets. Work could also be carried out on other species that have been implicated in platelet contamination, such as other *Staphylococci spp.* or *Enterobacter*, as they may potential demonstrate different results to what was demonstrated. Further, due to time limitations, only two replicates could be done for the western blot data and further replicates would likely reduce some of the large errors observed.

Overall it was apparent that the surface properties had an effect on biofilm formation, especially in regard to surface topography. Further, human plasma conditioning films were capable of altering multiple surface properties including topography, physicochemistry and surface chemistry. Finally, the presence of bacteria had a detrimental effect on platelet function, especially when platelets were in the presence of a biofilm. Whilst this work forms a good basis, more work would have to be carried out before recommending changes to the blood bags to ensure that they keep platelets viable during storage whilst reducing bacterial adhesion and biofilm formation.

8.0 References

Ali, H. *et al.* (2014) 'Characterization of the growth dynamics and biofilm formation of Staphylococcus epidermidis strains isolated from contaminated platelet units', *J. Med. Microbiol.*, 63(PART 6), pp. 884–891. doi: 10.1099/jmm.0.071449-0.

de Allori, M. C. G. *et al.* (2006) 'Antimicrobial resistance and production of biofilms in clinical isolates of coagulase-negative Staphylococcus strains.', *Biol. Pharm. Bull.*, 29(8), pp. 1592–6. Available at: <http://www.ncbi.nlm.nih.gov/pubmed/16880610>.

Anderson, G. G. and O'Toole, G. A. (2008) 'Innate and induced resistance mechanisms of bacterial biofilms.', *Curr. Top. Microbiol. Immunol.*, 322, pp. 85–105. Available at: <http://www.ncbi.nlm.nih.gov/pubmed/18453273> (Accessed: 27 May 2019).

Arman, M. *et al.* (2014) 'Amplification of bacteria-induced platelet activation is triggered by FcγRIIA, integrin αIIbβ3, and platelet factor 4.', *Blood*. American Society of Hematology, 123(20), pp. 3166–74. doi: 10.1182/blood-2013-11-540526.

Aucken, H. M. and Pitt, T. L. (1998) 'Antibiotic Resistance and Putative Virulence Factors of *Serratia Marcescens* with Respect to O and K Serotypes', *J. Med. Microbiol.* Microbiology Society, 47(12), pp. 1105–1113. doi: 10.1099/00222615-47-12-1105.

Bárdos, L. and Baránková, H. (2010) 'Cold atmospheric plasma: Sources, processes, and applications', *Thin Solid Films*, 518(23), pp. 6705–6713. doi: 10.1016/j.tsf.2010.07.044.

Baryshev, S. V *et al.* (2013) 'Characterization of surface modifications by white light interferometry: applications in ion sputtering, laser ablation, and tribology experiments.', *J. Vis. Exp.* MyJoVE Corporation, (72), p. e50260. doi: 10.3791/50260.

Beachey, E. H. *et al.* (1977) 'Interaction of lipoteichoic acid of group A streptococci with human platelets', *Infect Immun*, 16(2), pp. 649–654. Available at: http://www.ncbi.nlm.nih.gov/entrez/query.fcgi?cmd=Retrieve&db=PubMed&dopt=Citation&list_uids=324916.

Becker, K., Heilmann, C. and Peters, G. (2014) 'Coagulase-negative staphylococci.', *Clin. Microbiol. Rev.* American Society for Microbiology (ASM), 27(4), pp. 870–926. doi: 10.1128/CMR.00109-13.

Bellon-Fontaine, M.-N., Rault, J. and van Ossb, C. J. (1996) 'Microbial adhesion to solvents : a novel

method to determine the electron-donor / electron-acceptor or Lewis acid-base properties of microbial cells', *Colloids Surfaces B Biointerfaces*, 7(1–2), pp. 47–53.

Benavides, R., Edge, M. and Allen, N. S. (1995) 'The mode of action of metal stearate stabilisers in poly (vinyl chloride): II. Influence of pre-heating on induction times and carbonyl formation', *Polym. Degrad. Stab.* Elsevier, 49(1), pp. 205–211. doi: 10.1016/0141-3910(95)00047-P.

Benjamin, R. J. and Wagner, S. J. (2007) 'The residual risk of sepsis: Modeling the effect of concentration on bacterial detection in two-bottle culture systems and an estimation of false-negative culture rates', *Transfusion*, 47(8), pp. 1381–1389. doi: 10.1111/j.1537-2995.2007.01326.x.

Benz, P. M. *et al.* (2016) 'Vasodilator-Stimulated Phosphoprotein (VASP)-dependent and-independent pathways regulate thrombin-induced activation of Rap1b in platelets'. doi: 10.1186/s12964-016-0144-z.

Bjarnsholt, T. (2013) 'The role of bacterial biofilms in chronic infections.', *APMIS. Suppl.*, 136(136), pp. 1–51. doi: 10.1111/apm.12099.

Blajchman, M. A. *et al.* (2005) 'Bacterial detection of platelets: Current problems and possible resolutions', *Transfus. Med. Rev.*, 19(4), pp. 259–272. doi: 10.1016/j.tmr.2005.05.002.

Blajchman, M. A. *et al.* (2008) 'New Strategies for the Optimal Use of Platelet Transfusions', *Hematology*, 2008(1), pp. 198–204. doi: 10.1182/asheducation-2008.1.198.

Blumberg, N., Heal, J. M. and Phillips, G. L. (2010) 'Platelet transfusions: trigger, dose, benefits, and risks', *F1000 Med. Rep.*, 5(January), pp. 1–5. doi: 10.3410/M2-5.

Bodecchi, L. M. *et al.* (2005) 'Application of infrared spectroscopy and multivariate quality-control methods in PVC manufacturing', *Anal. Chim. Acta*, 554(1–2), pp. 207–217. doi: 10.1016/j.aca.2005.08.023.

Bozaci, E. *et al.* (2013) 'Effects of the atmospheric plasma treatments on surface and mechanical properties of flax fiber and adhesion between fiber-matrix for composite materials', *Compos. Part B Eng.* Elsevier Ltd, 45(1), pp. 565–572. doi: 10.1016/j.compositesb.2012.09.042.

Brecher *et al.* (2005) 'Bacterial contamination of blood products.', *Clin. Microbiol. Rev.*, 18(1), pp. 195–204. doi: 10.1128/CMR.18.1.195.

- Brecher, M. E. *et al.* (2000) 'Growth of bacteria in inoculated platelets: Implications for bacteria detection and the extension of platelet storage', *Transfusion*, 40(11), pp. 1308–1312. doi: 10.1046/j.1537-2995.2000.40111308.x.
- Bumbrah, G. S. and Sharma, R. M. (2016) 'Raman spectroscopy – Basic principle, instrumentation and selected applications for the characterization of drugs of abuse', *Egypt. J. Forensic Sci.* No longer published by Elsevier, pp. 209–215. doi: 10.1016/j.ejfs.2015.06.001.
- Busscher, H. J. and van der Mei, H. C. (2012) 'How do bacteria know they are on a surface and regulate their response to an adhering state?', *PLoS Pathog.*, 8(1), pp. 1–3. doi: 10.1371/journal.ppat.1002440.
- Cardile, A. P. *et al.* (2014) 'Human plasma enhances the expression of Staphylococcal microbial surface components recognizing adhesive matrix molecules promoting biofilm formation and increases antimicrobial tolerance In Vitro.', *BMC Res. Notes.* BioMed Central, 7, p. 457. doi: 10.1186/1756-0500-7-457.
- Castillo, L. and MacCallum, D. M. (2012) 'Cytokine measurement using cytometric bead arrays', in *Methods Mol. Biol.* Humana Press, pp. 425–434. doi: 10.1007/978-1-61779-539-8_29.
- Cavaillon, J. *et al.* (2003) 'Cytokine Cascade in Sepsis', *Scand. J. Infect. Dis.*, 35(9), pp. 535–544. doi: 10.1080/00365540310015935.
- Cheng, G. *et al.* (2007) 'Inhibition of bacterial adhesion and biofilm formation on zwitterionic surfaces.', *Biomaterials.* NIH Public Access, 28(29), pp. 4192–9. doi: 10.1016/j.biomaterials.2007.05.041.
- Cognasse, F., Osselaer, J. C. and Garraud, O. (2007) 'Les cytokines des plaquettes et leurs effets lors des transfusions de concentrés de plaquettes', *Transfus. Clin. Biol.* Elsevier Masson, 14(1), pp. 69–78. doi: 10.1016/J.TRACLI.2007.04.009.
- Corash, L. (2011) 'Bacterial contamination of platelet components: potential solutions to prevent transfusion-related sepsis', *Expert Rev. Hematol.*, 4(5), pp. 509–525. doi: <http://dx.doi.org.ezproxy.mmu.ac.uk/10.1586/ehm.11.53>.
- Cox, D., Kerrigan, S. W. and Watson, S. P. (2011) 'Platelets and the innate immune system: Mechanisms of bacterial-induced platelet activation', *J. Thromb. Haemost.*, 9(6), pp. 1097–1107. doi: 10.1111/j.1538-7836.2011.04264.x.

- Davlouros, P. *et al.* (2016) 'Role of Calcium in Platelet Activation: Novel Insights and Pharmacological Implications', *Med. Chem. (Los. Angeles).*, 12(2), pp. 131–138. doi: 10.2174/157340641202160208195923.
- Decousser, J.-W. *et al.* (2015) 'Susceptibility trends including emergence of linezolid resistance among coagulase-negative staphylococci and methicillin-resistant *Staphylococcus aureus* from invasive infections', *Int. J. Antimicrob. Agents*, 46(6), pp. 622–630. doi: 10.1016/j.ijantimicag.2015.07.022.
- Desrousseaux, C. *et al.* (2013) 'Modification of the surfaces of medical devices to prevent microbial adhesion and biofilm formation', *J. Hosp. Infect.*, 85(2), pp. 87–93. doi: 10.1016/j.jhin.2013.06.015.
- Dias, C. *et al.* (2018) 'Biofilms and antibiotic susceptibility of multidrug-resistant bacteria from wild animals', *PeerJ*. PeerJ, Inc, 6. doi: 10.7717/PEERJ.4974.
- Donlan, R. M. (2002) 'Biofilms: microbial life on surfaces. *Emerg Infect Diseases*', <http://www.cdc.gov/ncidod/EID/vol8no9/02-0063.htm>, 8(9), pp. 881–890. doi: 10.3201/eid0809.020063.
- Döppler, H. and Storz, P. (2013) 'Regulation of VASP by phosphorylation: consequences for cell migration.', *Cell Adh. Migr.* Taylor & Francis, 7(6), pp. 482–6. doi: 10.4161/cam.27351.
- Dunlap, C. A., Biresaw, G. and Jackson, M. A. (2005) 'Hydrophobic and electrostatic cell surface properties of blastospores of the entomopathogenic fungus *Paecilomyces fumosoroseus*', *Colloids Surfaces B Biointerfaces*, 46(4), pp. 261–266. doi: 10.1016/j.colsurfb.2005.11.014.
- ECDC (2013) *Annual epidemiological report 2012: Reporting on 2010 surveillance data and 2011 epidemic intelligence data*, *Ecdc.Europa.Eu*. Stockholm. Available at: www.ecdc.europa.eu (Accessed: 19 March 2019).
- Edelstein, L. C. (2017) 'The role of platelet microvesicles in intercellular communication', *Platelets*. Taylor & Francis, 28(3), pp. 222–227. doi: 10.1080/09537104.2016.1257114.
- Eginton, P. J. *et al.* (1995) 'The influence of substratum properties on the attachment of bacterial cells', *Colloids Surfaces B Biointerfaces*. Elsevier, 5(3–4), pp. 153–159. doi: 10.1016/0927-7765(95)01219-9.
- Fitzgerald, J. R., Foster, T. J. and Cox, D. (2006) 'The interaction of bacterial pathogens with platelets', *Nat. Rev. Microbiol.*, 4(6), pp. 445–457. doi: 10.1038/nrmicro1425.

- Frank, K. L. *et al.* (2007) 'In vitro effects of antimicrobial agents on planktonic and biofilm forms of *Staphylococcus lugdunensis* clinical isolates.', *Antimicrob. Agents Chemother.* American Society for Microbiology (ASM), 51(3), pp. 888–95. doi: 10.1128/AAC.01052-06.
- Garrett, T. R., Bhakoo, M. and Zhang, Z. (2008) 'Bacterial adhesion and biofilms on surfaces', *Prog. Nat. Sci.*, 18(9), pp. 1049–1056. doi: 10.1016/j.pnsc.2008.04.001.
- Givan, A. L. (2011) 'Flow Cytometry: An Introduction', in *Methods Mol. Biol.* Humana Press, pp. 1–29. doi: 10.1007/978-1-61737-950-5_1.
- Goldstein, J. I. *et al.* (2003) *Scanning Electron Microscopy and X-Ray*. Third. Springer, US. Available at: https://books.google.co.uk/books?id=ruF9DQxCDLQC&redir_esc=y (Accessed: 28 April 2018).
- Gönen, M. *et al.* (2010) 'Preparation and Characterization of Calcium Stearate Powders and Films Prepared by Precipitation and Langmuir–Blodgett Techniques', *Ind. Eng. Chem. Res.* American Chemical Society, 49(4), pp. 1732–1736. doi: 10.1021/ie901437d.
- Greco-Stewart, V. S. *et al.* (2012) 'Serratia marcescens strains implicated in adverse transfusion reactions form biofilms in platelet concentrates and demonstrate reduced detection by automated culture', *Vox Sang.*, 102(3), pp. 212–220. doi: 10.1111/j.1423-0410.2011.01550.x.
- Greco-Stewart, V. S. *et al.* (2013) 'Biofilm formation by *Staphylococcus capitis* strains isolated from contaminated platelet concentrates', *J. Med. Microbiol.*, 62(PART7), pp. 1051–1059. doi: 10.1099/jmm.0.050500-0.
- Greco, C. *et al.* (2007) 'Staphylococcus epidermidis forms biofilms under simulated platelet storage conditions', *Transfusion*, 47(7), pp. 1143–1153. doi: 10.1111/j.1537-2995.2007.01249.x.
- Guidetti, G. F., Canobbio, I. and Torti, M. (2015) 'PI3K/Akt in platelet integrin signaling and implications in thrombosis', *Adv. Biol. Regul.* Pergamon, 59, pp. 36–52. doi: 10.1016/J.JBIOR.2015.06.001.
- GuoHui, B. *et al.* (2013) 'Three different bacterial detection systems for platelet concentrates under inter-laboratory conditions', *Transfus. Apher. Sci.* Elsevier Ltd, 49(3), pp. 600–607. doi: 10.1016/j.transci.2013.07.029.
- Hamzeh-Cognasse, H. *et al.* (2015) 'Platelets and infections - Complex interactions with bacteria', *Front. Immunol.*, 6(FEB), pp. 1–18. doi: 10.3389/fimmu.2015.00082.

- Hartford, O. *et al.* (2001) 'The Fbe (SdrG) protein of *Staphylococcus epidermidis* HB promotes bacterial adherence to fibrinogen', *Microbiology*, 147(9), pp. 2545–2552. doi: 10.1099/00221287-147-9-2545.
- Heal, J. M. *et al.* (1993) 'The role of ABO matching in platelet transfusion.', *Eur. J. Haematol.*, 50(2), pp. 110–7. Available at: <http://www.ncbi.nlm.nih.gov/pubmed/8440356> (Accessed: 8 August 2018).
- Heilmann, C. *et al.* (1997) 'Evidence for autolysin-mediated primary attachment of *Staphylococcus epidermidis* to a polystyrene surface', *Mol. Microbiol.* John Wiley & Sons, Ltd (10.1111), 24(5), pp. 1013–1024. doi: 10.1046/j.1365-2958.1997.4101774.x.
- Hertle, R. (2005) 'The Family of Serratia Type Pore Forming Toxins', *Curr. Protein Pept. Sci.*, 6(4), pp. 313–325. doi: 10.2174/1389203054546370.
- Heubner, U. (2009) *Stainless Steel-When Health Comes First Environment and Human Health Series, Volume 2 Euro Inox*. Edited by Euro Inox. Available at: www.turkpasder.com (Accessed: 19 March 2019).
- Hillyer, C. *et al.* (2003) 'Bacterial contamination of blood components: risks, strategies, and regulation: joint ASH and AABB educational session in transfusion medicine.', *Hematol. 2003*, pp. 575–589. doi: 10.1182/asheducation-2003.1.575.
- Hong, H. *et al.* (2016) 'Detection of septic transfusion reactions to platelet transfusions by active and passive surveillance', *Blood*, 127(4), pp. 496–502. doi: 10.1182/blood-2015-07-655944.
- Hover, T. *et al.* (2016) 'Mechanisms of Bacterial (*Serratia marcescens*) Attachment to, Migration along, and Killing of Fungal Hyphae.', *Appl. Environ. Microbiol.* American Society for Microbiology, 82(9), pp. 2585–94. doi: 10.1128/AEM.04070-15.
- von Hundelshausen, P. *et al.* (2005) 'Heterophilic interactions of platelet factor 4 and RANTES promote monocyte arrest on endothelium.', *Blood*. American Society of Hematology, 105(3), pp. 924–30. doi: 10.1182/blood-2004-06-2475.
- Von Hundelshausen, P. *et al.* (2001) *RANTES Deposition by Platelets Triggers Monocyte Arrest on Inflamed and Atherosclerotic Endothelium*. Available at: <http://www.circulationaha.org> (Accessed: 27 May 2019).
- Ito, A. *et al.* (2009) 'Increased antibiotic resistance of *Escherichia coli* in mature biofilms.', *Appl.*

Environ. Microbiol. American Society for Microbiology, 75(12), pp. 4093–100. doi: 10.1128/AEM.02949-08.

Ito, Y. *et al.* (2018) 'Vasodilator-stimulated phosphoprotein (VASP) is not a major mediator of platelet aggregation, thrombogenesis, haemostasis, and antiplatelet effect of prasugrel in rats', *Sci. Rep.* Nature Publishing Group, 8(1), p. 9955. doi: 10.1038/s41598-018-28181-8.

Katsikogianni, M. *et al.* (2006) 'Adhesion of slime producing *Staphylococcus epidermidis* strains to PVC and diamond-like carbon/silver/fluorinated coatings', *J. Mater. Sci. Mater. Med.*, 17(8), pp. 679–689. doi: 10.1007/s10856-006-9678-8.

Katsikogianni, M. and Missirlis, Y. F. (2004) 'Concise review of mechanisms of bacterial adhesion to biomaterials and of techniques used in estimating bacteria-material interactions - True Open Access', *MEu. rKopatesaink oCgeiallnsn ain adn dM Ya.tFe.r iMaliss*, 8(August), pp. 37–57. doi: 10.1002/(sici)1097-4636(199823)43:3<338::aid-jbm16>3.0.co;2-b.

Kazarian, S. G. and Chan, K. L. A. (2006) 'Applications of ATR-FTIR spectroscopic imaging to biomedical samples', *Biochim. Biophys. Acta - Biomembr.* Elsevier, 1758(7), pp. 858–867. doi: 10.1016/J.BBAMEM.2006.02.011.

Kerr, T. J., Duncan, K. L. and Myers, L. (2013) 'Application of vibrational spectroscopy techniques for material identification from fire debris', *Vib. Spectrosc.* Elsevier B.V., 68(January 2018), pp. 225–235. doi: 10.1016/j.vibspec.2013.08.006.

Kerrigan, S. W. and Cox, D. (2010) 'Platelet-bacterial interactions', *Cell. Mol. Life Sci.*, 67(4), pp. 513–523. doi: 10.1007/s00018-009-0207-z.

Kim, S. B. *et al.* (2015) 'Risk factors for mortality in patients with *Serratia marcescens* bacteremia.', *Yonsei Med. J.* Yonsei University College of Medicine, 56(2), pp. 348–54. doi: 10.3349/ymj.2015.56.2.348.

Kini, R. M. *et al.* (2011) 'Toxins and hemostasis: From bench to bedside', *Toxins Hemost. From Bench to Bedside*, (August 2010), pp. 1–797. doi: 10.1007/978-90-481-9295-3.

Kleinschmidt, S. *et al.* (2015) 'Staphylococcus epidermidis as a cause of bacteremia', *Future Microbiol.* Future Medicine Ltd London, UK, 10(11), pp. 1859–1879. doi: 10.2217/fmb.15.98.

Kocoglu, M. E., Bayram, A. and Balci, I. (2005) 'Evaluation of negative results of BacT/Alert 3D automated blood culture system.', *J. Microbiol.*, 43(3), pp. 257–9. Available at:

<http://www.ncbi.nlm.nih.gov/pubmed/15995643> (Accessed: 9 May 2019).

Koltai, K. *et al.* (2017) 'Platelet aggregometry testing: Molecular mechanisms, techniques and clinical implications', *Int. J. Mol. Sci.* Multidisciplinary Digital Publishing Institute (MDPI). doi: 10.3390/ijms18081803.

Korenevsky, A. and Beveridge, T. J. (2007) 'The surface physicochemistry and adhesiveness of *Shewanella* are affected by their surface polysaccharides', *Microbiology*. Microbiology Society, 153(6), pp. 1872–1883. doi: 10.1099/mic.0.2006/003814-0.

De Korte, D. *et al.* (2006) 'Effects of skin disinfection method, deviation bag, and bacterial creening on clinical safety of platelet transfusions in the Netherlands', *Transfusion*, 46(3), pp. 476–485. doi: 10.1111/j.1537-2995.2006.00746.x.

Kostakioti, M., Hadjifrangiskou, M. and Hultgren, S. J. (2013) 'Bacterial biofilms: development, dispersal, and therapeutic strategies in the dawn of the postantibiotic era.', *Cold Spring Harb. Perspect. Med.* Cold Spring Harbor Laboratory Press, 3(4), p. a010306. doi: 10.1101/cshperspect.a010306.

Kunishima, S. *et al.* (2001) 'Presence of *Propionibacterium acnes* in blood components', *Transfusion*. Wiley/Blackwell (10.1111), 41(9), pp. 1126–1129. doi: 10.1046/j.1537-2995.2001.41091126.x.

Labbate, M. *et al.* (2007) 'Quorum-sensing regulation of adhesion in *Serratia marcescens* MG1 is surface dependent.', *J. Bacteriol.* American Society for Microbiology Journals, 189(7), pp. 2702–11. doi: 10.1128/JB.01582-06.

Laserna, J. (2006) 'Raman Spectroscopy: Introduction', in *Encycl. Anal. Chem.* Chichester, UK: John Wiley & Sons, Ltd. doi: 10.1002/9780470027318.a6401.

Lee, C. K. *et al.* (2012) 'Significant bacterial contamination risk reduction with the use of diversion pouch', *Transfus. Med.*, 22(6), pp. 404–408. doi: 10.1111/j.1365-3148.2012.01194.x.

Li, J. *et al.* (2015) 'Platelet-neutrophil interactions under thromboinflammatory conditions', *Cell. Mol. Life Sci.*, 72(14), pp. 2627–2643. doi: 10.1007/s00018-015-1845-y.

Lian, L. *et al.* (2005a) 'The relative role of PLC and PI3K in platelet activation', *Blood*. American Society of Hematology, 106(1), pp. 110–7. doi: 10.1182/blood-2004-05-2005.

- Lian, L. *et al.* (2005b) 'The relative role of PLCbeta and PI3Kgamma in platelet activation.', *Blood*. American Society of Hematology, 106(1), pp. 110–7. doi: 10.1182/blood-2004-05-2005.
- Lim, Y. A. *et al.* (2008) 'Change of platelet activation markers using flow cytometry in patients with hematology/oncology disorders after transfusion', *Platelets*. Taylor & Francis, 19(5), pp. 328–334. doi: 10.1080/09537100802129867.
- Limoli, D. H., Jones, C. J. and Wozniak, D. J. (2015) 'Bacterial Extracellular Polysaccharides in Biofilm Formation and Function.', *Microbiol. Spectr.* NIH Public Access, 3(3). doi: 10.1128/microbiolspec.MB-0011-2014.
- Lin, W.-H. *et al.* (2010) 'Functional roles of VASP phosphorylation in the regulation of chemotaxis and osmotic stress response', *Cytoskeleton (Hoboken)*. NIH Public Access, 67(4), p. 259. doi: 10.1002/CM.20443.
- Linnes, J. C., Mikhova, K. and Bryers, J. D. (2012) 'Adhesion of *Staphylococcus epidermidis* to biomaterials is inhibited by fibronectin and albumin.', *J. Biomed. Mater. Res. A*. NIH Public Access, 100(8), pp. 1990–7. doi: 10.1002/jbm.a.34036.
- Liumbruno, G. *et al.* (2009) 'Recommendations for the transfusion of plasma and platelets', *Blood Transfus.*, 7(2), pp. 132–150. doi: 10.2450/2009.0005-09.
- Liumbruno, G. M. *et al.* (2009) 'Reduction of the risk of bacterial contamination of blood components through diversion of the first part of the donation of blood and blood components', *Blood Transfus.*, 7(2), pp. 86–93. doi: 10.2450/2008.0026-08.
- Loeb, G. I. and Neihof, R. A. (2009) 'Marine Conditioning Films', in, pp. 319–335. doi: 10.1021/ba-1975-0145.ch016.
- Lorenzetti, M. *et al.* (2015) 'The Influence of Surface Modification on Bacterial Adhesion to Titanium-Based Substrates', *ACS Appl. Mater. Interfaces*. American Chemical Society, 7(3), pp. 1644–1651. doi: 10.1021/am507148n.
- Lorite, G. S. *et al.* (2011) 'The role of conditioning film formation and surface chemical changes on *Xylella fastidiosa* adhesion and biofilm evolution', *J. Colloid Interface Sci.* Academic Press, 359(1), pp. 289–295. doi: 10.1016/J.JCIS.2011.03.066.
- Loza-Correa, M. *et al.* (2017) 'Comparison of bacterial attachment to platelet bags with and without preconditioning with plasma', *Vox Sang.* Wiley/Blackwell (10.1111), 112(5), pp. 401–407. doi:

10.1111/vox.12513.

Lu, Q. and Malinauskas, R. A. (2010) 'Comparison of Two Platelet Activation Markers Using Flow Cytometry After In Vitro Shear Stress Exposure of Whole Human Blood', *Artif. Organs*. John Wiley & Sons, Ltd (10.1111), 35(2), p. no-no. doi: 10.1111/j.1525-1594.2010.01051.x.

Lu, Y. and Miller, J. D. (2002) 'Carboxyl Stretching Vibrations of Spontaneously Adsorbed and LB-Transferred Calcium Carboxylates as Determined by FTIR Internal Reflection Spectroscopy', *J. Colloid Interface Sci.* Academic Press, 256(1), pp. 41–52. doi: 10.1006/JCIS.2001.8112.

Mahmood, T. and Yang, P.-C. (2012) 'Western blot: technique, theory, and trouble shooting.', *N. Am. J. Med. Sci.* Wolters Kluwer -- Medknow Publications, 4(9), pp. 429–34. doi: 10.4103/1947-2714.100998.

Mallouk, N. *et al.* (2018) 'Assessment of a flow cytometry technique for studying signaling pathways in platelets: Monitoring of VASP phosphorylation in clinical samples', *Pract. Lab. Med.* Elsevier, 11, pp. 10–18. doi: 10.1016/J.PLABM.2018.02.002.

Martini, R. *et al.* (2012) 'Bacteriological analysis of platelets and cases of septic reactions associated with transfusion of contaminated samples', *Transfus. Apher. Sci.*, 47(3), pp. 313–318. doi: 10.1016/j.transci.2012.06.011.

McCann, M. T., Gilmore, B. F. and Gorman, S. P. (2008) 'Staphylococcus epidermidis device-related infections: pathogenesis and clinical management', *J. Pharm. Pharmacol.*, 60(12), pp. 1551–1571. doi: 10.1211/jpp/60.12.0001.

McMullan, D. (2006) 'Scanning electron microscopy 1928-1965', *Scanning*. John Wiley & Sons, Ltd, 17(3), pp. 175–185. doi: 10.1002/sca.4950170309.

Merritt, J. H., Kadouri, D. E. and O'Toole, G. A. (2005) 'Growing and analyzing static biofilms.', *Curr. Protoc. Microbiol.* NIH Public Access, Chapter 1, p. Unit 1B.1. doi: 10.1002/9780471729259.mc01b01s00.

Miller, M. B. and Bassler, B. L. (2001) 'Quorum Sensing in Bacteria', *Annu. Rev. Microbiol.*, 55(1), pp. 165–199. doi: 10.1146/annurev.micro.55.1.165.

Min, S. C. *et al.* (2006) 'Effects of physicochemical surface characteristics of *Listeria monocytogenes* strains on attachment to glass', *Food Microbiol.*, 23(3), pp. 250–259. doi: 10.1016/j.fm.2005.04.004.

- Mitik-Dineva, N. *et al.* (2008) 'Nano-structured surfaces control bacterial attachment', in *2008 Int. Conf. Nanosci. Nanotechnol.* IEEE, pp. 113–116. doi: 10.1109/ICONN.2008.4639259.
- Mohanty, D. (2009) 'Current concepts in platelet transfusion', *Asian J. Transfus. Sci.*, 3(1), p. 18. doi: 10.4103/0973-6247.45257.
- Mojet, B. L., Ebbesen, S. D. and Lefferts, L. (2010) 'Light at the interface: the potential of attenuated total reflection infrared spectroscopy for understanding heterogeneous catalysis in water', *Chem. Soc. Rev.* The Royal Society of Chemistry, 39(12), p. 4643. doi: 10.1039/c0cs00014k.
- Murphy, W. G. *et al.* (2008) 'Screening platelet concentrates for bacterial contamination: low numbers of bacteria and slow growth in contaminated units mandate an alternative approach to product safety', *Vox Sang.* Wiley/Blackwell (10.1111), 95(1), pp. 13–19. doi: 10.1111/j.1423-0410.2008.01051.x.
- Mussano, F. *et al.* (2016) 'Cytokine, chemokine, and growth factor profile of platelet-rich plasma', *Platelets.* Taylor & Francis, 27(5), pp. 467–471. doi: 10.3109/09537104.2016.1143922.
- National Institute of Standards and Technology (NIST) Web Book (no date) *cbook.cgi* (GIF Image, 2255 × 761 pixels) - Scaled (42%). Available at: <https://webbook.nist.gov/cgi/cbook.cgi?Scan=cob1069&Type=IR> (Accessed: 22 April 2017).
- National Nosocomial Infections Surveillance System (2004) 'National Nosocomial Infections Surveillance (NNIS) System Report, data summary from January 1992 through June 2004, issued October 2004.', *Am J Infect Control.* Elsevier, 32(8), pp. 470–85. doi: 10.1016/S0196655304005425.
- Ness, P. *et al.* (2001) 'Platelet Transfusion Reactions', *Transfusion*, 41(July), pp. 857–861.
- Ness, T. L. *et al.* (2004) 'CCR1 and CC chemokine ligand 5 interactions exacerbate innate immune responses during sepsis.', *J. Immunol.* American Association of Immunologists, 173(11), pp. 6938–48. doi: 10.4049/JIMMUNOL.173.11.6938.
- Nørbygaard, T. and Berg, R. W. (2002) 'Application of Ft-Raman Spectroscopy for Analysis of Phthalate Esters in Pvc Plastics', p. 2800.
- Noro, A. *et al.* (2013) 'Influence of surface topography and surface physicochemistry on wettability of zirconia (tetragonal zirconia polycrystal)', *J. Biomed. Mater. Res. - Part B Appl. Biomater.* Wiley-Blackwell, 101 B(2), pp. 355–363. doi: 10.1002/jbm.b.32846.

- O'Toole, G. A. (2011) 'Microtiter dish biofilm formation assay.', *J. Vis. Exp.* MyJoVE Corporation, (47). doi: 10.3791/2437.
- O'Toole, G. A. and Kolter, R. (1998) 'Flagellar and twitching motility are necessary for *Pseudomonas aeruginosa* biofilm development', *Mol. Microbiol.* John Wiley & Sons, Ltd (10.1111), 30(2), pp. 295–304. doi: 10.1046/j.1365-2958.1998.01062.x.
- van Oss, C. J., Chaudhury, M. K. and Good, R. J. (1988) 'Interfacial Lifshitz—van der Waals and Polar Interactions in Macroscopic Systems', *Chem. Rev.*, 88(6), pp. 927–941. doi: 10.1021/cr00088a006.
- Van Oss, C. J. and Giese, R. F. (1995) *THE HYDROPHILICITY AND HYDROPHOBICITY OF CLAY MINERALS*, *Clays Clay Miner.* Available at: [http://www.clays.org/journal/archive/volume 43/43-4-474.pdf](http://www.clays.org/journal/archive/volume%2043/43-4-474.pdf) (Accessed: 19 May 2019).
- Otto, M. (2009) 'Staphylococcus epidermidis - The "accidental" pathogen', *Nat. Rev. Microbiol.*, pp. 555–567. doi: 10.1038/nrmicro2182.
- Otto, M. (2014) 'Physical stress and bacterial colonization', *FEMS Microbiol. Rev.* Narnia, 38(6), pp. 1250–1270. doi: 10.1111/1574-6976.12088.
- Parikh, S. J. and Chorover, J. (2006) 'ATR-FTIR spectroscopy reveals bond formation during bacterial adhesion to iron oxide', *Langmuir*, 22(20), pp. 8492–8500. doi: 10.1021/la061359p.
- Parreira, P. *et al.* (2011) 'Effect of surface chemistry on bacterial adhesion, viability, and morphology', *J. Biomed. Mater. Res. Part A.* Wiley-Blackwell, 99A(3), pp. 344–353. doi: 10.1002/jbm.a.33178.
- Pawar, P. *et al.* (2004) 'Fluid shear regulates the kinetics and receptor specificity of Staphylococcus aureus binding to activated platelets.', *J. Immunol.*, 173(2), pp. 1258–1265. doi: 10.4049/jimmunol.173.2.1258.
- Persat, A. *et al.* (2015) 'HHS Public Access', 161(5), pp. 988–997. doi: 10.1016/j.cell.2015.05.005.The.
- Petrova, O. E. and Sauer, K. (2016) 'Escaping the biofilm in more than one way: desorption, detachment or dispersion', *Curr. Opin. Microbiol.* Elsevier Current Trends, 30, pp. 67–78. doi: 10.1016/J.MIB.2016.01.004.
- Ramírez-Arcos, S. *et al.* (2007) 'Canadian experience with detection of bacterial contamination in

- apheresis platelets', *Transfusion*. Wiley/Blackwell (10.1111), 47(3), pp. 421–429. doi: 10.1111/j.1537-2995.2007.01131.x.
- Rogers, K. L., Fey, P. D. and Rupp, M. E. (2009) 'Coagulase-Negative Staphylococcal Infections', *Infect. Dis. Clin. North Am.* Elsevier, 23(1), pp. 73–98. doi: 10.1016/J.IDC.2008.10.001.
- Rosenberg, M., Gutnick, D. and Rosenberg, E. (1980) 'Adherence of bacteria to hydrocarbons: A simple method for measuring cell-surface hydrophobicity', *FEMS Microbiol. Lett.* Wiley/Blackwell (10.1111), 9(1), pp. 29–33. doi: 10.1111/j.1574-6968.1980.tb05599.x.
- Sadani, D. T. *et al.* (2006) 'Repeat ABO-incompatible platelet transfusions leading to haemolytic transfusion reaction', *Transfus. Med.*, 16(5), pp. 375–379. doi: 10.1111/j.1365-3148.2006.00684.x.
- Sader, H. S. *et al.* (2014) 'Antimicrobial susceptibility of Gram-negative organisms isolated from patients hospitalised with pneumonia in US and European hospitals: Results from the SENTRY Antimicrobial Surveillance Program, 2009–2012', *Int. J. Antimicrob. Agents*. Elsevier, 43(4), pp. 328–334. doi: 10.1016/J.IJANTIMICAG.2014.01.007.
- Sanguhl, K. *et al.* (2011) 'Platelet aggregation pathway.', *Pharmacogenet. Genomics*. NIH Public Access, 21(8), pp. 516–21. doi: 10.1097/FPC.0b013e3283406323.
- Schrezenmeier, H. *et al.* (2007) 'Bacterial contamination of platelet concentrates: Results of a prospective multicenter study comparing pooled whole blood-derived platelets and apheresis platelets', *Transfusion*, 47(4), pp. 644–652. doi: 10.1111/j.1537-2995.2007.01166.x.
- Schuster, S. *et al.* (2014) 'The role of serum proteins in Staphylococcus aureus adhesion to ethylene glycol coated surfaces', *Int. J. Med. Microbiol.* Urban & Fischer, 304(8), pp. 949–957. doi: 10.1016/J.IJMM.2014.05.012.
- Shafrin, E. G. and Zisman, W. A. (1960) 'CONSTITUTIVE RELATIONS IN THE WETTING OF LOW ENERGY SURFACES AND THE THEORY OF THE RETRACTION METHOD OF PREPARING MONOLAYERS¹', *J. Phys. Chem.* American Chemical Society, 64(5), pp. 519–524. doi: 10.1021/j100834a002.
- Shattil, S. J. *et al.* (1985) 'Changes in the platelet membrane glycoprotein IIb/IIIa complex during platelet activation.', *J. Biol. Chem.*, 260(20), pp. 11107–14. Available at: <http://www.ncbi.nlm.nih.gov/pubmed/2411729> (Accessed: 27 May 2019).
- She, P. *et al.* (2016) 'Effects of human serum and apo-Transferrin on Staphylococcus epidermidis RP62A biofilm formation', *Microbiologyopen*. Wiley-Blackwell, 5(6), p. 957. doi:

10.1002/MBO3.379.

Shenkman, B. *et al.* (2004) 'Differential response of platelets to chemokines: RANTES non-competitively inhibits stimulatory effect of SDF-1alpha', *J. Thromb. Haemost.* Wiley/Blackwell (10.1111), 2(1), pp. 154–160. doi: 10.1111/j.1538-7836.2004.00527.x.

SHOT (2017) *Serious Hazards of Transfusion (SHOT) Working Expert Group (WEG) & Writing Group, on behalf of the SHOT Steering Group Steering Group (SG) during 2016*. Available at: https://www.shotuk.org/wp-content/uploads/SHOT-Report-2016_web_11th-July.pdf.

Silva, F. (2010) 'Serratia marcescens', *Rev. Chil. infectología*, 27(3), pp. 1–5. doi: 10.4067/S0716-10182010000300005.

Siow, K. S. *et al.* (2006) 'Plasma methods for the generation of chemically reactive surfaces for biomolecule immobilization and cell colonization - A review', *Plasma Process. Polym.*, 3(6–7), pp. 392–418. doi: 10.1002/ppap.200600021.

Skovager, A. *et al.* (2012) 'Influence of flow direction and flow rate on the initial adhesion of seven *Listeria monocytogenes* strains to fine polished stainless steel', *Int. J. Food Microbiol.* Elsevier B.V., 157(2), pp. 174–181. doi: 10.1016/j.ijfoodmicro.2012.04.028.

Solodovnichenko, V. S. *et al.* (2016) 'Synthesis of Carbon Materials by the Short-term Mechanochemical Activation of Polyvinyl Chloride', *Procedia Eng.* Institute of Hydrocarbons Processing SB RAS, 152, pp. 747–752. doi: 10.1016/j.proeng.2016.07.684.

Spiess, B. D. (2010) 'Platelet transfusions: the science behind safety, risks and appropriate applications.', *Best Pract. Res. Clin. Anaesthesiol.*, 24(1), pp. 65–83. Available at: <http://www.ncbi.nlm.nih.gov/pubmed/20402171> (Accessed: 8 August 2018).

Stojewska, M. *et al.* (2016) 'Evaluation of serum chemokine RANTES concentration as a biomarker in the diagnosis of early-onset severe infections in neonates', *Postepy Hig. Med. Dosw.*, 70, pp. 272–279. doi: 10.5604/17322693.1198990.

Störmer, M. and Vollmer, T. (2014) 'Diagnostic methods for platelet bacteria screening: current status and developments.', *Transfus. Med. Hemother.* Karger Publishers, 41(1), pp. 19–27. doi: 10.1159/000357651.

Szewzyk, U., Szewzyk, R. and Stenstrom, T. a (1993) 'Growth and Survival of *Serratia-marcescens* Under Aerobic and Anaerobic Conditions in the Presence of Materials from Blood Bags', *J Clin*

Microbiol, 31(7), pp. 1826–1830.

Szlavik, J. *et al.* (2012) 'Initial adhesion of *Listeria monocytogenes* to solid surfaces under liquid flow', *Int. J. Food Microbiol.*, 152(3), pp. 181–188. doi: 10.1016/j.ijfoodmicro.2011.09.006.

Taha, M. *et al.* (2018) 'Comparative characterisation of the biofilm-production abilities of staphylococcus epidermidis isolated from human skin and platelet concentrates', *J. Med. Microbiol.*, 67(2), pp. 190–197. doi: 10.1099/jmm.0.000673.

Tendero, C. *et al.* (2006) 'Atmospheric pressure plasmas: A review', *Spectrochim. Acta - Part B At. Spectrosc.*, 61(1), pp. 2–30. doi: 10.1016/j.sab.2005.10.003.

Thorpe, T. C. *et al.* (1990) 'BacT/Alert: An automated colorimetric microbial detection system', *J. Clin. Microbiol.*, 28(7), pp. 1608–1612.

Tuson, H. H. and Weibel, D. B. (2013) 'Bacteria-surface interactions', *Soft Matter*. NIH Public Access, 9(18), p. 4368. doi: 10.1039/C3SM27705D.

UK Blood Transfusion and Tissue Transplantation Services (2013) 'Guidelines for the Blood Transfusion Services in the United Kingdom'. Stationery Office, p. 399.

Varga-Szabo, D., Braun, A. and Nieswandt, B. (2009) 'Calcium signaling in platelets', *J. Thromb. Haemost.*, 7(7), pp. 1057–1066. doi: 10.1111/j.1538-7836.2009.03455.x.

Vaughan-Sarrazin, M. S., Bayman, L. and Cullen, J. J. (2011) 'Costs of Postoperative Sepsis', *Arch. Surg.* American Medical Association, 146(8), p. 944. doi: 10.1001/archsurg.2011.78.

Verran, J. *et al.* (2010) 'The retention of bacteria on hygienic surfaces presenting scratches of microbial dimensions', *Lett. Appl. Microbiol.*, 50(3), pp. 258–263. doi: 10.1111/j.1472-765X.2009.02784.x.

Vinik, A. I. *et al.* (2001) 'Platelet dysfunction in type 2 diabetes.', *Diabetes Care*. American Diabetes Association, 24(8), pp. 1476–85. doi: 10.2337/diacare.24.8.1476.

Wagner, S. J. *et al.* (2000) 'Blood donors and b', 40(March), pp. 335–338.

Wasiluk, A. *et al.* (2013) 'Expression of P-selectin (CD62P) on platelets after thrombin and ADP in hypotrophic and healthy, full-term newborns', *J. Matern. Neonatal Med.* Taylor & Francis, 26(13), pp. 1321–1324. doi: 10.3109/14767058.2013.784251.

Wentworth, J. K. T., Pula, G. and Poole, A. W. (2006) 'Vasodilator-stimulated phosphoprotein (VASP) is phosphorylated on Ser157 by protein kinase C-dependent and -independent mechanisms in thrombin-stimulated human platelets.', *Biochem. J.* Portland Press Ltd, 393(Pt 2), pp. 555–64. doi: 10.1042/BJ20050796.

Whitehead, K. A. *et al.* (2015) 'The effect of surface properties of polycrystalline, single phase metal coatings on bacterial retention', *Int. J. Food Microbiol.* Elsevier, 197, pp. 92–97. doi: 10.1016/j.ijfoodmicro.2014.12.030.

Whitehead, K. A., Colligon, J. and Verran, J. (2005) 'Retention of microbial cells in substratum surface features of micrometer and sub-micrometer dimensions', *Colloids Surfaces B Biointerfaces*, 41(2–3), pp. 129–138. doi: 10.1016/j.colsurfb.2004.11.010.

Whitehead, K. A. and Verran, J. (2006) 'The effect of surface topography on the retention of microorganisms', *Food Bioprod. Process.*, 84(4 C), pp. 253–259. doi: 10.1205/fbp06035.

Widerström, M. *et al.* (2012) 'Coagulase-negative staphylococci: update on the molecular epidemiology and clinical presentation, with a focus on *Staphylococcus epidermidis* and *Staphylococcus saprophyticus*', *Eur. J. Clin. Microbiol. Infect. Dis.* Springer-Verlag, 31(1), pp. 7–20. doi: 10.1007/s10096-011-1270-6.

Wu, S. *et al.* (2018) 'Role of the Surface Nanoscale Roughness of Stainless Steel on Bacterial Adhesion and Microcolony Formation.', *ACS omega.* American Chemical Society, 3(6), pp. 6456–6464. doi: 10.1021/acsomega.8b00769.

Wypych, G. (2017) *Handbook of plasticizers.* Available at: <https://www.sciencedirect.com/science/book/9781895198973> (Accessed: 16 March 2018).

Yaghoubi, H. and Taghavinia, N. (2011) 'Surface chemistry of atmospheric plasma modified polycarbonate substrates', *Appl. Surf. Sci.* Elsevier B.V., 257(23), pp. 9836–9839. doi: 10.1016/j.apsusc.2011.06.034.

Zeraik, A. E. and Nitschke, M. (2010) 'Biosurfactants as Agents to Reduce Adhesion of Pathogenic Bacteria to Polystyrene Surfaces: Effect of Temperature and Hydrophobicity', *Curr. Microbiol.* Springer-Verlag, 61(6), pp. 554–559. doi: 10.1007/s00284-010-9652-z.